Reaction-diffusion equations with membrane conditions describing tumor invasion

Giorgia Ciavolella

SORBONNE UNIVERSITÉ
CRÉATEURS DE FUTURS DEPUIS 1257

Università di Roma Tor Vergata

UNIVERSITÉ FRANCO ITALIENNE
UNIVERSITÀ ITALO FRANCESE

SORBONNE UNIVERSITÉ
UNIVERSITÀ DEGLI STUDI DI ROMA TOR VERGATA

Doctoral School **École Doctorale Sciences Mathématiques de Paris Centre**
Scuola di Dottorato in Matematica

University Department **Laboratoire Jacques-Louis Lions**

Thesis defended by **Giorgia CIAVOLELLA**

Defended on **October 4, 2022**

In order to become Doctor from Sorbonne Université and from Università degli Studi di Roma Tor Vergata

Academic Field **Applied Mathematics**

Speciality **Analysis of Partial Differential Equations**

Reaction-diffusion equations with membrane conditions describing tumor invasion

Thesis supervised by Roberto NATALINI
Benoit PERTHAME

Committee members

Referees	Marcello Edoardo DELITALA	Professor at Politecnico di Torino	
	Emmanuel GRENIER	Professor at ENS Lyon	
Examiners	Luís NEVES DE ALMEIDA	Senior Researcher at Sorbonne Université	Committee President
	Maria GROPPI	Professor at Università di Parma	
Supervisors	Roberto NATALINI	Senior Researcher at IAC-CNR Rome	
	Benoit PERTHAME	Professor at Sorbonne Université	

Keywords: Kedem-Katchalsky conditions, Reaction-diffusion equation, Numerical analysis, Tumor invasion

Mots clés : Conditions de Kedem-Katchalsky, Équation de réaction-diffusion, Analyse numérique, Invasion tumorale

This thesis has been prepared at the following research units.

Laboratoire Jacques-Louis Lions

Sorbonne Université
Campus Pierre et Marie Curie
4 place Jussieu
75005 Paris
France

Web Site https://ljll.math.upmc.fr/

Istituto per le Applicazioni del Calcolo 'Mauro Picone'

CNR
Via dei Taurini 19
00185 Roma
Italy

Web Site https://www.iac.cnr.it/

Reaction-diffusion equations with membrane conditions describing tumor invasion

Abstract

Reaction-diffusion membrane problems find several applications in physics, biology and medical sciences, both in the case of linear and nonlinear diffusion. We mainly focus on the biological setting of two domains separated by a permeable membrane. At first, extending the work by Sanchez-Palencia to the porous medium case, we rigorously derive the effective interface conditions, called Kedem-Katchalsky conditions, as the limit of transmission conditions when the thickness of the membrane converges to zero. This is biologically relevant and convenient for numerical simulations. Then, the following works regard this limit problem on a zero-thickness membrane, but in the linear case. Extending the theory developed by Pierre and his collaborators, we establish the existence of global weak solutions when initial data have an L^1 regularity and nonlinearities have a sub-quadratic growth. In another work, we look at the situation in which two populations react and diffuse in a single domain creating spatial patterns. We adapt this Turing theory to the case of a permeable membrane. The result is quite similar to the standard case, but pattern formation is influenced both by diffusion and permeability coefficients. Finally, we present a more applied study in collaboration with biologists from the Laboratoire de Biologie et Thérapeutique des Cancers of INSERM at Saint-Antoine Hospital in Paris. In fact, Kedem-Katchalsky conditions can well characterise the flow of tumor cells through the basal membrane, in the so-called invasion process. This is a key step in the metastatic cascade and it is allowed by several stages, among which we distinguish membrane degradation. With the aim of deepening the invasion phenomenon, we propose a mathematical model concerning degradation of a biological layer. We present numerical simulations and an *a priori* analysis on the sensitivity of our system and on the parameter estimation. This is a preparatory work waiting for experimental results.

Keywords: Kedem-Katchalsky conditions, Reaction-diffusion equation, Numerical analysis, Tumor invasion

Résumé

Les problèmes de membrane dans les systèmes de réaction-diffusion trouvent de nombreuses applications en physique, en biologie et en médecine, aussi bien dans le cas linéaire que non linéaire. Nous nous intéressons à ces systèmes pour le cas de membranes biologiques. L'exemple représentatif étant donné par deux domaines séparés par une membrane perméable. Dans un premier temps, nous commençons par adapter le travail de Sanchez-Palencia à l'égard de systèmes de type fluide dans un milieu poreux afin de déterminer les conditions de membrane effectives, usuellement appelées conditions de Kedem-Katchalsky, en faisant tendre l'épaisseur de la membrane vers 0. Le modèle limite est à la fois biologiquement pertinent et très bien adapté pour des simulations numériques. Les travaux suivants s'intéressent au cas de diffusion linéaire avec des conditions de membrane effectives. En étendant la théorie développée par Pierre et ses collaborateurs, nous établissons l'existence de solutions faibles globales lorsque les données initiales ont une régularité L^1 et que les non-linéarités ont une croissance sous-quadratique. Dans un autre travail, nous regardons la situation dans laquelle deux populations réagissent et diffusent dans un même domaine en créant des structures spatiales. Nous étendons cette théorie de Turing au cas d'une membrane perméable. Le résultat obtenu est assez similaire au cas sans membrane mais ici vont jouer un rôle aussi bien les coefficients de diffusion que ceux de perméabilité à l'interface. Enfin, nous présentons une étude plus appliquée en collaboration avec le Laboratoire de Biologie et Thérapeutique des Cancers de l'INSERM à l'Hôpital Saint Antoine à Paris. En effet, les conditions de Kedem-Katchalsky permettent de bien caractériser le flux de cellules tumorales à travers la membrane basale, dans le processus dit d'invasion. C'est une étape clé dans la cascade métastatique qui est composée de plusieurs phases, parmi lesquelles on distingue la dégradation de la membrane. Dans le but d'approfondir notre compréhension du phénomène d'invasion, nous proposons un modèle mathématique représentant la dégradation d'une couche biologique. Nous présentons des simulations numériques et une analyse *a priori* sur la sensibilité de notre système et sur l'estimation des paramètres. Il s'agit d'un travail préparatoire en attente des résultats expérimentaux.

Mots clés : Conditions de Kedem-Katchalsky, Équation de réaction-diffusion, Analyse numérique, Invasion tumorale

Laboratoire Jacques-Louis Lions – Sorbonne Université – Campus Pierre et Marie Curie – 4 place Jussieu – 75005 Paris – France

Istituto per le Applicazioni del Calcolo 'Mauro Picone' – CNR – Via dei Taurini 19 – 00185 Roma – Italy

Riassunto

I problemi di reazione-diffusione con membrana trovano numerose applicazioni in fisica, biologia e medicina, sia nel caso di diffusione lineare che non lineare. Ci interessiamo a questi sistemi nel caso di membrane biologiche. L'esempio rappresentativo é quello di due domini separati da una membrana permeabile. In un primo tempo, estendendo il lavoro di Sanchez-Palencia per le equazioni dei mezzi porosi, ricaviamo in modo rigoroso le condizioni di interfaccia, chiamate condizioni di Kedem-Katchalsky, come limite di condizioni di trasmissione quando lo spessore della membrana converge a zero. Ciò è rilevante dal punto di vista biologico e conveniente per le simulazioni numeriche. I lavori che seguono riguardano questo problema limite su una membrana di spessore zero, ma guardando al caso di diffusione lineare. In un secondo studio, estendendo la teoria sviluppata da Pierre e dai suoi collaboratori, stabiliamo l'esistenza di soluzioni deboli globali quando i dati iniziali hanno una regolarità L^1 e le nonlinearità hanno una crescita al più quadratica. In un altro lavoro, guardiamo alla situazione in cui due popolazioni reagiscono e si diffondono in un unico dominio creando strutture spaziali. Adattiamo questa teoria di Turing in presenza di una membrana permeabile. Il risultato è abbastanza simile alla classica teoria di Turing, ma la formazione di pattern é influenzata sia dai coefficienti di diffusione che di permeabilità della membrana. Infine, presentiamo un lavoro più applicato in collaborazione con dei biologi del Laboratoire de Biologie et Thérapeutique des Cancers dell'INSERM all'Ospedale Saint Antoine a Parigi. Infatti, le condizioni di Kedem-Katchalsky possono caratterizzare il flusso di cellule tumorali attraverso la membrana basale, nel cosiddetto processo di invasione. Questo è un passaggio chiave nella cascata metastatica ed è consentito da diverse fasi, tra le quali distinguiamo la degradazione della membrana. Con l'obiettivo di approfondire la nostra conoscenza del fenomeno invasivo, proponiamo un modello matematico che rappresenta la degradazione di una membrana biologica. Presentiamo anche simulazioni numeriche e un'analisi *a priori* della sensibilità del nostro sistema e della stima dei parametri. Si tratta di un lavoro preparatorio in attesa dei risultati sperimentali.

Parole chiave: Condizioni di Kedem-Katchalsky, Equazione di reazione-diffusione, Analisi numerica, Invasione tumorale

Acknowledgements

I could write a thesis on acknowledgements only, but this is not the case (unfortunately). These were 3 complicated and wonderful years and I could meet a lot of very nice people and friends. I have decided not to write a long list of names, risking of forgetting someone (don't be too upset, my equality-rule is winning over me, but if you are reading this you can recognise yourself in here). These years were made up by so many people, most of them met during this experience, but of course, I have to add also my best fan at home.

The first thanks are of course for Roberto (who supports me since my Master and who have introduced me to the mathematical biology research) and for Benoît (who accepted to work with us and to support our project). Thank you for allowing me to live this incredible cotutelle experience. Thank you to both of you for your care, your patient, your advice and your teachings. Thanks to my referees and examiners to have accepted to be part of my jury. Separately, of course, I have to thank Luis for all the experiences and laugh shared together. It is an honour to have met all of you.

I would like to thank also my collaborators for all the advice and knowledge shared together. Thank also to my co-organisers, co-friends now, for the amazing conferences that we set up and also to the wonderful participants (and friends) that we had. I hope to share other experiences like this with you again. Efcharistó! (Too difficult to let this latex document accept the greek alphabet).

During the first 2 years in Paris, I could get into a wonderful lab, full of very nice people. It was a pleasure to meet you all and, at the same time, a pity not to have taken advantage of the lab a bit more. However, I thank all of you for each small chat, laugh, advice and experience that we have shared together. A particular thank also to all my co-bureau. In Rome too, I could meet very friendly and nice people at the CNR. Thanks to the girls for the lunches and chatting together and to my third-floor mates.

I would also like to thank my super Master friends, with our aperò sur la Seine, all the billiard and games and, we don't have to forget that we can say we have done a (half) triathlon together! We have shared a lot of very nice experiences and trips. Of course, I cannot miss los Piratas, friends in the lab and outside too. Maravillosa tripulación! Shukran!

The last year was a bit crazier and more unstable: Rome, Paris and a bit in Bologna. However, it was an amazing and struggling year with my favourite "club" (cit). I would like to thank you! Thank you for your friendships, thank you for your support and your complications too, thank you for your craziness and laughs and thank you also for the more serious moments.

I have focused my thanks on people met at work, during these years, but I cannot forget my home-team. We are more apart right now but you are always there, back in Rome (more or less let's say). I promise you that this is the last "laurea" that you have to see and then I will stop. Thank you for always being there for me. It is always nice to go back home thank to you.

A great thanks to Francesca, my best sister, or better my half sister-half adopted daughter, and we could also say half-coloq. You could say to have done an Erasmus in Paris too. I cannot

count anymore how many times you have visited me, and I am truly glad to have you often with me. You contributed a lot to what I am now and you succeed in shaping me also during these 3 years. Thank you for always pushing me (for the good... and the bad). Of course, I thank also all my family who had to deal with all my bad moods, but we have also spent a lot of wonderful moments together (as always). You are very important to me. Finally, thanks to Thomas without which these years wouldn't have been the same, full of laugh and joy. Thank you for letting me discover so many things. Merci b e a u c o u p!

Contents

Chapter 1

Introduction

Partial differential equations describing the movement of cells through a membrane are of high interest in the biology of cancer because this invasive property is fundamental in the metastatic cascade. The invasive process is still largely unknown and it is of interest both from a biological point of view, since there are still various open questions, and from a mathematical one, due to the introduction of systems closed by membrane conditions called Kedem-Katchalsky conditions.

Following an initial biological background, we are going to present some analysis of the mathematical models describing invasion phenomena (Chapters 2, 3, 4) and, finally, a more applied work (Chapter 5) in collaboration with a group of biologists of the Inserm team, at the Saint Antoine Hospital in Paris.

1.1 Biological background and motivations

Tumors are complex diseases which strongly affect human society. The extraordinary diversity of cancer and its high incidence are constantly increasing the demand to control it and to get cues to the underlying causes, Sung *et al.* [121]. The disconcertingly complexity explains why the discipline of oncology is divided and focuses on organ-specific cancers. However, there are underlying common principles that allow to bring together and to better understand all types of cancer, Hanahan and Coussens [60], Hanahan and Weinberg [61, 62, 63].

The hallmarks of cancer. In 2000 and 2011, Hanahan and Weinberg [61, 62] postulated that the vast complexity of cancers shares a set of principles which are at the basis of cancer growth and progression. They proposed to call this set of common characteristics *hallmarks of cancer*. In fact, as normal cells evolve progressively to a neoplastic state, they acquire a succession of these hallmarks, that provide a rationalisation of the multistep process of human tumor pathogenesis. At first (in 2000), they identified six biological capabilities, which included the ability to sustain proliferative signalling, evade growth suppressors, resist cell death, enable replicative immortality, induce angiogenesis, and activate invasion and metastasis. They later recognised two additional hallmarks: avoiding immune destruction, and deregulating cellular energetics and metabolism. Moreover, two characteristics of cancer lesions are able to induce and promote the acquisition of these functional capabilities: genome instability and mutations, and tumor-promoting inflammation. These hallmark traits can be acquired at different stages in the multistep process of tumorogenesis, and different types of cancer may depend on particular hallmarks.

Cancer cells are not able to traverse all this stages alone. Indeed, they recruit a variety of normal cells that contribute in this multistep process of tumor development and progression, see Figure 1.1. We have to underline that solid tumors are not simply a mass of cells, but they are a more complex and heterogeneous environment. Thus, tumors can be seen as complex tissues or new abnormal organs, made of multiple cell types and the stroma, Egeblad *et al.* [43]. The stroma can be divided into several classes: the extracellular matrix (ECM), the non-cellular component of organs which provides structural and biochemical support to surrounding cells, and stromal cells. Among stromal cells of the tumor microenvironment, it is possible to select three different classes (cancer-associated fibroblastic cells, infiltrating immune cells, and angiogenic vascular cells) which are involved in at least seven of the previous hallmarks, Hanahan and Coussens [60]. Fibroblasts are a type of cells which normally synthesize the extracellular matrix and collagen. Their carcinoma-associated cells stimulate cancer cell growth, inflammation, angiogenesis and invasion. In particular, fibroblasts activated by the tumor microenvironment are the cause of the major changes in the ECM. To ensure growth, tumors need to develop their vasculature and this is realised with the recruitment of angiogenic vascular cells. Interaction between cancer cells and infiltrated immune cells also play a significant role in the initiation and progression of cancer. They do not only participate to the anti-cancer response, but they also facilitate angiogenesis and metastatic spread. They compete with the normal microenvironment and its changes can induce a procancerous state, affecting tumor growth and metastasis, Bissell and Hines [9], Kim and Friedman [74].

One of the most crucial and lethal characteristics of solid tumors is represented by the increased ability of cancer cells to migrate and invade other organs during the so-called *metastatic spread* (see Figure 1.2), Dillekås *et al.* [39]. This thesis aims to study from an analytical, numerical and modelistic point of view one of the hallmarks listed above: cancer cells invasion.

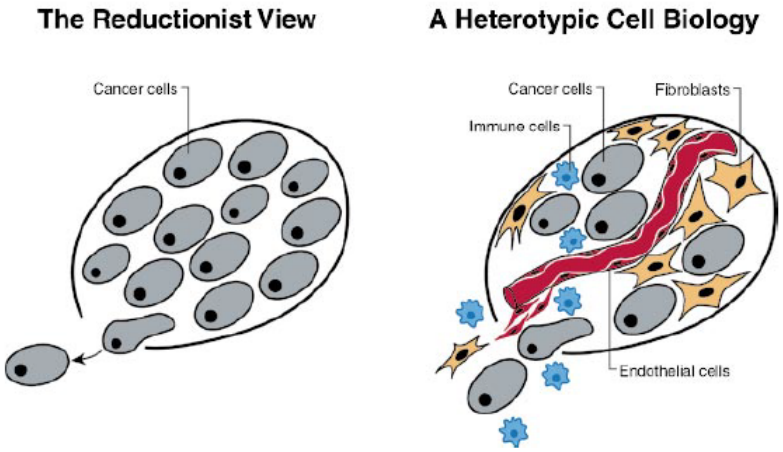

Figure 1.1: *On the left, the traditional and reductive way to see a tumor in the field of cancer research. On the right panel, innovative way to study a tumor, understanding the importance of its micro environment's connections. Reprinted from Cell,* 100.1*, D. Hanahan and R. A. Weinberg, "The hallmarks of cancer", pp.* 57−70*, Copyright (*2000*) with permission from Elsevier (Hanahan and Weinberg [62]).*

Metastatic process. Accumulation of mutations leads to uncontrolled cell proliferation and, thus, the formation of a small nodule. To grow beyond this size, they must attract new blood vessels by vasculogenesis and angiogenesis, in order to get more oxygen and nutrients, Carmeliet and Jain [23], Hillen and Griffioen [65]. Tumour vessels are tortuous and dilated. Consequently, tumour blood flow is chaotic and variable, inducing hypoxic (*i.e.* deprivation of adequate oxygen supply) and acidic regions in tumours. Among the cellular changes caused by hypoxia and other environmental factors, we distinguish what is known as *epithelial-to-mesenchymal transition* (EMT). This transition of epithelial cells to mesenchymal ones is a key molecular event in cancer invasiveness and metastatic dissemination. In fact, EMT reduces cell-cell adhesion and leads to dramatic changes in the physical and mechanical properties of cells, allowing the mesenchymal-like cancer cells to invade the surrounding stroma, Franssen [50], Liu *et al.* [84]. Extracellular matrix (ECM) provides substrate as well as a barrier to the advancing cells. Then, degradation is fundamental to penetrate into the ECM. Cancer cells can now intravasate and leave the original site. Life conditions inside blood vessels are hostile and circulating tumour cells (CTCs) can eventually extravasate, if combined environmental factors allowed it, such as platelets or the blood flow itself, Wirtz *et al.* [130]. Extravasation marks the gain of a new or secondary site that cancer cells can colonise forming a secondary tumor or metastasis.

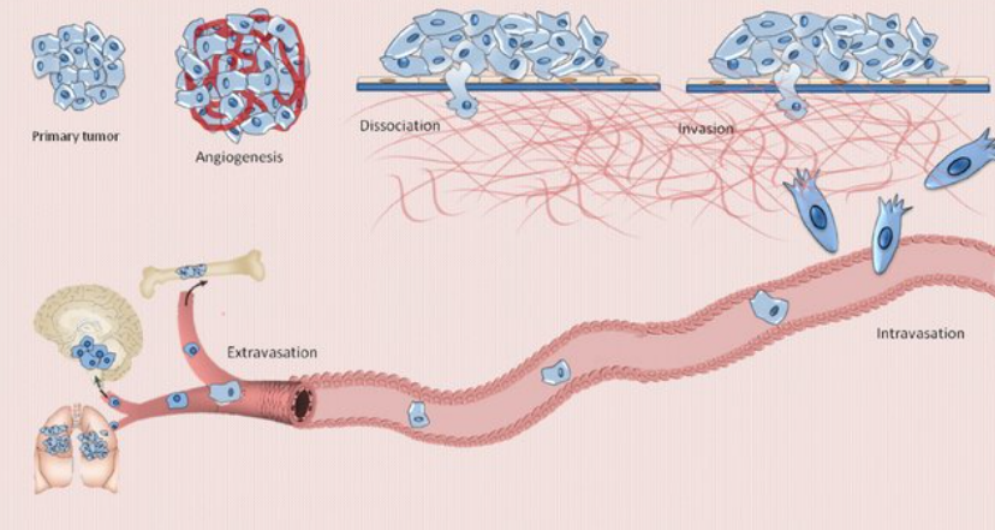

Figure 1.2: *The metastatic process. From a well-vascularised primary tumor, some cells can detach passing throught the basal membrane. Invasive cells may intravasate and, consequently known as circulating tumor cells, they circulate in the vascular system. Some of these eventually adhere to blood vessel walls and are able to extravasate and migrate into the secondary site, where they can form a secondary tumor or metastasis. Reprinted by permission from Springer: Springer, Tumor Biol., "Metastasis review: from bench to bedside", Alizadeh et al., Copyright (*2014*) (Alizadeh et al. [3])*

Invasion phenomenon. We have seen the main steps of the metastatic cascade which bring to the dissemination of cells of a primary tumor into other organs generating secondary tumors or metastasis. During this process, invasive ability plays a fundamental and challenging role. In particular, one of the most difficult barriers for cells to cross is the *basement membrane*. This kind of membrane separates the epithelial tissue (which generally covers and lines organs, cavities

and body surfaces) from the connective one (which connects body parts and grants stability), providing a barrier that isolates malignant cells from the surrounding environment over that supports cells. This membrane is composed by the basal lamina consisting of ECM and its main protein is called *laminin*, which allows the adherence of epithelial cells. While epithelial tissue consists mainly of cells, the basal lamina and connective tissue predominantly consist of ECM, a network of extracellular macromolecules and minerals that constantly undergoes remodelling according to environmental demand.

At the early stage, cancer cells proliferate locally in the epithelial tissue originating a carcinoma *in situ*, see Figure 1.3 in the case of a breast tumor. Unfortunately, they may mutate and acquire the ability to migrate by producing *matrix metalloproteinases* (MMPs), specific enzymes which degrade the basement membrane and the ECM, Overall and López-Otín [100]. Investigations have mainly focused on two members of this family of enzymes: MMP-2 and MMP-9, able to degrade a type of collagen abundant in the basal membrane, Köhrmann [76].

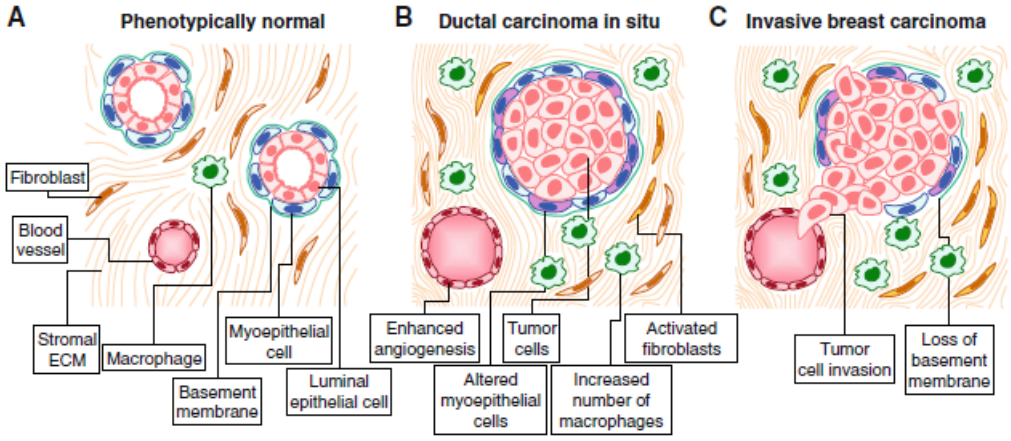

Figure 1.3: *Example of stromal alterations in breast cancer progression.* ***A.*** *In phenotipically normal tissue, central luminal epithelial cells are encircled by myoepithelial cells and basement membrane.* ***B.*** *A ductal carcinoma in situ, where tumor cells are still enclosed by a continuous basement membrane.* ***C.*** *Invasive breast carcinoma defined by the rupture of the basement membrane, loss of myoepithelial cells and invasion into the surrounding stroma and into the vasculature. Reprinted from J. Mammary Gland Biol. Neoplasia,* 15.4*, Cichon et al., "Microenvironmental Influences that Drive Progression from Benign Breast Disease to Invasive Breast Cancer", pp.* 389 – 397*, (*2010*), licensed under CC BY-ND (Cichon et al. [32]).*

1.2 Mathematical models describing tumor invasion

The models of interest are reaction-diffusion equations, one of the most common mathematical tools used in biological applications at the macroscopic level. In their general formulation, the evolution in time of the population density $u = u(t, x)$ is classically described in a divergence form by

$$\frac{\partial u}{\partial t} = div(D(u)\nabla u) + f, \tag{1.1}$$

where the reaction term $f = f(t, x, u(t, x))$ denotes the growth/degradation of the specie. We notice that the reaction depends on time, space and the density itself, but there could be other

quantities involved, such as other species densities. This kind of equations derives from a conservation principle such that, considered an arbitrary volume $V = V(t)$ with boundary ∂V, we have

$$\int_V \frac{\partial u}{\partial t} dx = -\int_{\partial V} \boldsymbol{J} \cdot \boldsymbol{n} dS + \int_V f dx, \tag{1.2}$$

namely the mass variation in the volume V is equal to the flow $\boldsymbol{J}$ across its boundary to which we add a mass that is either created or destroyed. In Equation (1.1), we characterise the flux through the Fick's law, *i.e.* $\boldsymbol{J} = -D(u)\nabla u$, describing a movement from regions of high concentration to others of lower concentration. We present here below two classical examples representing respectively the linear and nonlinear diffusion equation, ignoring for simplicity the reaction term.

Heat equation. The simplest example of linear diffusion equation is the heat equation (HE), corresponding to take $D(u) = D$, where D is a positive constant. We infer that the HE is in the form

$$\partial_t u = D\Delta u, \quad x \in \mathbb{R}^d, \quad t > 0. \tag{1.3}$$

This is a well-know equation and it has been largely studied. It was introduced to describe heat propagation in a solid material, this is where the name comes from. However, it can describe a large class of physical and biological phenomena, known as diffusion processes. Equation (1.3) can be derived also from a probabilistic model describing a microscopic dynamics in which each particle moves randomly. This random walk, in its continuous limit, is called Brownian motion.

The HE is quite nice, compared to its nonlinear counterpart introduced later on. One of its main property is the *strong maximum principle*, asserting that if the maximum of u is reached in the interior of the time-space domain $\Omega \times [0, T)$, then u is constant in $\overline{\Omega} \times [0, T]$. A consequence of it is the infinite speed of propagation that characterises the HE. In fact, given a nonnegative initial data, at an infinitesimal time u becomes strictly positive everywhere, see also Vazquez [126].

Finally, we can explicitly determine the solution of a Cauchy problem, obtained combining Equation (1.3) with an initial condition, finding out a Gaussian profile.

Porous medium equation. The porous medium equation (PME) is the simplest example of nonlinear degenerate parabolic equation assuming $D(u) = \gamma|u|^{\gamma-1}$ in Equation (1.1), Vazquez [127]. Then, it reads as follows

$$\partial_t u = \Delta u^\gamma, \quad \gamma > 1, \quad x \in \mathbb{R}^d, \quad t > 0. \tag{1.4}$$

Its degeneracy comes from the fact that $D(u) \geqslant 0$, and the vanishing $D(u)$ corresponds to the PME *degeneration* wherever $u = 0$. Equation (1.4) is equivalent to the heat Equation (1.3) in the case $\gamma = 1$. However, the nonlinearity and degeneracy of the PME bring several additional difficulties and these create a large gap with its linear and non-degenerate counterpart. The main qualitative difference is called *finite speed of propagation*, in contrast with the infinite speed of propagation of the HE, causing that the strong maximum principle cannot hold, see Vazquez [126, 127, Section 1.2.1]. In fact, starting with initial data with compact support, they remain so also at any finite time. The finite speed of propagation implies the appearance of a moving boundary, called *free boundary*, which separates the region where the density u is positive from the one in which it is zero. The change of character of the PME whenever $u = 0$ can be observed explicitly in the case $\gamma = 2$, in which

$$\partial_t u = 2u\Delta u + 2|\nabla u|^2. \tag{1.5}$$

The first term corresponding to a nonlinear perturbation of the HE dominates when u is larger than zero. It disappears approaching zero, in which case the second hyperbolic term is dominant.

Consequently, near the free boundary the PME is of *mixed type*: parabolic and hyperbolic. It infers that PMEs exhibit mixed properties. A similar calculation can be done for general $\gamma \neq 1$ after an appropriate change of variables that we will see in the following.

Another way to look at the PME is as part of a mechanical description of tissue and tumour development. In fact, tumors can be seen as a fluid flowing through a porous embedding, such as the extracellular matrix (ECM). To avoid over-crowding, cells move down a pressure gradient. This nonlinear and degenerate process allows to rewrite the PME as a filtration-equation of the form

$$\partial_t u + \nabla \cdot (u\boldsymbol{v}) = 0, \tag{1.6}$$

where we express the velocity field $\boldsymbol{v}$ linked to the internal pressure $p = \frac{\gamma}{\gamma-1}u^{\gamma-1}$ by the *Darcy law*, or equivalently

$$\boldsymbol{v} = -\mu\nabla p. \tag{1.7}$$

The function $\mu = \mu(t,x) \geqslant 0$ represents the cell mobility coefficient, that in the previous Equation (1.4) was taken equal to 1 for simplicity. Equation (1.6), closed with the Darcy law, is frequently used in the analysis of the porous medium type equations, since it allows to recover a self-contained equation for the pressure satisfying

$$\partial_t p = (\gamma - 1)\mu p\Delta p + \mu|\nabla p|^2. \tag{1.8}$$

This is the change of variable useful to clearly observe the double behaviour of the PME, around the degeneracy $p = 0$. We mention another extension of the PME which is the fast diffusion equation, consisting in the same equation as the PME but with $\gamma < 1$. Indeed, in this case the diffusion coefficient $D(u) = \gamma|u|^{\gamma-1}$ for $\gamma < 1$ goes now to infinity as $u \to 0$. This is why the PME is also mentioned as *slow diffusion equation*.

Finally, a fundamental example of solution with an explicit formula is called Barenblatt solution or Barenblatt-Pattle solution, which takes as initial data a Dirac mass and it has compact support in space for every fixed time.

Fast reaction limit. In this last paragraph, we want to introduce briefly a heat equation to which we add reaction terms that are fast respect to other terms, Moussa [93], Perthame and Skrzeczkowsi [105]. This kind of equations will be partly mentioned in Chapter 4. Their singular limits, as the reaction rates become extremely large, is called *fast reaction limit* or *instantaneous reaction limit*, which expresses the fact that instantaneous dynamics is also included in the system. There are two kinds of limit problems: free boundary problems and cross-diffusion systems. This limit has been intensively studied in many field of applications, such as diffusive irreversible chemical reactions, Evans [46], spatial segregation of competing species Dancer *et al.* [35] and cell polarisation Otsuji *et al.* [99], described by the system below.

Let $\Omega \subset \mathbb{R}^d$ a smooth, bounded spatial domain. We consider the following system of reaction-diffusion equations with Neumann boundary conditions,

$$\begin{cases} \partial_t u_\varepsilon - D_u\Delta u_\varepsilon = \varepsilon^{-1}(v_\varepsilon - F(u_\varepsilon)), \\ \partial_t v_\varepsilon - D_v\Delta v_\varepsilon = -\varepsilon^{-1}(v_\varepsilon - F(u_\varepsilon)), \end{cases} \tag{1.9}$$

where $t \geqslant 0$, $x \in \Omega$, $F : \mathbb{R}^+ \to \mathbb{R}^+$. Such equations have been used to model biological and physical phenomena such as cell polarisation.

One of the first basic properties of this system is mass conservation. Indeed, summing up the two equations we obtain

$$\partial_t(u_\varepsilon + v_\varepsilon) - \Delta[D_u u_\varepsilon + D_v v_\varepsilon] = 0,$$

from which we deduce, thanks to Neumann boundary conditions,

$$\int_\Omega u_\varepsilon(t,x) + v_\varepsilon(t,x)dx = const.$$

The name of fast reaction-diffusion is appropriate when studying the limit as $\varepsilon \to 0$. This limit usually lead to cross-diffusion systems. Formally, we expect that $(u_\varepsilon, v_\varepsilon) \to (u, v)$, where $v = F(u)$. Then, we infer that

$$\partial_t w - \Delta[D_u u + D_v F(u)] = 0, \quad w = u + F(u).$$

If we assume that the map $u \to w = u + F(u)$ is invertible, then we can write

$$D_u u + D_v F(u) = A(w).$$

Finally, we get

$$\begin{cases} \partial_t w - \Delta A(w) = 0 & x \in \Omega, t \geqslant 0, \\ \partial_n w = 0 & x \in \partial\Omega. \end{cases} \tag{1.10}$$

In the case of backward parabolicity, namely

$$A'(w) = \frac{D_u + D_v F'(u)}{1 + F'(u)} < 0,$$

the cross-diffusion System (1.10) is ill-posed.

1.3 Kedem-Katchalsky conditions

In this thesis, we are going to study the previous models in a bounded domain $\Omega \subset \mathbb{R}^d$ divided in two subdomains Ω_1 and Ω_3 separated by a zero-thickness interface $\Gamma_{1,3}$, that we will interpret as a biological membrane separating two medium. Then, the previous equations have to be coupled not only with homogeneous Dirichlet or Neumann boundary conditions on the external boundary, but also with membrane conditions on the inner membrane $\Gamma_{1,3}$. This is realised with the so-called *Kedem-Katchalsky conditions*, describing the crossing of the flux through the interface as

$$\nabla u_1 \cdot \boldsymbol{n} = \nabla u_3 \cdot \boldsymbol{n} = k(u_3 - u_1), \tag{1.11}$$

where $\boldsymbol{n}$ is the normal vector at the membrane and k is called permeability coefficient and it specifies how much the membrane is permeable to the specie u. The permeability can be constant or it can vary in time, space, depending also on other species densities. Conditions (1.11) outline the continuity of the flux and its proportionality to the jump of the density u at the membrane $\Gamma_{1,3}$.

They were introduced by Kedem and Katchalsky in 1961 in [72] in a thermodynamic context and they were applied to biological problems only later. In 2002, Quarteroni *et al.* [112] used these interface conditions in the study of the dynamics of the solute in the vessel and in the arterial wall. In 2006, Calabrò and Zunino [20] applied their theoretical results on elliptic partial differential equations to the study of the behavior of a biological model for the transfer of chemicals through thin biological membranes. In 2007, Serafini, in her PhD thesis [120], studied a model of the intracellular signal transduction processes in which molecules freely diffuse and the membrane transport events are allowed. In 2010, Cangiani and Natalini [21] considered models of nuclear transport of molecules such as proteins in living cells taking into account the active transport

of molecules along the cytoplasmic microtubules. We also find Kedem-Katchalsky conditions in recent works studying tumor invasion such as in Gallinato *et al.* ([53], 2017) or in Chaplain *et al.* ([24], 2019) and Giverso *et al.* ([57], 2022). A very recent on-going work deepening in the interactions between immune and tumour cells in microfluidic chips, Braun [12], Braun *et al.* [11, 13], use hyperbolic and parabolic models connected by Kedem-Katchalsky conditions. In [82] (2019), Li *et al.* proposed a rigorous derivation of bulk surface models which describe cell polarization and cell division including also transmission conditions. Let us also mention an example of transmission condition in electrochemistry: Bathory *et al.* ([8], 2019) proposed a problem frequently used when modelling the transfer of ions through the interface between two different materials. Also semi-discretization of mass diffusion problems requires numerical treatment in adjoint domains coupled at the interface (see Calabrò [20]).

We detail Kedem-Katchalsky conditions in the one dimensional case letting $I = (a, x_m) \cup (x_m, b)$ the spatial domain with a membrane in $x = x_m$. We call $x = x_m^+$ its right limit and $x = x_m^-$ the left limit. We consider the linear heat equation $\partial_t u + \partial_x J = 0$ where $J = -D\partial_x u$, with homogeneous Neumann boundary conditions in a and b. We need, then, two conditions to close the system in order to describe both sides of the interface.

Conservation of mass. We assume conservation of mass, since the passage throught the membrane do not cause a production or loss of mass, *i.e.* what enters in membrane pores will also exits. Then, we infer that

$$0 = \frac{d}{dt}\int_I u dx = -\int_I \partial_x J dx = J^+(x_m) - J^-(x_m), \tag{1.12}$$

where $J^\pm$ are the right and left limiting values of the flux. In conclusion, we derive the continuity of the flux.

Dissipation principle. We know to have dissipation of the time derivative L^2-norm of a HE solution. So, we expect that this holds also introducing a permeable membrane. Indeed, this quantity represents, with a negative sign, the entropy production which is a nonincreasing quantity, in relation to the second law of thermodynamics, see Jüngel [68], Eck *et al.* [41]. In fact, multiplying by u the HE, we get

$$0 = \frac{1}{2}\partial_t u^2 - D\partial_x^2\left(\frac{1}{2}u^2\right) + |\partial_x u|^2,$$

deducing that

$$\frac{d}{dt}\int_I u^2 = \int_I D\partial_x^2 u^2 - 2|\partial_x u|^2 \leqslant \int_I D\partial_x^2 u^2 = 0.$$

Consequently, we observe a decay in time of the L^2-norm of the solutions, that coupled to the previous flux continuity brings to state

$$\frac{d}{dt}\int_I u^2 \leqslant \int_{I_-} D\partial_x^2 u_-^2 + \int_{I_+} D\partial_x^2 u_+^2 = D\partial_x u_-^2(x_m) - D\partial_x u_+^2(x_m) =$$

$$= 2[(Du_-\partial_x u_- - Du_+\partial_x u_+)(x_m)] = 2J(u_+(x_m) - u_-(x_m)).$$

Imposing

$$2J(u_+(x_m) - u_-(x_m)) \leqslant 0,$$

we assure to always have a dissipation of the L^2-norm. This condition is satisfied taking $J = -k(u_+(x_m) - u_-(x_m))$. Finally, we derive Kedem-Katchalsky membrane conditions

$$D\partial_x u_+ = D\partial_x u_- = k(u_+(x_m) - u_-(x_m)). \tag{1.13}$$

1.4 Summary of the thesis

With the aim of studying tumour invasion models, this thesis focuses on the study of membrane conditions both concerning linear and nonlinear diffusion systems.

Part I concerns the derivation of the membrane conditions on a zero-thickness membrane.

In Chapter 2, we analyse the limit of a transmission problem on a thick membrane as its thickness converges to zero, obtaining rigorously the interface conditions. Studying a limiting effective problem on a zero-thickness membrane is relevant and convenient both biologically and mathematically. This analysis is performed for a porous medium type system, extending the analogous result in the elliptic and parabolic case by Sanchez-Palencia [118]. Consequently, in the following chapters, we treat only the effective membrane problem, with the so-called Kedem-Katchalsky conditions.

Part II focuses on linear diffusion problems. In fact, the idea is to build a stronger theoretical background for membrane problems.

In Chapter 3, we build an L^1 theory for reaction-diffusion membrane problems, adapting previous results by Pierre and collaborators [10, 78, 79, 107].

In Chapter 4, we provide membrane problems of a Turing instability theory. Indeed, working with reaction-diffusion systems the question that arises is whether the membrane has an effect on the formation of patterns.

Part III deals with an applied project with a team of biologists at the Saint Antoine Hospital.

Chapter 5 presents the mathematical results that will be later used with the experimental data, as soon as available. However, the experimental setting is illustrated as well as examples of the biological data, clarifying also the simulations point of view. We present the sensitivity of the model, as well as the inverse problem to recover the parameters value from future experimental data. Finally, a logistic fitting is also of interest.

1.4.1 Derivation of membrane conditions on a zero-thickness interface

Motivated by biological applications on tumor invasion through thin membranes, in Chapter 2 (taken from Ciavolella *et al.* [30]) we study the rigorous derivation of effective membrane conditions on a zero-thickness membrane. Starting from a trasmission problem with transmission conditions on the boundary of a membrane with thickness ε, we consider the limit as ε goes to 0 with the aim of determining the boundary conditions at the limit interface. Indeed, the membrane is smaller than the size of adjacent tissues. Then, it is reasonable to approximate it with a zero-thickness one (see Figure 1.4), as done for instance in Chaplain *et al.* [24] and Gallinato *et al.* [53]. In particular, we give a rigorous proof to the formal derivation by Chaplain *et al.* [24]. They have also performed a numerical study, observing that there is a correspondence between the two problems taking the thickness ε small enough and, in the case of a zero-thickness membrane, the computational cost is also lower. This is why this kind of question is interesting both biologically and mathematically.

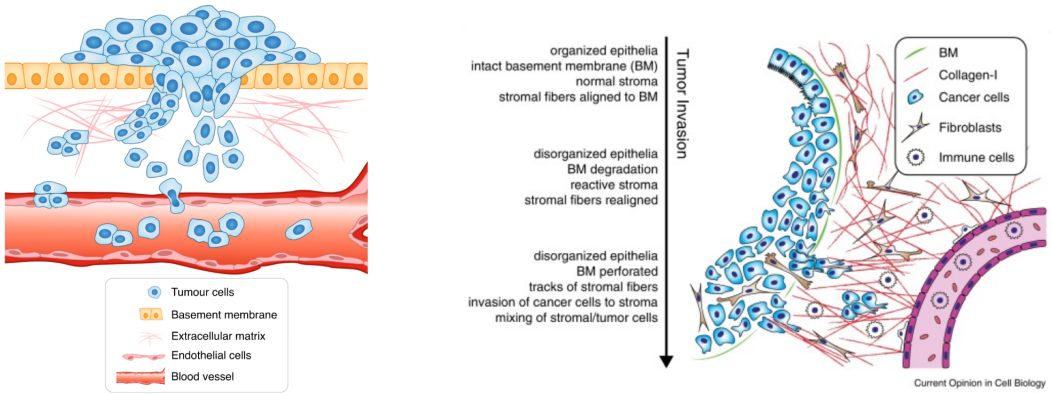

Figure 1.4: *On the left, the representation of the thick basal membrane (in yellow), which separates the upper domain where the primary tumor initially lives from the lower domain composed of extracellular matrix. Moreover, we observe cancer cells invasion through the membrane. On the right, it is shown the same process but with the approximated zero-thickness membrane (in green). Adapted from Br. J. Cancer,* 124.1*, Novikov et al., "Mutational drivers of cancer cell migration and invasion", pp.* $102-114$ *(*2021*), licensed under CC BY* 4.0 *(Novikov et al. [97]). Reproduced from Curr. Opin. Cell Biol.,* 36*, Clark and Vignjevic, "Modes of cancer cell invasion and the role of the microenvironment", pp.* $13-22$ *(*2015*), licensed under CC-BY-NC-ND (Clark and Vignjevic [33]).*

We consider a model in which the population density $u = u(t,x)$ evolves under a porous medium dynamics. We assume the domain $\Omega \in \mathbb{R}^3$ to be an open and bounded set. Moreover, Ω is composed of three subdomains $\Omega_{i,\varepsilon}$, for $i = 1,2,3$, where ε is the thickness of the membrane $\Omega_{2,\varepsilon}$, see Figure 1.5. Cells are allowed to move among these three domains with different constant mobilities $\mu_{i,\varepsilon}$, for $i = 1,2,3$, crossing the boundaries $\Gamma_{1,2,\varepsilon}$ (between $\Omega_{1,\varepsilon}$ and $\Omega_{2,\varepsilon}$) and $\Gamma_{2,3,\varepsilon}$ (between $\Omega_{2,\varepsilon}$ and $\Omega_{3,\varepsilon}$). Finally, we have $\Omega = \Omega_{1,\varepsilon} \cup \Omega_{2,\varepsilon} \cup \Omega_{3,\varepsilon}$, with $\Gamma_{1,2,\varepsilon} = \Omega_{1,\varepsilon} \cap \Omega_{2,\varepsilon}$, and $\Gamma_{2,3,\varepsilon} = \Omega_{2,\varepsilon} \cap \Omega_{3,\varepsilon}$. The transmission problem reads as

$$\begin{cases} \partial_t u_{i,\varepsilon} - \mu_{i,\varepsilon} \nabla \cdot (u_{i,\varepsilon} \nabla p_{i,\varepsilon}) = u_{i,\varepsilon} G(p_{i,\varepsilon}), & \text{in } (0,T) \times \Omega_{i,\varepsilon}, \quad i = 1,2,3, \\ \mu_{i,\varepsilon} u_{i,\varepsilon} \nabla p_{i,\varepsilon} \cdot \boldsymbol{n}_{i,i+1} = \mu_{i+1,\varepsilon} u_{i+1,\varepsilon} \nabla p_{i+1,\varepsilon} \cdot \boldsymbol{n}_{i,i+1}, & \text{on } (0,T) \times \Gamma_{i,i+1,\varepsilon}, \quad i = 1,2, \\ u_{i,\varepsilon} = u_{i+1,\varepsilon}, & \text{on } (0,T) \times \Gamma_{i,i+1,\varepsilon}, \quad i = 1,2, \\ u_{i,\varepsilon} = 0, & \text{on } (0,T) \times \partial\Omega, \end{cases} \tag{1.14}$$

where $p_{i,\varepsilon}$ is the density dependent pressure, given by the power law $p_{i,\varepsilon} = u_{i,\varepsilon}^{\gamma}$, for $\gamma > 1$. The problem that we expect to recover in the limit, formally derived by Chaplain *et al.* [24], is called *effective problem* and it is defined on the domain Ω divided into two open subdomains $\tilde{\Omega}_i$ for $i = 1,3$. The second domain $\Omega_{2,\varepsilon}$ collapses into the zero-thickness membrane $\tilde{\Gamma}_{1,3}$. Then, $\Omega = \tilde{\Omega}_1 \cup \tilde{\Gamma}_{1,3} \cup \tilde{\Omega}_3$. When shrinking the membrane $\Omega_{2,\varepsilon}$ to an infinitesimal region $\tilde{\Gamma}_{1,3}$, it is important to preserve the properties of the initial domain such that cell invasion is allowed. This is why, together with the limit as the thickness of the membrane approaches zero, we have to deal with the limit of the mobility rate inside the membrane. Consequently, we consider the assumptions on the mobility coefficients such that they satisfy $\mu_{i,\varepsilon} > 0$ for $i = 1,3$ and

$$\lim_{\varepsilon \to 0} \mu_{1,\varepsilon} = \tilde{\mu}_1 \in (0,+\infty), \qquad \lim_{\varepsilon \to 0} \frac{\mu_{2,\varepsilon}}{\varepsilon} = \tilde{\mu}_{1,3} \in (0,+\infty), \qquad \lim_{\varepsilon \to 0} \mu_{3,\varepsilon} = \tilde{\mu}_3 \in (0,+\infty). \tag{1.15}$$

Under the previous hypothesis, we prove weak convergence of solutions of Problem (1.14) to solutions of the following system

$$\begin{cases} \partial_t \tilde{u}_i - \tilde{\mu}_i \nabla \cdot (\tilde{u}_i \nabla \tilde{p}_i) = \tilde{u}_i G(\tilde{p}_i), & \text{in } (0,T)\times\tilde{\Omega}_i, \quad i=1,3, \\ \tilde{\mu}_{1,3}[\![\Pi]\!] = \tilde{\mu}_1\tilde{u}_1\nabla\tilde{p}_1\cdot\tilde{\boldsymbol{n}}_{1,3} = \tilde{\mu}_3\tilde{u}_3\nabla\tilde{p}_3\cdot\tilde{\boldsymbol{n}}_{1,3}, & \text{on } (0,T)\times\tilde{\Gamma}_{1,3}, \\ \tilde{u}=0, & \text{on } (0,T)\times\partial\Omega, \end{cases} \tag{1.16}$$

where Π satisfies $\Pi'(u) = up'(u)$, namely

$$\Pi(u) := \frac{\gamma}{\gamma+1}u^{\gamma+1}.$$

Conditions on $\tilde{\Gamma}_{1,3}$ are called non linear generalized Kedem-Katchalsky conditions. Their linear counterpart can be obtained taking $\Pi(u) = u + C$, $C \in \mathbb{R}$. They describe the continuity of the flux through the effective interface $\tilde{\Gamma}_{1,3}$ and their proportionality to the jump, denoted by the symbol $[\![\cdot]\!]$, of a quantity linked to cells pressure. In particular,

$$[\![\Pi]\!] := \frac{\gamma}{\gamma+1}(\tilde{u}^{\gamma+1})_3 - \frac{\gamma}{\gamma+1}(\tilde{u}^{\gamma+1})_1, \tag{1.17}$$

where the subscript indicates that $(\cdot)$ is evaluated as the limit to a point of the interface coming from the subdomain $\tilde{\Omega}_1$, $\tilde{\Omega}_3$, respectively.

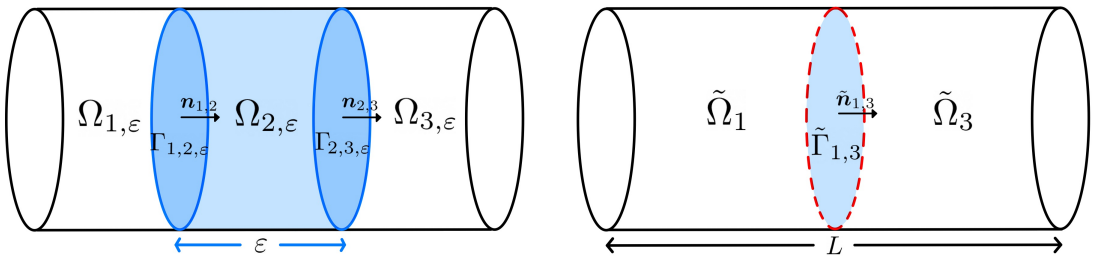

Figure 1.5: *We represent here the bounded cylindrical domain Ω of length L. On the left, we can see the subdomains $\Omega_{i,\varepsilon}$ with related outward normals. The membrane $\Omega_{2,\varepsilon}$ of thickness $\varepsilon > 0$ is delimited by $\Gamma_{i,i+1,\varepsilon} = \{x_3 = \pm\varepsilon/2\} \cap \Omega$ which are symmetric with respect to the effective interface, $\tilde{\Gamma}_{1,3} = \{x_3 = 0\} \cap \Omega$. On the right, we represent the limit domain as $\varepsilon \to 0$. The effective interface $\tilde{\Gamma}_{1,3}$ separates the two limit domains, $\tilde{\Omega}_1, \tilde{\Omega}_3$.*

Main result and main steps of the proof

We show here the main result on the derivation of Kedem-Katchalsky conditions and the idea of its proof.

Theorem 1.4.1 (Convergence to the effective problem)**.** *We consider a cylinder as in Figure 1.5. We add assumptions on the initial data, on the growth rate and on the mobility coefficients, see (1.15). With the use of appropriate a priori estimates, we are able to prove that weak*

solutions of the transmission problem, i.e. for all $\psi \in H^1(0,T;H_0^1(\Omega))$

$$-\int_0^T\int_\Omega u_\varepsilon \partial_t\psi + \sum_{i=1}^{3}\mu_{i,\varepsilon}\int_0^T\int_{\Omega_{i,\varepsilon}} u_{i,\varepsilon}\nabla p_{i,\varepsilon}\cdot\nabla\psi = \int_0^T\int_\Omega u_\varepsilon G(p_\varepsilon)\psi + \int_\Omega u_\varepsilon^0\psi(0,x), \tag{1.18}$$

converge to weak solutions of the effective problem, i.e.

$$\begin{aligned}-\int_0^T\int_\Omega \tilde{u}\partial_t w + \tilde{\mu}_1\int_0^T\int_{\tilde{\Omega}_1}\tilde{u}\nabla\tilde{p}\cdot\nabla w + \tilde{\mu}_3\int_0^T\int_{\tilde{\Omega}_3}\tilde{u}\nabla\tilde{p}\cdot\nabla w \\ + \tilde{\mu}_{1,3}\int_0^T\int_{\tilde{\Gamma}_{1,3}}[\![\Pi]\!]\left(w_{|x_3=0^+}-w_{|x_3=0^-}\right) = \int_0^T\int_\Omega \tilde{u}G(\tilde{p})w + \int_\Omega \tilde{u}^0 w^0,\end{aligned} \tag{1.19}$$

for all test functions $w(t,x)$ *with a proper regularity and* $w(T,x)=0$ *a.e. in* Ω.

As underlined before, this theorem completes the formal analysis in Chaplain *et al.* [24] in the case of a porous medium dynamic. The proof follows a previous result on elliptic and parabolic equations by Sanchez-Palencia [118]. His approach is based on H^1- *a priori* estimates on the density u_ε. In our case, the nonlinearity and the degeneracy of the porous medium equation bring several additional difficulties. Indeed, we do not have an L^2-bound on the density u_ε, since it can develop discontinuities, see Section 1.2 on the porous medium equation. However, we can state an H^1-estimate for the pressure. The nice part of working with a porous medium type equation is that we can either work with the density or with the pressure, since we can find an equation also for it, due to the relation $p = u^\gamma$, see Equation (1.8). This is very useful when more regularity on the gradient is needed.

The critical term then is the divergence one (the second one in Equation (1.18)). Indeed, we need:

- a control on the gradient of the pressure, considering also that in the second domain $\Omega_{2,\varepsilon}$ the mobility approaches zero in the limit;
- strong convergence of the density u_ε, differently from Sanchez-Palencia, since we have to ask that the product $u_\varepsilon\nabla p_\varepsilon$ converges weakly;
- a proper definition of the limit test functions w which are discontinuous.

With the previous properties, the theorem is proved with the use of standard tools and the procedure is quite technical. Here below, we provide the ideas to solve the previous points.

A priori estimates. An important result to state the convergence is the following *a priori* lemma, in which we also prove the H^1-bound of the pressure.

Lemma 1.4.1 (A priori estimates)**.** *Given appropriate assumptions, let* $(u_\varepsilon, p_\varepsilon)$ *be a solution of Problem* (1.14)*. There exists a positive constant* C *independent of* ε *such that*

(i) $\|u_\varepsilon\|_{L^\infty(0,T;L^\infty(\Omega))} \leqslant C,\ \|p_\varepsilon\|_{L^\infty(0,T;L^\infty(\Omega))} \leqslant C$

(ii) $\|\partial_t u_\varepsilon\|_{L^\infty(0,T;L^1(\Omega))} \leqslant C,\ \|\partial_t p_\varepsilon\|_{L^\infty(0,T;L^1(\Omega))} \leqslant C,$

(iii) $\|\nabla p_\varepsilon\|_{L^2(0,T;L^2(\Omega\setminus\Omega_{2,\varepsilon}))} \leqslant C.$

The proof here is quite standard, but, of course, keeping attention to transmission conditions.

We remark that the estimate *(iii)* is given by

$$\sum_{i=1}^{3} \mu_{i,\varepsilon} \int_0^T \int_{\Omega_{i,\varepsilon}} |\nabla p_{i,\varepsilon}|^2 \leqslant C.$$

Since $\mu_{2,\varepsilon} \to 0$, then we lack the estimate of the gradient in the domain $\Omega_{2,\varepsilon}$. Consequently, we need to construct an extension operator to have a uniform control of the pressure gradient in $L^2(\Omega)$.

Extension operator. A first main tool to deal with the limit $\varepsilon \to 0$ is an extension operator that 'truncates' and 'reflects' the solution from the outside of $\Omega_{2,\varepsilon}$ to the inside, see Figure 1.6. So, in particular we obtain that $\nabla \mathcal{P}_\varepsilon(p_\varepsilon) \in L^2(0,T; L^2(\Omega \setminus \tilde{\Gamma}_{1,3}))$ uniformly with respect to ε.

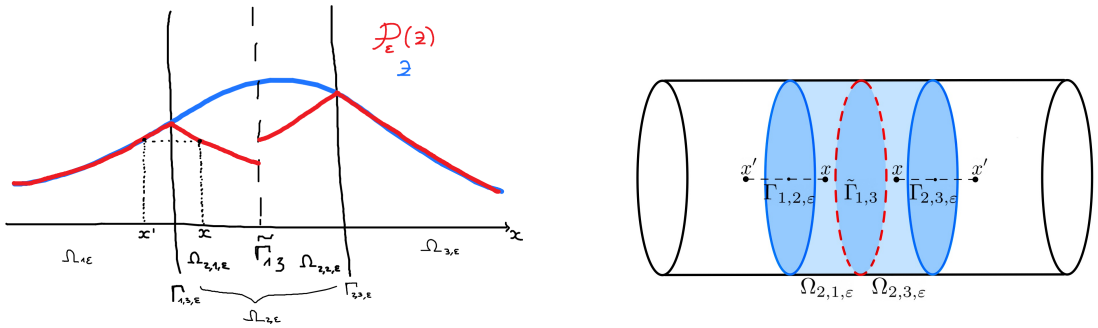

Figure 1.6: *On the left, schematic representation of the extension operator (in red) applied to a function z (in blue). Outside the central domain $\Omega_{2,\varepsilon}$, we take $\mathcal{P}_\varepsilon(z) = z$, whereas $\mathcal{P}_\varepsilon(z(t,x)) = z(t,x')$. On the right, the spatial symmetry used in the definition of the extension operator.*

Thanks to the properties of the operator linked to the *a priori* estimates on u_ε and p_ε, we can prove some compactness results of the extension operator, useful in the limit $\varepsilon \to 0$.

Lemma 1.4.2 (Compactness of the extension operator)**.** *Let $(u_\varepsilon, p_\varepsilon)$ be the solution of Problem (1.14). There exists a couple $(\tilde{u}, \tilde{p})$ with*

$$\tilde{u} \in L^\infty(0,T; L^\infty(\Omega \setminus \tilde{\Gamma}_{1,3})), \quad \tilde{p} \in L^2(0,T; H^1(\Omega \setminus \tilde{\Gamma}_{1,3})) \cap L^\infty(0,T; L^\infty(\Omega \setminus \tilde{\Gamma}_{1,3})),$$

such that, up to a subsequence, it holds

(i) $\mathcal{P}_\varepsilon(p_\varepsilon) \to \tilde{p}$ *strongly in* $L^p(0,T; L^p(\Omega \setminus \tilde{\Gamma}_{1,3}))$, *for* $1 \leq p < +\infty$,

(ii) $\mathcal{P}_\varepsilon(u_\varepsilon) \to \tilde{u}$ *strongly in* $L^p(0,T; L^p(\Omega \setminus \tilde{\Gamma}_{1,3}))$, *for* $1 \leq p < +\infty$,

(iii) $\nabla \mathcal{P}_\varepsilon(p_\varepsilon) \rightharpoonup \nabla \tilde{p}$ *weakly in* $L^2(0,T; L^2(\Omega \setminus \tilde{\Gamma}_{1,3}))$.

Proper test functions. Since in the limit we expect discontinuous test functions w, as we can see in (1.19), we define a new space E^* where these functions live. E^* is the space of finite combinations of functions defined as extension operators applied to regular functions. Indeed, since the extension operator builds a discontinuous function, then we obtain also discontinuous test functions w in E^*. Finally, we introduce the operator L_ε such that, taken $w \in C^1([0,T); E^*)$,

$L_\varepsilon(w) \in H^1(0,T;H_0^1(\Omega))$ and $L_\varepsilon(w) \to w$, uniformly as $\varepsilon \to 0$, for all $w \in C^1([0,T);E^*)$. In this way, we can substitute $\psi = L_\varepsilon(w)$ in the weak solution (1.18).

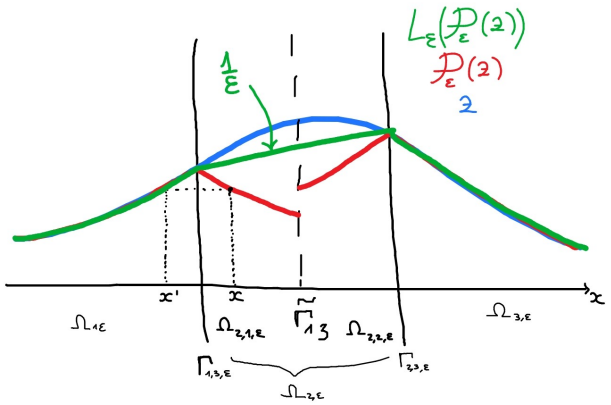

Figure 1.7: *Schematic representation of the operator L_ε (in green) applied to the extension operator $\mathcal{P}_\varepsilon$ (in red), since L_ε is defined on functions in the space E^* which are combinations of extension operators on regular function, called here z (in blue). Inside the domain $\Omega_{2,\varepsilon}$, L_ε is defined as a line with a slope $\frac{1}{\varepsilon}$, such that it diverges as $\varepsilon \to 0$.*

1.4.2 Existence of weak solutions for a reaction-diffusion membrane problem

As pointed out at the beginning of Section 1.4, we dedicate Chapter 3 to an analytical study of membrane problems in the linear case. Then, we study a reaction-diffusion membrane problem on a zero-thickness interface, with the previously derived Kedem-Katchalsky conditions. Chapter 3 is taken from Ciavolella and Perthame [31]. The interest is to build an existence theory for membrane problems in an L^1 setting. We analyse the existence of a global weak solution for a reaction-diffusion problem of m species which diffuse in a multi-dimensional domain and through a zero-thickness permeable membrane.

To describe the model, we consider, as depicted in Fig. 1.8, an inner transverse C^1 membrane $\Gamma^{1,3}$ separating a domain Ω in two connected sub-domains Ω^1 and Ω^3,

$$\Omega \;=\; \Omega^1 \cup \Omega^3 \subset \mathbb{R}^d, \quad d \geqslant 2, \qquad\qquad \Gamma^{1,3} = \partial\Omega^1 \cap \partial\Omega^3.$$

We assume Ω^1 and Ω^3 to be piecewise C^1 domains. In order to set boundary conditions, we introduce $\Gamma^1 = \partial\Omega^1 \setminus \Gamma^{1,3}$ and $\Gamma^3 = \partial\Omega^3 \setminus \Gamma^{1,3}$, assumed non-empty.

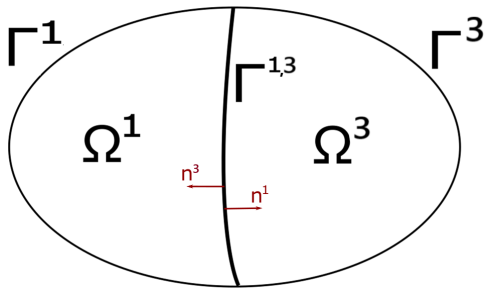

Figure 1.8: *Example of spatial domain Ω with an inner transverse membrane $\Gamma^{1,3}$ which decomposes Ω in open sets Ω^1 and Ω^3. The figure also shows the outward normals to the membrane.*

The system of interest is described by

$$\begin{cases} \partial_t u_i - D_i \Delta u_i = f_i(u_1, ..., u_m), & \text{in } Q_T := (0,T) \times \Omega, \\ u_i = 0, & \text{in } \Sigma_T := (0,T) \times (\Gamma^1 \cup \Gamma^3), \\ \partial_{\boldsymbol{n}^1} u_i^1 = \partial_{\boldsymbol{n}^1} u_i^3 = k_i(u_i^3 - u_i^1), & \text{in } \Sigma_{T,\Gamma} := (0,T) \times \Gamma^{1,3}, \\ u_i(0,x) = u_{0,i}(x) \geqslant 0, & \text{in } \Omega, \end{cases} \tag{1.20}$$

where we denote each species density for $i = 1, ..., m$ with

$$u_i = \begin{cases} u_i^1, & \text{in } \Omega^1, \\ u_i^3, & \text{in } \Omega^3. \end{cases}$$

Moreover, the diffusion coefficient D_i and the permeability at the membrane k_i (corresponding to $\tilde{\mu}_{1,3}$ in the previous *effective interface* Problem (1.16)) are positive constants. We call $\boldsymbol{n}^\lambda$ the outward normal of the domain Ω^λ for $\lambda = 1, 3$ such that $\boldsymbol{n}^3 = -\boldsymbol{n}^1$. Conditions $\partial_{\boldsymbol{n}^1} u_i^1 = \partial_{\boldsymbol{n}^1} u_i^3 = k_i(u_i^3 - u_i^1)$ are the (linear) Kedem-Katchalsky conditions derived in Chapter 2: flux continuity of the species density and flux proportionality to the jump of the density itself for $x \in \Gamma^{1,3}$.

This kind of equations is quite standard and very frequent in biological applications, namely to describe Lotka-Volterra systems, chemical reaction problems, gas combustion, electrodynamics. At the same time, even without a membrane, some questions are still open, also concerning weak solutions. A specific challenge has been to describe systems with the natural L^1-regularity and with high order nonlinearities, which are the common properties of many biological systems. This was the interest of Pierre and his collaborators [7, 10, 79, 107] and Laamri and Perthame [78].

In this context, we aim to introduce our work, extending the results just cited. Consequently, we gather the following assumptions for some constants $C, C_M, M > 0$ and for all $i = 1, ..., m$, for all $\mathbf{u} = (u_1, ..., u_m) \in [0, +\infty)^m$,

$$|f_i(\boldsymbol{u})| \leqslant C\Big(1 + \sum_{j=1}^m u_j^2\Big), \qquad \text{(sub-quadratic growth)}, \tag{1.21}$$

$$\sum_{j=1}^m f_j(\boldsymbol{u}) \leqslant C\Big(1 + \sum_{j=1}^m u_j\Big), \qquad \text{(mass control)}, \tag{1.22}$$

$$f_i(u_1, ..., u_{i-1}, 0, u_{i+1}, ..., u_m) \geqslant 0, \qquad \text{(quasi-positivity)}, \tag{1.23}$$

$$|f_i(\boldsymbol{u}) - f_i(\boldsymbol{v})| \leqslant C_M \sum_{j=1}^{m} |u_j - v_j|, \qquad \forall \boldsymbol{u}, \boldsymbol{v} \in [0, M]^m. \tag{1.24}$$

Mass control (1.22) and quasi-positivity (1.23) are the main hypothesis used also by Pierre [107] and Laamri and Perthame [78]. In fact, they assure nonnegativity of solutions and mass control. These hypothesis can be found also in membrane problems such as those analysed in Cangiani and Natalini [21] and Serafini [120] describing intracellular trasport, as seen in more details in Chapter 3.

Main result and steps of the proof

Our main contribution is the following global existence theorem with initial data of low regularity and reaction terms at most quadratic.

Theorem 1.4.2 (Existence and regularity)**.** *Assuming* (1.21)-(1.24) *and* $k_1 = ... = k_m$*. Then, for all* L^1*-initial data* $\boldsymbol{u}_0 = (u_{0,1}, ..., u_{0,m})$*, the previous System* (1.20) *has a nonnegative global weak solution which satisfies for all* $T > 0$ *and* $i = 1, ..., m$*,*

$$u_i \in L^2(Q_T) \quad \text{and} \quad (1 + |u_i|)^\alpha \in L^2\big(0, T; H^1(\Omega)\big), \qquad \forall \alpha \in \left[0, \frac{1}{2}\right), \tag{1.25}$$

$$u_i \in L^\beta\big(0, T; W^{1,\beta}(\Omega)\big) \quad \text{and} \quad u_i \in L^\beta\big(0, T; L^\beta(\Gamma^{1,3})\big), \qquad \forall \beta \in \left[1, \frac{d}{d-1}\right). \tag{1.26}$$

Remark 1.4.1. *We remark that, since* β *is at most* 2*, solutions are at least* $W^{1,1}$ *in space, whereas only* L^1 *at the membrane* $\Gamma^{1,3}$*, due to the jump highlighted in Kedem-Katchalsky conditions.*

We present a sketch of the proof, deeply analysed in Chapter 3. We follow four main steps, as in Pierre's method [107].

Regularization process. We build a regularized problem (see (3.16)) with a nonnegative classical global solution $\mathbf{u}^n$, considering a regularized version of the initial data and of the nonlinearities. We observe that regularised reaction terms share the same properties as the non-regularised ones, *i.e.* hypothesis (1.21)-(1.24).

An L^2 *a priori* Lemma. A fundamental hypothesis to prove existence is an L^1-bound of the regularised nonlinearities. Without this hypothesis, we can still prove an L^2-bound on the densities $\mathbf{u}^n$, then claiming a bound on the reaction terms thanks to sub-quadratic growth (1.21). This is why we need to have an L^2 *a priori* result.

Lemma 1.4.3 (Key estimate with L^1 data and membrane conditions)**.** *Consider smooth functions* $z_i : [0, +\infty) \times \Omega \to \mathbb{R}^+$*,* $f_i : [0, +\infty)^m \to \mathbb{R}$*, for all* $i = 1, ..., m$*, with* f_i *satisfying the assumption* (1.22)*. Assume* $z_{0,i} \in L^1(\Omega) \cap (\mathbf{H^1})^*$ *and that the differential equation holds with*

$k_i = k$

$$\begin{cases} \partial_t z_i - D_i \Delta z_i = f_i(z_1, ..., z_m), & in\ Q_T, \\ z_i = 0, & in\ \Sigma_T, \\ \partial_{\boldsymbol{n}^1} z_i^1 = \partial_{\boldsymbol{n}^1} z_i^2 = k_i(z_i^2 - z_i^1), & in\ \Sigma_{T,\Gamma}, \\ z(0,x) = z_{0,i}(x) \geqslant 0, & in\ \Omega. \end{cases} \tag{1.27}$$

Then, for some constant C_3 depending on $\|\boldsymbol{z}_0\|_{(\mathbf{H^1})^*}$, the inequality holds

$$\sum_{i=1}^{m} \int_{Q_T} |z_i|^2 \leqslant C_3.$$

This lemma is an extension of the Laamri-Perthame L^1 key estimate Lemma 2.1.1. Here, we have to add the restriction $k_i = k$, for all $i = 1, ..., m$, otherwise the proof does not work.

Concluding, under the *mass control hypothesis* (1.22) on the sum of the f_i, for $i = 1, ..., m$, we prove that the regularized problem with L^1 initial data has an L^2 solution. So, thanks to this lemma and the *sub-quadratic growth hypothesis* (1.21) on the f_i, for $i = 1, ..., m$, we obtain that the regularized reaction term $\mathbf{f}^n$ is bounded in L^1.

Existence of a super-solution. It is not possible to directly prove existence of weak solutions in the limit. Despite we prove the good convergence for the densities (see Appendix 3.B) and $\mathbf{f}^n$ is bounded in L^1, we cannot pass to the limit $n \to +\infty$ in the definition of weak solution $\mathbf{u}^n$, namely for all $i = 1, ..., m$

$$-\int_\Omega \psi(0,x) u_{0,i}^n + \int_{Q_T} (-\psi_t u_i^n + D_i \nabla\psi \nabla u_i^n) + \int_0^T \int_\Gamma D_i k_i [\![u_i^n]\!][\![\psi]\!] = \int_{Q_T} \psi f_i^n,$$

since we do not have the L^1 convergence of the nonlinearities. However, we can find an inequality in the formulation of weak solution, thus obtaining a super solution.

So, assuming convergence of the initial data $\mathbf{u}_0^n \to \mathbf{u}_0$ in $L^1(\Omega)$, we have now all the ingredients to extend Pierre's Theorem 2.1.2 on the existence of a supersolution, in the case $k_i = k$, for all $i = 1, ..., m$, and $\mathbf{f}^n$ bounded in L^1. The result is proved in Section 3.3.3. The proof follows the main guide lines in Pierre [107]. In order to avoid the convergence problem of the reaction terms, we use a truncation method. The idea is to obtain a reaction-diffusion inequality with nonlinearities bounded in the limit $n \to +\infty$ and for a fixed truncation level. Then, we are able to find a limit for the truncated weak supersolution formula as $n \to +\infty$. Finally, bringing the truncation level to infinity, we obtain the supersolution of Problem (1.20).

Existence of a solution. Proving that the previous supersolution is also a subsolution, we can conclude the proof. The main ingredient to state this is the mass control structure, which allows to apply Fatou's lemma on the sum of reaction terms and densities obtaining a subsolution.

1.4.3 Effect of a membrane on diffusion-driven Turing instability

In Chapter 4 (a detailed version of Ciavolella [29]), we continue the analysis on reaction-diffusion systems with Kedem-Katchalsky membrane conditions. In fact, the question that arises is whether the membrane affects the formation of patterns.

Reaction-diffusion systems are largely studied not only for the previous existence analysis, but also to figure out the development of pattern and form. This natural phenomenon describes

morphogenesis in embryo, complex and spatial patterns formed by bacteria, as well as the formation of spots and stripes on animals. In 1952, Turing [123] suggested that *a system of chemical substances, called morphogens, reacting together and diffusing through a tissue, is adequate to account for the main phenomena of morphogenesis.* The idea of Chapter 4 is to retrace the main steps explaining theoretically and numerically Turing patterns in the case of a membrane. Then, we consider a domain as in Figure 1.8. Using the same notation of Chapter 3, see also in Subsection 1.4.2, we define $Q_T^\lambda = (0,T)\times\Omega_\lambda$, $\Sigma_T^\lambda = (0,T)\times\Gamma_\lambda$, for $\lambda = 1,3$ and $\Sigma_{T,\Gamma} = (0,T)\times\Gamma_{1,3}$. We consider a two-species reaction-diffusion membrane problem as below.

$$\begin{cases} \partial_t u_1 - D_{u1}\,\Delta u_1 = f(u_1,v_1), & \\ & \text{in } Q_T^1,\\ \partial_t v_1 - D_{v1}\,\Delta v_1 = g(u_1,v_1), & \\ \nabla u_1\cdot n \;=\; 0 \;=\; \nabla v_1\cdot n, & \text{in } \Sigma_T^1,\\ D_{u1}\,\nabla u_1\cdot n = k_u(u_3-u_1), & \\ & \text{in } \Sigma_{T,\Gamma},\\ D_{v1}\,\nabla v_1\cdot n = k_v(v_3-v_1), & \end{cases} \qquad \begin{cases} \partial_t u_3 - D_{u3}\,\Delta u_3 = f(u_3,v_3), & \\ & \text{in } Q_T^3,\\ \partial_t v_3 - D_{v3}\,\Delta v_3 = g(u_3,v_3), & \\ \nabla u_3\cdot n \;=\; 0 \;=\; \nabla v_3\cdot n, & \text{in } \Sigma_T^3,\\ D_{u3}\,\nabla u_3\cdot n = k_u(u_3-u_1), & \\ & \text{in } \Sigma_{T,\Gamma},\\ D_{v3}\,\nabla v_3\cdot n = k_v(v_3-v_1). & \end{cases} \tag{1.28}$$

This is the same initial setting than the standard Turing theory, except for the membrane conditions and the addition of new parameters, *i.e.* the permeabilities k_u, k_v of the two species, central in the analysis to understand the role of the membrane.

Analytical part

At first, we assume that there exists a homogeneous steady state $(\overline{u},\overline{v})$ such that it nullifies the reaction terms. Then, we analyse its stability on the linearised version of Systems (1.28), namely

$$\begin{cases} \partial_t u_1 - D_{u1}\,\Delta u_1 = \overline{f}_u u_1 + \overline{f}_v v_1,\\ \partial_t v_1 - D_{v1}\,\Delta v_1 = \overline{g}_u u_1 + \overline{g}_v v_1,\\ \nabla u_1\cdot n \;=\; 0 \;=\; \nabla v_1\cdot n,\\ D_{u1}\,\nabla u_1\cdot n = k_u(u_3-u_1),\\ D_{v1}\,\nabla v_1\cdot n = k_v(v_3-v_1), \end{cases} \qquad \begin{cases} \partial_t u_3 - D_{u3}\,\Delta u_3 = \overline{f}_u u_3 + \overline{f}_v v_3,\\ \partial_t v_3 - D_{v3}\,\Delta v_3 = \overline{g}_u u_3 + \overline{g}_v v_3,\\ \nabla u_3\cdot n \;=\; 0 \;=\; \nabla v_3\cdot n,\\ D_{u3}\,\nabla u_3\cdot n = k_u(u_3-u_1),\\ D_{v3}\,\nabla v_3\cdot n = k_v(v_3-v_1), \end{cases} \tag{1.29}$$

where $\overline{f}_u, \overline{f}_v, \overline{g}_u, \overline{g}_v$ are the partial derivatives of the reaction terms evaluated in $(\overline{u},\overline{v})$. By definition, we derive the conditions for the dynamical system to perform a stable steady state and, then, for the complete System (1.29) such that the stable steady state $(\overline{u},\overline{v})$ becomes unstable adding diffusion. The analysis requires, as for the standard reaction-diffusion problem, the introduction of eigenvalue problems for the Laplace operators with Neumann and membrane conditions, namely

$$L = -D_u\Delta \quad \text{and} \quad \widetilde{L} = -D_v\Delta,$$

where we define

$$D_\phi = \begin{cases} D_{\phi 1}, \text{ in } \Omega_1,\\ D_{\phi 3}, \text{ in } \Omega_3. \end{cases} \qquad \phi = \begin{cases} \phi_1, & \text{in } \Omega_1,\\ \phi_3, & \text{in } \Omega_3, \end{cases}$$

for $\phi = u$ or v. So, we have for u

$$\begin{cases} Lw = \lambda w, & \text{in } \Omega_1 \cup \Omega_3, \\ \nabla w \cdot n = 0, & \text{in } \Gamma_1 \cup \Gamma_3, \\ D_{u1}\nabla w_1 \cdot n = D_{u3}\nabla w_3 \cdot n = k_u(w_3 - w_1), & \text{in } \Gamma_{1,3}, \end{cases}$$

and for v,

$$\begin{cases} \widetilde{L}z = \eta z, & \text{in } \Omega_1 \cup \Omega_3, \\ \nabla z \cdot n = 0, & \text{in } \Gamma_1 \cup \Gamma_3, \\ D_{v1}\nabla z_1 \cdot n = D_{v3}\nabla z_3 \cdot n = k_v(z_3 - z_1), & \text{in } \Gamma_{1,3}. \end{cases}$$

Consequently, a diagonalisation theory is needed, for details see Appendix 4.A, to claim existence of sequences of eigenvalues $\{\lambda_n\}_{n\in\mathbb{N}}, \{\nu_n\}_{n\in\mathbb{N}}$ and corresponding eigenfunctions $\{w_n\}_{n\in\mathbb{N}}, \{z_n\}_{n\in\mathbb{N}}$. Then, we state the instability theorem for a membrane problem

Theorem 1.4.3 (Turing instability theorem)**.** *Consider the linearised systems in* (1.29) *around the steady state* $(\overline{u}, \overline{v})$ *with* $D_v > 0$ *fixed. We assume*

$$\overline{f}_u + \overline{g}_v < 0 \quad \text{and} \quad \overline{f}_u\,\overline{g}_v - \overline{f}_v\,\overline{g}_u > 0,$$

such that we have stability for the dynamical system, and

$$\nu_{_D} := \frac{D_{ur}}{D_{ul}} = \frac{D_{vr}}{D_{vl}}, \qquad \nu_{_K} := \frac{k_u}{D_{ul}} = \frac{k_v}{D_{vl}} \qquad \text{and} \qquad \theta := \frac{D_{ul}}{D_{vl}} = \frac{D_{ur}}{D_{vr}}. \tag{1.30}$$

$$\lambda_{_n} = \theta\eta_{_n}, \quad \text{for all } n \in \mathbb{N}, \tag{1.31}$$

to have the same eigenfunctions w_n *and* z_n*. Then, for* θ *sufficiently small (that means* D_u *small), the steady state* $(\overline{u}, \overline{v})$ *is linearly unstable. Moreover, only a finite number of eigenvalues are unstable.*

Idea of the proof. The proof follows the main steps of the standard theory, see for example Murray [95], Perthame [106]. Then, we decompose u and v using the basis of eigenfunctions and such that we obtain solutions with exponential growth in time. The idea is that we want to impose a divergent exponential, in order to have an unstable steady state. So, we can write a *dispersion relation* for the exponential coefficient μ and, to infer $\mathrm{Re}(\mu) > 0$, we end up with condition

$$p(\eta_{_n}) := \theta\eta_{_n}^2 - \eta_{_n}(\overline{f}_u + \theta\,\overline{g}_v) + \det(A) < 0. \tag{1.32}$$

For the convex function $p(\eta_{_n})$ to be strictly negative, its minimum must be strictly negative. Finally, we can find a critical $\theta = \theta_c$ at which we have a bifurcation phenomena: for $\theta < \theta_c$, convergence to equilibrium is observed, for $\theta > \theta_c$ we can see patterns. To go further, we can explicate the range of eigenvalues such that $p(\eta_{_n}) < 0$ and, in particular, in the regime θ small we find a very large interval, hence it will contain some eigenvalues.

□

Numerical part

Eigenvalues and eigenfunctions of the one-dimensional Neumann membrane problem. We validate the previous theoretical results through numerical simulations in a one-dimensional domain $(0, x_m) \cup (x_m, L)$, with $x_m = \frac{L}{2}$. Differently from the standard theory,

we cannot find an explicit expression for the eigenvalues, but they are the zeroes of a given function. A simplification that we have done is to consider $\nu_{_D} = 1$, or equivalently $D_{u1} = D_{u3}$ and $D_{v1} = D_{v3}$, which is also biologically reasonable. In this case, taken cosinusoidal eigenfunctions

$$z_{1_n}(x) = C_1 \cos(a_{_n} x) \quad \text{and} \quad z_{3_n}(x) = \cos(b_{_n}(x - L)),$$

with

$$a_{_n}^2 = b_{_n}^2,$$

the eigenvalues are the positive roots of the function

$$r : \quad \xi \quad \longmapsto \quad \sqrt{\xi} \ \tan\left(\frac{\sqrt{\xi}}{\sqrt{D_{v3}}}\frac{L}{2}\right) - 2\frac{k_v}{\sqrt{D_{v3}}},$$

as illustrate in Figure 1.9.

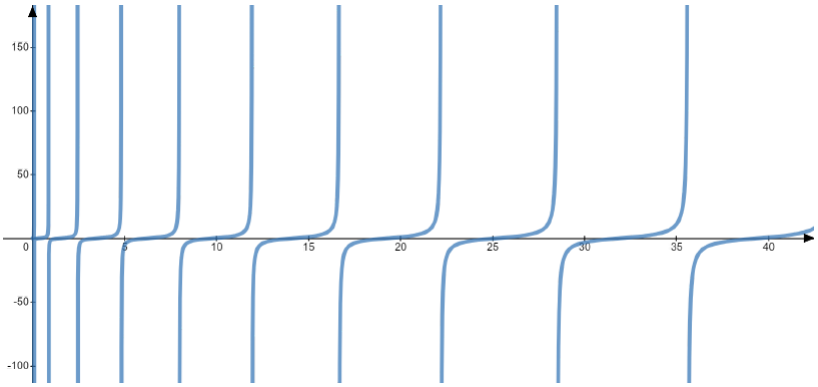

Figure 1.9: *We represent here the function $\xi \longmapsto r(\xi)$, considering $L = 1$, $\nu_{_D} = 1$, and $D_{v3} = D_{v1} = 10^{-2}$ and $k_v = 10^{-4}$. Its roots correspond to the eigenvalues $\eta_{_n}$.*

Numerical examples. We dedicate this last paragraph to some numerical examples. We use finite difference schemes with first-order discretisation of the boundary and membrane conditions in Matlab, see Appendix 4.B, as well as Morton and Mayers [92] and Quarteroni [112].

We choose a simple setting with mass conservation already analysed by Moussa *et al.* [93] in a Turing instabilities study, namely

$$f(u,v) = \varepsilon^{-1}(v - h(u)), \quad g(u,v) = -f(u,v), \quad \text{with } h(u) = u\,(u - 1)^2$$

and we notice the conditions

$$h \in C^2(\mathbb{R}^+, \mathbb{R}^+),\ h(0) = 0,\ h(u) > 0 \ \text{ for } u > 0 \ \text{ and } \ h'(u) = (1-u)(1-3u) > -1.$$

The small parameter ε measures the time scale of the reaction compared to diffusion, whether $\varepsilon = 1$ corresponds to a reaction-diffusion system. With this data, we can prove that we are in the good framework previously analysed to observe Turing instability.

Claim 1.4.1. *Considering the reaction terms just introduced, we claim that:*

1. *In the absence of diffusion, there is a unique stable equilibrium point $(\overline{u}, \overline{v})$ to which solutions converge monotonically.*

2. *The same steady state* $(\overline{u},\overline{v})$ *is asymptotically Turing unstable for the linearised reaction-diffusion system under the condition*

$$\theta+h'(\overline{u})<0.$$

Starting from initial data of the form

$$u_0(x)=\begin{cases}\frac{7}{15}+\frac{1}{5}\sin(4\pi x), & \text{for } 0\leqslant x\leqslant\frac{1}{2},\\ \frac{1}{5}+\frac{1}{5}\sin(4\pi x), & \text{for } \frac{1}{2}<x\leqslant 1\end{cases}\quad\text{and}\quad v_0(x)=\begin{cases}\frac{1}{3}-\frac{1}{5}\sin(4\pi x), & \text{for } 0\leqslant x\leqslant\frac{1}{2},\\ \frac{3}{5}-\frac{1}{5}\sin(4\pi x), & \text{for } \frac{1}{2}<x\leqslant 1,\end{cases}$$

we can calculate the steady state such that

$$\overline{u}=0.7545\in\left(\frac{1}{3},1\right),\quad \overline{v}=h(\overline{u})=0.0454\in\left(0,\frac{4}{27}\right)$$

and $h'(\overline{u})=\theta_c=-0.3101\in\left(-\frac{1}{3},0\right)$. We show time convergent solutions in the spatial interval [0,1]. To guarantee conditions (1.30), (1.31), we deduce that

$$D_{u1}=D_{u3}=\theta,\quad k_u=\theta\,k_v\quad\text{with } D_{v1}=D_{v3}=1\ \text{ and }\ \varepsilon=1, \tag{1.33}$$

where for $\theta<\theta_c=-0.3101$ there is a non-empty range of instability, see the previous claim and Figure 1.10.

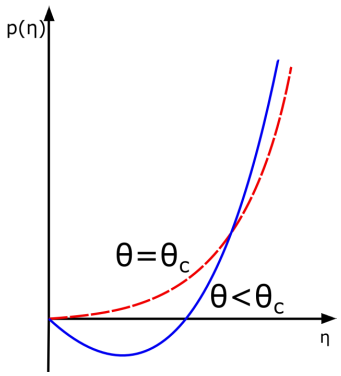

Figure 1.10: *Representation of the function* $p(\eta)=\theta\eta^2+\varepsilon^{-1}(\theta+h'(\overline{u})\eta)$ *in* (1.32) *determining the unstable modes. For* $\theta=\theta_c$ *(dashed line), there is a banal range of instability and consequent convergence to equilibrium of solutions, whereas for* $\theta<\theta_c$ *(solid line) we can find some eigenvalues generating instability.*

In the numerical examples (see Figure 1.1), we consider

- fixed permeability and decreasing values of $\theta<\theta_c$, observing, as in the standard Turing theory, an increase in Turing patterns,
- fixed values of θ and different values of the permeability k_v (remembering the relation $k_u=\theta k_v$), observing (in the non-banal case $k_v\in(0,+\infty)$) that patterns are present but they are non-smooth and they could be nearly constant functions with a discontinuity at the membrane.

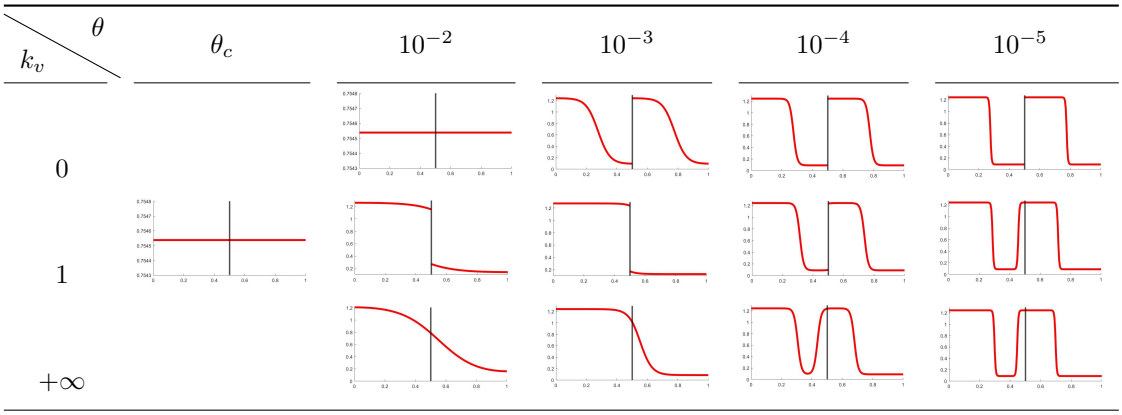

Table 1.1: *We summarise the evolution of patterns varying θ and k_v. The first column corresponds to the value $\boldsymbol{\theta = \theta_c}$, in which case there are no unstable modes. Then, for all k_v, convergence to the steady state is observed. The first and last row ($k_v = 0, +\infty$) corresponds to the case of reaction-diffusion systems respectively on a half domain and on the entire domain. This is evident looking back at the transformation of Kedem-Katchalsky conditions in this extreme cases. For $k_v = 1$, we observe both an increase of patterns decreasing θ and non-smooth patterns with a jump at the membrane.*

Finally, we illustrate also some simulations decreasing the parameter ε, previously fixed at $\varepsilon = 1$. In fact, in the limit $\varepsilon \to 0$, we are in the case of a fast reaction-diffusion system, see Section 1.2, and Turing instability turns out to be equivalent to the instability due to the ill-posedness for the limiting cross-diffusion equations, caused by backward parabolicity, Moussa *et al.* [93], Perthame and Skrzeczkowski [105]. For fixed $k_v = 1$, $\theta = 10^{-4}$ and varying ε, we obtain the following pictures.

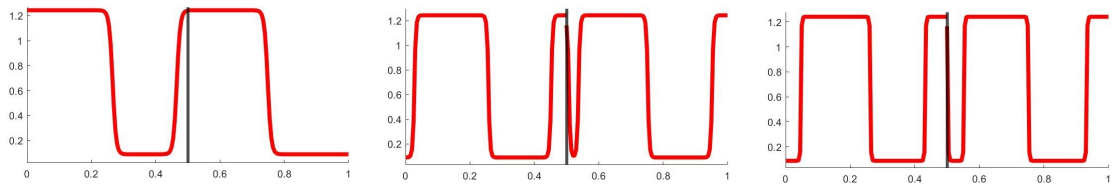

Figure 1.11: *This figure should be read from left to right.* $\boldsymbol{\varepsilon = 1/5}$. *Slops increase respect to the corresponding case $\varepsilon = 1$ in Table 1.1. The jump at the membrane is less significant since membrane derivatives are really small with the data chosen.* $\boldsymbol{\varepsilon = 1/20}$. *Oscillations are increasing respect to $\varepsilon = 1/5$, since numerically we are approaching zero.* $\boldsymbol{\varepsilon = 1/100}$. *Instabilities are dominant.*

1.4.4 Membrane degradation: modeling and simulations

We conclude this thesis with Chapter 5, which contains the mathematical results of an ongoing work with a team of biologists working in the Laboratoire de Biologie et Thérapeutique des Cancers of INSERM at the Saint Antoine Hospital in Paris. The collaboration started with the aim of studying cells invasive behaviour. For such experiments, biologists use the XCELLigence technology, Ke *et al.* [71], Martinez-Serra *et al.* [89], Obr *et al.* [98], Turker *et al.* [124], Zaoui *et*

al. [132]: two chambers separated by a porous membrane coated with an ECM-like layer. On the lower side of the membrane gold electrodes measure the *cell index*, proportional to the number of invasive cells, initially in the upper chamber. Thus, a model describing this setting contains three different equations: an advection-reaction-diffusion equation for the density of cells, which follows the evolution of cells diffusing in the upper chamber, possibly replicating and at the same time a directed movement towards the membrane is allowed; a reaction-diffusion equation for MMPs enzymes, produced by cells to degrade the ECM-like layer; a degradation equation for the layer, depending on the concentration of MMPs. If homogeneous Neumann boundary conditions characterise the absence of flow outside the chambers, Kedem-Katchalsky conditions at the inner membrane both for cells and enzymes regulate their flow to the lower chamber. Moreover, the permeability of the membrane depends on the damage and it evolves then in time.

As underlined before, experimental data focuse on the number of invasive cells. In fact, it is not possible to extrapolate information on degradation. We do not expect to have data on the enzymes, because it is not easy at this scale but, since they are the ones eating the membrane, degradation give us a cue on them too. This is why Chapter 5 focuses on modeling and numerical results of membrane degradation.

Experimental data. Another experimental device is designed to measure the capacity of cells to degrade the membrane: the QCM™ Gelatin Invadopodia Assay, composed by a well coated with fluorescent gelatin (simulating the ECM). We still do not have experimental data but we provide an example of them in Figure 1.12. This is the reason why Chapter 5 is at the moment constructed on mathematical results, looking forward to apply them to experiments.

Mathematical model. The model that we have built to describe the experimental pictures is set up on a rectangular domain $\Omega = [a, b] \times [c, d]$. We describe the evolution inside Ω of cell density $u(t, x)$, enzymes concentration $m(t, x)$ and damage at the gelatin $d(t, x) \in [0, 1]$, related to the amount of gelatin $q(t, x) = 1 - d(t, x) \in [0, 1]$, such as

$$\begin{cases} \partial_t u = div(D(d)\nabla u) + \alpha_1 u \left(1 - \frac{u}{\alpha_3}\right), & \text{in } \Omega, \\ \partial_t m = D_m \Delta m + \beta(1-d)u - \alpha m, & \text{in } \Omega, \\ \partial_t d = \gamma m(1-d), & \text{in } \Omega, \end{cases}$$

where

$$D(d) = D_L d + D_G(1-d) = D_G + (D_L - D_G)d.$$

Both u and m satisfy no-flux boundary conditions on $\partial\Omega$.

Cells are diffusing on the gelatin with coefficient $D_G > 0$ and in the liquid with coefficient $D_L > 0$. We remark that when the gelatin is intact ($d = 0$, then $q = 1$), cells move randomly on the gelatin, whereas when it is completely destroyed ($d = 1$, then $q = 0$), cells diffuse into the liquid. Finally, cells are proliferating, following a logistic growth. Equations for MMPs and damage are the same as for the invasion experiment. In particular, we consider that the production of enzymes starts when cells sense the gelatin $q = 1 - d$ and at this point degradation begins too.

Rescaling time and space, we also propose a nondimensional form in which we reduce the number of parameters to 5. System writes as

$$\begin{cases} \partial_t u = div((\theta + d)\nabla u) + k_2 u \left(1 - \frac{u}{\alpha_3}\right), & \text{in } \Omega, \\ \partial_t m = \Delta m + k_1(1 - pd)u - m, & \text{in } \Omega, \\ \partial_t d = \frac{1}{p} m(1 - pd), & \text{in } \Omega. \end{cases} \tag{1.34}$$

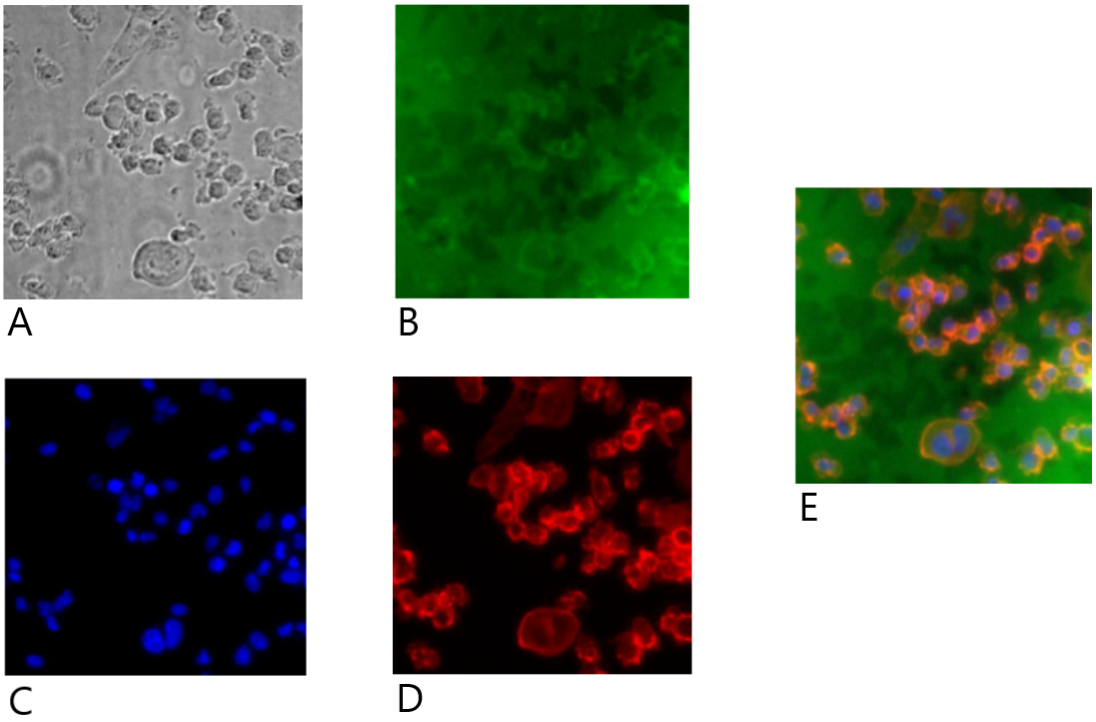

Figure 1.12: *Example of experimental data after 48h realised by N. Ferrand.* ***A.*** *Contrast phase image which represents cells.* ***B.*** *Image of the left gelatin (in green), whereas black areas are spots without gelatin.* ***C.*** *DAPI image representing cells nuclei in blue.* ***D.*** *Representation of actin cytosckeleton in red which delineates cells contouring.* ***E.*** *Overlap of images B,C,D that relates cells position and gelatin degradation. From this picture, we appreciate gelatin degradation which is quite high.*

Numerical results. Starting with a random initial data for u and a zero one both for m and d, we have selected values of parameters in System 1.34 from the literature, see Di Costanzo *et al.* [38], Braun [12] and Franssen *et al.* [49]. The type of simulations that we can show are as in Figure 1.13.

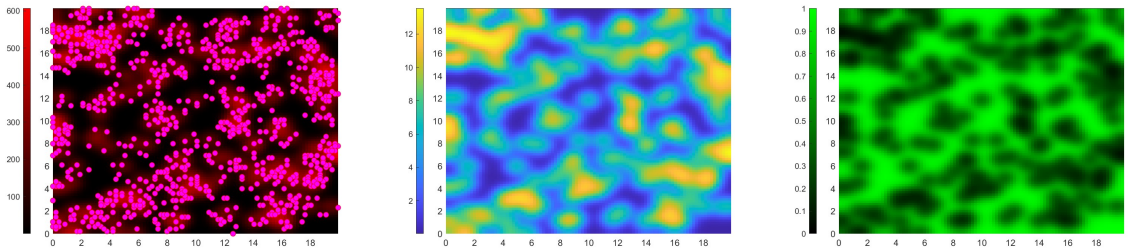

Figure 1.13: *Numerical solutions u, m and d of System (1.34). On the left, a representation of cells density u in a black-red scale overlapped with a more realistic representation of cells as particles (see Appendix 5.A). In the centre, a picture of enzymes concentration m and on the right gelatin q in green with black spots corresponding to the areas without gelatin. We can remark a correspondence between these spots, enzymes concentration and cells positions, validating the hypothesis that cells locally produce the enzymes, thus degrading below them and after they move.*

Sensitivity, parameter estimations and logistic fitting. An *a priori* study on the model offers valuable details on its behaviour, facilitating the comparison with future experimental results.

Trivially, changing the parameters value, we modify also solutions. However, it is relevant to know how much solutions of our Model (1.34) vary, modifying the parameters. We say that the model has a low sensitivity, if small variations on parameters do not heavily affect solutions, otherwise the model results sensitive to changes. Thus, we perform a *sensitivity analysis*, showing that we are dealing with a low sensitivity model, see Table 5.1.

At the same time, parameters are mathematical quantities. Actually, experimental data consists of pictures of cells and gelatin as in Figure 1.12. Consequently a parameter estimation technique is helpful to recover their values from biological pictures. This is achievable introducing an inverse problem in the form of a minimisation problem: given the final solutions (experimental data), it recovers the appropriate parameters that successfully describe the dynamics. We show the method in the case of artificial data, waiting to test it with biological ones.

Finally, the previous tools were tested on the model without cell proliferation. Indeed, working with a logistic growth we can estimate parameters with the logistic fitting introduced by Pearl and Reed [102]. We present their expression at the end of Subsection 5.6.3.

1.5 Discussion and perspectives

We present reaction-diffusion models with Kedem-Katchalsky conditions with the purpose of characterising cancer invasive process.

At first in Chapter 2, we derive appropriate membrane conditions in the limiting case in which the thickness of the membrane is converging to zero, since biological membranes are smaller than the adjacent tissues. A porous-medium type equation was considered in order to prove rigorously a previous result by Chaplain *et al.* [24]. More extensive studies should extend the proof to more realistic biological aspects, such as a more general description using filtration

equations, the inclusion of a multi-specie problem (a formal derivation is provided by Giverso *et al.* [57]), or considering non-constant permeability, possibly depending on other species such as MMP enzymes.

Concerning the study of a linear reaction-diffusion membrane problem, it is possible to take different desired directions. In Chapter 3, we considered an L^1-setting for our multi-species problem. We treat the case in which the permeability is constant and common to all the species. This translates into having for example different populations with the same characteristics in size such as taking all cells or all molecules of the same size. An alternative proof has to be written. In particular, it is useful to consider a more realistic setting in which membrane permeability depends on time and space variables. A very challenging question about existence includes also the addition of a transport or chemotactic term to describe a directed movements of cells towards the membrane.

We provide also only an introduction to Turing instability in Chapter 4. It would be interesting to deepen the numerous questions in the standard theory, trying to explain applications in the real world, such as in Murray [95] or in Perthame [106]. Moreover, a two-dimensional case can be faced and compared to the standard theory.

These are all open directions leading to a varied spectrum of mathematical tools. However, right now, the main perspective of our work is to complete the application path started in Chapter 5. As previously stressed, we supply the mathematical tools to soon handle biological data. A more analytical study can be also included to look at both existence of solutions and modeling improvements. Moreover, the main idea was to introduce the degradation model to have more information on the invasion problem. Then, always collaborating with biologists, we could examine invasion results using the XCELLigence technology. A similar mathematical and numerical study, as the one proposed for degradation, can be carried on for an invasion model with Kedem-Katchalsky conditions.

In conclusion, in this thesis we aim to illustrate a complete mathematical and biological model characterising tumor invasion. We are still engaged in this project and we have stressed the main points on which we have to work. Moreover, we have just given an idea of possible direct extensions of our study, but of course it is also very interesting to modify the models including more and more details on cells and their microenvironment behaviour. To give some examples, cells are not only able to degrade the basal membrane, but also to reconstruct it producing ECM, Connolly and Maxwell [34], Ghersi *et al.* [55], then we could add also a production term for the gelatin equation. Concerning the surrounding microenvironment, tumor cells do not act alone, but they have helpers which induce cells migration, such as microtubules (protein filaments inside cells), Denicolai *et al.* [37], or that influence hypoxic and acidic regions promoting tumor evolution and invasion, such as oxygen, glucose and lactate, Fiandaca *et al.* [48], Gatenby and Gawlinski [54], or which interact with transformed epithelial cells affecting tumor growth and metastasis, such as fibroblasts, Kim and Friedman [74], or which induce tumorigenic expansion, such as immune cells, Eikenberry *et al.* [44].

Part I

Rigorous derivation of Kedem-Katchalsky conditions for a porous medium type problem

We extend the work on elliptic and parabolic equations by Sanchez-Palencia [118] to derive Kedem-Katchalsky conditions also for a porous-medium type equation. This extension answers to the open question in the paper of Chaplain *et al.* [24], who started wandering what kind of conditions we can get in the limit of the thickness of a biological membrane going to zero. As underlined in the Introduction 1.4.1, biological membranes as the basal membrane are small compared to the size of adjacent tissues and biologically it is relevant to consider this kind of limit. Then, Chaplain *et al.* derive formally Kedem-Katchalsky conditions in a nonlinear generalised version. In fact, they close a nonlinear system composed by a general filtration equation. In the following Chapter 2, we prove rigorously this result in the specific case of a porous medium type equation which enables to have a power-law formulation of the pressure, fundamental in our method to get the desired *a priori* bounds on the main quantities. Moreover, mathematically the porous medium type equation represents the first most common non-linear and degenerate diffusion equation, characteristics that make it very challenging to analyse.

As previously stressed, despite the difficulties of the PME respect to a linear parabolic equation, we were able to follow the main steps provided by Sanchez-Palencia. This is why we do not provide his proof here. In his work, he studies conductivity problems that appear in mathematical physics such as thermal, electric or magnetic ones. In the electrostatic case, we can consider for example two materials at the interface of which the electric potential u satisfies continuity transmission conditions of the form (using mostly our notation)

$$u_1 = u_3,$$

$$\sigma_1 \nabla u_1 \cdot \boldsymbol{n} = \sigma_3 \nabla u_3 \cdot \boldsymbol{n},$$

where $u = u_1$ in the first material, $u = u_3$ in the second material, $\boldsymbol{n}$ is the normal vector at the interface and σ the dielectric constant. In particular, the second relation is the continuity of the normal component of the electric induction vector. In his paper, he considers the case in which the conductivity σ of an inner material, geometrically small, is small respect to the conductivity of the surrounding. He takes a bounded domain $\Omega \subset \mathbb{R}^3$, inside of which it is placed a lense-shaped domain I_ε which shrinks to a smooth surface in the limit. Conductivity inside I_ε depends on the parameter ε too. The aim of the work is to let ε and σ to zero to observe the limiting behaviour of the elliptic problem

$$\begin{cases} \Delta u = 0, & \text{in } \Omega \setminus I_\varepsilon \text{ and } I_\varepsilon, \\ u = g, & \text{in } \partial\Omega \\ u_{|_{I_\varepsilon}} = u_{|_{\Omega \setminus I_\varepsilon}}, & \text{in } \partial I_\varepsilon \\ \sigma \partial_n u_{|_{I_\varepsilon}} = \partial_n u_{|_{\Omega \setminus I_\varepsilon}}, & \text{in } \partial I_\varepsilon. \end{cases}$$

This work is based on an H^1-*a priori* estimate on the main quantity u and under the hypothesis

$$\lambda = \lim_{\varepsilon \to 0} \frac{\sigma(\varepsilon)}{\varepsilon} > 0,$$

it is proved that limit solutions satisfy appropriate Kedem-Katchalsky conditions at the interface. The same study is briefly performed in the parabolic case remarking again this convergence.

Chapter 2

Effective interface conditions for a porous medium type problem

This chapter is taken from Ciavolella G., David N., Poulain A. *Effective interface conditions for a porous medium type problem*, *submitted*, (2021) https://arxiv.org/abs/2105.02063.

2.1 Introduction

We consider a model of cell movement through a membrane where the population density $u = u(t, x)$ is driven by porous medium dynamics. We assume the domain to be an open and bounded set $\Omega \subset \mathbb{R}^3$. This domain Ω is divided into three open subdomains, $\Omega_{i,\varepsilon}$ for $i = 1, 2, 3$, where $\varepsilon > 0$ is the thickness of the intermediate membrane, $\Omega_{2,\varepsilon}$, see Figure 2.1. In the three domains, cells are moving with different constant mobilities, $\mu_{i,\varepsilon}$, for $i = 1, 2, 3$, and they are allowed to cross the adjacent boundaries of these domains which are $\Gamma_{1,2,\varepsilon}$ (between $\Omega_{1,\varepsilon}$ and $\Omega_{2,\varepsilon}$) and $\Gamma_{2,3,\varepsilon}$ (between $\Omega_{2,\varepsilon}$ and $\Omega_{3,\varepsilon}$). Then, we write $\Omega = \Omega_{1,\varepsilon} \cup \Omega_{2,\varepsilon} \cup \Omega_{3,\varepsilon}$, with $\Gamma_{1,2,\varepsilon} = \partial\Omega_{1,\varepsilon} \cap \partial\Omega_{2,\varepsilon}$, and $\Gamma_{2,3,\varepsilon} = \partial\Omega_{2,\varepsilon} \cap \partial\Omega_{3,\varepsilon}$. The system reads as

$$\begin{cases} \partial_t u_{i,\varepsilon} - \mu_{i,\varepsilon} \nabla \cdot (u_{i,\varepsilon} \nabla p_{i,\varepsilon}) = u_{i,\varepsilon} G(p_{i,\varepsilon}), & \text{in } (0,T) \times \Omega_{i,\varepsilon}, \quad i = 1,2,3, \\ \mu_{i,\varepsilon} u_{i,\varepsilon} \nabla p_{i,\varepsilon} \cdot \boldsymbol{n}_{i,i+1} = \mu_{i+1,\varepsilon} u_{i+1,\varepsilon} \nabla p_{i+1,\varepsilon} \cdot \boldsymbol{n}_{i,i+1}, & \text{on } (0,T) \times \Gamma_{i,i+1,\varepsilon}, \quad i = 1,2, \\ u_{i,\varepsilon} = u_{i+1,\varepsilon}, & \text{on } (0,T) \times \Gamma_{i,i+1,\varepsilon}, \quad i = 1,2, \\ u_{i,\varepsilon} = 0, & \text{on } (0,T) \times \partial\Omega. \end{cases} \tag{2.1}$$

We denote by $p_{i,\varepsilon}$ the density-dependent pressure, which is given by the following power law

$$p_{i,\varepsilon} = u_{i,\varepsilon}^{\gamma}, \quad \text{with } \gamma > 1.$$

In this chapter, we are interested in studying the convergence of System (2.1) as $\varepsilon \to 0$. When the thickness of the thin layer decreases to zero, the membrane collapses to a limiting interface, $\tilde{\Gamma}_{1,3}$, which separates two domains denoted by $\tilde{\Omega}_1$ and $\tilde{\Omega}_3$, see Figure 2.1. Then, the domain turns out to be $\Omega = \tilde{\Omega}_1 \cup \tilde{\Gamma}_{1,3} \cup \tilde{\Omega}_3$. We derive in a rigorous way the *effective problem* (2.2), and in particular, the transmission conditions on the limit density, $\tilde{u}$, across the effective interface.

Assuming that the mobility coefficients satisfy $\mu_{i,\varepsilon} > 0$ for $i = 1, 3$ and

$$\lim_{\varepsilon\to 0} \mu_{1,\varepsilon} = \tilde{\mu}_1 \in (0, +\infty), \qquad \lim_{\varepsilon\to 0} \frac{\mu_{2,\varepsilon}}{\varepsilon} = \tilde{\mu}_{1,3} \in (0, +\infty), \qquad \lim_{\varepsilon\to 0} \mu_{3,\varepsilon} = \tilde{\mu}_3 \in (0, +\infty),$$

we prove that, in a weak sense, solutions of Problem (2.1) converge to solutions of the following system

$$\begin{cases} \partial_t \tilde{u}_i - \tilde{\mu}_i \nabla \cdot (\tilde{u}_i \nabla \tilde{p}_i) = \tilde{u}_i G(\tilde{p}_i), & \text{in } (0,T) \times \tilde{\Omega}_i, \quad i = 1, 3, \\ \tilde{\mu}_{1,3} [\![\Pi]\!] = \tilde{\mu}_1 \tilde{u}_1 \nabla \tilde{p}_1 \cdot \tilde{\boldsymbol{n}}_{1,3} = \tilde{\mu}_3 \tilde{u}_3 \nabla \tilde{p}_3 \cdot \tilde{\boldsymbol{n}}_{1,3}, & \text{on } (0,T) \times \tilde{\Gamma}_{1,3}, \\ \tilde{u} = 0, & \text{on } (0,T) \times \partial\Omega, \end{cases} \tag{2.2}$$

where Π satisfies $\Pi'(u) = up'(u)$, namely

$$\Pi(u) := \frac{\gamma}{\gamma+1} u^{\gamma+1}.$$

We use the symbol $[\![\,\cdot\,]\!]$ to denote the jump across the interface $\tilde{\Gamma}_{1,3}$, *i.e.*

$$[\![\Pi]\!] := \frac{\gamma}{\gamma+1} (\tilde{u}^{\gamma+1})_3 - \frac{\gamma}{\gamma+1} (\tilde{u}^{\gamma+1})_1, \tag{2.3}$$

where the subscript indicates that $(\cdot)$ is evaluated as the limit to a point of the interface coming from the subdomain $\tilde{\Omega}_1$, $\tilde{\Omega}_3$, respectively.

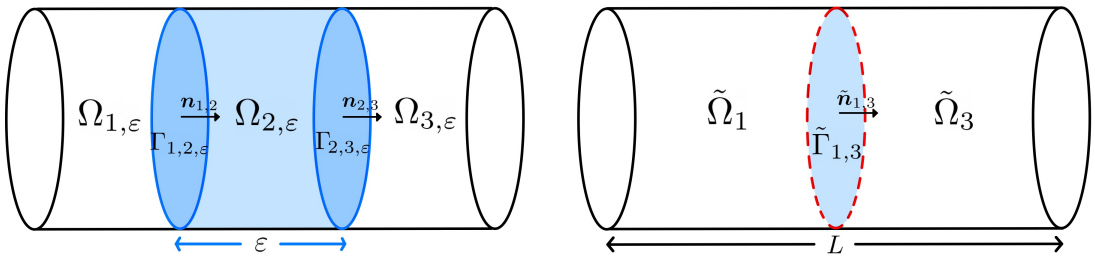

Figure 2.1: *We represent here the bounded cylindrical domain Ω of length L. On the left, we can see the subdomains $\Omega_{i,\varepsilon}$ with related outward normals. The membrane $\Omega_{2,\varepsilon}$ of thickness $\varepsilon > 0$ is delimited by $\Gamma_{i,i+1,\varepsilon} = \{x_3 = \pm\varepsilon/2\} \cap \Omega$ which are symmetric with respect to the effective interface, $\tilde{\Gamma}_{1,3} = \{x_3 = 0\} \cap \Omega$. On the right, we represent the limit domain as $\varepsilon \to 0$. The effective interface, $\tilde{\Gamma}_{1,3}$, separates the two limit domains, $\tilde{\Omega}_1, \tilde{\Omega}_3$.*

Motivations and previous works. Nowadays, a huge literature can be found on the mathematical modeling of tumour growth, see for instance Lowengrub *et al.* [86], Perthame [103], Preziosi and Tosin [109], Roose *et al.* [116], on a domain $\Omega \subseteq \mathbb{R}^d$ (with $d = 2, 3$ for *in vitro* experiments, $d = 3$ for *in vivo* tumours). Studying tumour's evolution, a crucial and challenging scenario is represented by cancer cells invasion through thin membranes. As stressed in the biological Introduction 1.1, one of the most difficult barriers for the cells to cross is the *basement membrane*, which separates the epithelial tissue from the connective one (mainly composed by ECM), providing a barrier that isolates malignant cells from the surrounding environment. At

the early stage, cancer cells proliferate locally in the epithelial tissue originating a carcinoma *in situ*. Unfortunately, cancer cells could mutate and acquire the ability to migrate by producing *matrix metalloproteinases* (MMPs), specific enzymes which degrade the basement membrane, allowing cancer cells to penetrate into it, invading the adjacent tissue. A specific study can be done on the relation between MMP and their inhibitors as in Ribba *et al.* [115]. Instead, we are interested in modeling cancer transition from *in situ* stage to the invasive phase. This transition is described both by System (2.1) and (2.2). In fact, for the both of them, the left domain can be interpreted as the domain in which the primary tumor lives, whereas the right one is the ECM. Between them, the basal membrane is penetrated by cancer cells either with a constant mobility (in the case of a thick membrane) or with particular membrane conditions, in the case of a zero-thickness interface (better analysed in the following).

Since in biological systems the membrane is often much smaller than the size of the other components, it is then convenient and reasonable to approximate the membrane as a zero-thickness one, as done in Chaplain *et al.* [24], Gallinato *et al.* [53], differently from Ribba *et al.* [115]. In particular, it is possible to mathematically describe cancer invasion through a zero thickness interface considering a limiting problem defined on two domains. The system is then closed by conditions on the effective interface which generalise the classical Kedem-Katchalsky ones, introduced in Section 1.3. In our description, they define continuity of cells density flux through the effective interface $\tilde{\Gamma}_{1,3}$ and their proportionality to the jump of a term linked to cells pressure. The coefficient of proportionality is related to the permeability of the effective interface with respect to a specific population.

For these reasons, studying the convergence as the thickness of the membrane tends to zero represents a relevant and interesting problem both from a biological and mathematical point of view. In the literature, this limit has been studied in different fields of applications other than tumour invasion, such as, for instance, thermal, electric or magnetic conductivity, Li *et al.* [81], Sanchez-Palencia [118], or transport of drugs and ions through an heterogeneous layer, Neuss-Radu and Jäger [96]. Physical, cellular and ecological applications characterised the bulk-surface model and the dynamical boundary value problem, derived in Li *et al.* [82] in the context of boundary adsorption-desorption of diffusive substances between a bulk (body) and a surface. Another class of limiting systems is offered by Li and Wang [80], in the case in which the diffusion in the thin membrane is not as small as its thickness. Again, this has a very large application field, from thermal barrier coatings (TBCs) for turbine engine blades to the spreading of animal species, from commercial pathways accelerating epidemics to cell membrane.

As it is now well-established, see for instance Byrne and Drasdo [19], living tissues behave like compressible fluids. Therefore, in the last decades, mathematical models have been more and more focusing on the fluid mechanical aspects of tissue and tumour development, see for instance Bresch *et al.* [14], Byrne and Chaplain [18], Byrne and Drasdo [19], Chaplain *et al.* [24], Greenspan [58], Perthame [103]. Tissue cells move through a porous embedding, such as the extra-cellular matrix (ECM). This nonlinear and degenerate diffusion process is well captured by filtration-type equations like the following, rather than the classical heat equation,

$$\partial_t u + \nabla \cdot (u\mathbf{v}) = F(u), \qquad \text{for } t > 0,\ x \in \Omega. \tag{2.4}$$

Here $F(u)$ represents a generic density-dependent reaction term and the model is closed with the velocity field equation

$$\mathbf{v} := -\mu \nabla p, \tag{2.5}$$

and a density-dependent law of state for the pressure $p := f(u)$. The function $\mu = \mu(t, x) \geq 0$ represents the cell mobility coefficient and the velocity field equation corresponds to the Darcy law of fluid mechanics. This relation between the velocity of the cells and the pressure gradient

reflects the tendency of the cells to move away from regions of high compression.

Our model is based on the one by Chaplain *et al.* [24], where the authors formally recover the *effective interface problem*, analogous to System (2.2), as the limit of a transmission problem, (or *thin layer problem*) *cf.* System (2.1), when the thickness of the membrane converges to zero. They also validate through simulations the numerical equivalence between the two models. When shrinking the membrane $\Omega_{2,\varepsilon}$ to an infinitesimal region, $\tilde{\Gamma}_{1,3}$, (*i.e.* when passing to the limit $\varepsilon \to 0$, where ε is proportional to the thickness of the membrane), it is important to guarantee that the effect of the thin membrane on cell invasion remains preserved. To this end, it is essential to make the following assumption on the mobility coefficient in the subdomain $\Omega_{2,\varepsilon}$,

$$\mu_{2,\varepsilon} \xrightarrow{\varepsilon\to 0} 0 \qquad \text{such that} \qquad \frac{\mu_{2,\varepsilon}}{\varepsilon} \xrightarrow{\varepsilon\to 0} \tilde{\mu}_{1,3}.$$

This condition implies that, when shrinking the pores of the membrane, the local permeability of the layer decreases to zero proportionally with respect to the local shrinkage. The function $\tilde{\mu}_{1,3}$ represents the *effective permeability coefficient* of the limiting interface $\tilde{\Gamma}_{1,3}$, *i.e.* the permeability of the zero-thickness membrane. We refer the reader to Chaplain *et al.* [24, Remark 2.4] for the derivation of the analogous assumption in the case of a fluid flowing through a porous medium. In Chaplain *et al.* [24], the authors derive the effective transmission conditions on the limiting interface, $\tilde{\Gamma}_{1,3}$, which relates the jump of the quantity $\Pi := \Pi(u)$, defined by $\Pi'(u) = uf'(u)$ and the normal flux across the interface, namely[1]

$$\tilde{\mu}_{1,3}[\![\Pi]\!] = \tilde{\mu}_i \tilde{u}_i \nabla f(\tilde{u}_i) \cdot \tilde{\boldsymbol{n}}_{1,3} = \tilde{\mu}_i \nabla \Pi(\tilde{u}_i) \cdot \tilde{\boldsymbol{n}}_{1,3}, \qquad \text{for } i = 1, 3 \qquad \text{on } \tilde{\Gamma}_{1,3}.$$

These conditions turns out to be the well-known Kedem-Katchalsky interface conditions when $f(u) := \ln(u)$, for which $\Pi(u) = u + C$, $C \in \mathbb{R}$, *i.e.* the linear diffusion case.

In this chapter, we provide a rigorous proof to the derivation of these limiting transmission conditions, for a particular choice of the pressure law. To the best of our knowledge, this question has not been addressed before in the literature for a non-linear and degenerate model such as System (2.1). Although our system falls into the class of models formulated by Chaplain *et al.*, we consider a less general case, making some choices on the quantities of interest. First of all, for the sake of simplicity, we assume the mobility coefficients $\mu_{i,\varepsilon}$ to be positive constants, hence they do not depend on time and space as in Chaplain *et al.* [24]. We take a reaction term of the form $uG(p)$, where G is a pressure-penalized growth rate. Moreover, we take a power-law as pressure law of state, *i.e.* $p = u^\gamma$, with $\gamma \geq 1$. Hence, our model turns out to be in fact a porous medium type model, since Equations (2.4, 2.5) read as follows

$$\partial_t u - \frac{\gamma}{\gamma + 1} \Delta u^{\gamma+1} = uG(p), \qquad \text{for } t > 0,\ x \in \Omega.$$

We recall that the nonlinearity and the degeneracy of the porous medium equation (PME) bring several additional difficulties to its analysis compared to its linear and non-degenerate counterpart, see Section 1.2. In particular, the main challenge is represented by the emergence of a free boundary, which separates the region where $u > 0$ from the region of vacuum. On this interface the equation degenerates, affecting the control and the regularity of the main quantities. For example, it is well-known that the density can develop jumps singularities, therefore preventing any control of the gradient in L^2, opposite to the case of linear diffusion. On the other hand, using the fundamental change of variables of the PME, $p = u^\gamma$, and studying the equation on the pressure rather than the equation on the density, turns out to be very useful

[1] This equation is reported in Chaplain *et al.* [24, Proposition 3.1], where we adapted the notation to that of our chapter.

when searching for better regularity of the gradient. Nevertheless, since the pressure presents 'corners' at the free boundary, it is not possible to bound its laplacian in L^2 (uniformly on the entire domain).

For these reasons, we could not straightforwardly apply some of the methods previously used in the literature in the case of linear diffusion. For instance, the result in Brezis *et al.* [16] is based on proving H^2-*a priori* bounds, which do not hold in our case. The authors consider elliptic equations in a domain divided into three subdomains, each one contained into the interior of the other. The coefficients of the second-order terms are assumed to be piecewise continuous with jumps along the interior interfaces. Then, the authors study the limit as the thickness of the interior reinforcement tends to zero. In Sanchez-Palencia [118], the author studies the same problem in the particular case of a lense-shaped region, I_ε, which shrinks to a smooth surface in the limit, facing also the parabolic case. The approach is based on H^1-*a priori* estimates, namely the L^2-boundedness of the gradient of the unknown. Considering the variational formulation of the problem, the author is able to pass to the limit upon applying an extension operator. In fact, if the mobility coefficient in I_ε converges to zero proportionally with respect to ε, it is only possible to establish uniform bounds outside of I_ε. The extension operator allows to 'truncate' the solution and then 'extend' it into I_ε reflecting its profile from outside. Therefore, making use of the uniform control outside of the ε-thickness layer, the author is able to pass to the limit in the variational formulation. Let us also mention that, in the literature, one can find different methods and strategies for reaction-diffusion problems with a thin layer. For instance, Marušić and Marušić-Paloka [90] introduce the notion of two-scale convergence for thin domains which allows the rigorous derivation of lower dimensional models. Some other papers have deepened the case of heterogeneous membrane. We cite Neuss-Radu and Jäger [96], where the authors develop a multiscale method which combines classical compactness results based on *a priori estimates* and weak-strong two-scale convergence results in order to be able to pass to the limit in a thin heterogeneous membrane. In Gahn [51], a transmission problem involving nonlinear diffusion in the thin layer is treated and an effective model was derived. Finally, in Gahn *et al.* [52], the accuracy of the effective approximations for processes through thin layers is studied by proving estimates for the difference between the original and the effective quantities.

The passage at the limit allows to infer the existence of weak solutions for the effective Problem (2.2), thanks to the existence result for the $\varepsilon-$problem provided in Appendix 2.A. In the case of linear diffusion, the existence of global weak solutions for the effective problem with the Kedem-Katchalsky conditions is provided by Chapter 3, taken from Ciavolella and Perthame [31]. In particular, the proof is under weak hypothesis such as L^1 initial data and reaction terms with sub-quadratic growth in an L^1-setting.

Outline of the chapter. The chapter is organised as follows. In Section 2.2, we introduce the assumptions and notations, including the definition of weak solution of the original problem, System (2.1). In Section 2.3, *a priori* estimates that will be useful to pass to the limit are proven.

Section 2.4 is devoted to prove the convergence of Problem (2.1), following the method introduced in Sanchez-Palencia [118] for the (non-degenerate) elliptic and parabolic cases. The argument relies on recovering the L^2-boundedness (uniform with respect to ε) of the velocity field, in our case, the pressure gradient. As one may expect, since the permeability of the membrane, $\mu_{2,\varepsilon}$, tends to zero proportionally with respect to ε, it is only possible to establish a uniform bound outside of $\Omega_{2,\varepsilon}$. For this reason, following Sanchez-Palencia [118], we introduce an extension operator (Subsection 2.4.1) and apply it to the pressure in order to extend the H^1-uniform bounds in the whole space $\Omega \setminus \tilde{\Gamma}_{1,3}$, hence proving compactness results. We remark that the main difference between the strategy in Sanchez-Palencia [118] and our adaptation, is given by the fact that due to the non-linearity of the equation, we have to infer strong compactness

of the pressure (and consequently of the density) in order to pass to the limit in the variational formulation. For this reason, we also need the L^1-boundedness of the time derivative, hence obtaining compactness with a standard Sobolev's embedding argument. Moreover, since solutions to the limit Problem (2.2) will present discontinuities at the effective interface, we need to build proper test functions which belong to $H^1(\Omega \setminus \tilde{\Gamma}_{1,3})$ that are zero on $\partial\Omega$ and are discontinuous across $\tilde{\Gamma}_{1,3}$ (Subsection 2.4.2).

Finally, using the compactness obtained thanks to the extension operator, we are able to prove the convergence of solutions to Problem (2.1) to couples $(\tilde{u}, \tilde{p})$ which satisfy Problem (2.2) in a weak sense, therefore inferring the existence of solutions of the effective problem, as stated in the following theorem.

Theorem 2.1.1 (Convergence to the effective problem)**.** *Solutions of Problem (2.1) converge weakly to solutions $(\tilde{u}, \tilde{p})$ of Problem (2.2) in the following weak form*

$$\begin{aligned} -\int_0^T \int_\Omega \tilde{u}\partial_t w + \tilde{\mu}_1 \int_0^T \int_{\tilde{\Omega}_1} \tilde{u}\nabla\tilde{p}\cdot\nabla w + \tilde{\mu}_3 \int_0^T \int_{\tilde{\Omega}_3} \tilde{u}\nabla\tilde{p}\cdot\nabla w \\ + \tilde{\mu}_{1,3} \int_0^T \int_{\tilde{\Gamma}_{1,3}} [\![\Pi]\!]\big(w_{|x_3=0^+} - w_{|x_3=0^-}\big) = \int_0^T \int_\Omega \tilde{u}G(\tilde{p})w + \int_\Omega \tilde{u}^0 w^0, \end{aligned} \tag{2.6}$$

for all test functions $w(t,x)$ with a proper regularity (defined in Theorem 2.4.1) and $w(T,x) = 0$ a.e. in Ω. We used the notation

$$[\![\Pi]\!] := \frac{\gamma}{\gamma+1}(\tilde{u}^{\gamma+1})_{|x_3=0^+} - \frac{\gamma}{\gamma+1}(\tilde{u}^{\gamma+1})_{|x_3=0^-},$$

and $(\cdot)_{|x_3=0^-} = \mathcal{T}_1(\cdot)$ as well as $(\cdot)_{|x_3=0^+} = \mathcal{T}_3(\cdot)$, with $\mathcal{T}_1, \mathcal{T}_3$ the trace operators defined in Section 2.2.

Section 2.5 concludes the chapter and provides some research perspectives.

2.2 Assumptions and notations

Here, we detail the problem setting and assumptions. For the sake of simplicity, we consider as domain $\Omega \subset \mathbb{R}^3$ a cylinder with axis x_3, see Figure 2.1. Let us notice that it is possible to take a more general domain $\hat{\Omega}$ defining a proper diffeomorfism $F : \hat{\Omega} \to \Omega$. Therefore, the results of this chapter extend to more general domains as long as the existence of the map F can be proved (this implies that $\hat{\Omega}$ is a connected open subset of $\mathbb{R}^d$ and has a smooth boundary). Therefore, we assume that the domain Ω has a C^1-piecewise boundary. We also want to emphasize the fact that our proofs hold in a 2D domain considering three rectangular subdomains. We introduce

$$u_\varepsilon := \begin{cases} u_{1,\varepsilon}, & \text{in } \Omega_{1,\varepsilon}, \\ u_{2,\varepsilon}, & \text{in } \Omega_{2,\varepsilon}, \\ u_{3,\varepsilon}, & \text{in } \Omega_{3,\varepsilon}, \end{cases} \qquad p_\varepsilon := \begin{cases} p_{1,\varepsilon}, & \text{in } \Omega_{1,\varepsilon}, \\ p_{2,\varepsilon}, & \text{in } \Omega_{2,\varepsilon}, \\ p_{3,\varepsilon}, & \text{in } \Omega_{3,\varepsilon}. \end{cases}$$

We define the interfaces between the domains $\Omega_{i,\varepsilon}$ and $\Omega_{i+1,\varepsilon}$ for $i = 1, 2$, as

$$\Gamma_{i,i+1,\varepsilon} = \partial\Omega_{i,\varepsilon} \cap \partial\Omega_{i+1,\varepsilon}.$$

We denote with $\boldsymbol{n}_{i,i+1}$ the outward normal to $\Gamma_{i,i+1,\varepsilon}$ with respect to $\Omega_{i,\varepsilon}$, for $i = 1, 2$. Let us notice that $\boldsymbol{n}_{i,i+1} = -\boldsymbol{n}_{i+1,i}$.

We define two trace operators

$$\begin{cases} \mathcal{T}_1 : W^{k,p}(\tilde{\Omega}_1) \longrightarrow L^p(\partial\tilde{\Omega}_1), \\ \mathcal{T}_3 : W^{k,p}(\tilde{\Omega}_3) \longrightarrow L^p(\partial\tilde{\Omega}_3), \end{cases} \qquad \text{for } 1 \leqslant p < +\infty, \quad k \geqslant 1.$$

Therefore, for any $z \in W^{k,p}(\Omega \setminus \tilde{\Gamma}_{1,3})$, we have the following decomposition

$$z := \begin{cases} z_1, & \text{in} \quad \tilde{\Omega}_1, \\ z_3, & \text{in} \quad \tilde{\Omega}_3. \end{cases}$$

Obviously, we have that $z_\alpha \in W^{k,p}(\tilde{\Omega}_\alpha)$ $(\alpha = 1, 3)$. Thus, we denote

$$z_{|_{\partial\tilde{\Omega}_\alpha}} := \mathcal{T}_\alpha z \in L^p(\partial\tilde{\Omega}_\alpha), \quad \alpha = 1, 3,$$

and the following continuity property holds, Brezis [15]

$$\|\mathcal{T}_\alpha z\|_{L^p(\partial\tilde{\Omega}_\alpha)} \leqslant C\|z\|_{W^{k,p}(\tilde{\Omega}_\alpha)}, \quad \alpha = 1, 3.$$

We assume $W^{k,p}(\Omega \setminus \tilde{\Gamma}_{1,3})$ is endowed with the norm

$$\|z\|_{W^{k,p}(\Omega\setminus\tilde{\Gamma}_{1,3})} = \|z\|_{L^p(\Omega\setminus\tilde{\Gamma}_{1,3})} + \sum_{j=1}^{k} \|D^j z\|_{L^p(\Omega\setminus\tilde{\Gamma}_{1,3})}.$$

We make the following assumptions on the initial data: there exists a positive constant p_H, such that

$$0 \leq p_\varepsilon^0 \leq p_H, \qquad 0 \leq u_\varepsilon^0 \leq p_H^{1/\gamma} =: u_H, \tag{A-data1}$$

$$\Delta\big((u_{i,\varepsilon}^0)^{\gamma+1}\big) \in L^1(\Omega_{i,\varepsilon}), \quad \text{for } i = 1, 2, 3. \tag{A-data2}$$

Moreover, we assume that there exists a function $\tilde{u}_0 \in L^1_+(\Omega)$ (*i.e.* $u_0 \in L^1(\Omega)$ and non-negative) such that

$$\|u_\varepsilon^0 - \tilde{u}_0\|_{L^1(\Omega)} \longrightarrow 0, \quad \text{as } \varepsilon \to 0. \tag{A-data3}$$

The growth rate $G(\cdot)$ satisfies

$$G(0) = G_M > 0, \quad G'(\cdot) < 0, \quad G(p_H) = 0. \tag{A-G}$$

The value p_H, called *homeostatic pressure*, represents the lowest level of pressure that prevents cell multiplication due to contact-inhibition.

We assume that the mobility coefficients satisfy $\mu_{i,\varepsilon} > 0$ for $i = 1, 3$ and

$$\lim_{\varepsilon\to 0} \mu_{1,\varepsilon} = \tilde{\mu}_1 > 0, \qquad \lim_{\varepsilon\to 0} \frac{\mu_{2,\varepsilon}}{\varepsilon} = \tilde{\mu}_{1,3} > 0, \qquad \lim_{\varepsilon\to 0} \mu_{3,\varepsilon} = \tilde{\mu}_3 > 0. \tag{2.7}$$

Notations. For all $T > 0$, we denote $\Omega_T := (0, T) \times \Omega$. We use the abbreviated form $u_\varepsilon := u_\varepsilon(t) := u_\varepsilon(t, x)$. From now on, we use C to indicate a generic positive constant independent of ε that may change from line to line. Moreover, we denote

$$\text{sign}_+(w) = \mathbb{1}_{\{w>0\}}, \qquad \text{sign}_-(w) = -\mathbb{1}_{\{w<0\}},$$

and

$$\operatorname{sign}(w) = \operatorname{sign}_+(w) + \operatorname{sign}_-(w).$$

We also define the positive and negative part of w as follows

$$(w)_+ := \begin{cases} w, & \text{for } w > 0, \\ 0, & \text{for } w \leqslant 0, \end{cases} \quad \text{and} \quad (w)_- := \begin{cases} -w, & \text{for } w < 0, \\ 0, & \text{for } w \geqslant 0. \end{cases}$$

We denote $|w| := (w)_+ + (w)_-$.

Now, let us write the variational formulation of Problem (2.1).

Definition 2.2.1 (Definition of weak solutions)**.** *Given $\varepsilon > 0$, a weak solution to Problem (2.1) is given by $u_\varepsilon, p_\varepsilon \in L^\infty(0,T;L^\infty(\Omega))$ such that $\nabla p_\varepsilon \in L^2(\Omega_T)$ and*

$$-\int_0^T \int_\Omega u_\varepsilon \partial_t \psi + \sum_{i=1}^{3} \mu_{i,\varepsilon} \int_0^T \int_{\Omega_{i,\varepsilon}} u_{i,\varepsilon} \nabla p_{i,\varepsilon} \cdot \nabla \psi = \int_0^T \int_\Omega u_\varepsilon G(p_\varepsilon)\psi + \int_\Omega u_\varepsilon^0 \psi(0,x), \tag{2.8}$$

for all test functions $\psi \in H^1(0,T;H_0^1(\Omega))$ such that $\psi(T,x) = 0$ a.e. in Ω.

2.3 A priori estimates

We show that the main quantities satisfy some uniform *a priori* estimates which will later allow us to prove strong compactness and pass to the limit.

Lemma 2.3.1 (A priori estimates)**.** *Given the assumptions in Section 2.2, let $(u_\varepsilon, p_\varepsilon)$ be a solution of Problem (2.1). There exists a positive constant C independent of ε such that*

(i) $0 \leq u_\varepsilon \leq u_H$ *and* $0 \leq p_\varepsilon \leq p_H$,

(ii) $\|\partial_t u_\varepsilon\|_{L^\infty(0,T;L^1(\Omega))} \leqslant C$, $\|\partial_t p_\varepsilon\|_{L^\infty(0,T;L^1(\Omega))} \leqslant C$,

(iii) $\|\nabla p_\varepsilon\|_{L^2(0,T;L^2(\Omega\setminus\Omega_{2,\varepsilon}))} \leqslant C$.

Remark 2.3.1. *We remark that statement (i) implies that for all $p \in [1,\infty]$, we have*

$$\|u_\varepsilon\|_{L^\infty(0,T;L^p(\Omega))} \leqslant C, \ \|p_\varepsilon\|_{L^\infty(0,T;L^p(\Omega))} \leqslant C.$$

Remark 2.3.2. *The following proof can be made rigorous by performing a parabolic regularization of the problem, namely by adding $\delta\Delta u_{i,\varepsilon}$, for $\delta > 0$, to the left-hand side of the equation and in the flux continuity conditions. In fact, the following estimates can be obtained uniformly both in ε and δ.*

Proof. Let us recall the equation satisfied by u_ε on $\Omega_{i,\varepsilon}$, namely

$$\partial_t u_{i,\varepsilon} - \mu_{i,\varepsilon} \nabla \cdot (u_{i,\varepsilon} \nabla u_{i,\varepsilon}^\gamma) = u_{i,\varepsilon} G(p_{i,\varepsilon}). \tag{2.9}$$

(i) $0 \leq u_\varepsilon \leq u_H$, $0 \leq p_\varepsilon \leq p_H$. The L^∞-bounds of the density and the pressure are a straight-forward consequence of the comparison principle applied to Equation (2.9), which can be rewritten as

$$\partial_t u_{i,\varepsilon} - \frac{\gamma}{\gamma+1} \mu_{i,\varepsilon} \Delta u_{i,\varepsilon}^{\gamma+1} = u_{i,\varepsilon} G(p_{i,\varepsilon}). \tag{2.10}$$

Indeed, summing up Equations (2.10) for $i = 1, 2, 3$, we obtain

$$\sum_{i=1}^{3} \partial_t u_{i,\varepsilon} - \frac{\gamma}{\gamma+1} \sum_{i=1}^{3} \mu_{i,\varepsilon} \Delta u_{i,\varepsilon}^{\gamma+1} = \sum_{i=1}^{3} u_{i,\varepsilon} G(p_{i,\varepsilon}). \tag{2.11}$$

Then, we also have

$$\sum_{i=1}^{3} \partial_t (u_H - u_{i,\varepsilon}) = \frac{\gamma}{\gamma+1} \sum_{i=1}^{3} \mu_{i,\varepsilon} \Delta (u_H^{\gamma+1} - u_{i,\varepsilon}^{\gamma+1}) + \sum_{i=1}^{3} (u_H - u_{i,\varepsilon}) G(p_{i,\varepsilon}) - u_H \sum_{i=1}^{3} G(p_{i,\varepsilon}).$$

Let us recall Kato's inequality, Kato [70], *i.e.*

$$\Delta(u)_- \geqslant \mathrm{sign}_-(u) \Delta u.$$

If we multiply by $\mathrm{sign}_-(u_H - u_{i,\varepsilon})$, thanks to Kato's inequality, we infer that

$$\begin{aligned} \sum_{i=1}^{3} \partial_t (u_H - u_{i,\varepsilon})_- &\leqslant \sum_{i=1}^{3} \left[\frac{\gamma}{\gamma+1} \mu_{i,\varepsilon} \Delta (u_H^{\gamma+1} - u_{i,\varepsilon}^{\gamma+1})_- + (u_H - u_{i,\varepsilon})_- G(p_{i,\varepsilon}) \right. \\ &\qquad \left. - u_H G(p_{i,\varepsilon}) \mathrm{sign}_-(u_H - u_{i,\varepsilon}) \right] \\ &\leqslant \sum_{i=1}^{3} \left[\frac{\gamma}{\gamma+1} \mu_{i,\varepsilon} \Delta (u_H^{\gamma+1} - u_{i,\varepsilon}^{\gamma+1})_- + (u_H - u_{i,\varepsilon})_- G(p_{i,\varepsilon}) \right], \end{aligned} \tag{2.12}$$

where we have used the assumption (A-G). We integrate over the domain Ω. Thanks to the boundary conditions in System (2.1), *i.e.* the density and flux continuity across the interfaces, and the homogeneous Dirichlet conditions on $\partial\Omega$, we gain

$$\begin{aligned} &\sum_{i=1}^{3} \int_{\Omega_{i,\varepsilon}} \mu_{i,\varepsilon} \Delta (u_H^{\gamma+1} - u_{i,\varepsilon}^{\gamma+1})_- \\ &= \sum_{i=1}^{2} \int_{\Gamma_{i,i+1,\varepsilon}} \left[\mu_i \nabla (u_H^{\gamma+1} - u_{i,\varepsilon}^{\gamma+1})_- - \mu_{i+1,\varepsilon} \nabla (u_H^{\gamma+1} - u_{i+1,\varepsilon}^{\gamma+1})_- \right] \cdot \boldsymbol{n}_{i,i+1} \\ &= \sum_{i=1}^{2} \left[\int_{\Gamma_{i,i+1,\varepsilon} \cap \{u_H < u_{i,\varepsilon}\}} \mu_i \nabla u_{i,\varepsilon}^{\gamma+1} \cdot \boldsymbol{n}_{i,i+1} - \int_{\Gamma_{i,i+1,\varepsilon} \cap \{u_H < u_{i+1,\varepsilon}\}} \mu_{i+1,\varepsilon} \nabla u_{i+1,\varepsilon}^{\gamma+1} \cdot \boldsymbol{n}_{i,i+1} \right] \\ &= \sum_{i=1}^{2} \int_{\Gamma_{i,i+1,\varepsilon} \cap \{u_H < u_{i,\varepsilon}\}} \left[\mu_i \nabla u_{i,\varepsilon}^{\gamma+1} - \mu_{i+1,\varepsilon} \nabla u_{i+1,\varepsilon}^{\gamma+1} \right] \cdot \boldsymbol{n}_{i,i+1} \\ &= 0. \end{aligned}$$

Hence, from Equation (2.12), we find

$$\frac{d}{dt} \sum_{i=1}^{3} \int_{\Omega_{i,\varepsilon}} (u_H - u_{i,\varepsilon})_- \leqslant G_M \sum_{i=1}^{3} \int_{\Omega_{i,\varepsilon}} (u_H - u_{i,\varepsilon})_-.$$

Finally, Gronwall's lemma and hypothesis (A-data1) on $u^0_{i,\varepsilon}$ imply

$$\sum_{i=1}^{3}\int_{\Omega_{i,\varepsilon}}(u_H-u_{i,\varepsilon})_-\leqslant e^{G_M t}\sum_{i=1}^{3}\int_{\Omega_{i,\varepsilon}}(u_H-u^0_{i,\varepsilon})_-=0.$$

We then conclude the boundedness of $u_{i,\varepsilon}$ by u_H for all $i=1,2,3$. From the relation $p_\varepsilon=u_\varepsilon^\gamma$, we conclude the boundedness of p_ε.

By arguing in an analogous way, replacing u_H by 0 and multiplying by $\mathrm{sign}_+(u_{i,\varepsilon})$, we obtain

$$\sum_{i=1}^{3}\int_{\Omega_{i,\varepsilon}}(u_{i,\varepsilon})_-\leqslant e^{G_M t}\sum_{i=1}^{3}\int_{\Omega_{i,\varepsilon}}(u^0_{i,\varepsilon})_-=0,$$

namely, $u_\varepsilon\geqslant 0$, and consequently, $p_\varepsilon\geqslant 0$.

(ii) $\boldsymbol{\partial_t u_\varepsilon,\partial_t p_\varepsilon\in L^\infty(0,T;L^1(\Omega))}$. We derive Equation (2.10) with respect to time to obtain

$$\partial_t(\partial_t u_{i,\varepsilon})=\mu_{i,\varepsilon}\gamma\Delta(p_{i,\varepsilon}\partial_t u_{i,\varepsilon})+\partial_t u_{i,\varepsilon}G(p_{i,\varepsilon})+u_{i,\varepsilon}G'(p_{i,\varepsilon})\partial_t p_{i,\varepsilon}.$$

Upon multiplying by $\mathrm{sign}(\partial_t u_{i,\varepsilon})$ and using Kato's inequality, we have

$$\partial_t(|\partial_t u_{i,\varepsilon}|)\leq\mu_{i,\varepsilon}\gamma\Delta(p_{i,\varepsilon}|\partial_t u_{i,\varepsilon}|)+|\partial_t u_{i,\varepsilon}|G(p_{i,\varepsilon})+u_{i,\varepsilon}G'(p_{i,\varepsilon})|\partial_t p_{i,\varepsilon}|,$$

since $u_{i,\varepsilon}$ and $p_{i,\varepsilon}$ are both nonnegative and $\partial_t p_{i,\varepsilon}=\gamma u_{i,\varepsilon}^{\gamma-1}\partial_t u_{i,\varepsilon}$. We integrate over $\Omega_{i,\varepsilon}$ and we sum over $i=1,2,3$, namely

$$\frac{\mathrm{d}}{\mathrm{d}t}\sum_{i=1}^{3}\int_{\Omega_{i,\varepsilon}}|\partial_t u_{i,\varepsilon}|\leq\gamma\underbrace{\sum_{i=1}^{3}\mu_{i,\varepsilon}\int_{\Omega_{i,\varepsilon}}\Delta(p_{i,\varepsilon}|\partial_t u_{i,\varepsilon}|)}_{\mathcal{J}}+G_M\int_{\Omega_{i,\varepsilon}}|\partial_t u_{i,\varepsilon}|,\tag{2.13}$$

where we use that $G'\leqslant 0$.

Now we show that the term $\mathcal{J}$ vanishes. Integration by parts yields

$$\mathcal{J}=\sum_{i=1}^{2}\int_{\Gamma_{i,i+1,\varepsilon}}\mu_{i,\varepsilon}\nabla(p_{i,\varepsilon}|\partial_t u_{i,\varepsilon}|)\cdot\boldsymbol{n}_{i,i+1}+\sum_{i=1}^{2}\int_{\Gamma_{i,i+1,\varepsilon}}\mu_{i+1,\varepsilon}\nabla(p_{i+1,\varepsilon}|\partial_t u_{i+1,\varepsilon}|)\cdot\boldsymbol{n}_{i+1,i}.$$

For the sake of simplicity, we denote $\boldsymbol{n}:=\boldsymbol{n}_{i,i+1}$. Let us recall that, by definition, $\boldsymbol{n}_{i+1,i}=-\boldsymbol{n}$. We have

$$\begin{aligned}\mathcal{J}&=\sum_{i=1}^{2}\int_{\Gamma_{i,i+1,\varepsilon}}(\mu_{i,\varepsilon}\nabla(p_{i,\varepsilon}|\partial_t u_{i,\varepsilon}|)-\mu_{i+1,\varepsilon}\nabla(p_{i+1,\varepsilon}|\partial_t u_{i+1,\varepsilon}|))\cdot\boldsymbol{n}\\&=\underbrace{\sum_{i=1}^{2}\int_{\Gamma_{i,i+1,\varepsilon}}|\partial_t u_{i,\varepsilon}|\mu_{i,\varepsilon}\nabla p_{i,\varepsilon}\cdot\boldsymbol{n}-|\partial_t u_{i+1,\varepsilon}|\mu_{i+1,\varepsilon}\nabla p_{i+1,\varepsilon}\cdot\boldsymbol{n}}_{\mathcal{J}_1}\\&\quad+\underbrace{\sum_{i=1}^{2}\int_{\Gamma_{i,i+1,\varepsilon}}\mu_{i,\varepsilon}p_{i,\varepsilon}\nabla|\partial_t u_{i,\varepsilon}|\cdot\boldsymbol{n}-\mu_{i+1,\varepsilon}p_{i+1,\varepsilon}\nabla|\partial_t u_{i+1,\varepsilon}|\cdot\boldsymbol{n}}_{\mathcal{J}_2}.\end{aligned}$$

Let us recall the membrane conditions of Problem (2.1), namely

$$\mu_{i,\varepsilon} u_{i,\varepsilon} \nabla p_{i,\varepsilon} \cdot \boldsymbol{n} = \mu_{i+1,\varepsilon} u_{i+1,\varepsilon} \nabla p_{i+1,\varepsilon} \cdot \boldsymbol{n}, \tag{2.14}$$

$$u_{i,\varepsilon} = u_{i+1,\varepsilon}, \tag{2.15}$$

on $(0,T) \times \Gamma_{i,i+1,\varepsilon}$, for $i = 1, 2$. From Equation (2.15), it is immediate to infer

$$\partial_t u_{i,\varepsilon} = \partial_t u_{i+1,\varepsilon}, \text{ on } (0,T) \times \Gamma_{i,i+1,\varepsilon}, \tag{2.16}$$

since

$$u_{i,\varepsilon}(t+h) - u_{i,\varepsilon}(t) = u_{i+1,\varepsilon}(t+h) - u_{i+1,\varepsilon}(t),$$

on $\Gamma_{i,i+1,\varepsilon}$ for all $h > 0$ such that $t + h \in (0,T)$.

Combing Equation (2.15) and Equation (2.14) we get

$$\mu_{i,\varepsilon} \nabla p_{i,\varepsilon} \cdot \boldsymbol{n} = \mu_{i+1,\varepsilon} \nabla p_{i+1,\varepsilon} \cdot \boldsymbol{n} \quad \text{ on } (0,T) \times \Gamma_{i,i+1,\varepsilon}. \tag{2.17}$$

Moreover, Equation (2.14) also implies

$$\mu_{i,\varepsilon} p_{i,\varepsilon} \nabla u_{i,\varepsilon} \cdot \boldsymbol{n} = \mu_{i+1,\varepsilon} p_{i+1,\varepsilon} \nabla u_{i+1,\varepsilon} \cdot \boldsymbol{n} \quad \text{ on } (0,T) \times \Gamma_{i,i+1,\varepsilon}, \tag{2.18}$$

which, combined with Equation (2.15) gives also

$$\mu_{i,\varepsilon} \nabla u_{i,\varepsilon} \cdot \boldsymbol{n} = \mu_{i+1,\varepsilon} \nabla u_{i+1,\varepsilon} \cdot \boldsymbol{n} \quad \text{ on } (0,T) \times \Gamma_{i,i+1,\varepsilon}. \tag{2.19}$$

Now we may come back to the computation of the term $\mathcal{J}$. By Equations (2.16), and (2.17) we directly infer that $\mathcal{J}_1$ vanishes.

We rewrite the term $\mathcal{J}_2$ as

$$\begin{aligned}
&\sum_{i=1}^{2} \int_{\Gamma_{i,i+1,\varepsilon}} \mu_{i,\varepsilon} p_{i,\varepsilon} \operatorname{sign}(\partial_t u_{i,\varepsilon})\, \partial_t(\nabla u_{i,\varepsilon} \cdot \boldsymbol{n}) - \mu_{i+1,\varepsilon} p_{i+1,\varepsilon} \operatorname{sign}(\partial_t u_{i+1,\varepsilon})\, \partial_t(\nabla u_{i+1,\varepsilon} \cdot \boldsymbol{n}) \\
&= \underbrace{\sum_{i=1}^{2} \int_{\Gamma_{i,i+1,\varepsilon}} \operatorname{sign}(\partial_t u_{i,\varepsilon})\, \partial_t(\mu_{i,\varepsilon} p_{i,\varepsilon} \nabla u_{i,\varepsilon} \cdot \boldsymbol{n} - \mu_{i+1,\varepsilon} p_{i+1,\varepsilon} \nabla u_{i+1,\varepsilon} \cdot \boldsymbol{n})}_{\mathcal{J}_{2,1}} \\
&\quad \underbrace{- \sum_{i=1}^{2} \int_{\Gamma_{i,i+1,\varepsilon}} |\partial_t p_{i,\varepsilon}| (\mu_{i,\varepsilon} \nabla u_{i,\varepsilon} \cdot \boldsymbol{n} - \mu_{i+1,\varepsilon} \nabla u_{i+1,\varepsilon} \cdot \boldsymbol{n})}_{\mathcal{J}_{2,2}},
\end{aligned}$$

where we used Equation (2.16), which also implies $\partial_t p_{i,\varepsilon} = \partial_t p_{i+1,\varepsilon}$ on $(0,T) \times \Gamma_{i,i+1,\varepsilon}$, for $i = 1, 2$. The terms $\mathcal{J}_{2,1}$ and $\mathcal{J}_{2,2}$ vanish thanks to Equation (2.18) and Equation (2.19), respectively.

Hence, from Equation (2.13), we finally have

$$\frac{\mathrm{d}}{\mathrm{d}t} \sum_{i=1}^{3} \int_{\Omega_{i,\varepsilon}} |\partial_t u_{i,\varepsilon}| \leq G_M \sum_{i=1}^{3} \int_{\Omega_{i,\varepsilon}} |\partial_t u_{i,\varepsilon}|,$$

and, using Gronwall's inequality, we obtain

$$\sum_{i=1}^{3}\int_{\Omega_{i,\varepsilon}}|\partial_t u_{i,\varepsilon}(t)| \leq e^{G_M t}\sum_{i=1}^{3}\int_{\Omega_{i,\varepsilon}}|(\partial_t u_{i,\varepsilon})^0|.$$

Thanks to the assumptions on the initial data, *cf.* Equation (A-data2), we conclude.

(iii) $p_\varepsilon \in L^2(0,T;H^1(\Omega\setminus\Omega_{2,\varepsilon}))$. As known, in the context of a filtration equation, we can recover the pressure equation upon multiplying the equation on $u_{i,\varepsilon}$, *cf.* System (2.1), by $p'(u_{i,\varepsilon}) = \gamma u_{i,\varepsilon}^{\gamma-1}$. Therefore, we obtain

$$\partial_t p_{i,\varepsilon} - \gamma\mu_{i,\varepsilon}p_{i,\varepsilon}\Delta p_{i,\varepsilon} = \mu_{i,\varepsilon}|\nabla p_{i,\varepsilon}|^2 + \gamma p_{i,\varepsilon}G(p_{i,\varepsilon}). \tag{2.20}$$

Studying the equation on p_ε rather than the equation on u_ε turns out to be very useful in order to prove compactness, since, as it is well-know for the porous medium equation (PME), the gradient of the pressure can be easily bounded in L^2, while the density solution of the PME can develop jump singularities on the free boundary, Vázquez [125].

We integrate Equation (2.20) on each $\Omega_{i,\varepsilon}$, and we sum over all i to obtain

$$\sum_{i=1}^{3}\int_{\Omega_{i,\varepsilon}}\partial_t p_{i,\varepsilon} = \sum_{i=1}^{3}\left(\gamma\mu_{i,\varepsilon}\int_{\Omega_{i,\varepsilon}}p_{i,\varepsilon}\Delta p_{i,\varepsilon} + \int_{\Omega_{i,\varepsilon}}\mu_{i,\varepsilon}|\nabla p_{i,\varepsilon}|^2 + \gamma\int_{\Omega_{i,\varepsilon}}p_{i,\varepsilon}G(p_{i,\varepsilon})\right). \tag{2.21}$$

Integration by parts yields

$$\begin{aligned}\sum_{i=1}^{3}\mu_{i,\varepsilon}\int_{\Omega_{i,\varepsilon}}p_{i,\varepsilon}\Delta p_{i,\varepsilon} &= -\sum_{i=1}^{3}\mu_{i,\varepsilon}\int_{\Omega_{i,\varepsilon}}|\nabla p_{i,\varepsilon}|^2 + \sum_{i=1}^{2}\int_{\Gamma_{i,i+1,\varepsilon}}\mu_{i,\varepsilon}p_{i,\varepsilon}\nabla p_{i,\varepsilon}\cdot\boldsymbol{n}_{i,i+1}\\ &\quad + \sum_{i=1}^{2}\int_{\Gamma_{i,i+1,\varepsilon}}\mu_{i+1,\varepsilon}p_{i+1,\varepsilon}\nabla p_{i+1,\varepsilon}\cdot\boldsymbol{n}_{i+1,i}\\ &= -\sum_{i=1}^{3}\mu_{i,\varepsilon}\int_{\Omega_{i,\varepsilon}}|\nabla p_{i,\varepsilon}|^2,\end{aligned}$$

since we have homogeneous Dirichlet boundary conditions on $\partial\Omega$ and the flux continuity conditions (2.17).

Hence, from Equation (2.21), we have

$$\sum_{i=1}^{3}\int_{\Omega_{i,\varepsilon}}\partial_t p_{i,\varepsilon} = \sum_{i=1}^{3}\mu_{i,\varepsilon}\left((1-\gamma)\int_{\Omega_{i,\varepsilon}}|\nabla p_{i,\varepsilon}|^2 + \gamma\int_{\Omega_{i,\varepsilon}}p_{i,\varepsilon}G(p_{i,\varepsilon})\right). \tag{2.22}$$

We integrate over time and we deduce that

$$\sum_{i=1}^{3}\left(\int_{\Omega_{i,\varepsilon}}p_{i,\varepsilon}(T) - \int_{\Omega_{i,\varepsilon}}p_{i,\varepsilon}^0 + \mu_{i,\varepsilon}(\gamma-1)\int_0^T\int_{\Omega_{i,\varepsilon}}|\nabla p_{i,\varepsilon}|^2\right) = \sum_{i=1}^{3}\gamma\int_0^T\int_{\Omega_{i,\varepsilon}}p_{i,\varepsilon}G(p_{i,\varepsilon}). \tag{2.23}$$

Finally, we conclude that

$$\sum_{i=1}^{3}\int_0^T\int_{\Omega_{i,\varepsilon}}\mu_{i,\varepsilon}|\nabla p_{i,\varepsilon}|^2 \leq \sum_{i=1}^{3}\frac{\gamma}{\gamma-1}\int_0^T\int_{\Omega_{i,\varepsilon}}p_{i,\varepsilon}G(p_{i,\varepsilon}) + \frac{1}{\gamma-1}\int_{\Omega_{i,\varepsilon}}p_{i,\varepsilon}^0, \tag{2.24}$$

Since we have already proved that $p_{i,\varepsilon}$ is bounded in $L^\infty(\Omega_T)$ and by assumption G is continuous, we finally find that

$$\sum_{i=1}^{3} \mu_{i,\varepsilon} \int_0^T \int_{\Omega_{i,\varepsilon}} |\nabla p_{i,\varepsilon}|^2 \leq C, \tag{2.25}$$

where C denotes a constant independent of ε. Since both $\mu_{1,\varepsilon}$ and $\mu_{3,\varepsilon}$ are bounded from below away from zero, we conclude that the uniform bound holds in $\Omega \setminus \Omega_{2,\varepsilon}$. □

Remark 2.3.3. *Let us also notice that, differently from Sanchez-Palencia [118], where the author studies the linear and uniformly parabolic case, proving weak compactness is not enough. Indeed, due to the presence of the nonlinear term $u\nabla p$, it is necessary to infer strong compactness of u. For this reason, the L^1-uniform estimate on the time derivative proven in Lemma 2.3.1 is fundamental.*

2.4 Limit $\varepsilon \to 0$

We have now the *a priori* tools to face the limit $\varepsilon \to 0$. We need to construct an extension operator with the aim of controlling uniformly, with respect to ε, the pressure gradient in $L^2(\Omega)$. Indeed, from (2.25), we see that one cannot find a uniform bound for $\|\nabla p_{2,\varepsilon}\|_{L^2(\Omega_{2,\varepsilon})}$. The blow-up of Estimate (2.25) for $i = 2$, is in fact the main challenge in order to find compactness on Ω. To this end, following Sanchez-Palencia [118], we introduce in Subsection 2.4.1 an extension operator which projects the points of $\Omega_{2,\varepsilon}$ inside $\Omega_{1,\varepsilon} \cup \Omega_{3,\varepsilon}$. Then, introducing proper test functions such that the variational formulation for $\varepsilon > 0$ in (2.8) and $\varepsilon \to 0$ in (2.6) are well-defined, we can pass to the limit (Subsection 2.4.2).

2.4.1 Extension operator and compactness

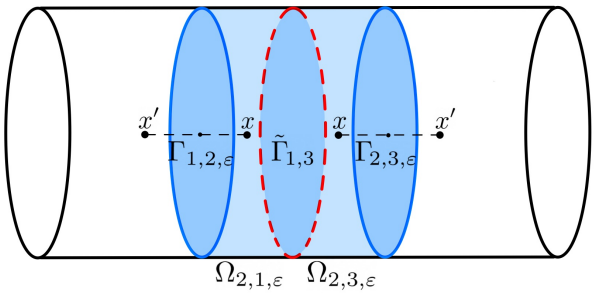

Figure 2.2: *Representation of the spatial symmetry used in the definition of the extension operator,* cf. *Equation* (2.26) *and of the two subdomains of $\Omega_{2,1,\varepsilon}$ and $\Omega_{2,3,\varepsilon}$.*

As mentioned above, in order to be able to pass to the limit $\varepsilon \to 0$, we first need to define the following extension operator

$$\mathcal{P}_\varepsilon : L^q(0,T; W^{1,p}(\Omega \setminus \Omega_{2,\varepsilon})) \to L^q(0,T; W^{1,p}(\Omega \setminus \tilde{\Gamma}_{1,3})), \quad \text{for} \quad 1 \leq p, q \leq +\infty,$$

as follows for a general function $z \in L^q(0,T;W^{1,p}(\Omega \setminus \Omega_{2,\varepsilon}))$,

$$\mathcal{P}_\varepsilon(z(t,x)) = \begin{cases} z(t,x), & \text{if} \quad x \in \Omega_{1,\varepsilon} \cup \Omega_{3,\varepsilon}, \\ z(t,x'), & \text{if} \quad x \in \Omega_{2,\varepsilon}, \end{cases} \tag{2.26}$$

where x' is the symmetric of x with respect to $\Gamma_{1,2,\varepsilon}$ (or $\Gamma_{2,3,\varepsilon}$) if $x \in \Omega_{2,1,\varepsilon}$ (respectively $x \in \Omega_{2,3,\varepsilon}$), defined by the function $g : x \to x'$ for $x = (x_1, x_2, x_3) \in \Omega_{2,\varepsilon}$ such that

$$g(x) = \begin{cases} (x_1, x_2, x_3 - 2\, d(\Gamma_{1,3,\varepsilon}, x)), & \text{if} \quad x \in \Omega_{2,1,\varepsilon}, \\ (x_1, x_2, x_3 + 2\, d(\Gamma_{2,3,\varepsilon}, x)), & \text{if} \quad x \in \Omega_{2,3,\varepsilon}, \end{cases}$$

where $d(\Gamma_{1,2,\varepsilon}, x)$ (respectively $d(\Gamma_{2,3,\varepsilon}, x)$) denotes the distance between x and the surface $\Gamma_{1,2,\varepsilon}$ (respectively $\Gamma_{2,3,\varepsilon}$). The point x' is illustrated in Figure 2.2. It can be easily seen that the function g and its inverse have uniformly bounded first derivatives. Hence, we infer that $\mathcal{P}_\varepsilon$ is linear and bounded, *i.e.*

$$\|\mathcal{P}_\varepsilon(z)\|_{L^q(0,T;W^{1,p}(\Omega\setminus\tilde{\Gamma}_{1,3}))} \leq C, \quad \forall z \in L^q(0,T;W^{1,p}(\Omega \setminus \Omega_{2,\varepsilon})), \text{ for } 1 \leq p,q \leq \infty.$$

Let us notice that the extension operator is well defined also from $L^1((0,T) \times (\Omega \setminus \Omega_{2,\varepsilon}))$ into $L^1((0,T) \times (\Omega \setminus \tilde{\Gamma}_{1,3}))$. Hence, we can apply it also on u_ε and $\partial_t p_\varepsilon$.

Remark 2.4.1. *Thanks to the properties of the extension operator, the estimates stated in Lemma 2.3.1 hold true also upon applying $\mathcal{P}_\varepsilon(\cdot)$ on $p_\varepsilon, u_\varepsilon$, and $\partial_t p_\varepsilon$, namely*

$$\begin{aligned}
&0 \leq \mathcal{P}_\varepsilon(p_\varepsilon) \leq p_H, \quad 0 \leq \mathcal{P}_\varepsilon(u_\varepsilon) \leqslant u_H, \\
&\partial_t \mathcal{P}_\varepsilon(p_\varepsilon) \in L^\infty(0,T;L^1(\Omega \setminus \tilde{\Gamma}_{1,3})), \\
&\nabla \mathcal{P}_\varepsilon(p_\varepsilon) \in L^2(0,T;L^2(\Omega \setminus \tilde{\Gamma}_{1,3})), \\
&\frac{\gamma}{\gamma+1} \nabla\big(\mathcal{P}_\varepsilon(u_\varepsilon^{\gamma+1})\big) \in L^2(0,T;L^2(\Omega \setminus \tilde{\Gamma}_{1,3})), \\
&\partial_t(\mathcal{P}_\varepsilon(u_\varepsilon^{\gamma+1})) \in L^\infty(0,T;L^1(\Omega \setminus \tilde{\Gamma}_{1,3})).
\end{aligned}$$

The last two bounds hold thanks to the following arguments

$$\frac{\gamma}{\gamma+1} \nabla\big(\mathcal{P}_\varepsilon(u_\varepsilon^{\gamma+1})\big) = \mathcal{P}_\varepsilon(u_\varepsilon) \nabla \mathcal{P}_\varepsilon(p_\varepsilon) \in L^2(0,T;L^2(\Omega \setminus \tilde{\Gamma}_{1,3})),$$

and

$$\partial_t\big(\mathcal{P}_\varepsilon(u_\varepsilon^{\gamma+1})\big) = (\gamma+1)\mathcal{P}_\varepsilon(p_\varepsilon)\partial_t \mathcal{P}_\varepsilon(u_\varepsilon) = (\gamma+1)\mathcal{P}_\varepsilon(p_\varepsilon)\mathcal{P}_\varepsilon(\partial_t u_\varepsilon) \in L^\infty(0,T;L^1(\Omega \setminus \tilde{\Gamma}_{1,3}).$$

Lemma 2.4.1 (Compactness of the extension operator)**.** *Let $(u_\varepsilon, p_\varepsilon)$ be the solution of Problem (2.1). There exists a couple $(\tilde{u}, \tilde{p})$ with*

$$\tilde{u} \in L^\infty(0,T;L^\infty(\Omega \setminus \tilde{\Gamma}_{1,3})), \quad \tilde{p} \in L^2(0,T;H^1(\Omega \setminus \tilde{\Gamma}_{1,3})) \cap L^\infty(0,T;L^\infty(\Omega \setminus \tilde{\Gamma}_{1,3})),$$

such that, up to a subsequence, it holds

(i) $\mathcal{P}_\varepsilon(p_\varepsilon) \to \tilde{p}$ strongly in $L^p(0,T;L^p(\Omega \setminus \tilde{\Gamma}_{1,3}))$, for $1 \leq p < +\infty$,

(ii) $\mathcal{P}_\varepsilon(u_\varepsilon) \to \tilde{u}$ strongly in $L^p(0,T;L^p(\Omega \setminus \tilde{\Gamma}_{1,3}))$, for $1 \leq p < +\infty$,

(iii) $\nabla \mathcal{P}_\varepsilon(p_\varepsilon) \rightharpoonup \nabla \tilde{p}$ *weakly in* $L^2(0,T;L^2(\Omega \setminus \tilde{\Gamma}_{1,3}))$.

Proof. (i). Since both $\partial_t \mathcal{P}_\varepsilon(p_\varepsilon)$ and $\nabla \mathcal{P}_\varepsilon(p_\varepsilon)$ are bounded in $L^1(0,T;L^1(\Omega \setminus \tilde{\Gamma}_{1,3}))$ uniformly with respect to ε, we infer the strong compactness of $\mathcal{P}_\varepsilon(p_\varepsilon)$ in $L^1(0,T;L^1(\Omega \setminus \tilde{\Gamma}_{1,3}))$. Let us also notice that since both u_ε and p_ε are uniformly bounded in $L^\infty(0,T;L^\infty(\Omega \setminus \tilde{\Gamma}_{1,3}))$ then the strong convergence holds in any $L^p(0,T;L^p(\Omega \setminus \tilde{\Gamma}_{1,3}))$ with $1 \le p < \infty$.

(ii). From *(i)*, we can extract a subsequence of $\mathcal{P}_\varepsilon(p_\varepsilon)$ which converges almost everywhere. Then, remembering that $u_\varepsilon = p_\varepsilon^{1/\gamma}$, with $\gamma > 1$ fixed, we have convergence of $\mathcal{P}_\varepsilon(u_\varepsilon)$ almost everywhere. Thanks to the uniform L^∞-bound of $\mathcal{P}_\varepsilon(u_\varepsilon)$, Lebesgue's theorem implies the statement. Let us point out that, in particular, the L^∞-uniform bound is also valid in the limit.

(iii). The uniform boundedness of $\nabla \mathcal{P}_\varepsilon(p_\varepsilon)$ in $L^2(0,T;L^2(\Omega \setminus \tilde{\Gamma}_{1,3}))$ immediately implies weak convergence up to a subsequence.

□

2.4.2 Test function space and passage to the limit $\varepsilon \to 0$

Since in the limit we expect a discontinuity of the density on $\tilde{\Gamma}_{1,3}$, we need to define a suitable space of test functions. Therefore we construct the space $E^\star$ as follows. Let us consider a function $\zeta \in \mathcal{D}(\Omega)$ (*i.e.* $C_c^\infty(\Omega)$). For any $\varepsilon > 0$ small enough, we build the function $v_\varepsilon = \mathcal{P}_\varepsilon(\zeta)$, using the extension operator previously defined. The space of all linear combinations of these functions v_ε is called $E^\star \subset H^1(\Omega \setminus \tilde{\Gamma}_{1,3})$, namely

$$E^\star = \left\{ \sum_{n=1}^{\infty} c_n v_{\varepsilon,n} \ \text{ s.t. } \ c_n \in \mathbb{R},\ v_{\varepsilon,n} = \mathcal{P}_\varepsilon(\zeta_n),\ \zeta_n \in C_c^\infty(\Omega) \right\}.$$

We stress that the functions of $E^\star$ are discontinuous on $\tilde{\Gamma}_{1,3}$.

In the weak formulation of the limit problem (2.6), we will make use of piece-wise C^∞-test functions (discontinuous on $\tilde{\Gamma}_{1,3}$) of the type $w(t,x) = \varphi(t)v(x)$, where $\varphi \in C^1([0,T))$ with $\varphi(T) = 0$ and $v \in E^*$. Therefore, w belongs to $C^1([0,T);E^*)$. On the other hand, in the variational formulation (2.8), *i.e.* for $\varepsilon > 0$, $H^1(0,T;H_0^1(\Omega))$ test functions are required. Thus, in order to study the limit $\varepsilon \to 0$, we need to introduce a proper sequence of test functions depending on ε that converges to w. To this end, we define the operator $L_\varepsilon : C^1([0,T);E^*) \to H^1(0,T;H_0^1(\Omega))$ such that

$$L_\varepsilon(w) \to w, \quad \text{uniformly as} \quad \varepsilon \to 0, \quad \forall w \in C^1([0,T);E^\star).$$

In this way, $L_\varepsilon(w)$ belongs to $H^1(0,T;H_0^1(\Omega))$, therefore, it can be used as test function in the formulation (2.8).

Following Sanchez-Palancia [118], for all $t \in [0,T]$ and $x = (x_1,x_2,x_3) \in \Omega$, we define

$$L_\varepsilon(w(t,x)) = \begin{cases} w(t,x), & \text{if} \quad x \notin \Omega_{2,\varepsilon}, \\ \dfrac{1}{2}\left[w\Big(t,x_1,x_2,\dfrac{\varepsilon}{2}\Big) + w\Big(t,x_1,x_2,-\dfrac{\varepsilon}{2}\Big)\right] & \\ \quad + \left[w\Big(t,x_1,x_2,\dfrac{\varepsilon}{2}\Big) - w\Big(t,x_1,x_2,-\dfrac{\varepsilon}{2}\Big)\right]\dfrac{x_3}{\varepsilon}, & \text{otherwise.} \end{cases}$$

It can be easily verified that $L_\varepsilon(w)$ is linear with respect to x_3 in $\Omega_{2,\varepsilon}$ and is continuous on $\partial\Omega_{2,\varepsilon}$.

Let us notice that it holds

$$\left|\frac{\partial L_\varepsilon(w)}{\partial x_3}\right| \leq \frac{C}{\varepsilon}. \tag{2.27}$$

Furthermore, thanks to the mean value theorem, the partial derivatives of $L_\varepsilon(w)$ with respect to x_1 and x_2 are bounded by a constant (independent of ε),

$$\left|\frac{\partial L_\varepsilon(w)}{\partial x_1}\right| \leq C, \qquad \left|\frac{\partial L_\varepsilon(w)}{\partial x_2}\right| \leq C,$$

and since the measure of $\Omega_{2,\varepsilon}$ is proportional to ε, we have

$$\int_0^T \int_{\Omega_{2,\varepsilon}} \left|\frac{\partial L_\varepsilon(w)}{\partial x_1}\right|^2 + \left|\frac{\partial L_\varepsilon(w)}{\partial x_2}\right|^2 \leq C\varepsilon. \tag{2.28}$$

Given $w \in C^1([0,T); E^\star)$, we take $L_\varepsilon(w)$ as a test function in the variational formulation of the problem, *i.e.* Equation (2.8), and we have

$$\begin{aligned} -\int_0^T \int_\Omega u_\varepsilon \partial_t L_\varepsilon(w) + \sum_{i=1}^3 \mu_{i,\varepsilon} \int_0^T \int_{\Omega_{i,\varepsilon}} u_{i,\varepsilon} \nabla p_{i,\varepsilon} \cdot \nabla L_\varepsilon(w) \\ = \int_0^T \int_\Omega u_\varepsilon G(p_\varepsilon) L_\varepsilon(w) + \int_\Omega u_\varepsilon^0 L_\varepsilon(w^0). \end{aligned} \tag{2.29}$$

Thanks to the *a priori* estimates already proven, *cf.* Lemma 2.3.1, Remark 2.4.1 and the convergence result on the extension operator, *cf.* Lemma 2.4.1, we are now able to pass to the limit $\varepsilon \to 0$ and recover the effective interface problem.

Theorem 2.4.1. *For all test functions of the form $w(t,x) := \varphi(t)v(x)$ with $\varphi \in C^1([0,T))$ and $v \in E^*$, the limit couple $(\tilde{u}, \tilde{p})$ of Lemma 2.4.1 satisfies the following equation*

$$\begin{aligned} -\int_0^T \int_\Omega \tilde{u}\partial_t w + \tilde{\mu}_1 \int_0^T \int_{\tilde{\Omega}_1} \tilde{u}\nabla\tilde{p}\cdot\nabla w + \tilde{\mu}_3 \int_0^T \int_{\tilde{\Omega}_3} \tilde{u}\nabla\tilde{p}\cdot\nabla w \\ + \tilde{\mu}_{1,3} \int_0^T \int_{\tilde{\Gamma}_{1,3}} [\![\Pi]\!] \left(w_{|x_3=0^+} - w_{|x_3=0^-}\right) = \int_0^T \int_\Omega \tilde{u} G(\tilde{p}) w + \int_\Omega \tilde{u}^0 w^0, \end{aligned}$$

where

$$[\![\Pi]\!] := \frac{\gamma}{\gamma+1}(\tilde{u}^{\gamma+1})_{|x_3=0^+} - \frac{\gamma}{\gamma+1}(\tilde{u}^{\gamma+1})_{|x_3=0^-},$$

and $(\cdot)_{|x_3=0^-} = \mathcal{T}_1(\cdot)$ as well as $(\cdot)_{|x_3=0^+} = \mathcal{T}_3(\cdot)$, with $\mathcal{T}_1, \mathcal{T}_3$ the trace operators defined in Section 2.2. By definition, this equation is the weak formulation of Problem (2.2).

Proof. We may pass to the limit in Equation (2.29), computing each term individually.

Step 1. Time derivative integral. We split the first integral into two parts

$$-\int_0^T \int_\Omega u_\varepsilon \partial_t L_\varepsilon(w) = \underbrace{-\int_0^T \int_{\Omega_{1,\varepsilon}\cup\Omega_{3,\varepsilon}} u_\varepsilon \partial_t L_\varepsilon(w)}_{\mathcal{I}_1} \underbrace{-\int_0^T \int_{\Omega_{2,\varepsilon}} u_\varepsilon \partial_t L_\varepsilon(w)}_{\mathcal{I}_2}.$$

Since outside of $\Omega_{2,\varepsilon}$ the extension operator coincides with the identity, and $L_\varepsilon(w) = w$, we have

$$\mathcal{I}_1 = -\int_0^T \int_{\Omega_{1,\varepsilon}\cup\Omega_{3,\varepsilon}} \mathcal{P}_\varepsilon(u_\varepsilon)\partial_t w = -\int_0^T \int_\Omega \mathcal{P}_\varepsilon(u_\varepsilon)\partial_t w + \int_0^T \int_{\Omega_{2,\varepsilon}} \mathcal{P}_\varepsilon(u_\varepsilon)\partial_t w.$$

Thanks to Remark 2.4.1, we know that the last integral converges to zero, since both $\mathcal{P}_\varepsilon(u_\varepsilon)$ and $\partial_t w$ are bounded in L^2 and the measure of $\Omega_{2,\varepsilon}$ tends to zero as $\varepsilon \to 0$. Then, by Lemma 2.4.1, we have

$$-\int_0^T \int_\Omega \mathcal{P}_\varepsilon(u_\varepsilon)\partial_t w \longrightarrow -\int_0^T \int_\Omega \tilde{u}\ \partial_t w, \quad \text{as } \varepsilon \to 0,$$

where we used the weak convergence of $\mathcal{P}_\varepsilon(u_\varepsilon)$ to $\tilde{u}$ in $L^2(0,T;L^2(\Omega \setminus \tilde{\Gamma}_{1,3}))$. The term $\mathcal{I}_2$ vanishes in the limit, since both u_ε and $\partial_t L_\varepsilon(w)$ are bounded in L^2 uniformly with respect to ε. Hence, we finally have

$$-\int_0^T \int_\Omega u_\varepsilon \partial_t L_\varepsilon(w) \longrightarrow -\int_0^T \int_\Omega \tilde{u}\ \partial_t w, \quad \text{as } \varepsilon \to 0. \tag{2.30}$$

Step 2. Reaction integral. We use the same argument for the reaction term, namely

$$\int_0^T \int_\Omega u_\varepsilon G(p_\varepsilon) L_\varepsilon(w) = \underbrace{\int_0^T \int_{\Omega_{1,\varepsilon}\cup\Omega_{3,\varepsilon}} u_\varepsilon G(p_\varepsilon) L_\varepsilon(w)}_{\mathcal{K}_1} + \underbrace{\int_0^T \int_{\Omega_{2,\varepsilon}} u_\varepsilon G(p_\varepsilon) L_\varepsilon(w)}_{\mathcal{K}_2}.$$

Using again the convergence result on the extension operator, *cf.* Lemma 2.4.1, we obtain

$$\mathcal{K}_1 = \int_0^T \int_{\Omega_{1,\varepsilon}\cup\Omega_{3,\varepsilon}} \mathcal{P}_\varepsilon(u_\varepsilon) G(\mathcal{P}_\varepsilon(p_\varepsilon)) w \longrightarrow \int_0^T \int_\Omega \tilde{u}\, G(\tilde{p}) w, \quad \text{as } \varepsilon \to 0,$$

since both $\mathcal{P}_\varepsilon(u_\varepsilon)$ and $G(\mathcal{P}_\varepsilon(p_\varepsilon))$ converge strongly in $L^2(0,T;L^2(\Omega \setminus \tilde{\Gamma}_{1,3}))$. Arguing as before, it is immediate to see that $\mathcal{K}_2$ vanishes in the limit. Hence

$$\int_0^T \int_\Omega u_\varepsilon G(p_\varepsilon) L_\varepsilon(w) \longrightarrow \int_0^T \int_\Omega \tilde{u} G(\tilde{p}) w, \quad \text{as } \varepsilon \to 0. \tag{2.31}$$

Step 3. Initial data integral. From (A-data3), it is easy to see that

$$\int_\Omega u_\varepsilon^0 L_\varepsilon(w^0) \longrightarrow \int_\Omega \tilde{u}^0 w^0, \quad \text{as } \varepsilon \to 0. \tag{2.32}$$

Step 4. Divergence integral. Now it remains to treat the divergence term in Equation (2.29), from which we recover the effective interface conditions at the limit.

Since the extension operator $\mathcal{P}_\varepsilon$ is in fact the identity operator on $\Omega \setminus \Omega_{2,\varepsilon}$, we can write

$$\begin{aligned} &\sum_{i=1}^3 \mu_{i,\varepsilon} \int_0^T \int_{\Omega_{i,\varepsilon}} u_{i,\varepsilon} \nabla p_{i,\varepsilon} \cdot \nabla L_\varepsilon(w) \\ &\quad = \underbrace{\sum_{i=1,3} \mu_{i,\varepsilon} \int_0^T \int_{\Omega_{i,\varepsilon}} \mathcal{P}_\varepsilon(u_{i,\varepsilon}) \nabla \mathcal{P}_\varepsilon(p_{i,\varepsilon}) \cdot \nabla w}_{\mathcal{H}_1} + \underbrace{\mu_{2,\varepsilon} \int_0^T \int_{\Omega_{2,\varepsilon}} u_{2,\varepsilon} \nabla p_{2,\varepsilon} \cdot \nabla L_\varepsilon(w)}_{\mathcal{H}_2}. \end{aligned} \tag{2.33}$$

We treat the two terms separately. Since we want to use the weak convergence of $\nabla\mathcal{P}_\varepsilon(p_\varepsilon)$ in $L^2(0,T;L^2(\Omega\setminus\tilde{\Gamma}_{1,3}))$ (together with the strong convergence of $\mathcal{P}_\varepsilon(u_\varepsilon)$ in $L^2(0,T;L^2(\Omega\setminus\tilde{\Gamma}_{1,3}))$) we need to write the term $\mathcal{H}_1$ as an integral over Ω. To this end, let $\overline{\mu}_\varepsilon := \overline{\mu}_\varepsilon(x)$ be a function defined as follows

$$\overline{\mu}_\varepsilon(x) := \begin{cases} \mu_{1,\varepsilon} & \text{for } x \in \Omega_{1,\varepsilon}, \\ 0 & \text{for } x \in \Omega_{2,\varepsilon}, \\ \mu_{3,\varepsilon} & \text{for } x \in \Omega_{3,\varepsilon}. \end{cases}$$

Then, we can write

$$\mathcal{H}_1 = \int_0^T \int_\Omega \overline{\mu}_\varepsilon \mathcal{P}_\varepsilon(u_\varepsilon)\nabla\mathcal{P}_\varepsilon(p_\varepsilon)\cdot\nabla w.$$

Let us notice that as ε goes to 0, $\overline{\mu}_\varepsilon$ converges to $\tilde{\mu}_1$ in $\tilde{\Omega}_1$ and $\tilde{\mu}_3$ in $\tilde{\Omega}_3$. Therefore, by Lemma 2.4.1, we infer

$$\mathcal{H}_1 \longrightarrow \tilde{\mu}_1 \int_0^T \int_{\tilde{\Omega}_1} \tilde{u}\ \nabla\tilde{p}\cdot\nabla w + \tilde{\mu}_3 \int_0^T \int_{\tilde{\Omega}_3} \tilde{u}\ \nabla\tilde{p}\cdot\nabla w, \quad \text{as} \quad \varepsilon\to 0. \tag{2.34}$$

Now we treat the term $\mathcal{H}_2$, which can be written as

$$\begin{aligned}\mathcal{H}_2 =& \mu_{2,\varepsilon}\int_0^T\int_{\Omega_{2,\varepsilon}} u_{2,\varepsilon}\nabla p_{2,\varepsilon}\cdot\nabla L_\varepsilon(w)\\ =& \mu_{2,\varepsilon}\int_0^T\int_{\Omega_{2,\varepsilon}}\left(u_{2,\varepsilon}\frac{\partial p_{2,\varepsilon}}{\partial x_1}\frac{\partial L_\varepsilon(w)}{\partial x_1} + u_{2,\varepsilon}\frac{\partial p_{2,\varepsilon}}{\partial x_2}\frac{\partial L_\varepsilon(w)}{\partial x_2}\right) + \mu_{2,\varepsilon}\int_0^T\int_{\Omega_{2,\varepsilon}} u_{2,\varepsilon}\frac{\partial p_{2,\varepsilon}}{\partial x_3}\frac{\partial L_\varepsilon(w)}{\partial x_3}.\end{aligned}$$

By the Cauchy-Schwarz inequality, the a priori estimate (2.25), and Equation (2.28), we have

$$\begin{aligned}&\mu_{2,\varepsilon}\int_0^T\int_{\Omega_{2,\varepsilon}} u_{2,\varepsilon}\frac{\partial p_{2,\varepsilon}}{\partial x_1}\frac{\partial L_\varepsilon(w)}{\partial x_1} + u_{2,\varepsilon}\frac{\partial p_{2,\varepsilon}}{\partial x_2}\frac{\partial L_\varepsilon(w)}{\partial x_2}\\ &\qquad\leqslant \mu_{2,\varepsilon}^{1/2}\|u_{2,\varepsilon}\|_{L^\infty((0,T)\times\Omega_{2,\varepsilon})}\left(\left\|\mu_{2,\varepsilon}^{1/2}\frac{\partial p_{2,\varepsilon}}{\partial x_1}\right\|_{L^2((0,T)\times\Omega_{2,\varepsilon})}\left\|\frac{\partial L_\varepsilon(w)}{\partial x_1}\right\|_{L^2((0,T)\times\Omega_{2,\varepsilon})}\right)\\ &\qquad\quad + \mu_{2,\varepsilon}^{1/2}\|u_{2,\varepsilon}\|_{L^\infty((0,T)\times\Omega_{2,\varepsilon})}\left(\left\|\mu_{2,\varepsilon}^{1/2}\frac{\partial p_{2,\varepsilon}}{\partial x_2}\right\|_{L^2((0,T)\times\Omega_{2,\varepsilon})}\left\|\frac{\partial L_\varepsilon(w)}{\partial x_2}\right\|_{L^2((0,T)\times\Omega_{2,\varepsilon})}\right)\\ &\qquad\leqslant C\ \mu_{2,\varepsilon}^{1/2}\ \varepsilon^{1/2}\to 0.\end{aligned}$$

On the other hand, by Fubini's theorem, the following equality holds

$$\begin{aligned}
&\mu_{2,\varepsilon} \int_0^T \int_{\Omega_{2,\varepsilon}} u_{2,\varepsilon} \frac{\partial p_{2,\varepsilon}}{\partial x_3} \frac{\partial L_\varepsilon(w)}{\partial x_3} \\
&\quad = \mu_{2,\varepsilon} \frac{\gamma}{\gamma+1} \int_0^T \int_{\Omega_{2,\varepsilon}} \frac{\partial u_{2,\varepsilon}^{\gamma+1}}{\partial x_3} \frac{\partial L_\varepsilon(w)}{\partial x_3} \\
&\quad = \mu_{2,\varepsilon} \frac{\gamma}{\gamma+1} \int_0^T \int_{-\varepsilon/2}^{\varepsilon/2} \int_{\tilde{\Gamma}_{1,3}} \frac{\partial u_{2,\varepsilon}^{\gamma+1}}{\partial x_3} \frac{\partial L_\varepsilon(w)}{\partial x_3} \,\mathrm{d}\sigma \,\mathrm{d}x_3 \\
&\quad = \mu_{2,\varepsilon} \frac{\gamma}{\gamma+1} \int_0^T \int_{-\varepsilon/2}^{\varepsilon/2} \int_{\tilde{\Gamma}_{1,3}} \frac{\partial u_{2,\varepsilon}^{\gamma+1}}{\partial x_3} \frac{w_{|x_3=\frac{\varepsilon}{2}} - w_{|x_3=-\frac{\varepsilon}{2}}}{\varepsilon} \,\mathrm{d}\sigma \,\mathrm{d}x_3 \\
&\quad = \frac{\mu_{2,\varepsilon}}{\varepsilon} \frac{\gamma}{\gamma+1} \int_0^T \int_{\tilde{\Gamma}_{1,3}} \left(w_{|x_3=\frac{\varepsilon}{2}} - w_{|x_3=-\frac{\varepsilon}{2}} \right) \int_{-\varepsilon/2}^{\varepsilon/2} \frac{\partial u_{2,\varepsilon}^{\gamma+1}}{\partial x_3} \,\mathrm{d}x_3 \,\mathrm{d}\sigma \\
&\quad = \frac{\mu_{2,\varepsilon}}{\varepsilon} \frac{\gamma}{\gamma+1} \int_0^T \int_{\tilde{\Gamma}_{1,3}} \left((u_{2,\varepsilon}^{\gamma+1})_{|x_3=\frac{\varepsilon}{2}} - (u_{2,\varepsilon}^{\gamma+1})_{|x_3=-\frac{\varepsilon}{2}} \right) \cdot \left(w_{|x_3=\frac{\varepsilon}{2}} - w_{|x_3=-\frac{\varepsilon}{2}} \right).
\end{aligned}$$

Therefore,

$$\lim_{\varepsilon\to 0} \mathcal{H}_2 = \lim_{\varepsilon\to 0} \frac{\mu_{2,\varepsilon}}{\varepsilon} \frac{\gamma}{\gamma+1} \int_0^T \int_{\tilde{\Gamma}_{1,3}} \left((u_{2,\varepsilon}^{\gamma+1})_{|x_3=\frac{\varepsilon}{2}} - (u_{2,\varepsilon}^{\gamma+1})_{|x_3=-\frac{\varepsilon}{2}} \right) \cdot \left(w_{|x_3=\frac{\varepsilon}{2}} - w_{|x_3=-\frac{\varepsilon}{2}} \right). \quad (2.35)$$

In order to conclude the proof, we state the following lemma, which is proven below.

Lemma 2.4.2. *The following limit holds uniformly in* $\tilde{\Gamma}_{1,3}$

$$w_{|x_3=\frac{\varepsilon}{2}} - w_{|x_3=-\frac{\varepsilon}{2}} \longrightarrow w_{|x_3=0^+} - w_{|x_3=0^-}, \qquad \text{as } \varepsilon \to 0. \quad (2.36)$$

Moreover,

$$\frac{\gamma}{\gamma+1} \left((u_{2,\varepsilon}^{\gamma+1})_{|x_3=\frac{\varepsilon}{2}} - (u_{2,\varepsilon}^{\gamma+1})_{|x_3=-\frac{\varepsilon}{2}} \right) \longrightarrow \frac{\gamma}{\gamma+1} \left((\tilde{u}^{\gamma+1})_{|x_3=0^+} - (\tilde{u}^{\gamma+1})_{|x_3=0^-} \right), \quad (2.37)$$

strongly in $L^2(0,T;L^2(\tilde{\Gamma}_{1,3}))$, *as* $\varepsilon \to 0$.

We may finally find the limit of the term $\mathcal{H}_2$, using Assumption (2.7), and applying Lemma 2.4.2 to Equation (2.35)

$$\begin{aligned}
&\frac{\mu_{2,\varepsilon}}{\varepsilon} \frac{\gamma}{\gamma+1} \int_0^T \int_{\tilde{\Gamma}_{1,3}} \left((u_{2,\varepsilon}^{\gamma+1})_{|x_3=\frac{\varepsilon}{2}} - (u_{2,\varepsilon}^{\gamma+1})_{|x_3=-\frac{\varepsilon}{2}} \right) \cdot \left(w_{|x_3=\frac{\varepsilon}{2}} - w_{|x_3=-\frac{\varepsilon}{2}} \right) \\
&\longrightarrow \tilde{\mu}_{1,3} \frac{\gamma}{\gamma+1} \int_0^T \int_{\tilde{\Gamma}_{1,3}} \left((\tilde{u}^{\gamma+1})_{|x_3=0^+} - (\tilde{u}^{\gamma+1})_{|x_3=0-} \right) \cdot \left(w_{|x_3=0^+} - w_{|x_3=0^-} \right),
\end{aligned}$$

as $\varepsilon \to 0$. Combining the above convergence to Equation (2.33) and Equation (2.34), we find the

limit of the divergence term as ε goes to 0,

$$\begin{aligned}
&\sum_{i=1}^{3} \mu_{i,\varepsilon} \int_0^T \int_{\Omega_{i,\varepsilon}} u_{i,\varepsilon} \nabla p_{i,\varepsilon} \cdot \nabla L_\varepsilon(w) \\
&\quad \longrightarrow \tilde{\mu}_1 \int_0^T \int_{\tilde{\Omega}_1} \tilde{u} \nabla \tilde{p} \cdot \nabla w + \tilde{\mu}_3 \int_0^T \int_{\tilde{\Omega}_3} \tilde{u} \nabla \tilde{p} \cdot \nabla w \\
&\qquad + \tilde{\mu}_{1,3} \frac{\gamma}{\gamma+1} \int_0^T \int_{\tilde{\Gamma}_{1,3}} \big((\tilde{u}^{\gamma+1})_{|x_3=0^+} - (\tilde{u}^{\gamma+1})_{|x_3=0^-} \big) \cdot \big(w_{|x_3=0^+} - w_{|x_3=0^-} \big),
\end{aligned}$$

which, together with Equations (2.29), (2.30), (2.31), and (2.32), concludes the proof.

□

We now turn to the proof of Lemma 2.4.2

Proof of Lemma 2.4.2. Since by definition $w(t,x) = \varphi(t)v(x)$, with $\varphi \in C^1([0,T))$ and $v \in E^*$, the uniform convergence in Equation (2.36) comes from the piece-wise differentiability of w.

A little bit trickier is the second convergence, *i.e.* Equation (2.37). We recall that on $\{x_3 = \pm\varepsilon/2\}$, $u_{2,\varepsilon}^{\gamma+1}$ coincides with $\mathcal{P}_\varepsilon(u_\varepsilon^{\gamma+1})$, since across the interfaces u_ε is continuous and $\mathcal{P}_\varepsilon(u_{i,\varepsilon}) = u_{i,\varepsilon}$, for $i = 1, 3$.

Let us recall that from Remark 2.4.1, we have

$$\big\|\mathcal{P}_\varepsilon(u_\varepsilon^{\gamma+1})\big\|_{L^2(0,T;H^1(\Omega\setminus\tilde{\Gamma}_{1,3}))} \leqslant C, \quad \text{and} \quad \big\|\partial_t\big(\mathcal{P}_\varepsilon(u_\varepsilon^{\gamma+1})\big)\big\|_{L^\infty(0,T;L^1(\Omega\setminus\tilde{\Gamma}_{1,3}))} \leqslant C.$$

Since we have the following embeddings

$$H^1(\Omega \setminus \tilde{\Gamma}_{1,3}) \subset\subset H^\beta(\Omega \setminus \tilde{\Gamma}_{1,3}) \subset L^1(\Omega \setminus \tilde{\Gamma}_{1,3}),$$

for every $\frac{1}{2} < \beta < 1$, upon applying Aubin-Lions lemma, Aubin [6], Lions [83], we obtain

$$\mathcal{P}_\varepsilon(u_\varepsilon^{\gamma+1}) \longrightarrow \tilde{u}^{\gamma+1}, \qquad \text{as } \varepsilon \to 0,$$

strongly in $L^2(0,T;H^\beta(\Omega \setminus \tilde{\Gamma}_{1,3}))$.

Thanks to the continuity of the trace operators $\mathcal{T}_\alpha : H^\beta(\tilde{\Omega}_\alpha \setminus \tilde{\Gamma}_{1,3}) \to L^2(\partial\tilde{\Omega}_\alpha)$, for $\frac{1}{2} < \beta < 1$ and $\alpha = 1, 3$, we finally recover that

$$\Big\|\mathcal{P}_\varepsilon(u_\varepsilon^{\gamma+1})_{|x_3=0^\pm} - \big(\tilde{u}^{\gamma+1}\big)_{|x_3=0^\pm}\Big\|_{L^2(0,T;L^2(\tilde{\Gamma}_{1,3}))} \leq C \big\|\mathcal{P}_\varepsilon(u_\varepsilon^{\gamma+1}) - \tilde{u}^{\gamma+1}\big\|_{L^2(0,T;H^\beta(\Omega\setminus\tilde{\Gamma}_{1,3}))} \to 0, \tag{2.38}$$

as $\varepsilon \to 0$. We recall that the trace vanishes on the external boundary, $\partial\Omega$, therefore we only consider the $L^2(0,T;L^2(\tilde{\Gamma}_{1,3}))$-norm.

Recalling that L is the length of Ω, trivially, we find the following estimate

$$\begin{aligned}
\left\|\mathcal{P}_\varepsilon(u_\varepsilon^{\gamma+1})_{|x_3=\pm\varepsilon/2} - \mathcal{P}_\varepsilon(u_\varepsilon^{\gamma+1})_{|x_3=0^\pm}\right\|^2_{L^2(0,T;L^2(\tilde{\Gamma}_{1,3}))} & \\
&= \int_0^T \int_{\tilde{\Gamma}_{1,3}} \left(\int_0^{\pm\varepsilon/2} \frac{\partial \mathcal{P}_\varepsilon(u_\varepsilon^{\gamma+1})}{\partial x_3} \right)^2 \\
&= \int_0^T \int_{\tilde{\Gamma}_{1,3}} \left(\int_L \frac{\partial \mathcal{P}_\varepsilon(u_\varepsilon^{\gamma+1})}{\partial x_3} \mathbb{1}_{[0,\pm\varepsilon/2]}(x_3) \right)^2 \\
&\leq \int_0^T \int_{\tilde{\Gamma}_{1,3}} \left(\int_L \left(\frac{\partial \mathcal{P}_\varepsilon(u_\varepsilon^{\gamma+1})}{\partial x_3} \right)^2 \int_L \left(\mathbb{1}_{[0,\pm\varepsilon/2]}(x_3) \right)^2 \right) \\
&\leqslant \frac{\varepsilon}{2} \|\nabla \mathcal{P}_\varepsilon(u_\varepsilon^{\gamma+1})\|_{L^2(0,T;L^2(\Omega\setminus\tilde{\Gamma}_{1,3}))} \\
&\leqslant \varepsilon\, C,
\end{aligned}$$

and combing it with Equation (2.38), we finally obtain Equation (2.37).

□

Remark 2.4.2. *Although not relevant from a biological point of view, let us point out that, in the case of dimension greater than 3, the analysis goes through without major changes. It is clear that the a priori estimates are not affected by the shape or the dimension of the domain (although some uniform constants C may depend on the dimension, this does not change the result in Lemma 2.3.1). The following methods, and in particular the definition of the extension operator and the functional space of test functions, clearly depends on the dimension, but the strategy is analogous for a d-dimensional cylinder with axis $\{x_1 = \cdots = x_{d-1} = 0\}$.*

Remark 2.4.3. *We did not consider the case of non-constant mobilities,* i.e. $\mu_{i,\varepsilon} := \mu_{i,\varepsilon}(x)$*, but continuity and boundedness are the minimal hypothesis to succeed in the proof.*

2.5 Conclusions and perspectives

We proved the convergence of a continuous model of cell invasion through a membrane when its thickness is converging to zero, hence giving a rigorous derivation of the effective transmission conditions already conjectured in Chaplain *et al.* [24]. Our strategy relies on the methods developed in Sanchez-Palencia [118], although we had to handle the difficulties coming from the nonlinearity and degeneracy of the system. A very interesting direction both from the biological and mathematical point of view, could be coupling the system to an equation describing the evolution of the MMP concentration. In fact, as observed in Chaplain *et al.* [24], the permeability coefficient can depend on the local concentration of MMPs, since it indicates the level of 'aggressiveness' at which the tumour is able to destroy the membrane and invade the tissue.

In a recent work by Giverso *et al.* [57], a formal derivation of the multi-species effective problem has been proposed. However, its rigorous proof remains an interesting and challenging open question. Indeed, introducing multiple species of cells, hence dealing with a cross-(nonlinear)-diffusion system, adds several challenges to the problem. As it is well-known, proving the existence of solutions to cross-diffusion systems with different mobilities is one of the most challenging and still open questions in the field. Nevertheless, even when dealing with the same constant mobility coefficients, the nature of the multi-species system (at least for dimension greater than one) usually requires strong compactness on the pressure gradient. We refer the reader to Gwiazda

et al. [59], Price and Xu [110] for existence results of the two-species model without membrane conditions.

Another direction of further investigation of the effective transmission problem (2.2) could be studying the so-called *incompressible limit*, namely the limit of the system as $\gamma \to \infty$. The study of this limit has a long history of applications to tumour growth models, and has attracted a lot of interest since it links density-based models to a geometrical (or free boundary) representation, *cf.* Kim and Požár [73], Perthame *et al.* [104].

Moreover, including the heterogeneity of the membrane in the model could not only be useful in order to improve the biological relevance of the model, but could bring interesting mathematical challenges, forcing to develop new methods or adapt already existent ones, Neuss-Radu and Jäger [96], from the parabolic to the degenerate case.

2.A Existence of weak solution of the initial problem

We prove in this appendix the existence of solution for System (2.1). Similarly to diffraction problems modelled by linear parabolic equations (see Section 3.13 in [**ladyvzenskaja1988linear**]), this result follows from the existence of solution for the Porous Medium Equation with discontinuous coefficients. Indeed, using a test function $w \in C^\infty(\Omega_T)$, solutions of the following weak formulation

$$\int_\Omega \partial_t u w + \mu(x) u \nabla u^\gamma \cdot \nabla w \, \mathrm{d}x = \int_\Omega u G(p) w \, \mathrm{d}x,$$

are actually solutions of the strong form (2.1). This is obtained from the fact that the interfaces $\Gamma_{i,i+1}$ (for $i = 1, 2$) are continuous and from the interface conditions.

Even though the proof of the existence of weak solutions follow the lines of Section 5.4 in [**vasquez**], we could not find a proof of this result in the case of discontinuous mobility coefficients in the literature, hence, for the sake of clarity, we give in this appendix the idea of the proof.

Theorem 2.A.1 (Existence of weak solutions for the initial problem)**.** *Assuming that $\mu_i > 0$ for $i = 1, 2, 3$, System (2.1) admits a weak solution $u \in L^1(\Omega_T)$ and $p \in L^1(0, T; H^1_0(\Omega))$.*

Proof. Step 1: Regularized problem. We first regularize the model to convert it into a non-degenerate parabolic model. We use a positive parameter n and define a positive initial condition

$$u_{0n} = u_0 + \frac{1}{n}. \tag{2.39}$$

Our regularized problem reads

$$\begin{cases} \partial_t u_{i,n} - \mu_i \nabla \cdot (B_n(u_{i,n}) \nabla p_{i,n}) = u_{i,n} G(p_{i,n}) & \text{in } (0,T) \times \Omega_i, \quad i = 1,2,3, \\ \mu_i u_{i,n} \nabla p_{i,n} \cdot \boldsymbol{n}_{i,i+1} = \mu_{i+1} u_{i+1,n} \nabla p_{i+1,n} \cdot \boldsymbol{n}_{i,i+1} & \text{on } (0,T) \times \Gamma_{i,i+1,}, \quad i = 1,2, \\ u_{i,n} = u_{i+1,n} & \text{on } (0,T) \times \Gamma_{i,i+1,}, \quad i = 1,2, \\ u_{i,n} = \frac{1}{n} & \text{on } (0,T) \times \partial\Omega, \end{cases} \tag{2.40}$$

where $B_n(\cdot)$ is a positive smooth function and $B_n(s) = \gamma s^{\gamma-1}$.

From results on diffraction problems from [**ladyvzenskaja1988linear**] we know that in weak form our regularized problem is only a quasi-linear parabolic PDE. Thus, from standard results on these equations, we can have the existence of a classical solution $u_n \in C^{1,2}(\Omega_T)$ of

Problem (2.40). Then, at this point the rest of the proof is similar to Section 5.4 in [**vasquez**]. We obtain at the end the existence of weak solutions $u \in L^1(\Omega_T)$ and $p \in L^1(0,T;H_0^1(\Omega))$ of Problem (2.1).

□

Part II

Reaction-diffusion membrane problems: existence of solutions and Turing instability analysis

In the previous Chapter 2, we derive nonlinear Kedem-Katchalsky conditions which closes effective problems defined by a porous medium dynamics. The same derivation can be done in the linear case, see for details Sanchez-Palencia [118]. We remember that this limit problem, defined on a zero-thickness membrane, is not only relevant and interesting from a biological point of view but also from a mathematical one, justified with the numerical analysis performed by Chaplain *et al.*. Here, we want to extend theoretical results on linear reaction-diffusion problems to the membrane case.

Chapter 3 is dedicated to the existence study for the effective interface problem in the linear case. Indeed, we study a reaction-diffusion membrane problem with Kedem-Katchalsky conditions. There is a huge literature concerning standard reaction-diffusion systems on a single domain. The existence problem is also a challenging question and we extend results from this standard theory to our membrane case. In particular, dealing with biological applications, we deepen an appropriate theory consisting of weak hypothesis both on the initial data, which are controlled in L^1, and on the nonlinearities, with a sub-quadratic growth.

Before presenting our results, we want to give the reader a background on standard results which are also useful to justify our following work.

Standard existence theory without membrane conditions. We show here the main theorems and ideas for the standard reaction-diffusion theory, useful for us to extend and build a theory also in the membrane case. We do not provide proofs, except for some ideas, but we will look at their readaptation in our specific membrane case in the following chapter.

We consider a general $m \times m$ reaction-diffusion system on a spatial multi-dimensional domain Ω, namely for all $i = 1, ..., m$

$$\begin{cases} \partial_t u_i - d_i \Delta u_i = f_i(u_1, ..., u_m), & \text{in } (0,T) \times \Omega, \\ \alpha_i \partial_n u_i + (1 - \alpha_i) u_i = 0, & \text{in } (0,T) \times \partial\Omega, \\ u_i(0, \cdot) = u_{i,0} \geqslant 0, \end{cases} \tag{2.41}$$

where $d_i > 0$, $\alpha_i \in [0,1]$, $\forall i = 1, ..., m$ and we assume for some constants $C_M, M > 0$ and for all $i = 1, ..., m$, for all $\mathbf{r} = (r_1, ..., r_m), \hat{\mathbf{r}} \in [0, +\infty)^m$,

$$\begin{aligned} & f_i(r_1, ..., r_{i-1}, 0, r_{i+1}, ..., r_m) \geqslant 0, \qquad \text{(quasi-positivity)}, \\ & |f_i(\boldsymbol{r}) - f_i(\hat{\boldsymbol{r}})| \leqslant C_M \ \textstyle\sum_{j=1}^m |r_j - r_j|, \quad \forall \boldsymbol{r}, \hat{\boldsymbol{r}} \in [0, M]^m. \end{aligned} \tag{2.42}$$

Even though they are standard, a huge literature about them highlight the interest and challenge in their study. Often systems in applications come naturally with the two properties related to reaction terms: quasi-positivity and mass-control structure, namely

$$\forall r \in [0, +\infty)^m, \ \forall i = 1, ..., m, \quad f_i(r_1, ..., r_{i-1}, 0, r_{i+1}, ..., r_m) \geqslant 0, \tag{2.43}$$

$$\forall r \in [0, +\infty)^m, \quad \sum_{1 \leqslant i \leqslant m} f_i(r) \leqslant C \left[1 + \sum_{1 \leqslant i \leqslant m} r_i \right], \tag{2.44}$$

which imply nonnegativity and mass-control of solutions. Moreover, nonlinearities are often quadratic. Therefore, in the interest of covering this common properties, Pierre and his collaborators [7, 10, 78, 79, 107] have deepened the question about global existence, when nonlinearities are also bounded in $L^1(Q_T)$. Some examples of reaction-diffusion systems with the previous prop-

erties are the Brussellator, problems of chemical reactions, Lotka-Volterra systems, describing interactions between prey and predators, systems modeling pollutants transfer in the atmosphere.

Even without the mass-control hypothesis (2.44), in his survey [107], Pierre proves an existence result of supersolutions for bounded L^1 nonlinearities.

Theorem 2.1.2. *Let $\boldsymbol{u}^n$ be a nonnegative solution of the approximate System (2.41) satisfying*

$$\sup_{n\geqslant 1, 1\leqslant i\leqslant m} \int_{Q_T} |f_i^n(\boldsymbol{u}^n)| < +\infty. \tag{2.45}$$

Assume that, for $i = 1, ..., m$, $u_{i,0}^n \to u_{i,0}$ in $L^1(\Omega)$. Then, as $n \to +\infty$, up to a subsequence, $\boldsymbol{u}^n$ converges in $L^1(Q_T)$ to a super-solution of System (2.41). Moreover, $u_i \in L^1(0, T, W_0^{1,1}(\Omega))$, in the case of Dirichlet homogeneous conditions.

Idea of the proof. The compactness results proved in Baras and Pierre [7], Bothe and Pierre [10] allows to have L^1-convergence for u. The lack of L^1-convergence of the nonlinearities obliges the introduction of a truncation operator which satisfies a reaction-diffusion inequality with controlled reaction in the limit. This is why we obtain a supersolution.

□

With the structure (2.43), (2.44), it is possible to deduce existence of global solutions of the reaction-diffusion system.

Theorem 2.1.3. *Besides (2.42), (2.44), the previous a priori hypothesis (2.45) holds. Let $u_0 \in L^1(\Omega)^m$, $u_0 \geqslant 0$. Then, System (2.41) has a global weak solution.*

Idea of the proof. Adding up the m equations of the approximate problem and applying Fatou's Lemma, we deduce the existence of a subsolution, which is then a solution, thanks to the previous theorem.

□

An interesting consequence of Theorem 2.1.3 is that global existence can be extended to systems with the structure (2.43), (2.44) and with at most quadratic nonlinearities. The idea is that (2.43), (2.44) imply also an *a priori* $L^2(Q_T)$-estimate on solutions, considering L^2 initial data, see Pierre [107, Proposition 5.13]. If the nonlinearities are at most quadratic, they are consequently bounded in $L^1(Q_T)$, and we can apply Theorem 2.1.3.

Theorem 2.1.4. *We assume (2.42), (2.44), and that the f_i are at most quadratic, i.e. there exists $C \geqslant 0$ such that $\forall i = 1, ..., m$, $\forall \mathbf{r} \in [0, +\infty)$,*

$$|f_i(\mathbf{r})| \leqslant C \left[1 + \sum_{i=1}^{m} r_i^2\right]. \tag{2.46}$$

For all nonnegative initial data $u_0 \in L^2(\Omega)^m$, there exists a global weak solution to System (2.41).

There are several difficulties in the construction of weak solutions for these parabolic problems. Firstly, f_i are often quadratic, and in this case we have seen that an L^1 bound is sufficient to have existence of weak solutions. Secondly, it is common to have an L^1 bound for the initial data, differently from Pierre's theory which uses L^2 control on the initial data. So, here we introduce the theory developed by Laamri and Perthame [78], which is an extension of the L^2 method by Pierre [107] previously seen.

Lemma 2.1.1. *Consider smooth functions $F, U : [0, +\infty) \times \Omega \to \mathbb{R}^+$, and $V : (0, +\infty) \times \Omega \to \mathbb{R}$ such that $\int_\Omega \Delta V(t, x)\, dx = 0$. Assume that $U_0 = U(t = 0, x) \in L^1(\Omega) \cap H^{-1}(\Omega)$ and that the differential relation holds with $B \geqslant 0$*

$$\begin{cases} \partial_t U - \Delta V = B - F \leqslant 0, & t \geqslant 0,\ x \in \Omega \subset \mathbb{R}^n \\ \partial_n U = 0, & \text{in } (0, +\infty) \times \partial\Omega \\ U(t = 0, x) = U_0 \geqslant 0, & \text{in } \Omega \end{cases} \tag{2.47}$$

Then, for some constants C depending on Ω, it holds the inequality

$$\int_0^T \int_\Omega UV \leqslant \frac{1}{2}\|U(T)\|^2_{H^{-1}} + \int_0^T \int_\Omega UV \leqslant K(T) + \frac{1}{2}\|U_0\|^2_{H^{-1}}, \tag{2.48}$$

where

$$K = \int_0^T \left[\, C\langle F\rangle + \langle V\rangle \,\right] \left[B|\Omega| t + \int_\Omega U_0 \right] dt, \quad \text{with } \langle F\rangle = \frac{1}{\Omega}\int_\Omega F\, dx.$$

Remark 2.1.1. *U and V are normally chosen as proportional to the sum of the densities of the m species u_i. We will see later on our choice in the case of a membrane problem.*

Idea of the proof. The proof is provided using the elliptic theory.

□

In Chapter 4, we analyse a well-known phenomena in reaction-diffusion equations: the formation of Turing patterns. Our study is again an extension to the membrane problem, but we recall briefly the main concepts in the classical theory, see for more details Murray [95], Perthame [106].

Standard Turing theory without membrane conditions. Diffusion has generally a stabilising effect. The novelty introduced by Turing is that, under certain conditions, adding diffusion in a system can create spatially inhomogeneous patterns, now called *diffusion-driven instability*. Let consider a simple counter-intuitive example of two chemical species u, v reacting together. Then, we have the system

$$\begin{cases} \frac{du}{dt} = au + bv \\ \frac{dv}{dt} = cu + dv, \end{cases} \tag{2.49}$$

with real coefficients a, b, c, d. We recall some definitions useful in the following.

Definition 2.1.1. *We consider the ordinary differential equation (ODE)*

$$\begin{aligned} &\tfrac{dz}{dt} = f(z), \qquad z \in \mathcal{D} \subset \mathbb{R}^n, \\ &z(0) = z_0. \end{aligned}$$

- *We say that $\overline{z} \in \mathcal{D}$ is an equilibrium point, or steady state, if $f(\overline{z}) = 0$.*
- *An equilibrium point is stable if for all $\varepsilon > 0$ such that the closed ball of radius ε centered in $\overline{z}$ is in $\mathcal{D}$, namely $\overline{B}_\varepsilon(\overline{z}) \subset \mathcal{D}$, there exists a $\delta \in (0, \varepsilon]$ such that $z(t) \in B_\varepsilon(\overline{z})$ for all $t \geqslant 0$ and $z_0 \in B_\delta(\overline{z})$.*
- *An equilibrium point is unstable if it is not stable.*

- *An equilibrium point is asymptotically stable if it is stable and for all* $z_0 \in B_\delta(\overline{z})$,

$$\lim_{t\to+\infty} z(t) = \overline{z}.$$

Stability of an equilibrium point can be verified looking at the spectrum of the matrix of the system. In particular, if all the eigenvalues have negative real part we talk of asymptotically stable equilibrium, whereas if there exists a positive real part eigenvalue we call it an unstable equilibrium.

So, System (2.49) has as equilibrium point $(\overline{u}, \overline{v}) = (0, 0)$. Looking at the matrix A of the system

$$A = \begin{pmatrix} a & b \\ c & d \end{pmatrix},$$

we assume that it has two eigenvalues with negative real part, namely we assume that its trace is negative and its determinant is positive, *i.e.*

$$\mathrm{tr}(A) = a + d < 0, \quad \det(A) = ad - bc > 0. \tag{2.50}$$

Consequently, we can affirm that $(\overline{u}, \overline{v})$ is an asymptotically stable point. Now we add diffusion. We get

$$\begin{cases} \partial_t u = D_u \Delta u + au + bv \\ \partial_t v = D_v \Delta v + cu + dv. \end{cases} \tag{2.51}$$

We have the same equilibrium point $(\overline{u}, \overline{v}) = (0, 0)$, but if $D_u \ll D_v$, it is unstable.

Theorem 2.1.5 (Turing instability theorem)**.** *We consider System* (2.51) *where we fix the domain* Ω*, the matrix* A *and* $D_v > 0$*. Assuming* (2.50) *with* $a > 0$ *(thus* u *is called an activator),* $d < 0$ *(thus* v *is called an inhibitor), then, for sufficiently small* D_u*, the steady state* $(0, 0)$ *is linearly unstable.*

Then, Turing instability happens with a short range activator and a long range inhibitor. We report a nice example given by Murray [95]. If we set a fire on a grass field without any inhibitor, the fire would spread uniformly. Now, we place several sprinklers on the grass and we set several fires. Then, if the range of diffusion of the fire is shorter than the one of the water from the sprinkler, the fire remains confined into several spots. So, different diffusion fronts generate patterns.

Idea of the proof. We will see later on a detailed proof in the case of a membrane, since the proof works also in that case. We remember only the main tool which is the Laplace eigenvalue problem $-\Delta w_k = \lambda_k w_k$, which allows to decompose u and v with the basis of eigenfunctions $\{w_k\}_{k\in\mathbb{N}}$. Looking for exponential in time solutions, we have to find conditions such that they explode in time to have instability. Moreover, for sufficiently small D_u, we can find the range of eigenvalues corresponding to the unstable ones.

□

We remember that we can find explicit expressions of the solutions of the Laplace problem on a domain [0,L]. For example, in the case of Neumann conditions, we have

$$\lambda_k = \left(\frac{\pi k}{L}\right)^2, \quad w_k(x) = \cos\left(\frac{\pi k x}{L}\right), \quad k \in \mathbb{N}.$$

Obviously, when Turing instability occurs, solutions can exhibit strange behaviours, but still they have to respect the characteristics here below.

Definition 2.1.2. *We say that an equilibrium forms Turing patterns if*

- *there is no blow-up,*
- *it is linearly unstable,*
- *there are no high-frequency oscillations, which corresponds to bounded unstable eigenfunctions (or unstable modes).*

Sometimes the presence of oscillations can mislead. This is the case of the backward-parabolic equation

$$\begin{cases} \partial_t u - \Delta A(u) = 0, & x \in \Omega, \\ \partial_n u = 0, & x \in \partial\Omega, \end{cases} \tag{2.52}$$

with $A'(u) < 0$. Indeed, we can calculate the eigenvalues of the Laplace problem, remarking that all of them can generate unstable modes, thus they can have high frequency. We can also observe numerically that unstable modes can have high oscillatory behaviour. Then, this does not respect the last point of the definition of Turing patterns, concluding that this is not Turing instability. We will see an example of this kind of system in Subsection 4.4.4.

Chapter 3

Existence of a global weak solution for a reaction-diffusion problem with membrane conditions

This chapter is adapted by permission from Springer: Springer, *J. Evol. Equ.*, *Existence of a global weak solution for a reaction-diffusion problem with membrane conditions*, Ciavolella G., Perthame B., Copyright (2021) https://doi.org/10.1007/s00028-020-00633-7.

3.1 Introduction

We analyse the existence of a global weak solution for a reaction-diffusion problem of m species which diffuse through a permeable membrane. This kind of problem is characterised by the so-called Kedem-Katchalsky conditions [72], see Section 1.3.

To describe the model, we consider, as depicted in Fig. 3.1, an inner transverse C^1 membrane $\Gamma^{1,3}$ separating a domain Ω in two connected sub-domains Ω^1 and Ω^3,

$$\Omega \;=\; \Omega^1 \cup \Omega^3 \subset \mathbb{R}^d, \quad d \geqslant 2, \qquad\qquad \Gamma^{1,3} = \partial\Omega^1 \cap \partial\Omega^3.$$

This is the same setting obtained in the limit in Chapter 2, Figure 2.1. We assume Ω^1 and Ω^3 to be piecewise C^1 domains. In order to set boundary conditions, we introduce $\Gamma^1 = \partial\Omega^1 \setminus \Gamma^{1,3}$ and $\Gamma^3 = \partial\Omega^3 \setminus \Gamma^{1,3}$. We assume that Γ^1 and Γ^3 are non-empty. We could also consider a different geometry such that Ω^1 includes Ω^3 and the membrane becomes the boundary of the inner domain (see for example Brezis [16], Li and Wang [80], Li *et al.* [82]). In contrast, the biological situation that we analyse is presented in Fig. 3.1 and that is why we leave open the problem with an inner domain.

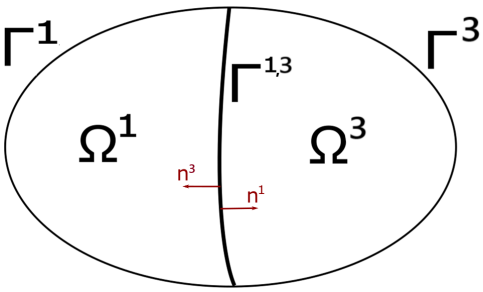

Figure 3.1: *Example of spatial domain Ω with an inner transverse membrane $\Gamma^{1,3}$ which decomposes Ω in open sets Ω^1 and Ω^3. The figure also shows the outward normals to the membrane.*

Ignoring a possible drift, the diffusion through the membrane is described by the system, for species $i = 1, .., m$,

$$\begin{cases} \partial_t u_i - D_i \Delta u_i = f_i(u_1, ..., u_m), & \text{in } Q_T := (0,T) \times \Omega, \\ u_i = 0, & \text{in } \Sigma_T := (0,T) \times (\Gamma^1 \cup \Gamma^3), \\ \partial_{\boldsymbol{n}^1} u_i^1 = \partial_{\boldsymbol{n}^1} u_i^3 = k_i(u_i^3 - u_i^1), & \text{in } \Sigma_{T,\Gamma} := (0,T) \times \Gamma^{1,3}, \\ u_i(0,x) = u_{0,i}(x) \geqslant 0, & \text{in } \Omega, \end{cases} \tag{3.1}$$

in which D_i and k_i are positive constants and $\boldsymbol{n}^\lambda$ is the outward normal of the domain Ω^λ for $\lambda = 1, 3$ such that $\boldsymbol{n}^3 = -\boldsymbol{n}^1$. In particular, we use the notation $\partial_{\boldsymbol{n}^1} u_i^\lambda = \nabla u_i^\lambda \cdot \boldsymbol{n}^1$. We denote each species density for $i = 1, ..., m$ with

$$u_i = \begin{cases} u_i^1, & \text{in } \Omega^1, \\ u_i^3, & \text{in } \Omega^3, \end{cases}$$

since each one lives in both sub-domains Ω^λ, for $\lambda = 1, 3$. There is a jump of u_i, $i = 1, ..., m$ across the membrane $\Gamma^{1,3}$ that we denote by $(u_i^3 - u_i^1) =: [\![u_i]\!]$. More precisely, for $x \in \Gamma^{1,3}$ and for all $i = 1, ..., m$, we define the trace in Sobolev sense

$$u_i^1(x) = \lim_{h \to 0^-} u_i(x + h\, \boldsymbol{n}^1(x)), \qquad u_i^3(x) = \lim_{h \to 0^-} u_i(x + h\, \boldsymbol{n}^3(x)).$$

The interest of this system stems from the boundary conditions. In fact, besides standard Dirichlet boundary condition on Γ^λ, for $\lambda = 1, 3$, we have used the Kedem-Katchalsky membrane conditions [72] on $\Gamma^{1,3}$. These conditions are made up by two principles (see Section 1.3): the conservation of mass, which brings to flux continuity, and the dissipation principle such that the L^2-norm of the solution is decreasing in time. This last property gives us that the flux is proportional to the jump of the density through the membrane with proportionality coefficient k_i, the membrane permeability constant.

For the applications we have in mind, System (3.1) has mass control, membrane conditions are conservative, and we are interested in developing a theory of weak solutions based on this L^1 bound even if the reaction terms are, for instance, quadratic. For usual reaction-diffusion systems, such a theory has been developed in a series of papers initiated by Pierre and developed later by several authors, as recalled at the beginning of Part II. In particular, we extend, to the case of membrane conditions, the method proposed by Pierre in [7, 10, 107] and extended by

Laamri and Pierre [79], Laamri and Perthame [78]. This method develops a theory to treat high order nonlinearities and low regularity initial data compatible with the natural L^1 regularity of solutions. Moreover, we show that for all $i = 1, ..., m$, $\lambda = 1, 3$, $u_i^\lambda \in W^{1,1}(\Omega^\lambda)$ (and even better), but it does not have L^1 derivatives in the whole Ω. In any case, since u_i, $i = 1, ..., m$ is a Sobolev function in Ω^1 and Ω^3, the trace makes sense in $\partial\Omega$ and thus the definition of the jumps $[\![u_i]\!]$, $i = 1, ..., m$ is meaningful. Finally, we define $\boldsymbol{u} = (u_1, ..., u_m)$ the vector solution which is characterized by nonnegative components and, as we will see later on, they are naturally L^1 functions but not L^2. One of the difficulties of a membrane problem is to derive an $L^2(Q_T)$ estimate.

In this chapter, we prove analytical results concerning existence and regularity of solutions in the case of the reaction-diffusion systems with Kedem-Katchalsky conditions (3.1). The chapter is composed of two sections. In Section 3.2, we introduce the assumptions and our main result about global existence of a weak solution for the Problem (3.1) with related lemmas. We also present a specific example in order to give a more concrete idea of the type of systems of interest for us. In Section 3.3, we prove this result introducing the approximate model of (3.1) (Subsection 3.3.1), proving and applying an a priori L^2 estimate on the solution (Subsection 3.3.2), proving a theorem about the existence of a supersolution of (3.1) (Subsection 3.3.3) and a second one on the existence of a solution (Subsection 3.3.4). At the end of this chapter, the reader can find three Appendices. Appendix 3.A and Appendix 3.B contain the proof of a regularity and compactness lemma useful in the third step of the proof of our main result. Appendix 3.C provides Sobolev and Poincaré embeddings in the case of membrane conditions and, in general, of non-uniform zero boundary conditions.

3.2 Assumptions and main results

3.2.1 Assumptions

We gather several assumptions on the reaction term $\mathbf{f}(\mathbf{u}) = (f_1(\mathbf{u}), ..., f_m(\mathbf{u}))$ that are used separately throughout the paper. With some constants C, C_M and $M > 0$, we assume that for all $i = 1, ..., m$ and for all $\boldsymbol{u} = (u_1, ..., u_m) \in [0, +\infty)^m$,

$$|f_i(\boldsymbol{u})| \leqslant C\Big(1 + \sum_{j=1}^{m} u_j^2\Big), \qquad \text{(sub-quadratic growth)}, \tag{3.2}$$

$$\sum_{j=1}^{m} f_j(\boldsymbol{u}) \leqslant C\Big(1 + \sum_{j=1}^{m} u_j\Big), \qquad \text{(mass control)}, \tag{3.3}$$

$$f_i(u_1, ..., u_{i-1}, 0, u_{i+1}, ..., u_m) \geqslant 0, \qquad \text{(quasi-positivity)}, \tag{3.4}$$

$$|f_i(\boldsymbol{u}) - f_i(\boldsymbol{v})| \leqslant C_M \sum_{j=1}^{m} |u_j - v_j|, \qquad \forall \boldsymbol{u}, \boldsymbol{v} \in [0, M]^m. \tag{3.5}$$

Thanks to assumption (3.4), solutions u_i are nonnegative, and (3.3) provides us with mass control since the total integral of the solution is bounded with exponential growth in time.

We do not consider that the f_i's depend on $(x, t) \in Q_T$, but we could extend these assumptions also to that case. We rather give an example modeling intracellular transport phenomena, Cangiani and Natalini [21], Dimitrio [40], Serafini [120], in order to understand the class of sys-

tems that we have in mind. Molecule trafficking across the nuclear envelope has been studied using reaction-diffusion equations with Kedem-Katchalsky conditions. Small molecules can pass through nuclear pore complexes (NPCs). The translocation of larger molecules is allowed by a system for active transport across the NPCs. The cargo protein binds to a nucleocytoplasmic transport receptor known as importin, which mediates the transport throught the nuclear envelope. The energy needed is provided by the Ran complex. In order to reproduce this intracellular dynamics, Cangiani and Natalini proposed a model in [21]. We denote by Ω^n and Ω^c respectively the nuclear and the cytoplasmic compartment with $\Gamma^{nc} = \partial\Omega^n$ the interface between them. In each compartment, we can write a system of coupled reaction-diffusion equations of type

$$\begin{cases} \partial_t R_t = d_r \Delta R_t + f_{rt}(R_t, T, T_r), \\ \partial_t R_d = d_r \Delta R_d + f_{rd}(R_t), \\ \partial_t T_r = d_{tr} \Delta T_r + f_{tr}(R_t, T, T_r), \\ \partial_t C = d_c \Delta C + f_c(C, T), \\ \partial_t T = d_t \Delta T + f_t(R_t, T, T_r, C), \\ \partial_t T_c = d_{tc} \Delta T_c + f_{tc}(C, T). \end{cases} \tag{3.6}$$

The two systems are coupled through Neumann homogeneous boundary conditions and Kedem-Katchalsky transmission conditions. Reactions have at most quadratic growth and they satisfy hypothesis (3.2)–(3.5). This is only an example of a biological system satisfying our assumptions. Its relevance will bring us to develop numerical results aiming to study biological phenomena fitting with the theory presented in this chapter.

3.2.2 Main result

The aim is to prove global existence when the f_i's are at most quadratic and for a membrane problem as (3.1). As mentioned before, we follow the literature concerning existence results for reaction-diffusion systems by Pierre *et al.* [7, 10, 107], by Laamri and Pierre [79] and by Laamri and Perthame [78]. A local result in the case of membrane conditions is available but taking into account local Lipschitz reaction terms with $u_0 \in H^s$, for $s > \frac{d}{2}$ (e.g. Serafini [120]).

Our main contribution is the following global existence theorem with initial data of low regularity and reaction terms at most quadratic. We first enunciate some definitions and introduce the appropriate test functions space for our problem. We recall that

$$Q_T = (0,T) \times \Omega, \quad \Sigma_T = (0,T) \times (\Gamma^1 \cup \Gamma^3), \quad \Sigma_{T,\Gamma} = (0,T) \times \Gamma^{1,3}.$$

Definition 3.2.1. *For $i = 1, ..., m$, we define the space of test functions*

$$\begin{aligned} \mathcal{D}_i := \big\{ \quad & (\psi^1, \psi^3) \in C^\infty([0,T] \times \overline{\Omega^1}) \times C^\infty([0,T] \times \overline{\Omega^3}), \\ & \psi \geqslant 0,\ \psi(\cdot, T) = 0,\ \psi = 0 \text{ in } \Sigma_T,\ \partial_{\boldsymbol{n}^1} \psi^1 = \partial_{\boldsymbol{n}^1} \psi^3 = k_i(\psi^3 - \psi^1) \text{ in } [0,T] \times \Gamma^{1,3} \big\}, \end{aligned}$$

where $\psi = \begin{cases} \psi^1, & \text{in } \Omega^1, \\ \psi^3, & \text{in } \Omega^3. \end{cases}$

We investigate the existence of a global weak solution of System (3.1) defined by duality as

Definition 3.2.2. *We define a weak solution of System (3.1) as a function $\boldsymbol{u} = (u_1, ..., u_m)$ such*

that for all $T > 0$ and $i = 1, ..., m$, $u_i \in L^1(Q_T)$, $f_i(\boldsymbol{u}) \in L^1(Q_T)$ and for $\psi \in \mathcal{D}_i$, it holds

$$-\int_\Omega \psi(0,x)u_{0,i} + \int_{Q_T} u_i(-\partial_t\psi - D_i\Delta\psi) = \int_{Q_T} \psi f_i. \tag{3.7}$$

We consider the space $\mathbf{H^1}$ and its dual as in Definitions 3.2.3 and 3.2.4.

Theorem 3.2.1 (Existence and regularity)**.** *Assume (3.2)-(3.5) and that $k_1 = ... = k_m$. Then, for all $\boldsymbol{u}_0 = (u_{0,1}, ..., u_{0,m})$, such that $\boldsymbol{u}_0 \in (L^1(\Omega)^+ \cap (\mathbf{H^1})^*)^m$, System (3.1) has a nonnegative global weak solution in the sense of Definition 3.2.2 which satisfies for all $T > 0$ and $i = 1, ..., m$,*

$$u_i \in L^2(Q_T) \quad \text{and} \quad (1+|u_i|)^\alpha \in L^2\big(0,T;H^1(\Omega)\big), \qquad \forall \alpha \in \left[0, \frac{1}{2}\right), \tag{3.8}$$

$$u_i \in L^\beta\big(0,T;W^{1,\beta}(\Omega)\big) \quad \text{and} \quad u_i \in L^\beta\big(0,T;L^\beta(\Gamma^{1,3})\big), \qquad \forall \beta \in \left[1, \frac{d}{d-1}\right). \tag{3.9}$$

3.2.3 Preliminary lemmas and proof organisation

In order to prove this result, we follow four main steps according to Pierre's method.

First step. Regularization process. We build a regularized problem with a nonnegative classical global solution $\boldsymbol{u}^n$.

Second step. An L^2 lemma. We extend the Laamri-Perthame [78] a priori L^2 estimate of the solution given an L^1 initial data to the case of membrane conditions (see Subsection 3.3.2). In particular, we gain

Lemma 3.2.1 (Key estimate with L^1 data and membrane conditions)**.** *Consider smooth functions $z_i : [0,+\infty) \times \Omega \to \mathbb{R}^+$, $f_i : [0,+\infty)^m \to \mathbb{R}$, for all $i = 1, ..., m$, with f_i satisfying the assumption (3.3). Assume $z_{0,i} \in L^1(\Omega) \cap (\mathbf{H^1})^*$ and that the equation holds with $k_i = k$*

$$\begin{cases} \partial_t z_i - D_i\Delta z_i = f_i(z_1, ..., z_m), & \text{in } Q_T, \\ z_i = 0, & \text{in } \Sigma_T, \\ \partial_{\boldsymbol{n}^1} z_i^1 = \partial_{\boldsymbol{n}^1} z_i^2 = k_i(z_i^2 - z_i^1), & \text{in } \Sigma_{T,\Gamma^{1,3}}, \\ z(0,x) = z_{0,i}(x) \geqslant 0, & \text{in } \Omega. \end{cases} \tag{3.10}$$

Then, for some constant C_3 depending on $\|\boldsymbol{z}_0\|_{(\mathbf{H^1})^*}$, the inequality holds

$$\sum_{i=1}^m \int_{Q_T} |z_i|^2 \leqslant C_3.$$

From this lemma we derive an L^1 bound for the reaction term $\boldsymbol{f}^n(\boldsymbol{u}^n)$ of the regularized system thanks to (3.2). The proof uses the solution of an elliptic problem $-\Delta w = f$ with membrane conditions which has a unique solution thanks to the Lax-Milgram theorem (see Evans [45, Section 6.2.1]) and we recall its statement in our context.

We assume H a real Hilbert space with norm $\|\cdot\|$ and inner product $(\cdot,\cdot)$. Let $\langle\cdot,\cdot\rangle$ denote the pairing of H with its dual space.

Theorem 3.2.2 (Lax-Milgram theorem)**.** *Given $B : H \times H \to \mathbb{R}$, a bilinear mapping for which there exist constants $\gamma, \delta > 0$ such that for all $w, z \in H$,*

$$|B[w,z]| \leqslant \gamma \|w\| \, \|z\| \quad \textit{(continuity)}\,, \qquad |B[w,w]| \geqslant \delta \|w\|^2 \quad \textit{(coercivity)}.$$

Finally, let $f : H \to \mathbb{R}$ be a bounded linear functional on H. Then there exists a unique $w \in H$ such that

$$B[w,z] = \langle f, z \rangle, \quad \forall z \in H.$$

We can apply the Lax-Milgram theorem for membrane problems (see Serafini [120]). In order to justify this, we introduce some definitions. The first ones concern the space $H = \mathbf{H^1}$ under consideration, the second is the bilinear form.

Definition 3.2.3. *We define $\mathbf{H^1} = H^1_{0,\Gamma}(\Omega^1) \times H^1_{0,\Gamma}(\Omega^3)$ as the Hilbert space of functions $H^1(\Omega^1) \times H^1(\Omega^3)$ satisfying Dirichlet homogeneous conditions on Γ^λ, $\lambda = 1, 3$. We endow it with the norm*

$$\|w\|_{\mathbf{H^1}} = \left(\|w^1\|^2_{H^1(\Omega^1)} + \|w^3\|^2_{H^1(\Omega^3)} \right)^{\frac{1}{2}}.$$

We let $(\cdot,\cdot)$ be the inner product in $\mathbf{H^1}$ and $\langle \cdot, \cdot \rangle$ denote the pairing of $\mathbf{H^1}$ with its dual space.

Definition 3.2.4. *We introduce the dual space of $\mathbf{H^1}$ as $(\mathbf{H^1})^* = \left(H^1_{0,\Gamma}(\Omega^1) \times H^1_{0,\Gamma}(\Omega^3) \right)^* = H^1_{0,\Gamma}(\Omega^1)^* \times H^1_{0,\Gamma}(\Omega^3)^*$.*

Now, we define a proper bilinear form associated to the Laplacian operator considering Dirichlet conditions on Γ^λ, $\lambda = 1, 3$ and membrane conditions on $\Gamma^{1,3}$.

Definition 3.2.5. *We consider the continuous, coercive bilinear form $B : \mathbf{H^1} \times \mathbf{H^1} \to \mathbb{R}$, such that*

$$B[w,z] = \int_\Omega \nabla w \nabla z + \int_{\Gamma^{1,3}} k_i (w^3 - w^1)(z^3 - z^1), \quad \textit{for } w, z \in \mathbf{H^1}.$$

We can readily check continuity and coercivity.
B is continuous: thanks to the Cauchy-Schwarz inequality and the continuity of the trace, we can write

$$\begin{aligned} |B[w,z]| &\leqslant \sum_{1 \leqslant \lambda \leqslant 3} \|\nabla w^\lambda\|_{L^2(\Omega^\lambda)} \|\nabla z^\lambda\|_{L^2(\Omega^\lambda)} + C k_i \| [\![w]\!] \|_{L^2(\Gamma^{1,3})} \| [\![z]\!] \|_{L^2(\Gamma^{1,3})} \\ &\leqslant \sum_{1 \leqslant \lambda, \sigma \leqslant 3} \left(\|w^\lambda\|_{H^1(\Omega^\lambda)} \|z^\lambda\|_{H^1(\Omega^\lambda)} + C k_i \|w^\lambda\|_{H^1(\Omega^\lambda)} \|z^\sigma\|_{H^1(\Omega^\sigma)} \right) \\ &\leqslant C \|w\|_{\mathbf{H^1}} \|z\|_{\mathbf{H^1}}. \end{aligned}$$

B is coercive: indeed, we can estimate

$$B[w,w] = \int_\Omega |\nabla w|^2 + \int_{\Gamma^{1,3}} k_i |w^3 - w^1|^2 \geqslant C \|w\|^2_{\mathbf{H^1}},$$

since, thanks to the Dirichlet conditions on Γ^λ, $\lambda = 1, 3$, and to Theorem 3.C.3, we have

$$\|w^\lambda\|_{H^1(\Omega^\lambda)} \leqslant C \|\nabla w^\lambda\|_{L^2(\Omega^\lambda)}, \quad \text{for } \lambda = 1, 3.$$

Therefore, using the Lax-Milgram theorem, taking an L^2 right-hand side, the elliptic membrane problem has a unique solution $w \in \mathbf{H^1}$ and, thanks to the Riesz–Fréchet representation theorem

(Brezis [15, Theorem 5.5]) and to the equivalence of the norm $B[w,w]^{\frac{1}{2}}$ and the original one in $\mathbf{H^1}$, we have

$$\|f\|_{(\mathbf{H^1})^*} = B[w,w]^{\frac{1}{2}}. \tag{3.11}$$

Moreover, throughout the paper, we are also allowed to integrate by parts functions in the Hilbert space $\mathbf{H^1}$, considering also the membrane.

Third step. Existence of a global weak supersolution. We prove a first theorem which asserts the convergence in $L^1(Q_T)$ of $\boldsymbol{u}^n$ to a supersolution of System (3.1). Another central result is the following compactness lemma which explains the regularity stated in Theorem 3.2.1 (see Appendix 3.A and 3.B),

Lemma 3.2.2 (A priori bounds)**.** *We consider w solution of the problem in dimension $d \geqslant 2$*

$$\begin{cases} \partial_t w - D\Delta w = f, & \text{in } Q_T, \\ w = 0, & \text{in } \Sigma_T, \\ \partial_{\boldsymbol{n}^1} w^1 = \partial_{\boldsymbol{n}^1} w^3 = k(w^3 - w^1), & \text{in } \Sigma_{T,\Gamma}, \\ w(0,x) = w_0(x) \geqslant 0, & \text{in } \Omega, \end{cases} \tag{3.12}$$

with $f \in L^1(Q_T)$ and $w_0 \in L^1(\Omega)$. Then,

- $w \in L^\beta\big(0,T;W^{1,\beta}(\Omega)\big)$, $\forall \beta \in \Big[1, \frac{d}{d-1}\Big)$ *and* $(1+|w|)^\alpha \in L^2\big(0,T;H^1(\Omega)\big)$ *for* $\alpha \in \big[0, \frac{1}{2}\big)$.
- *The mapping $(w_0, f) \longmapsto w$ is compact from $L^1(\Omega) \times L^1(Q_T)$ into $L^1\big(0,T;L^{\gamma_1}(\Omega)\big)$, for all $\gamma_1 < \frac{d}{d-2}$ and $L^{\gamma_2}(Q_T)$ for all $\gamma_2 < \frac{2+d}{d}$.*
- *The trace mapping $(w_0, f) \longmapsto Tr_\Gamma(w) \in L^\beta\big(0,T;L^\beta(\Gamma^{1,3})\big)$, $\beta \in \Big[1, \frac{d}{d-1}\Big)$ is also compact.*

Fourth step. Existence of a global weak solution. We conclude with a second theorem asserting the convergence in $L^1(Q_T)$ of u_i^n, $i = 1, ..., m$ to a solution of System (3.1).

3.3 Proof of the existence result

We are now ready to prove Theorem 3.2.1 according to the previous steps.

3.3.1 Regularized problem

First of all, we approximate the initial data and the reaction term as

$$u_{0,i}^n := \varphi_{\delta_n} * \inf\{u_{0,i}, n\} \quad \text{and} \quad f_i^n(\mathbf{u}^n) := \frac{f_i(\mathbf{u}^n)}{1 + \frac{1}{n}\sum_{1\leqslant j\leqslant m} |f_j(\mathbf{u}^n)|}. \tag{3.13}$$

For the initial data, we consider a regularized version thanks to a convolution with a mollifier sequence φ_{δ_n} which is only used to assert existence in the framework of Serafini [120]. We readily check that $\boldsymbol{f}^n$ satisfies assumptions (3.2)-(3.5). In particular, for (3.5), there is a C_M such that

$$|f_i^n(\boldsymbol{u}) - f_i^n(\boldsymbol{v})| \leqslant C_M \sum_{i=1}^m |u_i - v_i|, \quad \forall \boldsymbol{u}, \boldsymbol{v} \in [0,M]^m. \tag{3.14}$$

Moreover, we have

$$|f_i^n| \leqslant n \quad \text{and} \quad \epsilon_M^n := \sup_{\boldsymbol{u}\in[0,M]^m, i=1,2} |f_i^n(\boldsymbol{u}) - f_i(\boldsymbol{u})| \leqslant \frac{C(M)m}{n}. \tag{3.15}$$

We consider an approximation of System (3.1), for all $i = 1, ..., m$,

$$\begin{cases} \partial_t u_i^n - D_i \Delta u_i^n = f_i^n(u_1^n, ..., u_m^n), & \text{in } Q_T, \\ u_i^n = 0, & \text{in } \Sigma_T, \\ \partial_{\boldsymbol{n}^1} u_i^{n,1} = \partial_{\boldsymbol{n}^1} u_i^{n,3} = k_i(u_i^{n,3} - u_i^{n,1}), & \text{in } \Sigma_{T,\Gamma}, \\ u_i^n(0,x) = u_{0,i}^n(x), & \text{in } \Omega. \end{cases} \tag{3.16}$$

Since $\boldsymbol{f}^n$ is uniformly bounded for fixed n, from Serafini [120] we know that there exists a global classical solution $\boldsymbol{u}^n = (u_1^n, ..., u_m^n)$ to (3.16).

3.3.2 The L^2 lemma with membrane conditions

The second step of the proof is to apply to u_i^n, $i = 1, ..., m$ the following Laamri-Perthame [78] version of Pierre's lemma, adding our membrane conditions.

Lemma 3.3.1 (Key estimate with L^1 data and membrane conditions)**.** *Consider smooth functions $z_i : [0, +\infty) \times \Omega \to \mathbb{R}^+$, $f_i : [0, +\infty)^m \to \mathbb{R}$, for all $i = 1, ..., m$, with f_i satisfying the assumption (3.3). Assume $z_{0,i} \in L^1(\Omega) \cap (\mathbf{H^1})^*$ and that the differential equation holds*

$$\begin{cases} \partial_t z_i - D_i \Delta z_i = f_i(z_1, ..., z_m), & \text{in } Q_T, \\ z_i = 0, & \text{in } \Sigma_T, \\ \partial_{\boldsymbol{n}^1} z_i^1 = \partial_{\boldsymbol{n}^1} z_i^2 = k_i(z_i^2 - z_i^1), & \text{in } \Sigma_{T,\Gamma}, \\ z(0,x) = z_{0,i}(x) \geqslant 0, & \text{in } \Omega, \end{cases} \tag{3.17}$$

with $k_i = k$. Then, for some constant C_3 depending on $\|\boldsymbol{z}_0\|_{(\mathbf{H^1})^*}$, the inequality holds

$$\sum_{i=1}^m \int_{Q_T} |z_i|^2 \leqslant C_3.$$

It is an open problem to extend it to the case where the constants k_i are different and it is also noticeable that the other proofs (time integration or duality) also apply only with the condition $k_i = k$.

Proof. We consider $\widehat{u}_i = e^{-Ct} z_i$ for $i = 1, ..., m$, where C is the same constant than in (3.3). Substituting in the equation for z_i, we obtain that for all $i = 1, ..., m$,

$$\partial_t \widehat{u}_i - D_i \Delta \widehat{u}_i = e^{-Ct}[f_i(z_1, ..., z_m) - C z_i],$$

with the same boundary and initial conditions as in (3.17) but for $\widehat{u}_i$. Adding up and defining

$$\widehat{U} = \sum_{i=1}^m \widehat{u}_i, \qquad \widehat{V} = \sum_{i=1}^m D_i \widehat{u}_i,$$

we obtain

$$\partial_t \widehat{U} - \Delta \widehat{V} = e^{-Ct}[\sum_{i=1}^{m} f_i(z_1, ..., z_m) - C\sum_{i=1}^{m} z_i] \leqslant Ce^{-Ct} \leqslant C, \quad \text{in } Q_T \tag{3.18}$$

with conditions

$$\begin{cases} \widehat{U} = 0, & \text{in } \Sigma_T, \\ \partial_{\boldsymbol{n}^1} \widehat{U}^1 = \partial_{\boldsymbol{n}^1} \widehat{U}^3 = k(\widehat{U}^3 - \widehat{U}^1), & \text{in } \Sigma_{T,\Gamma}, \\ \widehat{U}(0,x) = \widehat{U}_0(x) \geqslant 0, & \text{in } \Omega. \end{cases}$$

Thanks to the Lax-Milgram theorem 3.2.2 (see also Brezis*et al.* [16]), we may define the solution of

$$\begin{cases} -\Delta \widehat{W} = \widehat{U}, & \text{in } Q_T \\ \widehat{W} = 0, & \text{in } \Sigma_T, \\ \partial_{\boldsymbol{n}^1} \widehat{W}^1 = \partial_{\boldsymbol{n}^1} \widehat{W}^3 = k(\widehat{W}^3 - \widehat{W}^1), & \text{in } \Sigma_{T,\Gamma}. \end{cases}$$

So, at this point, with $\underline{G} = \partial_t \widehat{W} + \widehat{V}$, we can write (3.18) as an elliptic inequality

$$\begin{cases} -\Delta \underline{G} \leqslant C, & \text{in } Q_T, \\ \underline{G} = 0, & \text{in } \Sigma_T, \\ \partial_{\boldsymbol{n}^1} \underline{G}^1 = \partial_{\boldsymbol{n}^1} \underline{G}^3 & = k(\partial_t \widehat{W}^3 - \partial_t \widehat{W}^1) + k\sum\limits_{i=1}^{m} D_i(\widehat{u}_i^3 - \widehat{u}_i^1) \\ & = k[\partial_t \widehat{W}] + k[\widehat{V}] = k(\underline{G}^3 - \underline{G}^1), \quad \text{in } \Sigma_{T,\Gamma}. \end{cases}$$

Lax-Milgram theorem 3.2.2 allows us to state the existence of a function $G \in \mathbf{H}^1$ satisfying the system

$$\begin{cases} -\Delta G = C, & \text{in } Q_T, \\ G = 0, & \text{in } \Sigma_T, \\ \partial_{\boldsymbol{n}^1} G^1 = \partial_{\boldsymbol{n}^1} G^2 = k(G^2 - G^1), & \text{in } \Sigma_{T,\Gamma}. \end{cases}$$

By comparison theorem, Serafini [120], we conclude that $\underline{G} \leqslant G$, in $\overline{Q}_T$. So, multiplying $\underline{G}$ by $\widehat{U}$ and integrating over space, we compute, since $\widehat{U} = -\Delta \widehat{W}$ and $\underline{G} \leqslant G$,

$$\int_\Omega \widehat{U}\underline{G} = -\int_\Omega \Delta \widehat{W} \partial_t \widehat{W} \; + \int_\Omega \widehat{U}\widehat{V} \leqslant \int_\Omega \widehat{U} G \leqslant \int_\Omega \frac{D\widehat{U}^2}{2} + \frac{G^2}{2D} \leqslant \frac{1}{2}\int_\Omega \widehat{U}\widehat{V} + C_1,$$

thanks to Young's inequality applied to $\sqrt{D}\widehat{U}$ and $\frac{G}{\sqrt{D}}$ with $D = \min_{i=1,...,m} D_i > 0$, see Brezis [15], the fact that by definition $D\widehat{U} \leqslant \widehat{V}$, and the L^2-bound of G. Then, reorganising the terms on the right and left hand-side, we derive

$$-\int_\Omega \Delta \widehat{W} \partial_t \widehat{W} \; + \frac{1}{2}\int_\Omega \widehat{U}\widehat{V} \leqslant C_1.$$

Following Subsection 3.2.3 and the definition of the Hilbert space $\mathbf{H^1}$ (see Definition 3.2.3), we

can integrate by parts obtaining

$$\frac{1}{2}\frac{d}{dt}\int_\Omega |\nabla \widehat{W}|^2 \ + \ \frac{1}{2}\int_\Omega \widehat{U}\widehat{V} \ \leqslant \ \int_{\partial\Omega} \partial_n \widehat{W}\partial_t \widehat{W} + C_1.$$

Next, we remark that

$$\begin{aligned}\int_0^T\int_{\partial\Omega} \partial_n \widehat{W}\partial_t \widehat{W} \ &= \int_0^T\int_{\Gamma^{1,3}} \partial_{\boldsymbol{n}^1} \widehat{W}^1(\partial_t \widehat{W}^1 - \partial_t \widehat{W}^3)\\ &= -\int_0^T\int_{\Gamma^{1,3}} k(\widehat{W}^3 - \widehat{W}^1)\partial_t(\widehat{W}^3 - \widehat{W}^1) = -\frac{k}{2}\int_0^T \frac{d}{dt}\int_{\Gamma^{1,3}} (\widehat{W}^3 - \widehat{W}^1)^2.\end{aligned}$$

Therefore, integrating in time and using the relation (3.11), we arrive to

$$\frac{1}{2}\|\widehat{U}(T)\|^2_{(\mathbf{H^1})^*} \ + \ \frac{1}{2}\int_{Q_T} \widehat{U}\widehat{V} \ \leqslant \ \frac{1}{2}\|\widehat{U}_0\|^2_{(\mathbf{H^1})^*} + C_1. \tag{3.19}$$

Finally, thanks to Equation (3.19), we can assert that

$$\sum_{i=1}^m D_i \int_{Q_T} {\widehat{u_i}}^2 \leqslant C_2.$$

This concludes the proof of Lemma 3.3.1 since $z_i^2 = e^{2Ct}{\widehat{u_i}}^2$.

□

3.3.3 Existence of a global weak supersolution

At this point we can complete the existence result of Theorem 3.2.1, since, thanks to Lemma 3.3.1 and to assumption (3.2), we know that the reaction term $\boldsymbol{f}^n$ is bounded in L^1. With this in hands, we can assert the existence of a supersolution of System (3.1).

Theorem 3.3.1 (Existence of a supersolution)**.** *Let $\boldsymbol{u}^n = (u_1^n, ..., u_m^n)$ be a nonnegative solution of the approximate System (3.16). Consider $k_1 = ... = k_m$. As defined in (3.13), $f_i^n(\boldsymbol{u}^n)$ is bounded in $L^1(Q_T)$, for $i = 1, ..., m$ and $\mathbf{u}_0^n \to \mathbf{u}_0$ in $L^1(\Omega)$. Then, up to a sub-sequence, $\boldsymbol{u}^n$ converges in $L^1(Q_T)$ and a.e. to a supersolution $\boldsymbol{u}$ of System (3.1) which means that for $i = 1, ..., m$, and $\beta \in \left[1, \frac{d}{d-1}\right)$,*

$$f_i(\boldsymbol{u}) \in L^1(Q_T), \quad u_i \in L^\beta\big(0,T; W^{1,\beta}(\Omega)\big), \quad Tr_\Gamma(u_i) \in L^\beta\big(0,T; L^\beta(\Gamma^{1,3})\big),$$

$$-\int_\Omega \psi(0,x)u_{0,i} + \int_{Q_T}(-\psi_t u_i + D_i\nabla\psi\nabla u_i) + \int_0^T\int_{\Gamma^{1,3}} D_i k_i [\![u_i]\!][\![\psi]\!] \geqslant \int_{Q_T} \psi f_i, \tag{3.20}$$

for all $\psi \in \mathcal{D}_i$, $\psi \geqslant 0$.

Proof. We divide the proof in several steps which are adaptations from Pierre's method.

Compactness of $\boldsymbol{u}^n$ and $Tr_\Gamma(\boldsymbol{u}^n)$. Combining Lemma 3.3.1 and assumption (3.2), we notice that $f_i^n(\boldsymbol{u}^n)$ is bounded in $L^1(Q_T)$ for $i = 1, ..., m$.

Next, we apply the compactness Lemma 3.2.2 (see also Lemma 3.A.1 and its proof in Ap-

pendix 3.A, 3.B) to the solution $\mathbf{u}^n$ of the approximate System (3.16). Accordingly, after extraction, the following convergences, hold

$$\begin{cases} \boldsymbol{u}^n \to \boldsymbol{u}, & \text{in } L^1\big(0,T;L^{\gamma_1}(\Omega)\big)^m, \quad \forall \gamma_1 \in \Big[1, \frac{d}{d-2}\Big), \\ \boldsymbol{u}^n \to \boldsymbol{u}, & \text{a.e. in } Q_T, \\ \nabla \boldsymbol{u}^n \rightharpoonup \nabla \boldsymbol{u}, & \text{in } [L^\beta(Q_T)^d]^m, \quad \forall \beta \in \Big[1, \frac{d}{d-1}\Big), \\ Tr_\Gamma(\boldsymbol{u}^n) \to Tr_\Gamma(\boldsymbol{u}), & \text{in } L^1\big(0,T;L^\beta(\Gamma^{1,3})\big)^m, \quad \forall \beta \in \Big[1, \frac{d}{d-1}\Big). \end{cases} \tag{3.21}$$

Pointwise convergence of the f_i^n's. Since u_i^n satisfies (3.7) for all $i = 1, ..., m$, i.e.

$$-\int_\Omega \psi(0,x)u_{0,i}^n + \int_{Q_T}(-\psi_t u_i^n + D_i \nabla\psi \nabla u_i^n) + \int_0^T \int_{\Gamma^{1,3}} D_i k_i [\![u_i^n]\!][\![\psi]\!] = \int_{Q_T} \psi f_i^n, \tag{3.22}$$

and our goal is to pass to the limit as $n \to +\infty$, we need to study the convergence of f_i^n.
Thanks to the choice of $\boldsymbol{f}^n$: a.e. convergence of ϵ_M^n to zero and the continuity with respect to its argument, we infer

$$f_i^n(\boldsymbol{u}^n) \to f_i(\boldsymbol{u}) \text{ a.e. in } Q_T.$$

By Fatou's lemma, we know that

$$\int_{Q_T} |\boldsymbol{f}(\boldsymbol{u})| \leqslant \liminf_{n\to+\infty} \int_{Q_T} |\boldsymbol{f}^n(\boldsymbol{u}^n)|$$

and, in particular, it holds

$$\boldsymbol{f}(\boldsymbol{u}) \in L^1(Q_T)^m.$$

So far we did not prove L^1-convergence of $f_i^n(\boldsymbol{u}^n)$, therefore we cannot pass to the limit in the Equation (3.22) obtaining a weak solution of System (3.1). However we can find an inequality in the formulation of the weak solution of System (3.1), thus obtaining a supersolution. We arrive at this applying a truncation method.

Truncation method. The idea is that, with an appropriate truncation, we succeed in obtaining a reaction-diffusion inequality in which the reaction terms are under control as $n \to +\infty$ with a fixed truncation level. In this way, we are able to pass to the limit in the truncated weak supersolution formula, as $n \to +\infty$. At this point, bringing the truncation level to infinity, we gain the supersolution property in Theorem 3.3.1.

In order to build the truncation T_b at level b, since we will have to differentiate twice T_b, we replace T_b by a C^2-regularized version (otherwise T_b'' would be a Dirac mass), still denoted by T_b, so that on $[0, +\infty)$ we have

$$0 \leqslant T_b' \leqslant 1, \quad -1 \leqslant T_b'' \leqslant 0, \quad T_b(\sigma) = \sigma \quad \forall \sigma \in [0,b], \quad T_b'(\sigma) = 0 \quad \forall \sigma \in (b, +\infty).$$

We fix $\eta \in (0,1)$ and we denote for all $i = 1, ..., m$,

$$U_i^n = \sum_{j\neq i} u_j^n, \quad W_i^n = u_i^n + \eta U_i^n.$$

The idea is to consider the limit for $n \to +\infty$, then $\eta \to 0$ and, finally, $b \to +\infty$.
The main point is to use the inequality satisfied by $v^n := T_b(W_i^n)$, taking into account the

previous properties of T_b' and T_b'',

$$-\Delta v^n = -\Delta T_b(u_i^n + \eta U_i^n) = -T_b''(u_i^n + \eta U_i^n)|\nabla u_i^n + \eta \nabla U_i^n|^2 \; - \; T_b'(u_i^n + \eta U_i^n)[\Delta u_i^n + \eta \Delta U_i^n]$$
$$\geqslant -T_b'(u_i^n + \eta U_i^n)[\Delta u_i^n + \eta \Delta U_i^n].$$

This implies

$$v_t^n - D_i \Delta v^n \geqslant T_b'(u_i^n + \eta U_i^n)[f_i^n + \eta \sum_{j \neq i} f_j^n] + \eta T_b'(u_i^n + \eta U_i^n) \sum_{j \neq i} (D_j - D_i) \Delta u_j^n =: R_i^n + \eta S_i^n,$$

where

$$R_i^n = T_b'(u_i^n + \eta U_i^n)[f_i^n + \eta \sum_{j \neq i} f_j^n], \qquad S_i^n = T_b'(u_i^n + \eta U_i^n) \sum_{j \neq i} (D_j - D_i) \Delta u_j^n. \tag{3.23}$$

So the truncation $T_b(W_i^n)$ solves the problem

$$\begin{cases} v_t^n - D_i \Delta v^n \geqslant R_i^n + \eta S_i^n, \\ v^n_{|_{\Gamma^\lambda}} = 0, \quad \lambda = 1, 3, \\ \partial_{\boldsymbol{n}^1} v^{n,1}_{|_\Gamma} = T_b'(u_i^{n,1} + \eta U_i^{n,1})[\partial_{\boldsymbol{n}^1} u_i^{n,1} + \eta \partial_{\boldsymbol{n}^1} U_i^{n,1}] \\ \qquad\qquad = T_b'(u_i^{n,1} + \eta U_i^{n,1})[k_i(u_i^{n,3} - u_i^{n,1}) + \eta \sum_{j \neq i} k_j (u_j^{n,3} - u_j^{n,1})] =: T'_{b,n,1} V_i^n, \\ \partial_{\boldsymbol{n}^1} v^{n,3}_{|_\Gamma} = T_b'(u_i^{n,3} + \eta u_i^{n,3})[\partial_{\boldsymbol{n}^1} u_i^{n,3} + \eta \partial_{\boldsymbol{n}^1} u_i^{n,3}] \\ \qquad\qquad = T_b'(u_i^{n,3} + \eta u_i^{n,3})[k_i(u_i^{n,3} - u_i^{n,1}) + \eta \sum_{j \neq i} k_j (u_j^{n,2} - u_j^{n,1})] =: T'_{b,n,3} V_i^n, \\ v^n(0,x) = T_b\big(u_i^n(0,x) + \eta U_i^n(0,x)\big). \end{cases} \tag{3.24}$$

Consequently, we may write for all $i = 1, ..., m$, for all $\psi \in \mathcal{D}_i$,

$$-\int_\Omega \psi(0) v^n(0) - \int_{Q_T} \psi_t v^n - \int_0^T \int_{\Gamma^{1,3}} D_i(\psi^1 \partial_{\boldsymbol{n}^1} v^{n,1} - \psi^3 \partial_{\boldsymbol{n}^1} v^{n,3}) + D_i \int_{Q_T} \nabla v^n \nabla \psi$$
$$\geqslant \int_{Q_T} (R_i^n + \eta S_i^n)\psi,$$
$$-\int_\Omega \psi(0) v^n(0) + \int_{Q_T} (-\psi_t v^n + D_i \nabla v^n \nabla \psi) - \int_0^T \int_{\Gamma^{1,3}} D_i V_i^n (\psi^1 T'_{b,n,1} - \psi^3 T'_{b,n,3})$$
$$\geqslant \int_{Q_T} (R_i^n + \eta S_i^n)\psi. \tag{3.25}$$

So, as we said, the truncated function is a supersolution but with reaction terms (see the following) converging in L^1 or bounded independently from n.

• *Limit for $n \to +\infty$ with b, η fixed.*

Since $\boldsymbol{u}^n$ was a convergent solution (see (3.21)) and $T_b(W_i^n)$ represents the truncation at level b with b fixed, by the dominated convergence theorem,

$$v^n = T_b(W_i^n) \overset{n \to +\infty}{\longrightarrow} T_b(W_i) = T_b(u_i + \eta U_i) \quad \text{in } L^1(Q_T) \text{ and a.e..}$$

Since $T_b'(\sigma) = 0$ for $\sigma > b$, by definition, it holds $R_i^n = 0$ on the set $u_i^n + \eta U_i^n > b$. But on

$u_i^n + \eta U_i^n \leqslant b$, for $s = 1, ..., m$, u_s^n are uniformly bounded. In fact,

$$u_i^n \leqslant b \text{ and } u_j^n \leqslant \frac{b}{\eta}, \quad \forall j \neq i. \tag{3.26}$$

By the dominated convergence theorem, using (3.3), we find

$$R_i^n \overset{n\to\infty}{\longrightarrow} R_i := T_b'(u_i + \eta U_i)[f_i + \eta \sum_{j\neq i} f_j] \quad \text{in } L^1(Q_T).$$

On the other hand, we remark that

$$\nabla v^n = \nabla T_b(W_i^n) = T_b'(u_i^n + \eta U_i^n)[\nabla u_i^n + \eta \nabla U_i^n] \rightharpoonup \nabla v = T_b'(u_i + \eta U_j)[\nabla u_i + \eta \nabla U_j] \quad \text{in } L^1(Q_T)$$

and we have also convergence of the traces on $\Gamma^{1,3}$ and Γ^λ, $\lambda = 1, 3$. Therefore, to pass to the limit as $n \to +\infty$ in (3.25), we only need to control $\int_{Q_T} \psi S_i^n$. We have (see the proof later on)

Lemma 3.3.2. *(Pierre [107]) There exists C depending on b, ψ and the data, but not on n, $\eta \in (0, 1)$ such that*

$$\left| \int_{Q_T} \psi \, S_i^n \right| \leqslant C\eta^{-\frac{1}{2}}.$$

So we can pass to the limit as $n \to +\infty$ in (3.25) with b, η fixed and we obtain

$$-\int_\Omega \psi(0)v(0) + \int_{Q_T} (-\psi_t v + D_i \nabla v \nabla \psi) - \int_0^T \int_{\Gamma^{1,3}} D_i V_i (\psi^1 T_b'(W_i^1) - \psi^3 T_b'(W_i^3))$$

$$\geqslant \int_{Q_T} R_i \psi + \eta \int_{Q_T} S_i^n \psi \geqslant \int_{Q_T} R_i \psi - C\eta^{\frac{1}{2}},$$

with $V_i = [k_i(u_i^3 - u_i^1) + \eta \sum_{j\neq i} k_j (u_j^3 - u_j^1)]$.

• *Limit for $\eta \to 0$ with b fixed.* Then, $W_i \to u_i$, $V_i \to b_i(u_i^3 - u_i^1)$ and $R_i \to T_b'(u_i) f_i$.

• *Limit for $b \to +\infty$.* Then, the truncation is converging to the function itself and its derivative to 1 and so we obtain the statement (3.20):

$$-\int_\Omega \psi(0, x) u_{0,i} + \int_{Q_T} (-\psi_t u_i + D_i \nabla \psi \nabla u_i) + \int_0^T \int_{\Gamma^{1,3}} D_i k_i [\![u_i]\!][\![\psi]\!] \geqslant \int_{Q_T} \psi f_i.$$

□

We now turn to the **proof of Lemma 3.3.2**.

Proof. Remembering (3.23), in order to prove Lemma 3.3.2, we need that

$$\left| \int_{Q_T} \psi T_b'(W_i^n) \sum_{j\neq i} (D_j - D_i) \Delta u_j^n \right| \leqslant C\eta^{-\frac{1}{2}}.$$

Consequently, we have to study the following integral

$$\begin{aligned}\int_{Q_T}\psi T_b'(W_i^n)\Delta u_j^n &= \int_{Q_T}\operatorname{div}(\psi T_b'(W_i^n)\nabla u_j^n) - \int_{Q_T}\operatorname{div}(\psi T_b'(W_i^n))\nabla u_j^n\\ &= \int_0^T\int_{\Gamma^{1,3}}(\psi^1 T_b'(W_i^{n,1})\partial_{\boldsymbol{n}^1}u_j^{n,1} + \psi^3 T_b'(W_i^{n,3})\partial_{\boldsymbol{n}^3}u_j^{n,3})\\ &\quad - \int_{Q_T}[T_b'(W_i^n)\nabla\psi + \psi T_b''(W_i^n)\nabla W_i^n]\nabla u_j^n.\end{aligned}$$

We remark that

$$\left|\int_0^T\int_{\Gamma^{1,3}}(\psi^1 T_b'(W_i^{n,1})\partial_{\boldsymbol{n}^1}u_j^{n,1} + \psi^3 T_b'(W_i^{n,3})\partial_{\boldsymbol{n}^3}u_j^{n,3})\right| \leqslant C,$$

$$\left|\int_{Q_T} T_b'(W_i^n)\nabla\psi\nabla u_j^n\right| \leqslant C,$$

since $\psi^\lambda \in C^\infty([0,T]\times\overline{\Omega^\lambda})$ for $\lambda = 1,3$, $|T_b'| \leqslant 1$ and, thanks to Lemma 3.A.1, $u_j^n \in L^1\big(0,T;W^{1,1}(\Omega)\big)$ and it is L^1 on the membrane. The other integral can be computed using the Cauchy-Schwarz inequality and considering the cases $\{W_i^n \leqslant b\}$ and $\{W_i^n > b\}$ in Q_T:

$$\left|\int_{Q_T}\psi T_b''(W_i^n)\nabla W_i^n\nabla u_j^n\right| = \left|\int_{\{W_i^n\leqslant b\}\cup\{W_i^n>b\}}\psi T_b''(W_i^n)\nabla W_i^n\nabla u_j^n\right| =$$

$$= \left|\int_{\{W_i^n\leqslant b\}}\psi T_b''(W_i^n)\nabla W_i^n\nabla u_j^n\right| \leqslant C\left(\int_{\{W_i^n\leqslant b\}}|\nabla u_j^n|^2\right)^{\frac12}\left(\int_{\{W_i^n\leqslant b\}}|\nabla W_i^n|^2\right)^{\frac12},$$

since $T_b'(\sigma) = 0$ for $\sigma > b$, by definition, and so also $T_b''(\sigma) = 0$. In order to control the second integral in the right-hand side, we can use the lemma (see the proof later on):

Lemma 3.3.3. *(Pierre [107]) Let w be solution of (3.12). Then, for all $b > 0$,*

$$D\int_{\{|w|\leqslant b\}}|\nabla w|^2 \leqslant b\left[\int_{Q_T} f + \int_\Omega |w_0|\right]. \tag{3.27}$$

Applying Lemma 3.3.3 and considering (3.26), we infer

$$\left(\int_{\{W_i^n\leqslant b\}}|\nabla W_i^n|^2\right)^{\frac12} \leqslant C.$$

Concerning the first integral at the right-hand side, we remark that

$$\left(\int_{\{W_i^n\leqslant b\}}|\nabla u_j^n|^2\right)^{\frac12} = \left(\int_{\left\{U_i^n\leqslant\frac{b}{\eta}-\frac{u_i^n}{\eta}\right\}}|\nabla u_i^n|^2\right)^{\frac12} \leqslant \left(\int_{\left\{u_j^n\leqslant\frac{b}{\eta}\right\}}|\nabla u_i^n|^2\right)^{\frac12} \leqslant \frac{b^{\frac12}}{\eta^{\frac12}}C^{\frac12} \quad \text{for } i\neq j,$$

$$\left(\int_{\{W_j^n\leqslant b\}}|\nabla u_j^n|^2\right)^{\frac12} = \left(\int_{\{u_j^n\leqslant b-\eta U_j^n\}}|\nabla u_j^n|^2\right)^{\frac12} \leqslant \left(\int_{\{u_j^n\leqslant b\}}|\nabla u_j^n|^2\right)^{\frac12} \leqslant (bC)^{\frac12}.$$

This concludes the proof of Lemma 3.3.2. □

We now turn to the **proof of Lemma 3.3.3**.

Proof. We multiply the Equation (3.12) by a truncation (non regularized) function $T_b(w)$ and integrate over Q_T to obtain

$$\int_{Q_T} T_b(w)\partial_t w - \int_{Q_T} DT_b(w)\Delta w = \int_{Q_T} T_b(w)f,$$

$$\int_\Omega \int_{w_0}^{w(T)} T_b(w)dw - \int_0^T \int_{\Gamma^{1,3}} D[T_b(w^1)\partial_{\boldsymbol{n}^1} w^1 + T_b(w^3)\partial_{\boldsymbol{n}^3} w^3] + \int_{Q_T} DT_b'(w)|\nabla w|^2 = \int_{Q_T} T_b(w)f.$$

We denote the antiderivative of T_b as $\mathcal{T}(\sigma) = \int_0^\sigma T_b(s)ds$. So, we compute

$$\int_\Omega \int_{w_0}^{w(T)} T_b(w)dw = \int_\Omega \mathcal{T}\big(w(T)\big) - \int_\Omega \mathcal{T}(w_0),$$

$$-\int_0^T \int_{\Gamma^{1,3}} D[T_b(w^1)\partial_{\boldsymbol{n}^1} w^1 + T_b(w^3)\partial_{\boldsymbol{n}^3} w^3] = \int_0^T \int_{\Gamma^{1,3}} D\ k\ (w^3 - w^1)(T_b(w^3) - T_b(w^1)) \geqslant 0.$$

Since $\int_\Omega \mathcal{T}\big(w(T)\big) \geqslant 0$ and $T_b(w) \leqslant b$, we deduce

$$D\int_{\{|w|\leqslant b\}} |\nabla w|^2 \leqslant b\left[\int_{Q_T} f + \int_\Omega |w_0|\right].$$

This concludes the proof of Lemma 3.3.3.

□

3.3.4 Global existence of a weak solution

We conclude the proof of Theorem 3.2.1. As before, we consider the approximate system as built in Subsection 3.3.1. Following the previous Theorem 3.3.1, we prove that the supersolution (3.20) is also a subsolution and, then, a solution of our System (3.1).

Theorem 3.3.2. *We consider System (3.1) together with the conditions on the reaction term (3.2)-(3.5) and $\boldsymbol{u}_0 \in (L^1(\Omega)^+ \cap (\mathbf{H^1})^*)^m$. Moreover, we take $k_1 = ... = k_m$. Then, System (3.1) has a weak solution on $(0, +\infty)$.*

Proof. By Theorem 3.3.1, up to a sub-sequence, the approximate solution $\boldsymbol{u}^n$ converges to a weak supersolution. Let us prove that it is also a weak subsolution. We recall some results obtained before:

$$\begin{cases} \boldsymbol{u}^n \to \boldsymbol{u}, & \text{in } L^1\big(0,T;L^{\gamma_1}(\Omega)\big)^m, \quad \forall \gamma_1 \in \left[1, \frac{d}{d-2}\right), \\ \nabla \boldsymbol{u}^n \rightharpoonup \nabla \boldsymbol{u}, & \text{in } [L^\beta(Q_T)^d]^m, \quad \forall \beta \in \left[1, \frac{d}{d-1}\right), \\ Tr_\Gamma(\boldsymbol{u}^n) \to Tr_\Gamma(\boldsymbol{u}), & \text{in } L^1\big(0,T;L^\beta(\Gamma)\big)^m, \quad \forall \beta \in \left[1, \frac{d}{d-1}\right), \end{cases}$$

where for $i = 1, ..., m$, $f_i(\boldsymbol{u}) \in L^1(Q_T)$ and $\forall \psi \in \mathcal{D}_i$, we have (3.20). We introduce the following

notations:

$$W^n = \sum_{1\leqslant i\leqslant m} u_i^n, \quad Z^n = \sum_{1\leqslant i\leqslant m} D_i u_i^n, \quad V^n = \sum_{1\leqslant i\leqslant m} D_i k_i (u_i^{n,3} - u_i^{n,1}),$$
$$W = \sum_{1\leqslant i\leqslant m} u_i, \quad Z = \sum_{1\leqslant i\leqslant m} D_i u_i, \quad V = \sum_{1\leqslant i\leqslant m} D_i k_i (u_i^3 - u_i^1).$$

Adding up the equations for u_i^n, for $i = 1, ..., m$, in the weak form, we deduce

$$-\int_\Omega \psi(0) W_0^n + \int_{Q_T} (-\psi_t W^n + \nabla\psi \nabla Z^n) + \int_0^T \int_{\Gamma^{1,3}} [\![V^n]\!][\![\psi]\!] = \int_{Q_T} \psi \sum_{1\leqslant i\leqslant m} f_i^n. \tag{3.28}$$

Since we have assumed (3.3), $-\sum_{1\leqslant i\leqslant m} f_i^n + C(1 + W^n) \geqslant 0$, with $\boldsymbol{f}^n(\boldsymbol{u}^n) \to \boldsymbol{f}(\boldsymbol{u})$ a.e. in Q_T and W^n converges in $L^1(Q_T)$. Applying Fatou's lemma on $-\sum_{1\leqslant i\leqslant m} f_i^n + C(1 + W^n) \geqslant 0$, we infer

$$\int_{Q_T} -\psi \sum_{1\leqslant i\leqslant m} f_i(\boldsymbol{u}) \leqslant \liminf_{n\to+\infty} \int_{Q_T} -\psi \sum_{1\leqslant i\leqslant m} f_i^n(\boldsymbol{u}^n).$$

By a.e convergence of all functions, by $L^1(Q_T)$-convergence of W^n and by Fatou's lemma, we have at the limit for (3.28) that

$$-\int_\Omega \psi(0) W_0 + \int_{Q_T} (-\psi_t W + \nabla\psi \nabla Z) + \int_0^T \int_{\Gamma^{1,3}} [\![V]\!][\![\psi]\!] \leqslant \int_{Q_T} \psi \sum_{1\leqslant i\leqslant m} f_i.$$

Consequently, W is not only a supersolution but also a subsolution. This means that the sum W is a solution and, since its addends u_i are weak supersolutions by Theorem 3.3.1, $\boldsymbol{u}$ is a global weak solution and the proof is completed. □

Finally, following all the four steps of the proof (from Subsection 3.3.1 to Subsection 3.3.4), we have proved Theorem 3.2.1 in the case of interest with quadratic nonlinearities. We point out that this result, as well as Theorem 3.3.1 and 3.3.2, needs the restricted assumption $k_1 = ... = k_m$, since it arises in Subsection 3.3.2. As said before, we leave as an open problem to remove this restriction. It would also be interesting to see if the method in Cañizo *et al.* [22] can be applied to nearly constant membrane coefficients rather than to the diffusion coefficients. Another open problem, previously introduced, concerns the geometry of the domain. In fact, as we can see in Brezis [16], Li and Wang [80], Li *et al.* [82], we could consider the membrane as the boundary of the domain Ω^3 which is included in $\Omega^1 = \Omega \setminus \Omega^3$.

3.A Regularity

We now analyse in detail regularity in our problem referring to Lemma 3.2.2 that we have rewritten here below, whereas in the next Appendix, we discuss about compactness. We extend previous results for reaction-diffusion systems without membrane, Baras and Pierre [7], Bothe and Pierre [10], Laamri and Pierre [79], Laamri and Perthame [78], Pierre [107], and we refer to Quittner and Souplet [113] for the general theory of parabolic equations. We also refer to Laamri and Pierre [79] for a regularity lemma.

Lemma 3.A.1 (A priori bounds)**.** *We consider w solution of the following problem in dimension $d \geqslant 2$*

$$\begin{cases} \partial_t w - D\Delta w = f, & \text{in } Q_T, \\ w = 0, & \text{in } \Sigma_T, \\ \partial_{\boldsymbol{n}^1} w^1 = \partial_{\boldsymbol{n}^1} w^3 = k(w^3 - w^1), & \text{in } \Sigma_{T,\Gamma}, \\ w(0,x) = w_0(x) \geqslant 0, & \text{in } \Omega, \end{cases} \tag{3.29}$$

with $f \in L^1(Q_T)$ and $w_0 \in L^1(\Omega)$. Then,

- $w \in L^\beta\big(0,T;W^{1,\beta}(\Omega)\big)$, $\forall \beta \in \Big[1, \frac{d}{d-1}\Big)$ *and* $(1+|w|)^\alpha \in L^2\big(0,T;H^1(\Omega)\big)$ *for* $\alpha \in \big[0, \frac{1}{2}\big)$.
- *The mapping $(w_0, f) \longmapsto w$ is compact from $L^1(\Omega) \times L^1(Q_T)$ into $L^1\big(0,T;L^{\gamma_1}(\Omega)\big)$, for all $\gamma_1 < \frac{d}{d-2}$ and $L^{\gamma_2}(Q_T)$ for all $\gamma_2 < \frac{2+d}{d}$.*
- *The trace mapping $(w_0, f) \longmapsto Tr_\Gamma(w) \in L^\beta\big(0,T;L^\beta(\Gamma^{1,3})\big)$, $\beta \in \Big[1, \frac{d}{d-1}\Big)$ is also compact.*

Notice that we do not use the information $w \in L^2(Q_T)$ here but $w \in L^\infty(0,T;L^1(\Omega))$. That is used in Pierre and Rolland [108] and leads to the exponent $\beta < \frac{4}{3}$.

Proof. The proof is based on manipulating nonlinear quantities and Sobolev imbeddings. We divide it in several steps.

Some L^2 regularity of ∇w. Multiplying the equation of w in (3.29) by $\frac{w}{(1+|w|^{\frac{1}{\mu}})^\mu}$ and integrating on Ω, we obtain three terms which we estimate separately.

We begin with the Laplacian term. Recalling the membrane conditions and applying the Leibniz rule and the divergence theorem, arguing by a regularization and a limit technique, we gain, since $\frac{w}{(1+|w|^{\frac{1}{\mu}})^\mu}$ is an increasing function,

$$\begin{aligned} \int_\Omega \frac{w}{(1+|w|^{\frac{1}{\mu}})^\mu}\,\Delta w &= \int_{\Gamma^{1,3}} \frac{w^1}{(1+|w^1|^{\frac{1}{\mu}})^\mu}\partial_{n_1} w^1 + \int_{\Gamma^{1,3}} \frac{w^3}{(1+|w^3|^{\frac{1}{\mu}})^\mu}\partial_{n_2} w^3 - \int_\Omega \frac{|\nabla w|^2}{(1+|w|^{\frac{1}{\mu}})^{\mu+1}} \\ &= \int_{\Gamma^{1,3}} \left(\frac{w^1}{(1+|w^1|^{\frac{1}{\mu}})^\mu} - \frac{w^3}{(1+|w^3|^{\frac{1}{\mu}})^\mu} \right) k(w^3 - w^1) - \int_\Omega \frac{|\nabla w|^2}{(1+|w|^{\frac{1}{\mu}})^{\mu+1}} \\ &\leqslant - \int_\Omega \frac{|\nabla w|^2}{(1+|w|^{\frac{1}{\mu}})^{\mu+1}}. \end{aligned}$$

We analyse now the reaction term. We remark that $0 \leqslant \frac{w}{(1+|w|^{\frac{1}{\mu}})^\mu} \leqslant 1$ and, using that $f \in L^1(Q_T)$, we conclude

$$\int_\Omega \left| \frac{w}{(1+|w|^{\frac{1}{\mu}})^\mu}\, f \right| \leqslant \int_\Omega |f| = \|f\|_{L^1(\Omega)}.$$

Next, for the time derivative, we define the anti-derivative $0 \leqslant \psi_\mu(w) = \int_0^w \frac{v\,dv}{(1+|v|^{\frac{1}{\mu}})^\mu} \leqslant w$, then

$$\frac{w}{(1+|w|^{\frac{1}{\mu}})^\mu}\,\partial_t w \;=:\; \partial_t \psi_\mu(w).$$

Therefore, combining the previous equality and inequalities, we find

$$\int_\Omega \partial_t \psi_\mu(w) \;+\; D\int_\Omega \frac{|\nabla w|^2}{(1+|w|^{\frac{1}{\mu}})^{\mu+1}} \leqslant \|f\|_{L^1(\Omega)}.$$

At this point, we can integrate in time and obtain

$$D\int_{Q_T} \frac{|\nabla w|^2}{(1+|w|^{\frac{1}{\mu}})^{\mu+1}} \leqslant \int_\Omega \psi_\mu\big(w_0(x)\big) + \|f\|_{L^1(Q_T)} \leqslant \|w_0\|_{L^1(\Omega)} + \|f\|_{L^1(Q_T)}.$$

Since, for all $\mu > 1$ there is a C_μ such that

$$(1+|w|^{\frac{1}{\mu}})^{\mu+1} \leqslant C_\mu (1+|w|)^{2(1-\alpha)}, \qquad \alpha = \frac{1}{2}\left(1-\frac{1}{\mu}\right),$$

we conclude that

$$\int_{Q_T} (1+|w|)^{2(\alpha-1)}|\nabla w|^2 \leqslant \frac{C_\mu}{D}\left[\|w_0\|_{L^1(\Omega)} + \|f\|_{L^1(Q_T)}\right], \qquad 0<\alpha<\frac{1}{2}.$$

And thus, there is a constant C_α which also depends on $\|w_0\|_{L^1(\Omega)} + \|f\|_{L^1(Q_T)}$ such that

$$\int_{Q_T} |\nabla(1+|w|)^\alpha|^2 \leqslant C_\alpha, \qquad 0<\alpha<\frac{1}{2}. \tag{3.30}$$

Integrability of w. The Sobolev imbedding (see Appendix 3.C) gives

$$\left(\int_\Omega (1+|w|)^{\alpha 2^*}\right)^{\frac{2}{2^*}} \leqslant C\int_\Omega |\nabla(1+|w|)^\alpha|^2, \qquad 2^* = \frac{2d}{d-2}. \tag{3.31}$$

which is only useful when $\alpha 2^* > 1$, i.e. $\frac{d-2}{2d} < \alpha$. Then, we can interpolate between L^1 and $L^{\alpha 2^*}$ and find

$$\left(\int_\Omega (1+|w|)^\gamma\right)^{\frac{1}{\gamma}} \leqslant C\left(\int_\Omega (1+|w|)\right)^\theta \left(\int_\Omega |\nabla(1+|w|)^\alpha|^2\right)^{\frac{1-\theta}{2\alpha}}, \qquad \frac{1}{\gamma} = \theta + \frac{1-\theta}{\alpha 2^*}.$$

We may choose $\frac{1-\theta}{2\alpha} = 1$, and, recalling that $\alpha < \frac{1}{2}$, we find the integrability

$$w \in L^1\big(0,T; L^{\gamma_1}(\Omega)\big) \qquad \text{with} \qquad \gamma_1 = \frac{d}{2\big(d(1-\alpha)-1\big)} < \frac{d}{d-2}.$$

We may also choose $\frac{\gamma(1-\theta)}{2\alpha} = 1$, $\alpha < \frac{1}{2}$ and find the integrability

$$w \in L^{\gamma_2}(Q_T) \qquad \text{with} \qquad \gamma_2 = \frac{2\big(1+\alpha d\big)}{d} < \frac{2+d}{d}.$$

Regularity of ∇w. On the other hand, Hölder inequality gives

$$\int_\Omega |\nabla w|^\beta = \int_\Omega \frac{|\nabla w|^\beta}{(1+|w|)^\eta}(1+|w|)^\eta \leqslant \left(\int_\Omega \frac{|\nabla w|^{\beta r}}{(1+|w|)^{\eta r}}\right)^{\frac{1}{r}} \left(\int_\Omega (1+|w|)^{\eta p}\right)^{\frac{1}{p}}$$
$$\leqslant C\left(\int_\Omega |\nabla(1+|w|)^\alpha|^2\right)^{\frac{1}{r}} \left(\int_\Omega (1+|w|)^{\eta p}\right)^{\frac{1}{p}}$$

with

$$\frac{1}{r}+\frac{1}{p}=1, \qquad \beta=\frac{2}{r}\leqslant 2, \quad \eta r = 2(1-\alpha).$$

We can choose $\eta p = \gamma_1$ from above, which requires $\eta\left(\frac{1}{2(1-\alpha)}+\frac{1}{\gamma_1}\right)=1$, $\beta=\frac{\eta}{1-\alpha}=\frac{2\gamma_1}{\gamma_1+2(1-\alpha)}$ and we find, thanks to the estimate (3.30),

$$\int_\Omega |\nabla w|^\beta \in L^1(0,T) \qquad \text{with} \qquad \beta < \frac{d}{d-1}.$$

This concludes the proof of the gradient estimate. Moreover, considering that $\beta<\gamma_2$, thanks to Sobolev imbeddings, we can infer that $w\in L^\beta(0,T;L^\beta(\Omega))$.

The trace. The regularity of the trace derives from its continuity property Brezis [15, p. 315], i.e.

$$\int_0^T \|\mathrm{Tr}(w)\|^\beta_{W^{1-\frac{1}{\beta},\beta}(\Gamma^{1,3})} \leqslant \int_0^T \|w\|^\beta_{W^{1,\beta}(\Omega)}, \quad 1\leqslant\beta<\frac{d}{d-1}. \tag{3.32}$$

3.B Compactness

In order to conclude the proof of Lemma 3.A.1, it remains to adapt compactness arguments to the case of the membrane problem. A proof based on a dual approach, see Baras and Pierre [7], Bothe and Pierre [10], could be used. We rather go to a direct proof.

Compactness in space. It can be obtained using the Rellich-Kondrachov theorem, Adams and Fournier [2], since we know the approximate family is bounded in the spaces $W^{1,\beta}(\Omega^\lambda)$, $\lambda=1,\ 3$ which are compactly embedded in $L^{\gamma_1}(\Omega^\lambda)$, with $\gamma_1<\frac{d}{d-2}$.

Compactness in time. We use the Fréchet-Kolmogorov criteria, see Brezis [15] for instance. Let $\varphi(x)$ be a nonnegative, radially symmetric, $C_c^\infty(\mathbb{R}^d)$ standard mollifier with mass 1. We define the family $(\varphi_\delta)_{\delta>0}$ by

$$\varphi_\delta(x)=\frac{1}{\delta^d}\,\varphi\left(\frac{x}{\delta}\right), \qquad \|\varphi_\delta\|_{L^1(\Omega)}=1. \tag{3.33}$$

Moreover, we have

$$\|g*\varphi_\delta\|_{L^p(\Omega)}\leqslant \|\varphi_\delta\|_{L^1(\Omega)}\|g\|_{L^p(\Omega)}, \tag{3.34}$$

and it holds (Evans [45, p. 273]) that for any function $g\in W^{1,p}(\Omega)$,

$$\|g*\varphi_\delta - g\|_{L^p(\Omega)}\leqslant \delta\|\nabla g\|_{L^p(\Omega)}. \tag{3.35}$$

About the derivative of order k of φ_δ, we know that

$$\nabla^k \varphi_\delta(x) = \frac{1}{\delta^{d+k}} \nabla^k \varphi\left(\frac{x}{\delta}\right), \qquad \|\nabla^k \varphi_\delta\|_{L^1(\Omega)} \leqslant \frac{C}{\delta^k}. \tag{3.36}$$

Proof. To complete the proof of time compactness, we shall prove that, as $h \to 0$,

$$\int_0^{T-h} \int_\Omega |w(t+h,x) - w(t,x)| dx dt \to 0. \tag{3.37}$$

By comparison with the mollified versions, the triangular equality yields

$$\begin{aligned}\int_0^{T-h} \int_\Omega |w(t+h,x) - w(t,x)| dx dt \leqslant & \int_0^{T-h} \int_\Omega |w(t,x) - w(t,\cdot) * \varphi_\delta(x)| dx dt \\ & + \int_0^{T-h} \int_\Omega |w(t+h,x) - w(t+h,\cdot) * \varphi_\delta(x)| dx dt \\ & + \int_0^{T-h} \int_\Omega |w(t+h,\cdot) * \varphi_\delta(x) - w(t,\cdot) * \varphi_\delta(x)| dx dt\end{aligned}$$

Here, δ depends on h (to be specified later on) and converges to zero. It suffices to prove that each integral converges to zero as $h \to 0$.

First term. We analyse the first term in the right-hand side. It holds that

$$\int_0^{T-h} \int_\Omega |w(t,x) - w(t,\cdot) * \varphi_\delta(x)| dx dt \leqslant \delta \int_0^{T-h} \|\nabla w(t,x)\|_{L^1(\Omega)} dt \leqslant C\delta(h), \tag{3.38}$$

thanks to w regularity and to (3.35), which proves that it converges to zero as $h \to 0$.

Second term. For the second integral, we can proceed as for the fist one obtaining

$$\int_0^{T-h} \int_\Omega |w(t+h,x) - w(t+h,\cdot) * \varphi_\delta(x)| dx dt \leqslant C\delta(h). \tag{3.39}$$

Third term. Remembering (3.29), the last term can be written as

$$\int_0^{T-h} \int_\Omega |w(t+h,\cdot) * \varphi_\delta(x) - w(t,\cdot) * \varphi_\delta(x)| dx\, dt = \int_0^{T-h} \int_\Omega \left| \int_t^{t+h} \frac{\partial w}{\partial s}(s,x) * \varphi_\delta(x) ds \right| dx\, dt$$

$$= \int_0^{T-h} \int_\Omega \left| \int_t^{t+h} [D\Delta w + f] * \varphi_\delta ds \right| dx\, dt = \int_0^{T-h} \int_\Omega \left| \int_t^{t+h} Dw * \Delta\varphi_\delta + f * \varphi_\delta\, ds \right| dx\, dt$$

after exchanging derivatives in the convolution. From (3.34) we deduce

$$\begin{aligned}\int_0^{T-h} \int_\Omega |w(t+h,\cdot) * \varphi_\delta(x) - w(t,\cdot) * \varphi_\delta(x)| dx\, dt \leqslant & \int_0^{T-h} \int_t^{t+h} D\|w\|_{L^1(\Omega)} \|\Delta\varphi_\delta\|_{L^1(\Omega)} \\ & + \int_0^{T-h} \int_t^{t+h} \|f\|_{L^1(\Omega)} \|\varphi_\delta\|_{L^1(\Omega)}.\end{aligned}$$

Finally, thanks to (3.33) and (3.36), we obtain choosing $\delta = h^{1/4}$

$$\int_0^{T-h}\int_\Omega |w(t+h,\cdot)*\varphi_\delta(x) - w(t,\cdot)*\varphi_\delta(x)|dx\,dt \leqslant C[\frac{h}{\delta^2}+h] \leqslant C\sqrt{h}$$

and (3.37) follows combining this estimate with (3.38) and (3.39). □

Applying the Fréchet-Kolmogorov theorem, Brezis [15], we conclude that the set of functions $w \in L^1(Q_T)$ under consideration is compact in $L^1(Q_T)$. Consequently, we claim compactness in $L^1\big(0,T;L^{\gamma_1}(\Omega)\big)$ with $\gamma_1 < \frac{d}{d-2}$ and in $L^{\gamma_2}(Q_T)$ with $\gamma_2 < \frac{2+d}{d}$. In fact, since we have L^1-convergence of L^p-functions, we deduce convergence in the space L^q, for $q < p$.

Compactness of traces in $L^\beta\big(0,T;L^\beta(\Gamma^{1,3})\big)$. Space compactness can be deduced, in each Ω^λ, from trace continuity and a compactness result for the boundary (Demengel *et al.* [36, Section 3.6.2]) such that $W^{1-\frac{1}{\beta},\beta}(\Gamma^{1,3}) \subset\subset L^\beta(\Gamma^{1,3})$. Time compactness is again achieved through the Fréchet-Kolmogorov theorem. Following the same proof as before and changing the order of the time integrals, we need to recall Kedem-Katchalsky membrane conditions from which we can infer that $\partial_t Tr_\Gamma(w) \in L^1(0,T;L^1(\Gamma^{1,3}))$ and so we can conclude the proof.

□

3.C Sobolev and Poincaré inequalities with membrane

For completeness, we explain why the Sobolev embeddings can be extended to the membrane problem, leading to (3.30) and (3.31). More precisely, we explain how to arrive to

$$\|\phi_\alpha(w^1)\|^2_{L^{2^*}(\Omega^1)} + \|\phi_\alpha(w^3)\|^2_{L^{2^*}(\Omega^3)} \leqslant C\left(\|\nabla\phi_\alpha(w^1)\|^2_{L^2(\Omega^1)} + \|\nabla\phi_\alpha(w^3)\|^2_{L^2(\Omega^3)}\right).$$

There are two difficulties. First, the boundary condition is not Dirichlet everywhere. Second we are dealing with a singular domain Ω and so we cannot use directly the Sobolev or Poincaré inequalities in Ω, but only some easy generalizations that we explain now.

We are going to prove the

Theorem 3.C.1 (Gagliardo-Nirenberg-Sobolev inequality with membrane)**.** *We consider the bounded domain $\Omega = \Omega^1 \cup \Omega^3 \subset \mathbb{R}^d$, $d \geqslant 2$, with piecewise C^1 sub-domains Ω^1 and Ω^3 and a C^1 membrane $\Gamma^{1,3} = \partial\Omega^1 \cap \partial\Omega^3$ which decomposes Ω in the two parts. We take the function $v = (v^1, v^3) \in \mathbf{H^1}$ (see Definition 3.2.3), then, for $\lambda = 1, 3$,*

$$\|v^\lambda\|_{L^{2^*}(\Omega^\lambda)} \leqslant C(\Omega^\lambda)\ \|\nabla v^\lambda\|_{L^2(\Omega^\lambda)^d}, \tag{3.40}$$

and consequently

$$[\ \|v^1\|_{L^{2^*}(\Omega^1)} + \|v^3\|_{L^{2^*}(\Omega^3)}\ ] \leqslant C(\Omega^1,\Omega^3)\ [\ \|\nabla v^1\|_{L^2(\Omega^1)^d} + \|\nabla v^3\|_{L^2(\Omega^3)^d}\ ]. \tag{3.41}$$

The reason why we want to prove this theorem is that the domain Ω described above is not enough regular to use the usual Gagliardo-Nirenberg-Sobolev inequality (Brezis [15, p. 284]). Consequently, we need to build smoother domains containing each Ω^λ, $\lambda = 1, 3$, in which we can apply known results and then, with a restriction to Ω, we can find (3.40) and (3.41). The construction is made considering an extension of $\Gamma^{1,3}$ and a domain with the same internal structure as Ω such that it contains Ω and each extension of the Ω^λ is of class C^1.

We first recall the standard Sobolev inequality (Brezis [15, p. 284]) in a bounded open set.

Theorem 3.C.2 (Sobolev embedding)**.** *Let Q be a bounded open subset of class C^1 in $\mathbb{R}^d$. There is a constant C_Q such that for all $v \in H^1(Q)$, we have*

$$v \in L^{2^*}(Q) \quad \text{and} \quad \|v\|_{L^{2^*}(Q)} \leqslant C_Q \left[\|v\|_{L^2(Q)} + \|\nabla v\|_{L^2(Q)^d} \right].$$

Proof. We recall how to prove Theorem 3.C.2 departing from the case of the full space. We use the regularity of the domain which assures us the existence of a linear and continuous extension operator $T : H^1(Q) \to H^1(R^d)$, which is also the extension from $L^2(Q)$ into $L^2(\mathbb{R}^d)$ (Brezis [15, p. 272]). So, we obtain that:

- taken $v \in H^1(Q)$, $\quad T(v) \in H^1(\mathbb{R}^d)$ and $T(v) = v$ on Q; (3.42)
- $\|T(v)\|^2_{L^2(\mathbb{R}^d)} \leqslant C^2_{\text{exten}L^2}(Q)\ \|v\|^2_{L^2(Q)}$; (3.43)
- $\|\nabla T(v)\|^2_{L^2(\mathbb{R}^d)^d} \leqslant C^2_{\text{exten}H^1}(Q)\ \|v\|^2_{H^1(Q)}$. (3.44)

Moreover, for construction (see the proof of the extension theorem, Brezis [15, p. 272]), this operator is in $H^1_0(R^d)$. Consequently, using a corollary of the Sobolev inequality (Evans [45, p. 265]), we get that

$$T(v) \in L^{2^*}(\mathbb{R}^d) \text{ and } \|T(v)\|_{L^{2^*}(\mathbb{R}^d)} \leqslant C_{\text{sob}}(d,2)\ \|\nabla T(v)\|_{L^2(\mathbb{R}^d)^d}.$$

We proceed with some estimates due to the application of (3.42), (3.43), (3.44). First of all, we deduce

$$\|\nabla v\|^2_{L^2(Q)^d} = \|\nabla T(v)\|_{L^2(Q)^d} \leqslant \|\nabla T(v)\|_{L^2(\mathbb{R}^d)^d} \leqslant C_{\text{exten}H^1}(Q)\ \|v\|^2_{H^1(Q)}$$

$$= C_{\text{exten}H^1}(Q)\ \left[\|v\|_{L^2(Q)} + \|\nabla v\|_{L^2(Q)^d} \right].$$

Since $T(v) \in L^{2^*}(\mathbb{R}^d)$ and $T(v) = v$ on Q, we get $v \in L^{2^*}(Q)$ and

$$\|v\|^2_{L^{2^*}(Q)} = \|T(v)\|^2_{L^{2^*}(Q)} \leqslant \|T(v)\|^2_{L^{2^*}(\mathbb{R}^d)} \leqslant (C_{\text{sob}}(d,2))^2\ \|\nabla T(v)\|^2_{L^2(\mathbb{R}^d)^d}$$

$$\leqslant (C_{\text{sob}}(d,2))^2\ C^2_{\text{exten}H^1}(Q)\ \left[\|v\|^2_{L^2(Q)} + \|\nabla v\|^2_{L^2(U)^d} \right].$$

The proof of Theorem 3.C.2 is complete. □

Since we do not impose Dirichlet conditions on the full boundary, we need the following generalized Poincaré inequality (Morrey [91, Theorem 3.6.4]).

Theorem 3.C.3 (Poincaré inequality)**.** *Suppose Q a bounded and connected open subset of $\mathbb{R}^d$ of class C^1 and consider a portion of its boundary $\Sigma_0 \subset \partial Q$ such that $|\Sigma_0| > 0$. Then, there exists a constant $C(Q, \Sigma_0)$ such that*

$$\forall v \in H^1(Q) \text{ such that } Tr_{\Sigma_0}(v) = 0, \quad \|v\|^2_{L^2(Q)} \leqslant C(Q,\Sigma_0)\|\nabla v\|^2_{L^2(Q)^d}. \tag{3.45}$$

Proof. If the statement is not true, we can find a sequence v_n such that each $v_n \in H^1(Q)$ and

$$\|v_n\|^2_{L^2(Q)} > n \left[\|\nabla v_n\|^2_{L^2(Q)^d} + \left(\int_{\Sigma_0} |v_n| dS \right)^2 \right].$$

On account of the homogeneity (normalizing), we may assume that $\|v_n\|_{L^2(Q)} = 1$, for each n. So we infer that

$$n \left[\|\nabla v_n\|^2_{L^2(Q)^d} + \left(\int_{\Sigma_0} |v_n| dS \right)^2 \right] < 1, \tag{3.46}$$

which implies that

$$\|\nabla v_n\|^2_{L^2(Q)^d} < \frac{1}{n}.$$

Therefore, $\nabla v_n \to 0$ in $L^2(Q)$. Moreover, v_n is bounded in $H^1(Q)$, so, up to a sub-sequence, it converges weakly in $H^1(Q)$ to some v. So $\nabla v_n \rightharpoonup \nabla v$, that means $\nabla v = 0$. This shows that v is a constant (since Q is connected). For the continuity of the trace operator and (3.46), we deduce

$$0 = \lim_{n \to +\infty} \int_{\Sigma_0} |v_n| dS = \int_{\Gamma_0} |v| dS = |c| |\Gamma_0|,$$

and so $v = 0$.
At the same time, thanks to the Rellich-Kondrachov compactness theorem, Adam [2], Brezis [15], Evans [45], up to a sub-sequence, v_n converges strongly in $L^2(Q)$ to $v = 0$. Hence, since $\|v_n\|_{L^2(Q)} = 1$, we arrive to a contradiction.

□

At this point we are able to give the proof of Theorem 3.C.1.

Proof. We apply Theorems 3.C.2 and 3.C.3. First of all we consider the extension of $\Gamma^{1,3}$ into the space $\mathbb{R}^d$ such that now $\Gamma^{1,3}$ separates the space into two pieces P^λ with $\lambda = 1, 3$. Since we have Dirichlet boundary conditions on Γ^λ, we can extend the function to zero in the whole P^λ. So now, considering Q^λ a domain of class C^1 such that $\Omega^\lambda \subset Q^\lambda \subset P^\lambda$ and for $\lambda, \sigma = 1, 3$, $Q^\lambda \cap P^\sigma$ is a portion of $\Gamma^{1,3}$, we can apply Theorems 3.C.2 and 3.C.3 to

$$\tilde{v}^\lambda = \begin{cases} v^\lambda, & \text{in } \Omega^\lambda, \\ 0, & \text{in } \Gamma^\lambda \cup \{Q^\lambda \setminus \Omega^\lambda\}. \end{cases}$$

This proves Theorem 3.C.1 in Q^λ and, so, in Ω^λ.

□

Chapter 4

Effect of a membrane on diffusion-driven Turing instability

4.1 Introduction

Pattern formation in a system of reacting substances that possess the ability to diffuse was postulated in 1952 by Turing [123] and it was numerically studied in 1972 by Gierer and Meinhardt [56]. A huge literature followed this path in describing animal pigmentation as for the well-studied zebrafish (Watanabe and Kondo [129], Yamaguchi *et al.* [131]), the arrangement of hair and feather in Painter *et al.* [101], the mammalian palate in Economou *et al.* [42], teeth in Cho *et al.* [28], tracheal cartilage rings in Sala *et al.* [117] and digit pattering in Raspopovic *et al.* [114]. In particular, there were found evidences asserting that internal anatomy does not play an influential role in this phenomenon. So, spatial patterns develop autonomously without any pre-pattern structure and they are mathematically described by Turing mechanism. Reaction-diffusion equations are not the only kind of system that exhibits the formation of patterns. Receptor-based models, Klika *et al.* [75], Marciniak-Czochra *et al.* [87] are an example of organisation mechanisms in a system coupling reaction-diffusion equations and ordinary differential equations. These models are based on the idea that cell differentiate according to positional information. This pre-pattern or morphogen mechanism has been experimentally proven in many morphogenetic events in early development, whereas it is not applicable to the complex structure of the adult body, Kondo *et al.* [77].

Here, we consider another kind of situation which is always a reaction-diffusion system but with a membrane as introduced by Kedem-Katchalsky. In Chapter 3, the reader can find a previous analytical study on a reaction-diffusion system of $m \geqslant 2$ species with membrane conditions of the Kedem-Katchalsky type. The main result concerns the existence of a global weak solution in the case of low regularity initial data and at most quadratic non-linearities in an L^1-setting. Moreover, it is proven a regularity result such that we have space and time L^2 solutions. In particular, solutions are L^β in time and $W^{1,\beta}$ in space with $\beta \in [1, 2)$, except on the membrane Γ where we loose the derivatives regularity. So, now the question that arises is whether it is possible to observe patterns in the case species react and diffuse in a domain with an inner membrane

and under which conditions.

For our purpose, we consider as before the domain $\Omega = \Omega_1 \cup \Omega_3$ with internal interface $\Gamma_{1,3}$ and boundary $\partial\Omega = \Gamma_1 \cup \Gamma_3$, where $\Gamma_1 := \partial\Omega_1 \setminus \Gamma_{1,3}$, $\Gamma_3 := \partial\Omega_3 \setminus \Gamma_{1,3}$. We denote as $\boldsymbol{n}_1$ (respectively, $\boldsymbol{n}_3$) the outward normal to Ω_1 (respectively, Ω_3). We call $\boldsymbol{n} := \boldsymbol{n}_1 = -\boldsymbol{n}_3$. On the two domains $Q_T^1 := (0,T) \times \Omega_1$ and $Q_T^3 := (0,T) \times \Omega_3$, we consider a reaction-diffusion membrane problem for two species u and v as below.

$$\begin{cases} \partial_t u_1 - D_{u1}\,\Delta u_1 = f(u_1, v_1), \\ \partial_t v_1 - D_{v1}\,\Delta v_1 = g(u_1, v_1), & \text{in } Q_T^1, \\ \nabla u_1 \cdot n \;=\; 0 \;=\; \nabla v_1 \cdot n, & \text{in } \Sigma_T^1, \\ D_{u1}\,\nabla u_1 \cdot n = k_u(u_3 - u_1), \\ D_{v1}\,\nabla v_1 \cdot n = k_v(v_3 - v_1), & \text{in } \Sigma_{T,\Gamma}, \end{cases} \qquad \begin{cases} \partial_t u_3 - D_{u3}\,\Delta u_3 = f(u_3, v_3), \\ \partial_t v_3 - D_{v3}\,\Delta v_3 = g(u_3, v_3), & \text{in } Q_T^3, \\ \nabla u_3 \cdot n \;=\; 0 \;=\; \nabla v_3 \cdot n, & \text{in } \Sigma_T^3, \\ D_{u3}\,\nabla u_3 \cdot n = k_u(u_3 - u_1), \\ D_{v3}\,\nabla v_3 \cdot n = k_v(v_3 - v_1). & \text{in } \Sigma_{T,\Gamma}, \end{cases} \tag{4.1}$$

with $\Sigma_T^1 := (0,T) \times \Gamma_1$, $\Sigma_T^3 := (0,T) \times \Gamma_3$ and $\Sigma_{T,\Gamma} := (0,T) \times \Gamma_{1,3}$.

In this chapter, we are interested in the effect of the membrane, represented by the permeability coefficients k_u, k_v, for Turing instability to arise under particular conditions on the latter membrane coefficients and on the diffusion ones. With this aim, we extend Turing's theory to the case of membrane operators. We recall the definition of a Turing unstable steady state in the case of a linearised system, Murray [95].

Definition 4.1.1. *We say that a steady state is Turing unstable for the linearised system if it is stable in the absence of diffusion and unstable introducing diffusion. It is also called diffusion driven instability.*

This is the kind of instability that induces spatially structured patterns.

As for the standard reaction-diffusion problems, in order to prove Turing instability, we need to introduce a diagonalization theory for compact and self-adjoint membrane operators (see Appendix 4.A). We introduce the eigenvalue problem of the Laplace operator with Neumann and membrane conditions for each specie u and v. We call

$$L = -D_u\Delta \quad \text{and} \quad \widetilde{L} = -D_v\Delta, \tag{4.2}$$

where we define

$$D_\phi = \begin{cases} D_{\phi 1}, \text{ in } \Omega_1, \\ D_{\phi 3}, \text{ in } \Omega_3. \end{cases} \qquad \phi = \begin{cases} \phi_1, & \text{in } \Omega_1, \\ \phi_3, & \text{in } \Omega_3, \end{cases} \tag{4.3}$$

for $\phi = u$ or v. So, we have for u

$$\begin{cases} Lw = \lambda w, & \text{in } \Omega_1 \cup \Omega_3, \\ \nabla w \cdot n = 0, & \text{in } \Gamma_1 \cup \Gamma_3, \\ D_{u1}\nabla w_1 \cdot n = D_{u3}\nabla w_3 \cdot n = k_u(w_3 - w_1), & \text{in } \Gamma, \end{cases} \tag{4.4}$$

and for v,

$$\begin{cases} \widetilde{L}z = \eta z, & \text{in } \Omega_1 \cup \Omega_3, \\ \nabla z \cdot n = 0, & \text{in } \Gamma_1 \cup \Gamma_3, \\ D_{v1}\nabla z_1 \cdot n = D_{v3}\nabla z_3 \cdot n = k_v(z_3 - z_1), & \text{in } \Gamma. \end{cases} \tag{4.5}$$

Thanks to the diagonalization theory introduced in Theorem 4.A.1, we infer the following result.

Proposition 4.1.1. *There exist increasing and diverging sequences of real numbers* $\{\lambda_n\}_{n\in N}$ *and* $\{\eta_n\}_{n\in\mathbb{N}}$ *which are the eigenvalues of* L *and* $\widetilde{L}$*, respectively. We call* $\{w_n\}_{n\in N}$ *and* $\{z_n\}_{n\in\mathbb{N}}$ *in* $L^2(\Omega_1)\times L^2(\Omega_3)$*, the corresponding orthonormal basis of eigenfunctions. In particular, we have that* $\lambda_0 = 0, w_0 = 1/|\Omega|^{\frac{1}{2}}$ *and* $\eta_0 = 0, z_0 = 1/|\Omega|^{\frac{1}{2}}$.

Finally, we are able to state our main theorem (for more details see Theorem 4.2.1).

Theorem 4.1.1. *Assume the coefficients of System (4.1) are such that* $w_n = z_n$*, for all* $n \in \mathbb{N}$*. Consider the linearised system around the steady state* $(\overline{u},\overline{v})$ *with* $D_v > 0$ *fixed and assume appropriate conditions on the linearised reaction terms. Then, for* D_u *sufficiently small, the steady state* $(\overline{u},\overline{v})$ *is linearly unstable. Moreover, only a finite number of eigenvalues are unstable.*

The chapter is organised in four sections and two appendices. In Section 4.2, we introduce assumptions allowing us to find conditions in order to have Turing instability in the case of a membrane problem. We refer to Theorem 4.2.1 as main result. In Section 4.3, we restrict the analysis to the one dimensional case, so that we explicit the eigenfunctions and the equations defining the eigenvalues. In Section 4.4, Turing analysis is completed by some numerical examples performed with a finite difference implicit scheme in Matlab. We investigate in one dimension the effect of the membrane on Turing patterns. In Subsection 4.4.1, we propose our choice of reaction terms and data setting for the numerical examples. In Subsection 4.4.2 and 4.4.3, we illustrate some simulations varying respectively the diffusion and the permeability coefficients. In Subsection 4.4.4, thanks to the choice made for the reaction terms, we analyse oscillatory limiting solutions to a fast reaction-diffusion system. In Section 4.5, a brief conclusion can be found. At the end of the chapter, the reader can find two appendices. In Appendix 4.A, we introduce the diagonalization theorem for compact, self-adjoint membrane operators and we apply it to the operators L^{-1} and $\widetilde{L}^{-1}$. In Appendix 4.B, we give more details concerning the numerical method behind the simulations presented in Section 4.4 and we provide also the Matlab code.

4.2 Conditions for Turing instability

In order to study Turing instability, we first assume that there exists a homogeneous steady state $(\overline{u},\overline{v})$ which is a non-negative solution of

$$f(\overline{u},\overline{v}) = 0, \quad g(\overline{u},\overline{v}) = 0.$$

Then, we analyse its stability for the linearised dynamical system around this steady state. Later, we come back to the linearisation of Equations (4.1), *i.e.*,

$$\begin{cases} \partial_t u_1 - D_{u1}\,\Delta u_1 = \overline{f}_u u_1 + \overline{f}_v v_1, \\ \partial_t v_1 - D_{v1}\,\Delta v_1 = \overline{g}_u u_1 + \overline{g}_v v_1, \\ \nabla u_1 \cdot n \;=\; 0 \;=\; \nabla v_1 \cdot n, \\ D_{u1}\,\nabla u_1 \cdot n = k_u(u_3 - u_1), \\ D_{v1}\,\nabla v_1 \cdot n = k_v(v_3 - v_1), \end{cases} \qquad \begin{cases} \partial_t u_3 - D_{u3}\,\Delta u_3 = \overline{f}_u u_3 + \overline{f}_v v_3, \\ \partial_t v_3 - D_{v3}\,\Delta v_3 = \overline{g}_u u_3 + \overline{g}_v v_3, \\ \nabla u_3 \cdot n \;=\; 0 \;=\; \nabla v_3 \cdot n, \\ D_{u3}\,\nabla u_3 \cdot n = k_u(u_3 - u_1), \\ D_{v3}\,\nabla v_3 \cdot n = k_v(v_3 - v_1), \end{cases} \tag{4.6}$$

in which $\overline{f}_u, \overline{f}_v, \overline{g}_u, \overline{g}_v$ are the partial derivatives of the reaction terms evaluated in $(\overline{u},\overline{v})$, and we look for conditions such that the previous steady state is unstable. We follow the standard

theory in Murray [95], Perthame [106].

Conditions for the dynamical system to perform a stable steady state. With no spatial variation (eliminating the diffusion term), we can study the stability of the previous steady state applying a linearisation method around $(\overline{u}, \overline{v})$, as in (4.6). Setting

$$z = \begin{pmatrix} u - \overline{u} \\ v - \overline{v} \end{pmatrix},$$

we get

$$\partial_t z = Az, \quad \text{where } A = \begin{pmatrix} \overline{f}_u & \overline{f}_v \\ \overline{g}_u & \overline{g}_v \end{pmatrix}.$$

We look for solutions in the exponential form $z \propto e^{\mu t}$, where μ is the eigenvalue related to the matrix A. The steady state $z = 0$ is linearly stable if $Re(\mu) < 0$. In that case we can observe an exponential decay to zero. This condition is guaranteed if

$$\mathrm{tr}(A) = \overline{f}_u + \overline{g}_v < 0 \quad \text{and} \quad \det(A) = \overline{f}_u\,\overline{g}_v - \overline{f}_v\,\overline{g}_u > 0. \tag{4.7}$$

In particular, we assume

$$\overline{f}_u > 0 \quad \text{and} \quad \overline{g}_v < 0, \tag{4.8}$$

i.e. u is called activator and v is the inhibitor.

Conditions to obtain an unstable steady state in the case of spatial variation. Now we consider the complete reaction-diffusion systems linearised around the steady state as in (4.6). Referring to the diagonalization theory in Appendix 4.A, there exist orthonormal basis of eigenfunctions $\{w_n\}_{n\in N}$ for L and $\{z_n\}_{n\in\mathbb{N}}$ for $\widetilde{L}$ in $L^2(\Omega_1) \times L^2(\Omega_3)$. We use these basis to decompose u and v as

$$u(t,x) = e^{\mu t} \sum_{n\in\mathbb{N}} \alpha_n w_n(x), \qquad v(t,x) = e^{\mu t} \sum_{n\in\mathbb{N}} \beta_n z_n(x), \tag{4.9}$$

where $e^{\mu t}\alpha_n = (u, w_n)_{\mathbf{L^2}}$ and $e^{\mu t}\beta_n = (v, z_n)_{\mathbf{L^2}}$, for all $n \in \mathbb{N}$, with $\mathbf{L^2}$ which is defined as the L^2 product space.

Definition 4.2.1. *We define* $\mathbf{L^2} = L^2(\Omega_1) \times L^2(\Omega_3)$. *We endow it with the norm*

$$\|w\|_{\mathbf{L^2}} = \left(\|w_1\|^2_{L^2(\Omega_1)} + \|w_3\|^2_{L^2(\Omega_3)} \right)^{\frac{1}{2}}.$$

We let $(\cdot,\cdot)_{\mathbf{L^2}}$ *be the inner product in* $\mathbf{L^2}$.

Substituting (4.9) into the linearised reaction-diffusion System (4.6) and using (4.4) and (4.5), we infer

$$\begin{cases} \sum_n (\alpha_n \mu w_n + \alpha_n \lambda_n w_n) = \sum_n \left(\overline{f}_u \alpha_n w_n + \overline{f}_v \beta_n z_n \right), \\ \sum_n (\beta_n \mu z_n + \beta_n \eta_n z_n) = \sum_n \left(\overline{g}_u \alpha_n w_n + \overline{g}_v \beta_n z_n \right), \end{cases} \tag{4.10}$$

with boundary conditions well satisfied. Indeed, for $x \in \Gamma_{1,3}$ we deduce that

$$\begin{aligned} \sum_{n\in\mathbb{N}} (\, \alpha_n e^{\mu t} k_u (w_{3n}(x) - w_{1n}(x)) \,) &= \sum_{n\in\mathbb{N}} k_u (\, \alpha_n e^{\mu t} w_{3n}(x) - \alpha_n e^{\mu t} w_{1n}(x)) \,), \\ \sum_{n\in\mathbb{N}} (\, \beta_n e^{\mu t} k_v (z_{3n}(x) - z_{1n}(x)) \,) &= \sum_{n\in\mathbb{N}} k_v (\, \beta_n e^{\mu t} z_{3n}(x) - \beta_n e^{\mu t} z_{1n}(x)) \,), \end{aligned} \tag{4.11}$$

whereas on the external boundary Neumann conditions are trivial. In view of the structure of (4.10), it will be convenient, for analysis, to impose $w_n = z_n$, for all $n \in \mathbb{N}$. This is the case under the following conditions.

Lemma 4.2.1 (Conditions for $w_n = z_n$, for all $n \in \mathbb{N}$)**.** *Let*

$$\nu_D := \frac{D_{u3}}{D_{u1}} = \frac{D_{v3}}{D_{v1}}, \qquad \nu_K := \frac{k_u}{D_{u1}} = \frac{k_v}{D_{v1}} \qquad \text{and} \qquad \theta := \frac{D_{u1}}{D_{v1}} = \frac{D_{u3}}{D_{v3}}. \tag{4.12}$$

A sufficient condition to have $w_n = z_n$, for all $n \in \mathbb{N}$, is the following relation

$$\lambda_n = \theta \eta_n, \qquad \text{for all } n \in \mathbb{N}. \tag{4.13}$$

Proof. With relations (4.12), w_n and z_n solve the same eigenvalue problem (see Problems (4.4) and (4.5)) for all $n \in \mathbb{N}$. From the diagonalization theory (see Theorem 4.A.1), there exists a solutions sequence of eigenvalues and related eigenfunctions. In particular, with condition (4.13), $w_n \propto z_n$, *i.e.* $w_n = C z_n$, for all $n \in \mathbb{N}$ but since these basis are orthonormal, the constant C is equal to 1.

□

We are now ready to state our main theorem.

Theorem 4.2.1 (Turing instability theorem)**.** *Consider the linearised Systems (4.6) around the steady state $(\overline{u},\overline{v})$ with $D_v > 0$ fixed. We assume (4.7)-(4.8), and (4.12)-(4.13). Then, for θ sufficiently small (that means D_u), the steady state $(\overline{u},\overline{v})$ is linearly unstable. Moreover, only a finite number of eigenvalues are unstable.*

Proof. Using the orthogonality of the eigenfunctions in Equation (4.10) and assuming conditions (4.12) and (4.13) in Lemma 4.2.1, we arrive to

$$\begin{cases} \alpha_n \mu + \alpha_n \lambda_n = \overline{f}_u \alpha_n + \overline{f}_v \beta_n, \\ \beta_n \mu + \beta_n \eta_n = \overline{g}_u \alpha_n + \overline{g}_v \beta_n. \end{cases} \tag{4.14}$$

This linear system has α_n and β_n as unknowns. In order to have nonnegative solutions we need to assure that the determinant of the coefficients of the system is zero, *i.e.*

$$\det \begin{pmatrix} \mu + \lambda_n - \overline{f}_u & -\overline{f}_v \\ -\overline{g}_u & \mu + \eta_n - \overline{g}_v \end{pmatrix} = 0.$$

Hence, we infer that we have the so-called *dispersion relation*

$$\mu^2 + \mu[\eta_n - \overline{g}_v + \lambda_n - \overline{f}_u] + \eta_n \lambda_n - \lambda_n \overline{g}_v + \overline{f}_u \eta_n + \det(A) = 0. \tag{4.15}$$

As underlined in (4.13), the eigenvalues are proportional. Therefore, through condition (4.12), we can write that $\lambda_n = \theta\, \eta_n$. As a consequence, we can rewrite (4.15) to have an equation of $\mu(\eta_n)$. Indeed, we get that

$$\mu^2 + \mu[\eta_n(1+\theta) - \mathrm{tr}(A)] + \theta \eta_n^2 - \eta_n(\overline{f}_u + \theta\, \overline{g}_v) + \det(A) = 0. \tag{4.16}$$

For the steady state to be unstable to spatial disturbances, we require that $\mathrm{Re}(\mu(\eta_n)) > 0$. Since we are working with condition (4.7), the first order coefficient of this polynomial is positive.

Consequently, we need to impose that

$$p(\eta_n) := \theta\eta_n^2 - \eta_n(\overline{f}_u + \theta\,\overline{g}_v) + \det(A) < 0. \tag{4.17}$$

Because η_n, θ and $\det(A)$ are positive quantities, the polynomial in (4.17) can take negative values only for

$$\overline{f}_u + \theta\overline{g}_v > 0 \tag{4.18}$$

sufficiently large and $\theta\det(A)$ sufficiently small. We remember that one of the conditions to have stability without diffusion was $\mathrm{tr}(A) = \overline{f}_u + \overline{g}_v < 0$. This implies that $\theta \neq 1$, in other words $D_u \neq D_v$.

Inequality (4.18) is necessary but not sufficient for $\mathrm{Re}(\mu(\eta_n)) > 0$. For the convex function $p(\eta_n)$ to be strictly negative for some nonzero η_n, the minimum must be strictly negative. So if we look for the minimum, we find its coordinates

$$\eta_{\min} = \frac{\overline{f}_u + \theta\overline{g}_v}{2\theta} \quad \text{and} \quad p_{\min} = \det(A) - \frac{(\overline{f}_u + \theta\overline{g}_v)^2}{4\theta}. \tag{4.19}$$

Then, the condition $p_{\min} < 0$ corresponds to $\frac{(\overline{f}_u+\theta\overline{g}_v)^2}{4\theta} > \det(A)$. Finally, given specific functions f and g, we can find the values of θ which assure that the minimum $p_{\min} < 0$. We call θ_c the critical diffusion ratio such that $p_{\min} = 0$, *i.e.* the appropriate root of

$$\overline{g}_v^2\,\theta_c^2 + 2\,(\overline{f}_u\overline{g}_v - 2\det(A))\,\theta_c + \overline{f}_u^2 = 0. \tag{4.20}$$

It corresponds to the value of θ at which there is a bifurcation phenomenon (see Subsection 4.4.2 in which we analyse some related examples).

The range of values of η_n such that $p(\eta_n) < 0$ is $\eta_- < \eta_n < \eta_+$, with

$$\eta_- = \frac{|\overline{f}_u + \theta\overline{g}_v| - \sqrt{|\overline{f}_u + \theta\overline{g}_v|^2 - 4\theta\det(A)}}{2\theta}, \quad \eta_+ = \frac{|\overline{f}_u + \theta\overline{g}_v| + \sqrt{|\overline{f}_u + \theta\overline{g}_v|^2 - 4\theta\det(A)}}{2\theta}. \tag{4.21}$$

If we consider the solutions given by (4.9), the dominant contribution as t increases are the modes for which $\mathrm{Re}(\mu(\eta_n)) > 0$ since all the other modes tend to zero exponentially. By consequence, we can consider the following approximation for large t

$$u(t,x) \sim \sum_{\substack{n\in\mathbb{N}\\ \eta_-<\eta_n<\eta_+}} \alpha_n e^{\mu(\eta_n)t} z_n(x) \quad \text{and} \quad v(t,x) \sim \sum_{\substack{n\in\mathbb{N}\\ \eta_-<\eta_n<\eta_+}} \beta_n e^{\mu(\eta_n)t} z_n(x).$$

So, the larger is the range defined by η_- and η_+, the larger is the number of unstable modes not decreasing in time and, then, the modes which infer Turing instability. In order to estimate this interval, we can restrict to the regime θ small which is the most common in data. In that way, Taylor expansion of the square root gives

$$\eta_\pm = \frac{\overline{f}_u + \theta\overline{g}_v}{2\theta}\left[1 \pm \sqrt{1 - \frac{4\det(A)\theta}{(\overline{f}_u + \theta\overline{g}_v)^2}}\right] \sim \frac{\overline{f}_u}{2\theta}\left[1 \pm \left(1 - \frac{2\det(A)\theta}{(\overline{f}_u + \theta\overline{g}_v)^2}\right)\right].$$

Finally, we obtain

$$\eta_- \sim \frac{\det(A)}{\overline{f}_u} = O(1) \quad \text{and} \quad \eta_+ \sim \frac{\overline{f}_u}{\theta} \gg 1.$$

Taking θ sufficiently small (that means D_u), the interval (η_-, η_+) becomes very large, therefore

we can find some eigenvalues η_n in this interval. We remember that η_n are increasing eigenvalues converging to infinity and so there is only a finite number of them in that interval. This concludes the proof of the theorem.

□

4.3 One dimensional case

In the one dimensional case, we can construct an explicit solution of the eigenvalue problem. We consider the domain $(0, x_m) \cup (x_m, L)$, with $x_m = L/2$. Given relations (4.12)-(4.13) and with our short notation (4.3) for D_v, the eigenfunctions are determined by

$$\begin{cases} -\partial_x^2 z_n = \frac{\eta_n}{D_v} z_n, \\ \partial_x z_{1n}(0) = 0 = \partial_x z_{3n}(L), \\ \partial_x z_{1n}(x_m) = \nu_D \partial_x z_{3n}(x_m) = \nu_K (z_{3n}(x_m) - z_{1n}(x_m)). \end{cases} \tag{4.22}$$

We decompose z_n, for all $n \in \mathbb{N}$, as a combination of sinus and cosinus. Nevertheless, Neumann boundary conditions impose a cosinusoidal form. Hence, since eigenfunctions are defined up to a multiplicative constant, we deduce that z_n, for all $n \in \mathbb{N}$, has components

$$z_{1n}(x) = C_1 \cos(a_n x) \quad \text{and} \quad z_{3n}(x) = \cos(b_n (x - L)).$$

In order to verify Equations (4.22), we get, for all $n \in \mathbb{N}$,

$$a_n^2 = \frac{\eta_n}{D_{v1}} \quad \text{and} \quad b_n^2 = \frac{\eta_n}{D_{v3}},$$

so, in particular,

$$a_n^2 = \nu_D b_n^2, \quad \text{with } \nu_D = \frac{D_{u3}}{D_{u1}} = \frac{D_{v3}}{D_{v1}}.$$

Since the eigenfunctions satisfy Kedem-Katchalsky membrane conditions, we also have the following conditions on $x_m = L/2$, for all $n \in \mathbb{N}$,

$$\begin{cases} -C_1 \, b_n \sin\left(b_n \sqrt{\nu_D} \, \frac{L}{2}\right) = \sqrt{\nu_D} \, b_n \sin\left(b_n \frac{L}{2}\right), \\ D_{v3} \, b_n \sin\left(b_n \frac{L}{2}\right) = k_v \left(\cos\left(b_n \frac{L}{2}\right) - C_1 \cos\left(b_n \sqrt{\nu_D} \, \frac{L}{2}\right)\right), \end{cases}$$

Then, we infer that, for all $n \in \mathbb{N}$, either $b_n = 0$, so $\eta_n = 0$ and $z_{1n} = z_{3n} = \text{const}$, or if $b_n \neq 0$,

$$\begin{cases} C_1 = -\sqrt{\nu_D} \, \frac{\sin\left(b_n \frac{L}{2}\right)}{\sin\left(b_n \sqrt{\nu_D} \frac{L}{2}\right)}, \\ D_{v3} \, b_n \tan\left(b_n \frac{L}{2}\right) = k_v \left[1 + \sqrt{\nu_D} \, \frac{\tan\left(b_n \frac{L}{2}\right)}{\tan\left(b_n \sqrt{\nu_D} \frac{L}{2}\right)}\right]. \end{cases}$$

Hence, we have a system of two equations with 2 unknowns: C_1 and η_n. We conclude that, for

all $n \in \mathbb{N}$,

$$\begin{cases} C_1 = -\sqrt{\nu_D}\, \dfrac{\sin\left(\frac{\sqrt{\eta_n}}{\sqrt{D_{v3}}}\frac{L}{2}\right)}{\sin\left(\frac{\sqrt{\eta_n}}{\sqrt{D_{v1}}}\frac{L}{2}\right)}, & \text{(4.25a)} \\ \sqrt{\eta_n}\,\sqrt{D_{v3}}\tan\left(\dfrac{\sqrt{\eta_n}}{\sqrt{D_{v3}}}\dfrac{L}{2}\right) = k_v\left[1+\sqrt{\nu_D}\,\dfrac{\tan\left(\frac{\sqrt{\eta_n}}{\sqrt{D_{v3}}}\frac{L}{2}\right)}{\tan\left(\frac{\sqrt{\eta_n}}{\sqrt{D_{v1}}}\frac{L}{2}\right)}\right]. & \text{(4.25b)} \end{cases}$$

We can express the eigenvalues as the positive roots of the continuous function $r : \mathbb{R}^+ \to \mathbb{R}$, such that

$$r: \quad \xi \quad \longmapsto \quad \sqrt{\xi}\,\frac{\tan\left(\frac{\sqrt{\xi}}{\sqrt{D_{v1}}}\frac{L}{2}\right)\,\tan\left(\frac{\sqrt{\xi}}{\sqrt{D_{v3}}}\frac{L}{2}\right)}{\left[\tan\left(\frac{\sqrt{\xi}}{\sqrt{D_{v1}}}\frac{L}{2}\right)+\sqrt{\nu_D}\,\tan\left(\frac{\sqrt{\xi}}{\sqrt{D_{v3}}}\frac{L}{2}\right)\right]} - \frac{k_v}{\sqrt{D_{v3}}}. \tag{4.26}$$

see Figure (4.1).

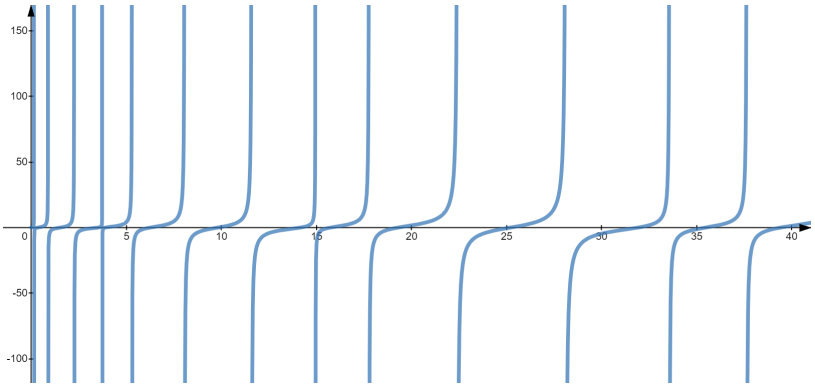

Figure 4.1: *We represent here the function $\xi \longmapsto r(\xi)$ in (4.26), considering $L = 1$, $D_{v1} = 10^{-1}$, $D_{v3} = 10^{-2}$ and $k_v = 10^{-4}$. Its roots correspond to the eigenvalues η_n.*

In order to simplify Equation (4.25b), in the following, we restrict to the case $\nu_D = 1$, *i.e.* $D_{v1} = D_{v3}$ and $D_{u1} = D_{u3}$, which is a reasonable assumption when the medium in the left and right domain have similar properties of diffusivity. Then, relation (4.25b) can be written for all $n \in \mathbb{N}$ as

$$C_1 = -1 \quad \text{and} \quad \sqrt{\eta_n}\,\tan\left(\frac{\sqrt{\eta_n}}{\sqrt{D_{v3}}}\,\frac{L}{2}\right) = 2\,\frac{k_v}{\sqrt{D_{v3}}}. \tag{4.27}$$

The simplified function $r(\cdot)$ of the form

$$r(\xi) = \sqrt{\xi}\,\tan\left(\frac{\sqrt{\xi}}{\sqrt{D_{v3}}}\,\frac{L}{2}\right) - 2\frac{k_v}{\sqrt{D_{v3}}}, \tag{4.28}$$

is depicted in Figure 4.2.

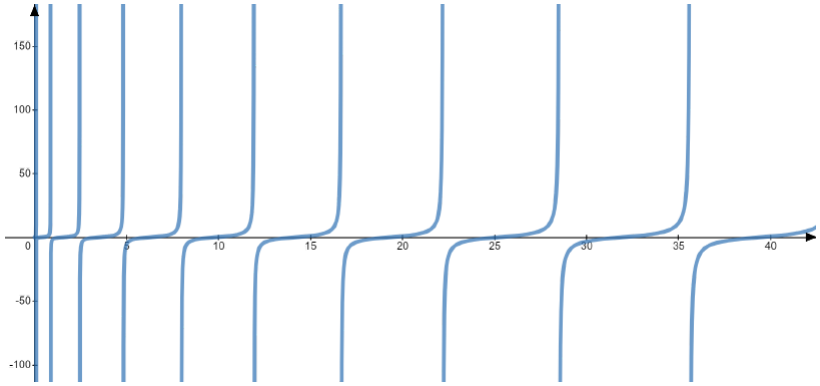

Figure 4.2: *Same as Figure 4.1, with* $\nu_{_D} = 1$*, and* $D_{v3} = D_{v1} = 10^{-2}$*. That is relation* (4.28)*, in place of* (4.26)*.*

4.4 Numerical examples

We investigate through numerical examples the effect of the membrane on appearance and shape of Turing's instability. We use the finite difference scheme of a Θ-method with $\Theta = 1$, Morton and Mayers [92], Quarteroni *et al.* [111], with a first-order discretization of the boundary and membrane conditions (see Appendix 4.B). At first, we present in details the expression of the reaction terms and the general data setting that we are using (Subsection 4.4.1). Then, we show some examples. In Subsection 4.4.2, we perform numerical examples with different choices for the value of θ (see Equation (4.12)), referring to the analyses performed in Section 4.2 concerning the values of θ_c (see Equation (4.20)). In Subsection 4.4.3, we exhibit simulations for different values of the membrane permeability coefficients. Finally, in Subsection 4.4.4, we perform oscillatory behaviours when a fast reaction-diffusion system converges to ill-posed cross-diffusion equations and we observe the evolution of these instabilities under the effect of the membrane permeability parameter.

4.4.1 Choice of reaction terms and data setting

We choose a simple setting with mass conservation, already analysed by Moussa *et al.* [93] in a Turing instabilities study. In the following, we consider System (4.1) with

$$f(u,v) = \varepsilon^{-1}(v - h(u)), \quad g(u,v) = -f(u,v), \quad \text{with } h(u) = \alpha\, u\,(u-1)^2 \tag{4.29}$$

and (see also Figure 4.3) we notice the conditions

$$h \in C^2(\mathbb{R}^+, \mathbb{R}^+),\ h(0) = 0,\ h(u) > 0 \ \text{ for } u > 0 \ \text{ and } \ h'(u) = \alpha(1-u)(1-3u) > -1. \tag{4.30}$$

We observe that there is mass conservation which is the first basic property of System (4.1) with (4.29). Looking at the latter condition $h'(u) > -1$, the admissible values of α are $0 < \alpha < 3$. In the numerical examples, we choose the value $\alpha = 1$. The small parameter $\varepsilon > 0$ measures the time scale of the reaction compared to diffusion. The smaller is ε, the more numerous are the patterns. Indeed, in the limit $\varepsilon \to 0$, we are dealing with a fast reaction-diffusion system (see Section 1.2) and its Turing instability turns out to be equivalent to the instability due to the ill-posedness for the limiting cross-diffusion equations, caused by backward parabolicity,

Moussa *et al.* [93], Perthame and Skrzeczkowski [105]. In the following numerical examples, we take $\varepsilon = 1$ which corresponds to a standard reaction-diffusion system, whereas in Subsection 4.4.4 we let vary ε to obtain the numerical zero-limit.

We briefly prove that the reaction terms in (4.29), with general values of ε, α and h, satisfy the analysis in Section 4.2.

Claim 4.4.1. *Considering reaction terms in (4.29), we claim that:*

1. *In the absence of diffusion, there is a unique stable equilibrium point $(\overline{u}, \overline{v})$ to which solutions converge monotonically.*

2. *The same steady state $(\overline{u}, \overline{v})$ is asymptotically Turing unstable for the linearised reaction-diffusion system under the condition*

$$\theta + h'(\overline{u}) < 0. \tag{4.31}$$

Proof. Statement 1.
We take the dynamical system

$$\frac{d}{dt}\begin{pmatrix} u \\ v \end{pmatrix} = \begin{pmatrix} \varepsilon^{-1}(v - h(u)) \\ -\varepsilon^{-1}(v - h(u)) \end{pmatrix},$$

which has steady state $(\overline{u}, \overline{v})$ such that $\overline{v} = h(\overline{u})$. Thanks to mass conservation of the system, we can write $M := u(t) + v(t) = u(0) + v(0)$ and $\frac{d}{dt}u = \varepsilon^{-1}(M - u - h(u)) =: \varepsilon^{-1}G(u(t))$. Since u, v are positive functions, the function G has the following properties: $G(0) = M > 0$, $G'(u) < 0$ and $G(+\infty) = -\infty$. Consequently, there exists a unique stable equilibrium point $(\overline{u}, \overline{v})$, monotonically achieved (since $G(u) > 0$ for $u \leqslant \overline{u}$ and $G(u) < 0$ for $u \geqslant \overline{u}$), that cancels G such that $\overline{u} = M - \overline{v}$ and $\overline{v} = h(\overline{u})$.
Statement 2.
Applying the same general steps as in the proof of Theorem 4.2.1, for the steady state to be unstable under spatial disturbances we require (see (4.18)) that $\theta + h'(\overline{u}) < 0$, with $-\varepsilon^{-1}(\theta + h'(\overline{u}))$ sufficiently large and θ sufficiently small. This is a necessary and sufficient condition when it is assured that the minimum of the polynomial $p(\eta)$ in (4.17) is negative. Looking back at Equations (4.19) with reactions in (4.29), we get

$$\eta_{\min} = \varepsilon^{-1}\,\frac{|h'(\overline{u}) + \theta|}{2\theta} \quad \text{and} \quad p_{\min} = -\theta\eta_{\min}^2. \tag{4.32}$$

It is clear that $p_{\min} < 0$ for all $\eta_{\min} \neq 0$, *i.e.* for $\theta \neq -h'(\overline{u})$. Otherwise, $p_{\min}$ is equal to zero and, then, we have found the critical diffusion ratio $\theta_c = -h'(\overline{u})$ at which there is a bifurcation phenomenon. Moreover, calculating the range where we can find unstable modes, like in (4.21), we deduce that

$$\eta_- = 0 \;\text{ and }\; \eta_+ = -\varepsilon^{-1}\left(1 + \theta^{-1}h'(\overline{u})\right). \tag{4.33}$$

This range is larger if condition (4.31) with $-\varepsilon^{-1}(\theta + h'(\overline{u}))$ sufficiently large and θ sufficiently small are satisfied. In particular, varying the parameter ε, we observe that the smaller it is, the larger is the range (η_-, η_+), *i.e.* a larger number of eigenvalues generating instability can be found. This concludes the proof of the claim.

□

We can easily calculate the steady state $(\overline{u}, \overline{v})$ thanks to the mass conservative structure of the system, as pointed out in the previous proof. Indeed, adding up the reaction-diffusion equations

for u and v and integrating over the space, we get for all $t \geqslant 0$,

$$\int_0^L u(x,t) + v(x,t)dx = \int_0^L u_0(x) + v_0(x)dx.$$

Then, we conclude that the steady state depends on the length of the domain (here $[0, L]$) and on the initial data, *i.e.*

$$\overline{u} + \overline{v} = \frac{1}{L} \int_0^L u_0(x) + v_0(x)dx, \qquad \text{with } \overline{v} = h(\overline{u}). \tag{4.34}$$

In particular, this steady state is Turing unstable when $h'(\overline{u}) < -\theta$, as it can be deduced from relation (4.31). So, $h'(\overline{u}) < 0$ which means that $h'(\overline{u}) \in \left(-\frac{\alpha}{3}, 0\right)$. Then, we infer that the Turing unstable steady state is such that $\overline{u} \in \left(\frac{1}{3}, 1\right)$ and $\overline{v} \in \left(0, \alpha\frac{4}{27}\right)$ (see Figure 4.3).

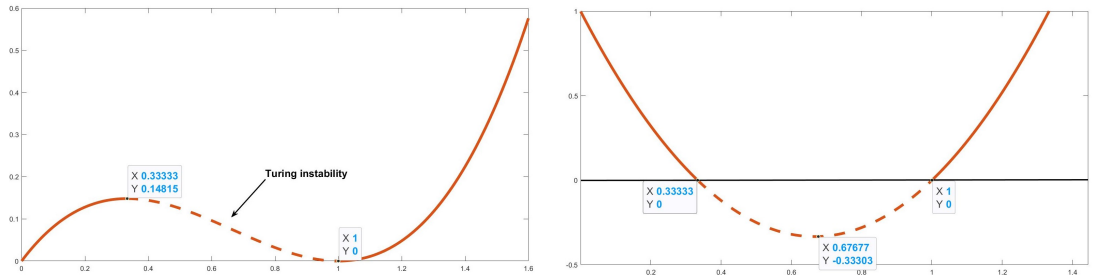

Figure 4.3: *We represent $h(u)$ in (4.29)-(4.30) (left picture) and $h'(u)$ (right picture) with $\alpha = 1$. In dashed lines, the instability region for $\overline{u}$ and $h(\overline{u}) = \overline{v}$.*

Finally, we present the main data chosen for simulations in Subsection 4.4.2 - 4.4.4. We show the time convergent solutions (in the left for u and in the right for v) in the spatial interval $[0, L]$, with $L = 1$ and with a discretization step $\Delta x = \frac{L}{200}$. As shown in Figure 4.4, we take the initial data as

$$u_0(x) = \begin{cases} \frac{7}{15} + \frac{1}{5}\sin(4\pi x), & \text{for } 0 \leqslant x \leqslant \frac{1}{2}, \\ \frac{1}{5} + \frac{1}{5}\sin(4\pi x), & \text{for } \frac{1}{2} < x \leqslant 1 \end{cases} \quad \text{and} \quad v_0(x) = \begin{cases} \frac{1}{3} - \frac{1}{5}\sin(4\pi x), & \text{for } 0 \leqslant x \leqslant \frac{1}{2}, \\ \frac{3}{5} - \frac{1}{5}\sin(4\pi x), & \text{for } \frac{1}{2} < x \leqslant 1. \end{cases}$$

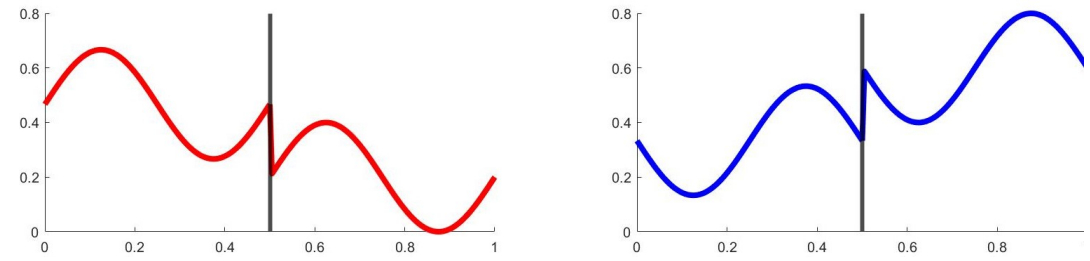

Figure 4.4: *Representation of the initial data u_0 (in the left) and v_0 (in the right).*

Looking back at (4.34), we deduce that the steady state $(\overline{u}, \overline{v})$ is such that $\overline{u} + \overline{v} = \frac{4}{5}$ with $\overline{v} = h(\overline{u})$. With $\alpha = 1$, we conclude that

$$\overline{u} = 0.7545 \in \left(\frac{1}{3}, 1\right), \quad \overline{v} = h(\overline{u}) = 0.0454 \in \left(0, \frac{4}{27}\right) \quad \text{and} \quad h'(\overline{u}) = -0,3101 \in \left(-\frac{1}{3}, 0\right). \tag{4.35}$$

If not specified, we guarantee conditions (4.12) and (4.13) in Lemma 4.2.1 with $\nu_{_D} = 1$ such that

$$D_{u1} = D_{u3} = \theta, \quad k_u = \theta\, k_v \quad \text{with } D_{v1} = D_{v3} = 1 \text{ and } \varepsilon = 1. \tag{4.36}$$

4.4.2 Effect of the diffusion ratio

We illustrate the effect of different values of the diffusion ratio θ in (4.12). We consider the reaction terms in (4.29), initial data as in Figure 4.4 and data setting as in (4.36) with $k_v = 1$ fixed. We remember that when we vary θ, there exists a critical diffusion ratio θ_c for Turing's instability. As analysed in the proof of Claim 4.4.1 and in (4.32), we can define

$$\theta_c = -\,h'(\overline{u}) \quad \text{and} \quad \eta_{_{min}} = \frac{1}{2\theta\,\varepsilon}\,|\theta + h'(\overline{u})|, \quad p_{_{min}} = -\,\theta\,\eta_{_{min}}^2, \tag{4.37}$$

where θ_c is the critical diffusion ratio at which $p_{_{min}}$, the minimum of the polynomial (4.17) calculated in $\eta_{_{min}}$, is zero. For $\theta = \theta_c$, we remark that $\eta_{_{min}} = p_{_{min}} = 0$. Otherwise, for $\theta < \theta_c$, the minimum is strictly negative (see Figure 4.5) and so we can calculate the non-empty range of instability. However, in the case $\theta > \theta_c$, *i.e.* $\theta > |h'(\overline{u})|$, we cannot find Turing patterns, since condition (4.31) does not hold.

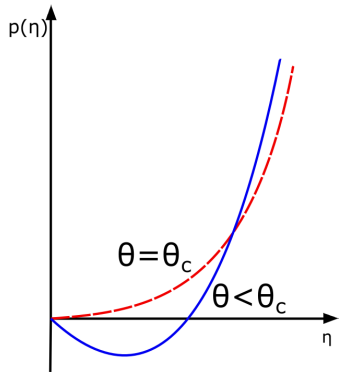

Figure 4.5: *Representation of the function in* (4.17) *determining the unstable modes with the reaction terms in* (4.29) *for* $\theta = \theta_c$ *(dashed line) and for* $\theta < \theta_c$ *(solid line). So,* $p(\eta) = \theta\eta^2 + \varepsilon^{-1}(\theta + h'(\overline{u}))\eta$ *with* $\varepsilon^{-1} = 2$, $h'(\overline{u}) = -0.3101$ *and* $\theta = 10^{-1} < \theta_c$.

In the numerical examples, we consider decreasing values of $\theta \leqslant \theta_c$ in order to see both what happens in an appropriate neighbourhood of θ_c and far away from this threshold. Looking back at (4.35), we infer that $\theta_c = -h'(\overline{u}) = 3.101 \cdot 10^{-1}$. We recall the expression for η_-, η_+ in (4.33) and the one dimension Equation (4.27) that defines the eigenvalues of u and v:

$$\eta_- = 0, \quad \eta_+ = -\varepsilon^{-1}(1 + \theta^{-1}h'(\overline{u})) \quad \text{and} \quad \sqrt{\eta_n}\,\tan\left(\frac{\sqrt{\eta_n}}{\sqrt{D_{v3}}}\,\frac{L}{2}\right) = 2\,\frac{k_v}{\sqrt{D_{v3}}}.$$

Case 1. We take $\theta = \theta_c = 3.101 \cdot 10^{-1}$ and the other parameters according to (4.36) ($k_v = 1$, $k_u = 3.101 \cdot 10^{-1}$).

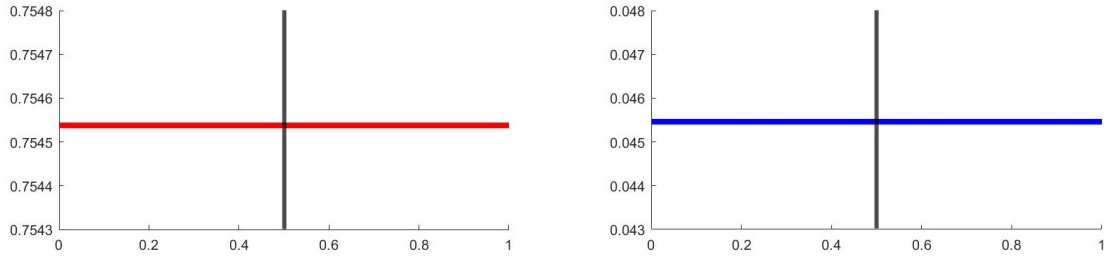

Figure 4.6: *Taking $\theta = \theta_c$, as we can see in Figure 4.5, we cannot define an unstable range (η_-, η_+) such that the polynomial $p(\eta)$ is strictly negative. In fact, we are at the bifurcation point. That is why, on a long time scale, we do not observe patterns neither for u (in the left) nor for v (in the right). Instead, as we are working with a reaction-diffusion equation with dissipative membrane conditions, we notice the convergence to the equilibrium $(\overline{u}, \overline{v})$ in (4.35).*

Case 2. We take $\theta = 7.8 \cdot 10^{-2}$ and the other parameters according to (4.36) ($k_v = 1$, $k_u = 7.8 \cdot 10^{-2}$). In this case, $\eta_+ = 2.97$ and so only the first eigenvalue $\eta_1 = 2.96$ corresponds to an unstable mode ($\eta_n > \eta_+$, for $n \geqslant 2$).

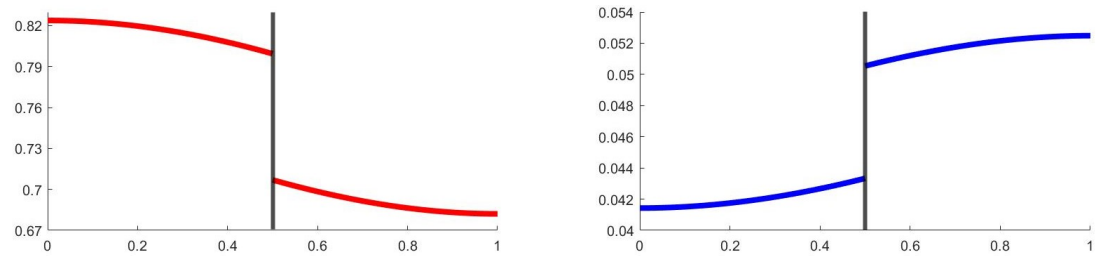

Figure 4.7: *Since $\theta < \theta_c$, on a long time scale, solutions do not reach the steady state even if they are nearby. Considering the only $\eta_1 \in (\eta_-, \eta_+)$, we do not observe a really interesting pattern but a piecewise function. We can appreciate the inclination of the solutions in the left and right limit at the membrane: they satisfy Kedem-Katchalsky conditions. We remark that with membrane problems, a nearly constant function with a jump at the membrane stands for a pattern.*

Case 3. We consider $\theta = 3 \cdot 10^{-4}$ and the other parameters according to (4.36) ($k_v = 1$, $k_u = 3 \cdot 10^{-4}$). These data give $\eta_+ = 1032.6$ and so we have 6 eigenvalues in (η_-, η_+).

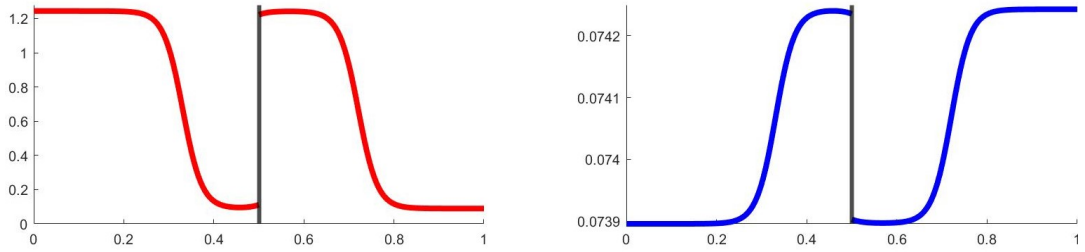

Figure 4.8: *Choosing $\theta = 3 \cdot 10^{-4}$, we succeed in having more considerable patterns for both the species u and v in the temporal limit. Moreover, it is again clear the well-verification of membrane conditions. As remark, we underline that until 5 eigenvalues in (η_-, η_+), over long time interval, the shape does not change significantly respect to Figure 4.7. Then, the diffusion ratio θ has to be sufficiently small to appreciate more complex patterns.*

Case 4. We take $\theta = 10^{-5}$ and the other parameters according to (4.36) ($k_v = 1$, $k_u = 10^{-5}$). In this case, $\eta_+ = 31009$ and so we have several eigenvalues in (η_-, η_+).

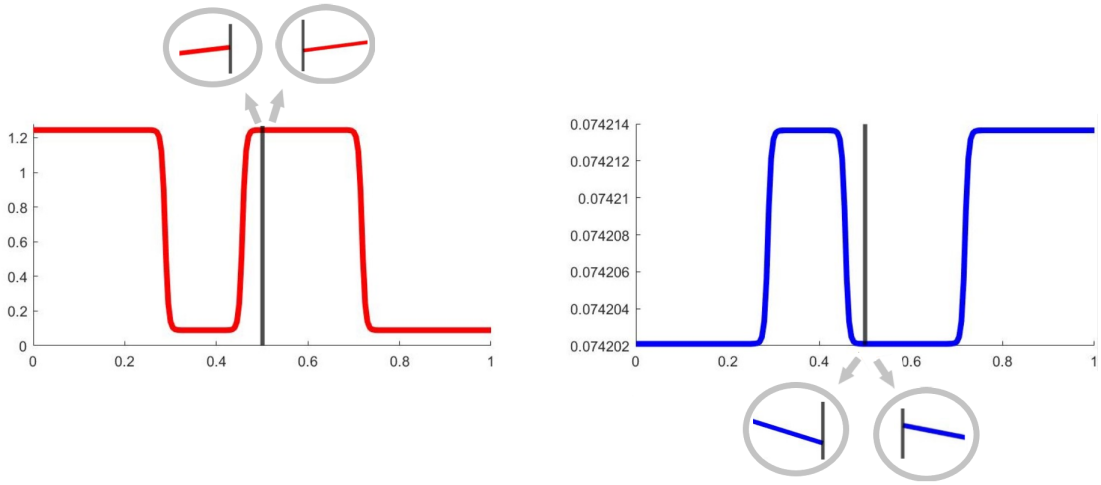

Figure 4.9: *Here, θ is on a very different scale respect to θ_c and there is a big number of unstable modes η_n. Hence, we observe remarkable and beautiful patterns both for u and v. The jump at the membrane is not evident with this choice of parameter. Then, in the zoom circles, we can appreciate the inclination of the solutions in the left and right limit at the membrane remarking that they satisfy Kedem-Katchalsky conditions.*

In conclusion, fixing $k_v \in (0, +\infty)$ and decreasing θ from its critical value θ_c, we can notice a remarkable change in patterns. In particular, starting from the convergence to the equilibrium for $\theta = \theta_c$ in Figure 4.6, we then approach three different, but discontinuous, shapes. Considering a reduced number of eigenvalues in the unstable range, solutions show a basic pattern which is a nearly constant function with a jump at the membrane (as in Figure 4.7). Decreasing θ, we get more complex and stiffer shapes depending on the number of unstable modes found in the interval (η_-, η_+) (see Figures 4.8 , 4.9).

4.4.3 Values of the permeability coefficients

We show here another set of simulations in which we vary only the permeability coefficient $k_v \in [0, +\infty]$ (then, k_u, given the coupling $k_u = \theta k_v$ deducible from (4.12)) in the data chosen in (4.36). So, we better discover the effect of the membrane on Turing patterns. In particular, we can distinguish two limiting situations: $k_v = 0 = k_u$, which is the one without transmission and it corresponds to have two separate and not communicating domains, and $k_v = +\infty = k_u$ (numerically realised taking $k_v = 10^8$), *i.e.* we have full permeability at the membrane, so it corresponds to have a unique connected domain. In this two extreme cases, we recover the results of a standard reaction-diffusion system without the effect of the membrane. Considering different values of the permeability coefficients, we can estimate the position of the eigenvalues on the real lines and then, in the unstable interval, in order to follow the same arguments as in the previous subsection. Indeed, we recall the dependence on k_v of the eigenvalues equation (4.27) such that if $\eta_n \neq 0$, we have that

$$\sqrt{\eta_n}\ \tan\left(\frac{\sqrt{\eta_n}}{\sqrt{D_{v3}}}\,\frac{L}{2}\right) = 2\,\frac{k_v}{\sqrt{D_{v3}}}.$$

In the case $k_v = 0 = k_u$, the previous equation reduces to $\sin\left(\frac{L}{2}\frac{\sqrt{\eta_n}}{\sqrt{D_{v3}}}\right) = 0$ and so we can calculate the eigenvalues as

$$\eta_n = D_{v3}\,\frac{(2n)^2\pi^2}{L^2}.$$

In the case $k_v = +\infty = k_u$, we have $\cos\left(\frac{L}{2}\frac{\sqrt{\eta_n}}{\sqrt{D_{v3}}}\right) = 0$ and, then, the eigenvalues are of the form

$$\eta_n = D_{v3}\,\frac{(2n+1)^2\pi^2}{L^2}.$$

We can affirm that the eigenvalues η_n^k related to a certain value of $k = k_u, k_v \in (0, +\infty)$ are situated between the eigenvalues η_n^0 for $k = 0$ and the ones for $k = +\infty$, *i.e.* η_n^∞. Moreover, fixing n and varying k, the eigenvalues η_n^k pass continuously from η_n^0 to η_n^∞. This can be observed in two different ways: from a numerical result or a more analytical one.

Numerical result
For $L = 1$, we consider the continuous function

$$q: \quad \xi \quad \longmapsto \quad \xi\,\tan\left(\frac{\xi}{2}\right) - 2\,\frac{k_v}{D_{v3}}. \tag{4.38}$$

Numerically, we find the zeros $\xi_n = \frac{\sqrt{\eta_n}}{\sqrt{D_{v3}}}$, $n \geqslant 0$ for different values of $\frac{k_v}{D_{v3}}$ and, then, of k_v (see Table 4.1).

k_v/D_{v3}	ξ_1	ξ_2	ξ_3	ξ_4
0	0	2π	4π	6π
0.5	0.41π	2.09π	4.05π	6.04π
5	0.83π	2.56π	4.39π	6.29π
10^8	π	3π	5π	7π

Table 4.1: *We report the values of the first four zeroes $\xi_n = \frac{\sqrt{\eta_n}}{\sqrt{D_{v3}}}$, $n = 1, ..., 4$ for different values of k_v, since D_{v3} is fixed, including the two limiting cases and two intermediate ones.*

Then, we recover the previous eigenvalue formulas for the two limiting situations and we can also observe that for fixed n, the eigenvalues $\eta_n^{k_v}$ increase continuously with k_v towards η_n^{∞}.

Analytical result
Another way to look at this phenomenon and to better observe continuity of the ξ_n's changing k_v and fixing n, it is to represent the function in (4.38) (see Figure 4.10). We consider $n = 1$ and so the interval $\xi \in (0, \pi)$. Since we have a monotonous function for $\xi \in (0, \pi)$, there exists a unique intersection with the horizontal line $y = k := 2\frac{k_v}{D_{v3}} = 2\frac{k_u}{D_{u3}}$ and for $0 < k_1 < k_2 < +\infty$, we get $0 < \xi_1^{k_1} < \xi_1^{k_2} < +\infty$.

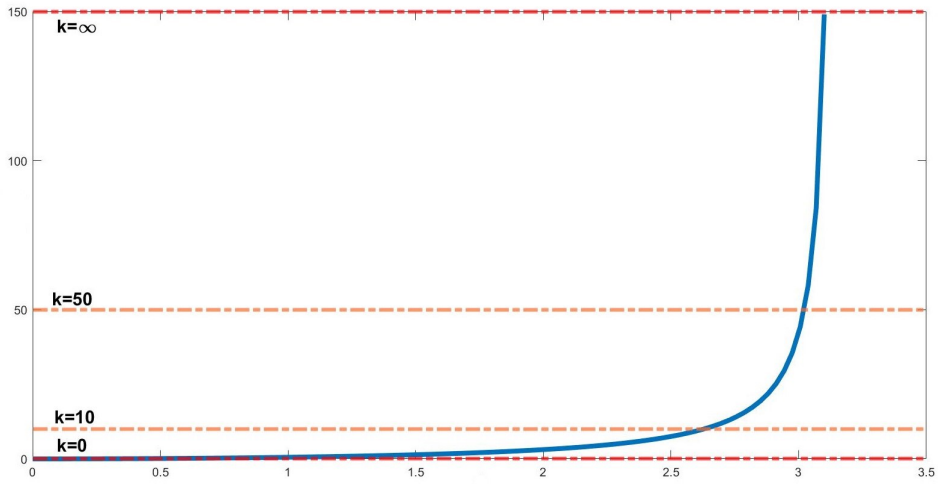

Figure 4.10: *Representation of the first root ξ_1 of q in (4.38), as the intersection between the function $\tilde{q} : \xi \longmapsto \xi \tan\left(\frac{\xi}{2}\right)$ for $\xi \in (0, \pi)$ (solid line) and one of the dashed lines defined by the permeability coefficient by the relation $k := 2\frac{k_v}{D_{v3}} = 2\frac{k_u}{D_{u3}}$.*

Remark 4.4.1. *For $k_u = k_v = 0$, the eigenvalue 0 is double. This is because we have two different domains with Neumann boundary conditions and so for both we find the zero eigenvalue.*

In Example 4.4.1, we refer to Table 4.1 and to the fact that the first non-zero eigenvalue for $k_v = +\infty = k_u$ is smaller than the one for $k_v = 0 = k_u$. So, we look for an unstable range such that $\eta_1^{\infty} \in (\eta_-, \eta_+)$ but $\eta_1^0 \notin (\eta_-, \eta_+)$. Then, we expect to see a different behaviour of the solutions. We perform also an intermediate case in which k_v is small but positive in order to see the evolution in shapes passing from a situation in which there are no unstable modes to another one in which there is only one of them. In Example 4.4.2, we show the appearance and the evolution of patterns in both the limiting cases and an intermediate one.

Example 4.4.1. *We look for some appropriate values of the diffusion coefficients in order to have $\eta_+ \in [D_{v3}\pi^2, D_{v3}4\pi^2)$. In that way, we expect to see patterns for $k_v \in (0, +\infty]$, since the first eigenvalue is in the unstable range (see Table 4.1). Instead, for $k_v = 0$, there is any non-zero eigenvalue in (η_-, η_+), then solutions should converge to the steady state in (4.35). Therefore, choosing $\theta = 10^{-2}$ in (4.36), we infer that $\eta_+ = 30.01 \in [\pi^2, 4\pi^2)$. The results are the following.*

Case 1. *We take $k_v = 0$ and the other data according to (4.36) ($\theta = 10^{-2}$, $k_u = 0$). For construction, we gain the absence of patterns.*

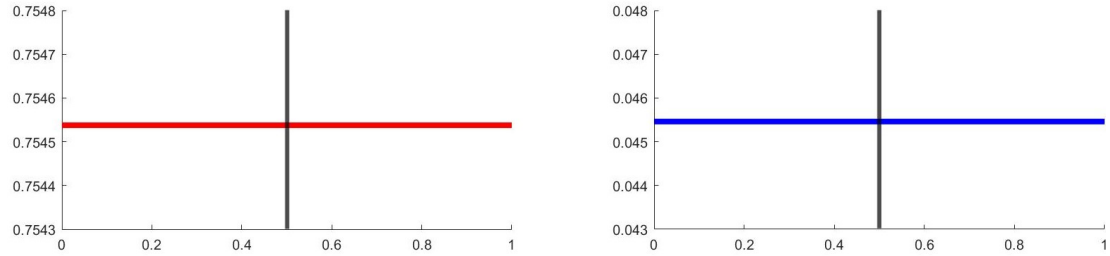

Figure 4.11: *As expected, taking $k_v = 0$, we can appreciate the convergence to the steady state $(\overline{u}, \overline{v})$ previously found. Indeed, we choose the data in order to not include positive eigenvalues in the unstable interval (η_-, η_+) in the case of zero permeability.*

Case 2. *We take $k_v = 10^{-2}$ and the other data according to (4.36) ($\theta = 10^{-2}$, $k_u = 10^{-6}$). We gain a single unstable mode which is $\eta_1 = 0.04$.*

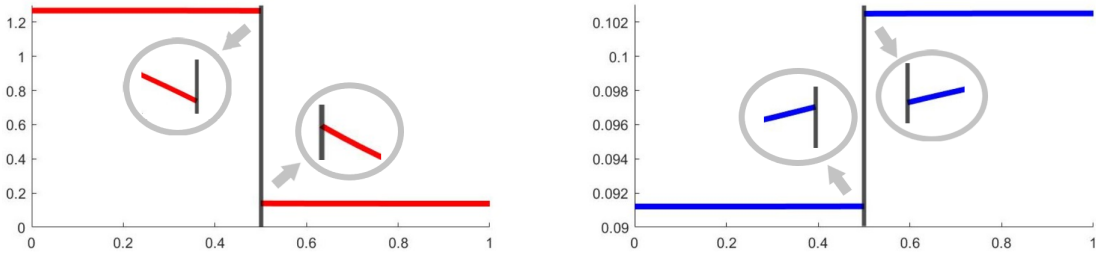

Figure 4.12: *In the case $k_v = 10^{-2}$, we can find a small positive eigenvalue in a neighbourhood of zero which is then in the unstable range $(0, 30.01)$. Then, we observe the appearance of a simple pattern which is only a piecewise function with a jump at the membrane. In the zoom circles, we focus the attention on solutions derivatives at the membrane to better appreciate that membrane conditions are satisfied. Moreover, the sign of the derivatives corresponds to the sign of the jump.*

Case 3. *We consider $k_v = 10^8$ and the other data according to (4.36) ($\theta = 10^{-2}$, $k_u = 10^4$).*

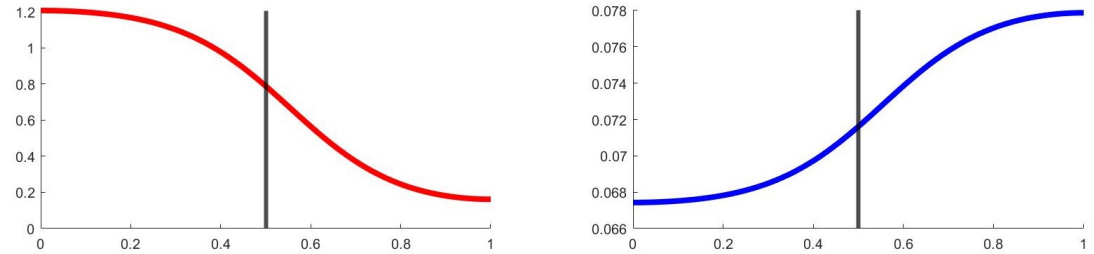

Figure 4.13: *As built, for $k_v = +\infty$, we see the appearance of continuous patterns, since the permeability coefficients are really big. Indeed, the shape corresponds to the one seen in Figure 4.12 but, at the membrane, the jump is now reduced to zero.*

Example 4.4.2. *We show the evolution of patterns varying $k_v \in [0, +\infty]$ and fixing θ. We choose the setting of Case 3 in Figure 4.8. Then, we take $\theta = 3 \cdot 10^{-4}$ in (4.36).*

Case 1. *We consider $k_v = 0$ and the other parameters according to the data in (4.36) ($\theta = 3 \cdot 10^{-4}$, $k_u = 0$). The number of eigenvalues in the unstable interval (η_-, η_+) is 5.*

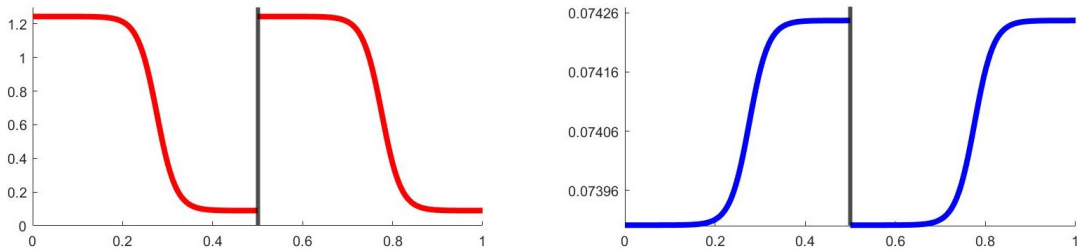

Figure 4.14: *Choosing $k_v = 0$, we clearly see patterns for u and v. In particular, they are similar to the one observed in Figure 4.8. A remarkable difference is at the membrane where Kedem-Katchalsky conditions are broken and they become standard homogeneous Neumann boundary conditions.*

Case 2. *We take $k_v = 10$ and the other parameters according to (4.36) ($\theta = 3 \cdot 10^{-4}$, $k_u = 3 \cdot 10^{-3}$).*

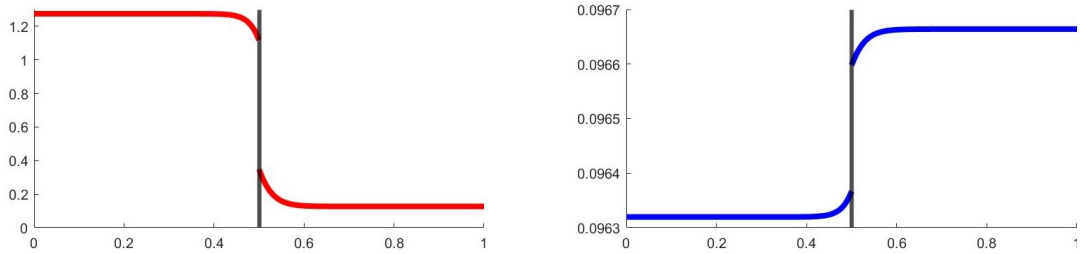

Figure 4.15: *With $k_v = 10$, solutions converge to an unexpected shape. There are 6 unstable modes which are not enough to generate a convergence to a more complex pattern, as it could happen with only 3 eigenvalues more in the case $\theta = 10^{-4}$ (as represented in the summary Table 4.2 in Section 4.5).*

Case 3. *We choose $k_v = 10^8$ with the other data as in (4.36) ($\theta = 3 \cdot 10^{-4}$, $k_u = 10^4$).*

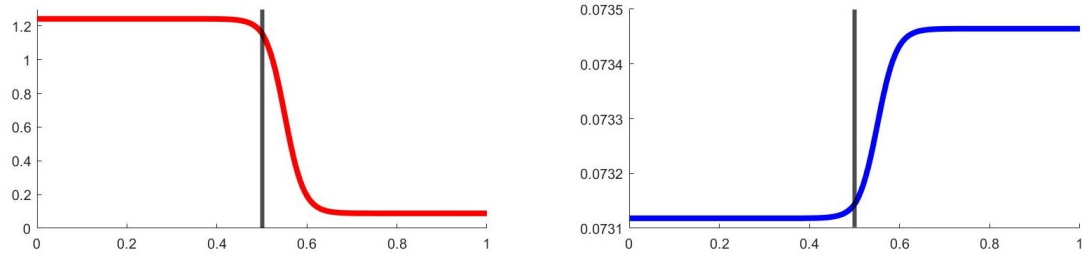

Figure 4.16: *With k_v and k_u sufficiently large, the jump at the membrane (seen in Figure 4.15) is reduced to an infinitesimal. Since, the number of unstable modes is small, the same behaviour in Figure 4.13 is recover.*

To sum up, in this two examples we can observe a particular pattern behaviour, for intermediate $k_v \in (0, +\infty)$ and for a small number of unstable modes, or equivalently, θ nearby θ_c, which does not occur with smooth Turing instability. Indeed, the transition from the case of two separate domain for $k_v = 0$ to a unique entire one for $k_v = +\infty$ is realized through a discontinuous state, which is a nearly constant function with a jump at the membrane.

4.4.4 Effect of the parameter ε

Another interesting parameter is ε, as briefly explained choosing reaction terms in Subsection 4.4.1. We remember that the smaller we take ε, the faster are the reactions and the more numerous are the patterns. However, in the limit $\varepsilon \to 0$, Turing instability for fast reaction-diffusion systems turns out to be equivalent to the instability due to backward parabolicity for the limiting cross-diffusion equations, Moussa *et al.* [93], Perthame and Skrzeczkowski [105], see also Section 1.2. Here, we show the changing of patterns for the solutions u (left) and v (right) decreasing the value of ε in different membrane scenarios. Again, we consider the data setting presented in Subsection 4.4.1. In particular, we choose data in (4.36) with $\theta = 10^{-4}$ and a varying ε.

As previously stressed, we need to look at the instability interval (η_-, η_+) in (4.33) which increases in size as ε decreases to zero. This implies that the number of eigenvalues (given by Equation (4.27)) in that interval increases as ε goes to zero. Then, fixing the membrane permeability k_v, we expect to see more complicated shapes as $\varepsilon \to 0$. Instead, fixing ε and varying k_v, we gain or lose (depending on the ε value) at most one unstable mode. This is why fixing ε patterns with different k_u, k_v are comparable.

Case 1. We consider $k_v = 0$ and the other parameters according to data in (4.36) ($\theta = 10^{-4}$, $k_u = 0$, ε varies). Indeed, we have not communicating domains in which we consider a reaction-diffusion system with reaction that is faster decreasing ε.

$\varepsilon = 10.$

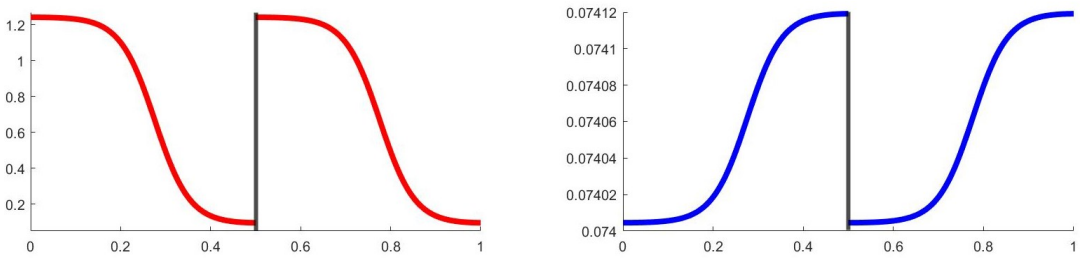

Figure 4.17: *We represent the convergent solutions for* $\varepsilon = 10$*. Diffusion prevails over reaction, then solutions are smooth and we can appreciate the emergence of patterns.*

$\varepsilon = 1.$

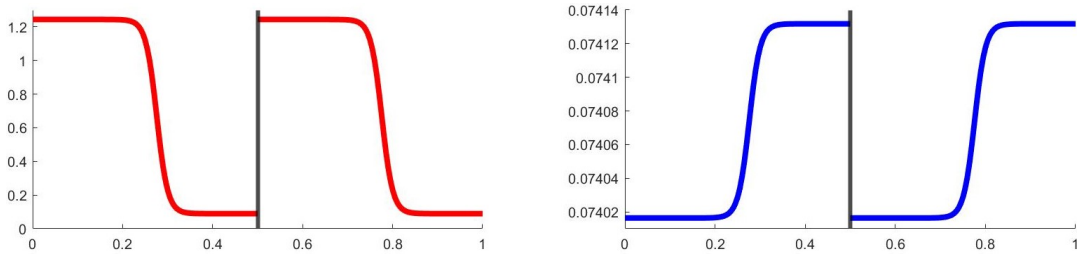

Figure 4.18: *In the case* $\varepsilon = 1$*, solutions does not change significantly respect to* $\varepsilon = 10$ *(we have only* 5 *unstable modes) but the slope is increasing. This scenario corresponds to the standard reaction-diffusion diffusion one analysed until now.*

$\varepsilon = 1/5.$

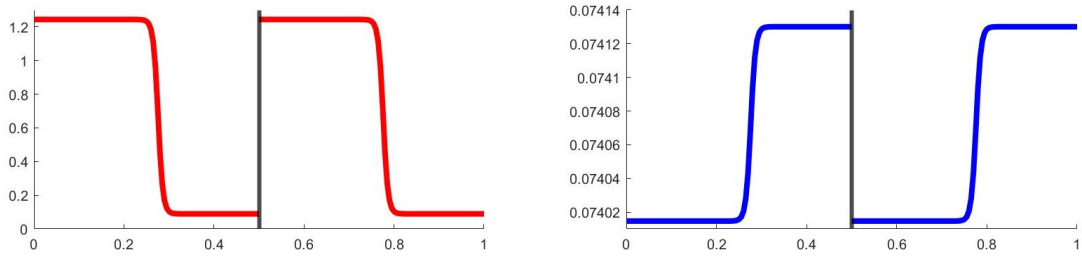

Figure 4.19: *It is with* $\varepsilon = 1/5$ *that we can see that the patterns are becoming more discontinuous, since numerically we are approaching the zero limit.*

$\varepsilon = 1/20.$

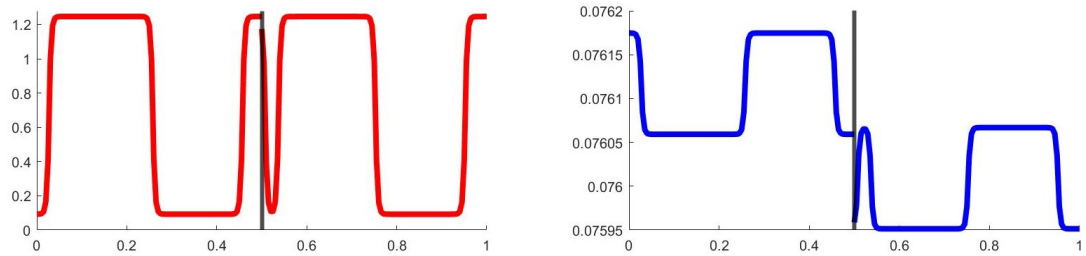

Figure 4.20: *With $\varepsilon = 1/20$, high frequency of oscillations are clearly appreciated. Numerically, we are converging to zero and then Turing instability is equivalent to instability and discontinuity of the ill-posedness of the backward parabolicity for the cross-diffusion system.*

$\varepsilon = 1/100.$

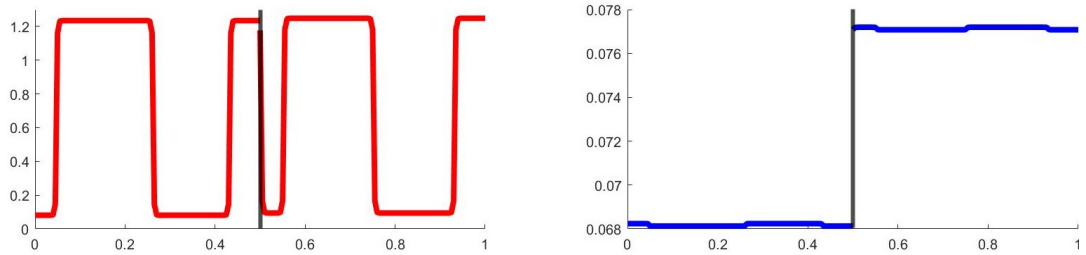

Figure 4.21: *Discontinuities are dominant with $\varepsilon = 1/100$. The right picture representing v has similar shapes has the one for $\varepsilon = 1/20$ but here the jump is more remarkable. The number of eigenvalues in the unstable range is really high and the slope in the patterns is diverging. We are far away from the smooth and regular patterns observed with slower reactions.*

Case 2. We consider $k_v = 1$ and the other parameters according to data in (4.36) ($\theta = 10^{-4}$, $k_u = 10^{-4}$, ε varies). The passage through the membrane is now allowed.

$\underline{\varepsilon = 10.}$

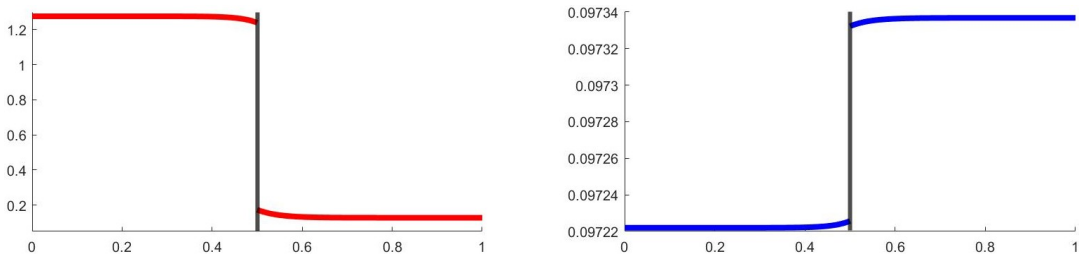

Figure 4.22: *With $\varepsilon = 10$, the slow reaction is not prevailing significantly on the diffusion (since increasing the value of ε, reactions converge to zero). The permeability of the membrane promotes dissipation but a slope nearby the interface is still observed.*

$\underline{\varepsilon = 1.}$

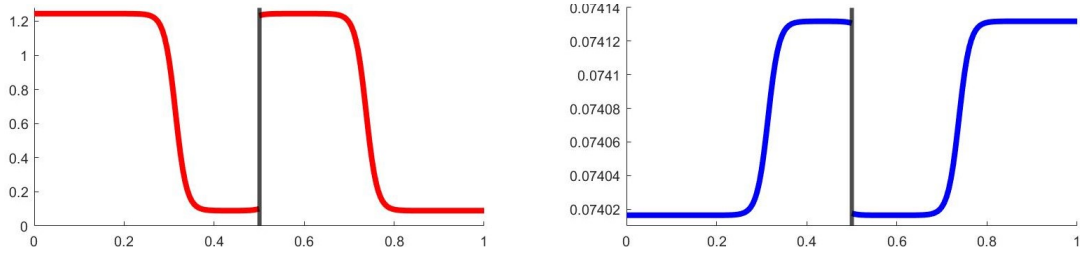

Figure 4.23: *Coming back to a standard reaction-diffusion equation with $\varepsilon = 1$, we observe a similar shape as in the case $k_v = 0$ but we can appreciate a little slope nearby the membrane.*

$\underline{\varepsilon = 1/5.}$

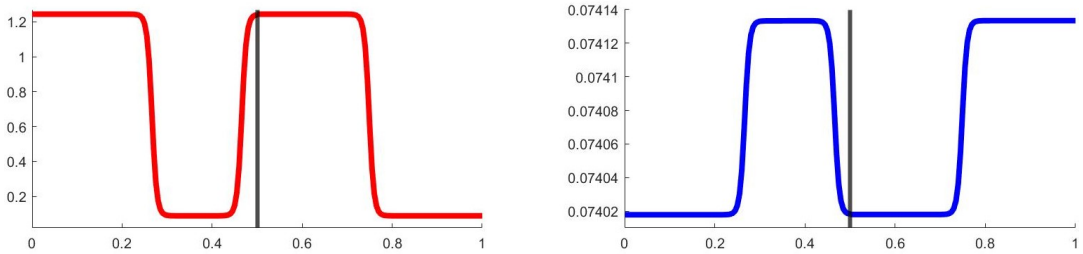

Figure 4.24: *Reducing ε, slopes increase but the jump at the membrane is less significant since membrane derivatives are really small with the data chosen.*

$\varepsilon = 1/20.$

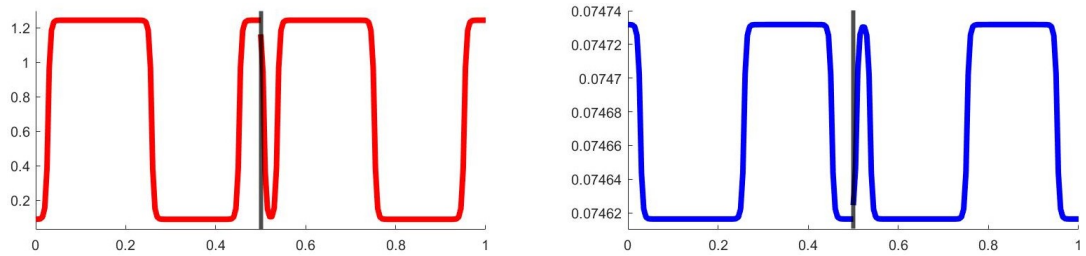

Figure 4.25: *As in the case $k_v = 0$, oscillations are increasing respect to Figure 4.24.*

$\varepsilon = 1/100.$

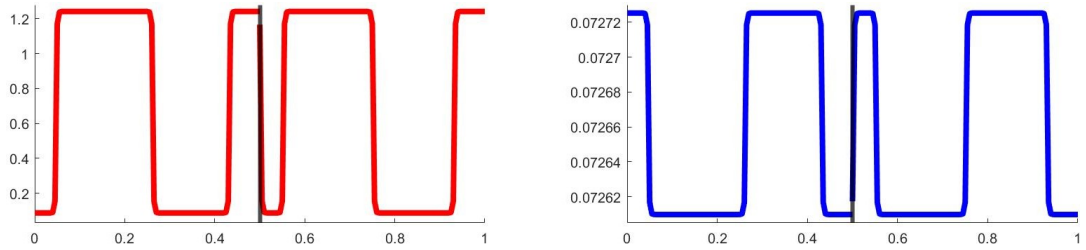

Figure 4.26: *Taking $\varepsilon = 1/100$ and $k_v > 0$, instabilities are dominant and patterns for v (in the right) are more remarkable than in the case $k_v = 0$, even if the shape is still unchanged.*

Case 3. We consider $k_v = 10^8$ and the other parameters according to data in (4.36) ($\theta = 10^{-4}$, $k_u = 10^4$, ε varies). We remember that the membrane is fully permeable and then we observe a reaction-diffusion system on the whole interval $[0, 1]$, since membrane conditions are reduced to continuity conditions.

$\varepsilon = 10.$

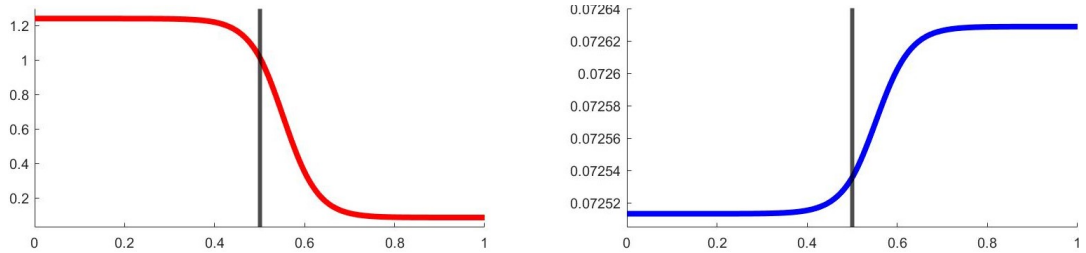

Figure 4.27: *The jump between the right and left side solutions in Figure 4.22 is now filled and we can observe continuous solutions.*

$\varepsilon = 1.$

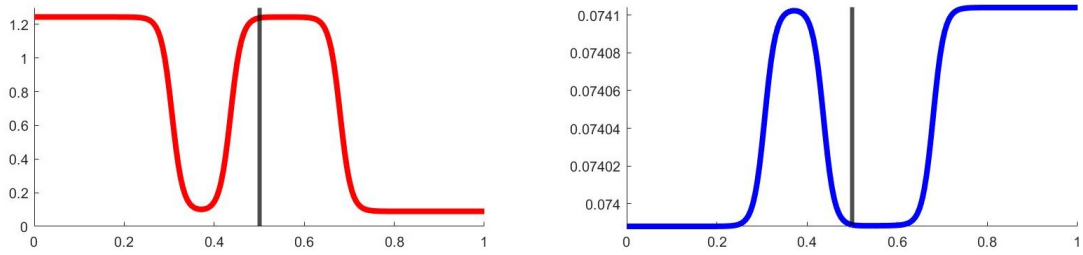

Figure 4.28: *With $\varepsilon = 1$, the continuous solutions are similar to the following case $\varepsilon = 1/5$ but they are more regular.*

$\varepsilon = 1/5.$

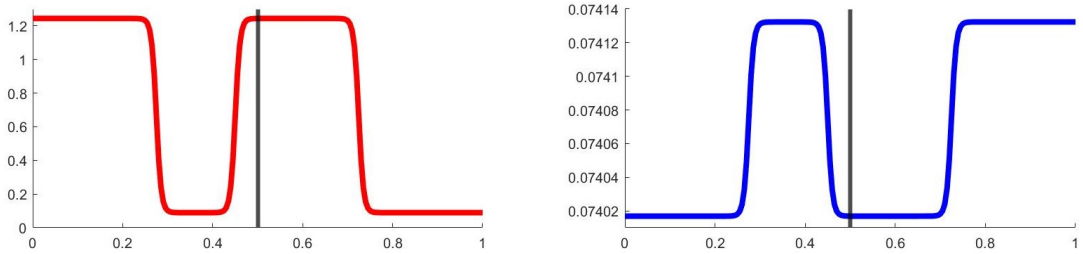

Figure 4.29: *With $\varepsilon = 1/5$, pictures can be well predicted from Figure 4.24.*

$\varepsilon = 1/20.$

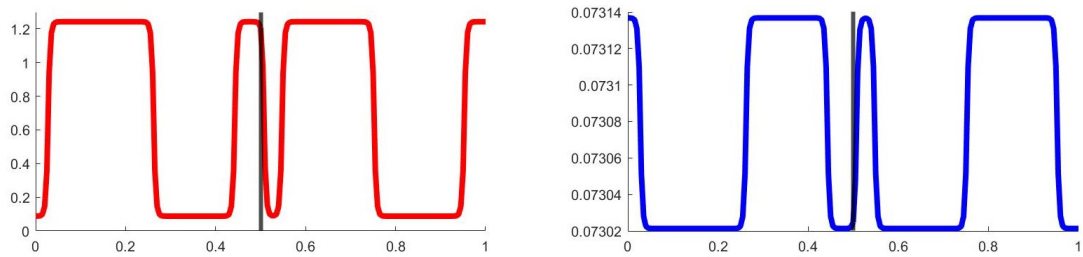

Figure 4.30: *Again with $\varepsilon = 1/20$, we are approaching the zero numerical limit. Then, the appearance of membrane continuous, but not smooth instabilities can be observed in both u and v.*

$\varepsilon = 1/100$.

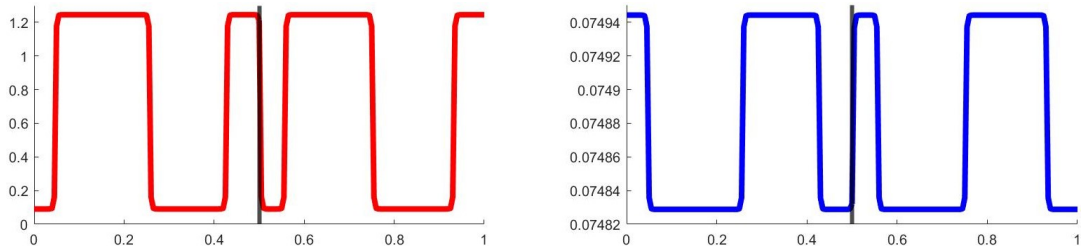

Figure 4.31: *For $\varepsilon = 1/100$, oscillations are now continuous at the membrane respect to Figure 4.26*

Finally, as ε converges to zero, we numerically observe convergence to instability due to backward parabolicity for the limiting cross-diffusion equations. Indeed, we remark that, from a numerical point of view, the convergence to zero is already attained with $\varepsilon = 1/100$. Fixing ε and varying k_v, we observe similar behaviour as in the previous subsections.

4.5 Conclusions

Turing instability for a standard reaction-diffusion problem is known to be a universal mechanism for pattern formation. We questioned the effect on pattern formation of a permeable membrane at which we have dissipative conditions. This interest follows both a path started in the study of membrane problems, Ciavolella *et al.* [30], Ciavolella and Perthame [31], and their importance in biology. Then, we have studied Turing instability from both an analytical and a numerical point of view for a reaction-diffusion membrane problem of two species u and v as in (4.1).

Our method relies on a diagonalization theory for membrane operators. A detailed proof of related results in Appendix 4.A is left to more analytical studies. Thanks to this theory, in Section 4.2, we could perform an analogous analysis of Turing instability as in the standard case without membrane under the hypothesis to have equal eigenfunctions for the membrane Laplace operator associated to the two species. This condition is related, thanks to Lemma 4.2.1, to restrictions (4.12) and (4.13). We left as an open problem the identification of cases in which these constraints can be eliminated.

In order to pass to the numerical analysis, we have introduced in Section 4.3 the one dimensional problem and the explicit solutions of the eigenvalue problem. Membrane Laplace eigenvalues are implicitly defined by Equation (4.27), since we have chosen to introduce the condition $\nu_D = 1$. This could be avoided under biological reasons considering, then, Equation (4.25b). Moreover, choosing a proper domain, it is possible to extend the analyses in the two-dimensional case.

Concerning numerical examples in Section 4.4, it is possible to take more complex and more realistic data. A more extensive study, with other nonlinearities, is of interest. Moreover, we have fixed the diffusion coefficient D_v whose role is of interest also.

In Table 4.2, we sum up the different patterns observed in Subsection 4.4.2 and 4.4.3, decreasing the diffusion ratio $\theta = \frac{D_{u1}}{D_{u3}} = \frac{D_{v1}}{D_{v3}}$ from the critical value $\theta_c = 3.1 \cdot 10^{-1}$ (from left to right in the rows) and increasing the permeability coefficient values $k_v \in [0, +\infty]$ (from top to down in the columns). We consider only the activator u and we take reaction terms as in (4.29),

initial data as in Figure 4.4 and data setting as in (4.36). We recall that the spatial interval of study is $[0, 1]$. We stress on the fact that the first ($k_v = 0$) and last ($k_v = +\infty$) row correspond to Turing instabilities observed in a reaction-diffusion problem on a half domain and on the full one respectively. Hence, it is coherent that decreasing θ the number of patterns increases in the biggest domain.

k_v \ θ	θ_c	10^{-2}	10^{-3}	10^{-4}	10^{-5}
0	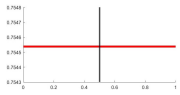	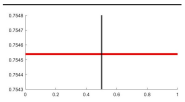	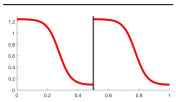	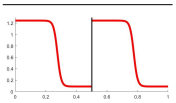	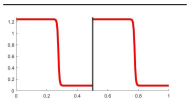
1		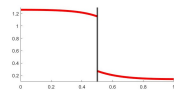	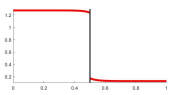	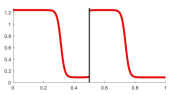	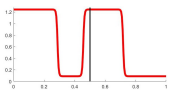
$+\infty$		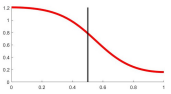	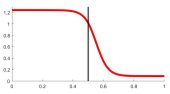	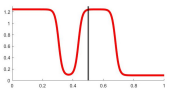	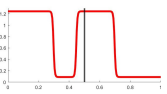

Table 4.2: *We summarise the evolution of patterns varying θ and k_v. The first column corresponds to the value $\boldsymbol{\theta = \theta_c}$, in which case there are no unstable modes. Then, for all k_v, convergence to the steady state is observed. For $\boldsymbol{\theta = 10^{-2}}$, we have again zero eigenvalues for $k_v = 0$ and one eigenvalue for $k_v \in (0, +\infty]$. So, we observe convergence respectively to a steady state and a simple pattern, discontinuous in the case $k_v = 1$. For θ small enough ($\boldsymbol{\theta = 10^{-3}, 10^{-4}, 10^{-5}}$), we observe more complex patterns with the main discontinuity property in the case of a non-trivial k_v (second row). We remark that in the picture for $\theta = 10^{-5}$ and $k_v = 1$, the jump is really small compared to the axis scale (see Figure 4.9).*

Surprisingly, not only adding diffusion but also adding dissipative membrane conditions, we observe the equilibria stability's break. As in the classical Turing analysis, decreasing θ, we get more complex patterns. Contrary to standard Turing instability, with non-trivial membrane permeability, discontinuity at the membrane characterizes the steady state. Moreover, for θ in a neighbourhood of θ_c and $k_v \in (0, +\infty)$, a singular pattern appears. Indeed, it is a simple nearly constant function with a jump at the membrane.

In Subsection 4.4.4, we have numerically studied a fast reaction-diffusion membrane system, leaving a rigorous analysis as an open problem. Again, discontinuity characterises instability for $k_v \in (0, +\infty)$.

4.A Diagonalization theory on membrane operators

We introduce the diagonalization result, Brezis [15], Evans [45], for membrane operators which assures the existence of a sequence of eigenvalues and eigenfunctions that solve each problem in (4.4) and (4.5).

Theorem 4.A.1 (Diagonalization theorem for compact, self-adjoint membrane operators.)**.** *Let A be a compact, self-adjoint membrane operator on a separable Hilbert space $\mathcal{H}$ with infinite dimension. There exists a sequence of real numbers $\{\lambda_n\}_{n\in\mathbb{N}}$ such that $\{|\lambda_n|\}_{n\in\mathbb{N}}$ is non increasing, converges to zero and such that:*

- *for any n such that λ_n is non-zero, λ_n is an eigenvalue of A and $E_n := \ker(A - \lambda_n I)$ is a subspace of $\mathcal{H}$ with finite dimension; moreover, if λ_n and λ_m are distinct, their corresponding eigenspaces are orthogonal;*
- *if $E :=$ Span $\bigcup_{\substack{n \in \mathbb{N} \\ \lambda_n \neq 0}} E_n$, then $\ker(A) = E^{\perp}$;*

Indeed, Theorem 4.A.1 applies to the inverse operators L^{-1} and $\widetilde{L}^{-1}$. Therefore, we can find also for L and $\widetilde{L}$ a sequence of eigenvalues and a basis of eigenfunctions.

We show here below that the inverse operators verify the hypothesis of this theorem. At first, we introduce the bilinear forms associated to the membrane operators. Then, we prove the hypothesis of the Lax-Milgram Theorem 3.2.2. As in Chapter 3, we deal with an elliptic problem, but with Neumann homogeneous conditions rather than Dirichlet homogeneous ones. Again, the following definition is requested.

Definition 4.A.1. *We define the Hilbert space of functions $\mathbf{H^1} = H^1_{0,\Gamma}(\Omega_1) \times H^1_{0,\Gamma}(\Omega_3)$ as the Hilbert space of functions $H^1(\Omega_1) \times H^1(\Omega_3)$ satisfying Neumann homogeneous conditions on Γ_λ, $\lambda = 1, 3$. We endow it with the norm*

$$\|w\|_{\mathbf{H^1}} = \left(\|w_1\|^2_{H^1(\Omega_1)} + \|w_3\|^2_{H^1(\Omega_3)} \right)^{\frac{1}{2}}.$$

We let $(\cdot, \cdot)_{\mathbf{H^1}}$ be the inner product in $\mathbf{H^1}$.

As in Definition 3.2.5, we define the continuous bilinear forms associated with these membrane elliptic operators as

$$\begin{aligned} B[\varphi, \phi] &= \textstyle\int_{\Omega_1} D_{u1} \nabla\varphi_1 \nabla\phi_1 + \int_{\Omega_3} D_{u3} \nabla\varphi_3 \nabla\phi_3 + \int_{\Gamma} k_u (\varphi_3 - \varphi_1)(\phi_3 - \phi_1), \\ \widetilde{B}[\varphi, \phi] &= \textstyle\int_{\Omega_1} D_{v1} \nabla\varphi_1 \nabla\phi_1 + \int_{\Omega_3} D_{v3} \nabla\varphi_3 \nabla\phi_3 + \int_{\Gamma} k_v (\varphi_3 - \varphi_1)(\phi_3 - \phi_1), \end{aligned} \tag{4.39}$$

for $\varphi, \phi \in \mathbf{H^1}$. We remark that B and $\widetilde{B}$ are symmetric. To apply the Lax-Milgram theory, Brezis [15], Evans [45], we only need to verify coercivity, since here we work with Neumann conditions and not Dirichlet ones as for the bilinear form in 3.2.5. For simplicity, we consider the membrane operator L and the bilinear form B. We can follow the same steps for $\widetilde{L}$ and $\widetilde{B}$. *B is coercive.* Indeed, if we assume $\int_{\Omega_1 \cup \Omega_3} \varphi = 0$, we can estimate

$$B[\varphi, \varphi] = \int_{\Omega_1} D_{u1} |\nabla\varphi_1|^2 + \int_{\Omega_3} D_{u3} |\nabla\varphi_3|^2 + \int_{\Gamma} k_i |\varphi_3 - \varphi_1|^2 \geqslant C \|\varphi\|^2_{\mathbf{H^1}}$$

with a membrane version of the Poincaré-Wirtinger inequality on a product space (this theory would not be analysed in this chapter since it is more a functional analysis result which is not of main interest in Turing theory). With the same assumption, we can check coercivity of $\widetilde{B}$. Therefore, the Lax-Milgram theory applies in this context assuming that $\int_{\Omega_1 \cup \Omega_3} w = 0$. Then there exists a unique function $w \in \mathbf{H^1}$ solving

$$B[w, \varphi] = (\lambda w, \varphi)_{\mathbf{H^1}}, \quad \forall \varphi \in \mathbf{H^1}. \tag{4.40}$$

Whenever (4.40) holds, we write

$$w = \lambda L^{-1} w.$$

The inverse operator $L^{-1} : (\mathbf{H^1})^{-1} \to \mathbf{H^1}$ is a compact operator in $L^2(\Omega_1) \times L^2(\Omega_3)$, since according to the Rellich-Kondrachov theorem $\mathbf{H^1} \subset\subset \mathbf{L^2}$. Moreover, it is also a self-adjoint one,

Taylor [122]. Indeed, the operators L and $\widetilde{L}$ are self-adjoints (we can prove it, since they are maximal monotone symmetric operators, Brezis [15], Serafini [120]).

The standard spectral theory for compact and self-adjoint operators seen in Theorem 4.A.1 applies in this context. We deduce that there exists a sequence of real number $\{\sigma_n\}_{n\in\mathbb{N}}$ such that $\{|\sigma_n|\}_{n\in\mathbb{N}}$ is non increasing and converging to zero. Moreover, if σ_n and σ_m are distinct, their corresponding eigenspaces are orthogonal. We call $\{w_n\}_{n\in\mathbb{N}}$ the basis of eigenfunctions of L^{-1}. So, we infer that L has an orthonormal basis of $L^2(\Omega_1)\cup L^2(\Omega_3)$ of eigenfunctions $\{w_n\}_{n\in\mathbb{N}}$ related to a sequence of increasing and diverging eigenvalues $\{\lambda_n\}_{n\in\mathbb{N}}$ such that $\lambda_n = \frac{1}{\sigma_n}$, for all $n \in \mathbb{N}$.

Remark 4.A.1. *The mean zero property can be interpreted as if we are taking the eigenfunctions in the orthogonal space of the constants. In fact, the existence of a sequence of eigenvalues and of orthogonal eigenfunctions in the diagonalization theorem can be proven through a minimisation process starting from the first zero eigenvalue and looking for the eigenspaces as the orthogonal spaces of its eigenfunction which is a constant.*

4.B Numerical method

We illustrate the one-dimension numerical method, Morton and Mayers [92], Quarteroni *et al.* [111], used to perform the examples in Section 4.4. We present the discretization on the interval $I = (a, x_m) \cup (x_m, b) =: I_1 \cup I_3$ of the one-dimension reaction-diffusion System (4.1).

In the following, for simplicity, we write the numerical expressions for the equations of u, but with the same steps we can obtain the discretization also for v. We consider a space discretization (see Almeida *et al.* [4]) of each subdomain I_1 and I_3 in $N_1 + 1$ and $N_3 + 1$ points respectively. We observe that this distinction allows to consider not centred membranes. In our case with the membrane in the middle point x_m, we infer that $N_1 = N_3$. Concerning the membrane, the key aspect is to discretize this point as two distinct ones since the Kedem-Katchalsky conditions are constructed defining the right and left limit of the density on the membrane (see for example Chapter 3). Moreover, the space step turns out to be $\Delta x = \frac{x_m - a}{N_1+1} = \frac{b-x_m}{N_3+1}$, with $N_1, N_3 \in \mathbb{N}$. The mesh is formed by the intervals

$$I_i = \left(x_{i-\frac{1}{2}}, x_{i+\frac{1}{2}}\right),\ i = 1, ..., N_1 + 1, \qquad J_j = \left(x_{j-\frac{1}{2}}, x_{j+\frac{1}{2}}\right),\ j = 1, ..., N_3 + 1.$$

The intervals are centred in $x_i = i\Delta x$, $i = 1, ..., N_1 + 1$ and $x_j = j\Delta x$, $j = 1, ..., N_3 + 1$ with $I_{N_1+1} = J_1$. Moreover, as the reader can remark, we add ghost points to build the extremal intervals in the left I_1, I_{N_1+1} and in the right J_1, J_{N_3+1}. Then, we consider the ghost points for $i = 0, N_1 + 2$ and $j = 0, N_3 + 2$. At a given time, the spatial discretization of $u(t, x)$, interpreted in the finite volume sense, is of the form

$$u_i(t) \approx \frac{1}{\Delta x}\int_{I_i} u_1(t, x)\, dx, \qquad \widehat{u}_j(t) \approx \frac{1}{\Delta x}\int_{J_j} u_3(t, x)\, dx,$$

for $i = 1, ..., N_1 + 1$ and $j = 1, ..., N_3 + 1$. Concerning the time discretization, we consider the time step Δt such that the mesh points are of the form $t^n = N_t\Delta t$, with $N_t \in \mathbb{N}$. The discrete approximation of $u(t, x)$, for $n \in \mathbb{N}$, $i = 1, ..., N_1 + 1$ and $j = 1, ..., N_3 + 1$, is now

$$u_i^n \approx \frac{1}{\Delta x}\int_{I_i} u_1(t^n, x)\, dx, \qquad \widehat{u}_j^n \approx \frac{1}{\Delta x}\int_{J_j} u_3(t^n, x)\, dx.$$

We write the time discretization as an Euler method and the space one with a generic Θ-method.

In the simulations, we have chosen $\Theta = 1$, meaning that the method is an implicit and always stable one. For the sake of simplicity, we consider a unique index i instead of i, j. In the following, we take $0 \leqslant n \leqslant N_t$ and we call $\delta_x^2 u_i^n = u_{i-1}^n - 2u_i^n + u_{i+1}^n$. Then, we obtain

$$u_i^{n+1} - u_i^n = \mu_1[\Theta\, \delta_x^2 u_i^{n+1} + (1-\Theta)\delta_x^2 u_i^n] + \Delta t f_i^n, \qquad \text{for } i = 1, ..., N_1 + 1,$$

with $\mu_1 = \frac{D_{u1}\Delta t}{\Delta x^2}$ and

$$\widehat{u}_i^{n+1} - \widehat{u}_i^n = \mu_3[\Theta\, \delta_x^2 \widehat{u}_i^{n+1} + (1-\Theta)\delta_x^2 \widehat{u}_i^n] + \Delta t \widehat{f}_i^n, \qquad \text{for } i = 1, ..., N_3 + 1,$$

with $\mu_3 = \frac{D_{u3}\Delta t}{\Delta x^2}$. Finally, we deduce the systems

for $i = 1, ..., N_1 + 1$,

$$\begin{aligned} &-\mu_1\Theta u_{i-1}^{n+1} + (1 + 2\mu_1\Theta)u_i^{n+1} - \mu_1\Theta u_{i+1}^{n+1} \\ &\qquad = \mu_1(1-\Theta)u_{i-1}^n + (1 - 2\mu_1(1-\Theta))u_i^n + \mu_1(1-\Theta)u_{i+1}^n + \Delta t f_i^n \end{aligned} \tag{4.41}$$

for $i = 1, ..., N_3 + 1$,

$$\begin{aligned} &-\mu_3\Theta \widehat{u}_{i-1}^{n+1} + (1 + 2\mu_3\Theta)\widehat{u}_i^{n+1} - \mu_3\Theta \widehat{u}_{i+1}^{n+1} \\ &\qquad = \mu_3(1-\Theta)\widehat{u}_{i-1}^n + (1 - 2\mu_3(1-\Theta))\widehat{u}_i^n + \mu_3(1-\Theta)\widehat{u}_{i+1}^n + \Delta t \widehat{f}_i^n \end{aligned} \tag{4.42}$$

Now, we exhibit the first order discretization of the boundary conditions. Starting from Neumann, we can distinguish the condition in a and b as

$$u_0^{n+1} = u_1^{n+1}, \qquad \widehat{u}_{N_3+2}^{n+1} = \widehat{u}_{N_3+1}^{n+1}, \tag{4.43}$$

which give the relation of the extremal ghost points. From the Kedem-Katchalsky membrane conditions, we deduce the expression of the membrane ghost points

$$u_{N_1+2}^{n+1} = u_{N_1+1}^{n+1} + \frac{\Delta x\, k_u}{D_{u1}}(\widehat{u}_1^{n+1} - u_{N_1+1}^{n+1}), \qquad \widehat{u}_0^{n+1} = u_1^{n+1} - \frac{\Delta x\, k_u}{D_{u3}}(\widehat{u}_1^{n+1} - u_{N_1+1}^{n+1}). \tag{4.44}$$

Substituting the ghost values found in (4.43) and (4.44) in the systems (4.41) and (4.42), we get the equations at the extremal points:

At the left limit on the membrane,

$$\begin{aligned} &-\mu_1\Theta u_{N_1}^{n+1} + \left(1 + \mu_1\Theta + \Theta\frac{\Delta t\, k_u}{\Delta x}\right) + u_{N_1+1}^{n+1} - \Theta\frac{\Delta t\, k_u}{\Delta x}\widehat{u}_1^{n+1} \\ &= \mu_1(1-\Theta)u_{N_1}^n + \left(1 - \mu_1(1-\Theta) - (1-\Theta)\frac{\Delta t\, k_u}{\Delta x}\right) + u_{N_1+1}^n + (1-\Theta)\frac{\Delta t\, k_u}{\Delta x}\widehat{u}_1^n. \end{aligned} \tag{4.45}$$

At the right limit on the membrane,

$$-\Theta\frac{\Delta t\, k_u}{\Delta x}\, u_{N_1+1}^{n+1} + \left(1 + \mu_3\Theta + \Theta\frac{\Delta t\, k_u}{\Delta x}\right)\widehat{u}_1^{n+1} - \mu_3\Theta\widehat{u}_2^{n+1}$$

$$= (1-\Theta)\frac{\Delta t\, k_u}{\Delta x}\, u^n_{N_1+1} + \left(1-\mu_3(1-\Theta) - (1-\Theta)\frac{\Delta t\, k_u}{\Delta x}\right)\widehat{u}^n_1 + \mu_3(1-\Theta)\widehat{u}^n_2. \tag{4.46}$$

In a,

$$(1+\mu_1\Theta)u_1^{n+1} - \mu_1\Theta u_2^{n+1} = (1-\mu_1(1-\Theta))u_1^n + \mu_1(1-\Theta)u_2^n. \tag{4.47}$$

In b,

$$-\mu_3\Theta\widehat{u}^{n+1}_{N_3} + (1+\mu_3\Theta)\widehat{u}^{n+1}_{N_3+1} = \mu_3(1-\Theta)\widehat{u}^n_{N_3} + (1-\mu_3(1-\Theta))\widehat{u}^n_{N_3+1}. \tag{4.48}$$

To conclude, system (4.41) for $i = 1, ..., N_1$ and (4.42) for $i = 1, ..., N_3$, written for the internal points of the grid, combined with the equations for the extremal points (4.45), (4.46), (4.47) and (4.48), build the discretized system of u. The same equations with the proper coefficients can be found for v.

Calling the vector solutions at time t^n as

$$U^n = \left(u^n_1, \ldots, u^n_{N_1+1}, \widehat{u}^n_1, \ldots, \widehat{u}^n_{N_3+1}\right)^T, \qquad V^n = \left(v^n_1, \ldots, v^n_{N_1+1}, \widehat{v}^n_1, \ldots, \widehat{v}^n_{N_3+1}\right)^T$$

and the reaction vectors as

$$F^n = \left(f^n_1, \ldots, f^n_{N_1+1}, \widehat{f}^n_1, \ldots, \widehat{f}^n_{N_3+1}\right)^T, \; G^n = \left(g^n_1, \ldots, g^n_{N_1+1}, \widehat{g}^n_1, \ldots, \widehat{g}^n_{N_3+1}\right)^T,$$

we can write the discretized systems in a matrix form as $AU^{n+1} = BU^n + \Delta t F^n$ coupled with $CV^{n+1} = DV^n + \Delta t G^n$, where

$$\mathrm{A} := \begin{pmatrix}
1+\mu_1\Theta & -\mu_1\Theta & 0 & \cdots & & & & & 0 \\
-\mu_1\Theta & 1+2\mu_1\Theta & & & & & & & \\
0 & & & & & & & & \\
 & & 1+2\mu_1\Theta & -\mu_1\Theta & & & & & \\
 & & -\mu_1\Theta & 1+\mu_1\Theta+\Theta\frac{\Delta t k_u}{\Delta x} & -\Theta\frac{\Delta t k_u}{\Delta x} & & & & \\
 & & & -\Theta\frac{\Delta t k_u}{\Delta x} & 1+\mu_3\Theta+\Theta\frac{\Delta t k_u}{\Delta x} & -\mu_3\Theta & & & \\
 & & & & -\mu_3\Theta & 1+2\mu_3\Theta & & & \\
 & & & & & & & & 0 \\
 & & & & & & 1+2\mu_3\Theta & -\mu_3\Theta & \\
0 & \cdots & & & & 0 & -\mu_3\Theta & 1+\mu_3\Theta &
\end{pmatrix}$$

and, with the notation $\Theta' := 1-\Theta$,

$$\mathrm{B} := \begin{pmatrix}
1-\mu_1\Theta' & \mu_1\Theta' & 0 & \cdots & & & & & 0 \\
\mu_1\Theta' & 1-2\mu_1\Theta' & & & & & & & \\
0 & & & & & & & & \\
 & & 1-2\mu_1\Theta' & \mu_1\Theta' & & & & & \\
 & & \mu_1\Theta' & 1-\mu_1\Theta'-\Theta'\frac{\Delta t k_u}{\Delta x} & \Theta'\frac{\Delta t k_u}{\Delta x} & & & & \\
 & & & \Theta'\frac{\Delta t k_u}{\Delta x} & 1-\mu_3\Theta'-\Theta'\frac{\Delta t k_u}{\Delta x} & \mu_3\Theta' & & & \\
 & & & & \mu_3\Theta' & 1-2\mu_3\Theta' & & & \\
 & & & & & & & & 0 \\
 & & & & & & 1-2\mu_3\Theta' & \mu_3\Theta' & \\
0 & \cdots & & & & 0 & \mu_3\Theta' & 1-\mu_3\Theta' &
\end{pmatrix}.$$

Substituting μ_1, μ_3, k_u with the notation $\sigma_l = \frac{D_{v1}\Delta t}{\Delta x^2}$, $\sigma_r = \frac{D_{v3}\Delta t}{\Delta x^2}$ and k_v, we can write the matrix C and D.

Part III

Biological application

In Part I - II, we focused on the mathematical aspects of tumor invasion models studying them both analytically and numerically. We have seen the importance of considering a zero-thickness membrane with the derived Kedem-Katchalsky conditions. Moreover, we have deepened into the existence of weak solutions in reaction-diffusion systems, within an L^1 setting, with the previous membrane conditions. Finally, we have introduced an asymptotic behaviour showing the formation of spatial patterns.

Chapter 5 aims to deal with biological experiments on tumor invasion. It is part of a new project in collaboration with the Laboratoire de Biologie et Thérapeutique des Cancers of INSERM at Saint-Antoine Hospital in Paris. Actually, we are not really going to use the previous analysis, since before discussing about invasion experiments we need to have more information about membrane degradation. Indeed, we remember that, as seen in the biological Introduction 1.1, tumor cells are initially isolated from the surrounding environment thanks to a basement membrane, thus the necessity to degrade it producing MMPs enzymes. We cannot have data neither on membrane degradation or enzymes evolution from biological experiments on invasion, then the need of a secondary model that could help us in better describing these two processes.

In the next chapter, we introduce then a mathematical model that wants to describe experimental results enlightening the degradation process of a biological membrane. Waiting for biological experiments, we can still perform some modeling and numerical analysis to have then all the tools to face biological data. For the mathematical analysis, we will mainly follow the PhD thesis of Braun [12].

Chapter 5

Membrane degradation: modeling and simulations

In the following, we show results of an on-going project in collaboration with biologists Nathalie Ferrand and Michèle Sabbah, working in the Laboratoire de Biologie et Thérapeutique des Cancers of INSERM at the Saint Antoine Hospital in Paris, and mathematicians Roberto Natalini (IAC-CNR, Rome) and Benoit Perthame (LJLL, Sorbonne Université, Paris).

5.1 Introduction

Tumors are complex diseases characterised by high diversity and incidence, Sung *et al.* [121]. One of the most crucial and lethal processes is represented by the increased ability of cancer cells to migrate and invade other organs during the so-called *metastatic spread*, Dillekås *et al.* [39]. Indeed, primary tumors are initially confined in a well-defined area. However, cancer cells could acquire useful mutations that allow them to penetrate different barriers and to disseminate themselves into secondary organs of our body. Then, we observe the transition from an *in situ* stage to an invasive one. It is now well known that metastatic cancer cells typically move in clusters which have greater predisposition of forming metastasis than single cells, Aceto *et al.* [1], Bubba *et al.* [17], Hong *et al.* [66].

One of the most difficult barriers for cells to cross is the basement membrane, also composed by ECM. This kind of membrane separates the epithelial tissue from the connective one (predominantly consisting in ECM) and, among its functions, we can distinguish a supportive role and an isolating one. Unfortunately, mutated cancer cells, called *invasive cells* can produce matrix metalloproteinases (MMPs) enzymes capable of modifying the ECM and, then, to degrade the basal membrane, allowing invasion. This process is, for instance, observed for breast tumors, as considered in our study.

Many questions concerning invasion details remain unanswered. Over the last decade, the research interest on this process is increasing in order to highlight the main cues with the aim of controlling and treating the phenomenon (Chaplain *et al.* [24], Ciavolella *et al.* [30], Franssen *et al.* [49], Gallinato *et al.* [53], Giverso *et al.* [57]).

This chapter can be included in this branch of research. In particular, we are interested in better describing one of the main biological phenomenon responsible for the invasion one, which is membrane degradation. In fact, *in vitro* invasion investigations (using the XCELLigence technology) are not able to give details on it. Consequently, we build here a mathematical model

which describes degradation of an ECM-like biological membrane through the production of MMPs by cancer cells. At the same time, we provide numerical simulations with a sensitivity analysis followed by a parameters estimation study. This is a preparatory work waiting for experimental results consisting of cells seeded in wells containing at their bottom fluorescent gelatin. We focus the attention on breast cancer, the most common malignancy among women. If non-metastatic, it has high chance of healing, but, at the contrary, advanced breast cancer with metastasis are considered incurable with the actual therapies, Harbeck *et al.* [64], Waks and Winer [128] .

5.2 Experimental settings and sample results

We present here the experimental setting with which we have to deal. The study is on three different cell lines: an epithelial non-invasive cell line isolated from the breast tissue (MCF7), a breast carcinoma cell line, called MDA MB 231, and another one built from the previous MCF7 cells invalidated for the protein WISP2 (MCF7 Sh WISP2), which increases the mesenchymal and invasive behaviour, Ferrand *et al.* [47].

Invasion experiments are realized using the XCELLigence technology, Ke *et al.* [71], Martinez-Serra *et al.* [89], Obr *et al.* [98], Turker *et al.* [124], Zaoui *et al.* [132]. This technique has been recently adopted to ameliorate results from the classic *Boyden Chamber* method. Both of them are characterized by the common main structure: a single well is divided into two chambers by a porous membrane. In the top chamber, a certain number of cells are injected on the surface of a serum free medium. Then, we observe a random movement of cells towards the middle membrane where they adhere. If in migration experiments cells are allowed to penetrate through membrane pores to accede to the bottom chamber, in invasion assays (Connolly and Maxwell [34]) a gelatin layer is added on the top membrane to create a barrier for cells. Consequently, in order to invade the bottom chamber, cells need to produce the enzymes MMPs which locally degrade the gelatin. On the bottom side of the membrane, gold electrodes measure the invasive phenomenon, allowing a *real time cells analysis* (RTCA), differently from the *Boyden Chamber* method in which experimentalists need to count manually the number of cells which has penetrated the membrane. Instead, RTCA systems measure impedance changings due to an increase in occupied space from cells adhering to microelectrodes. The impedance measurement provides quantitative information on cell number, viability, and morphology of adherent cells. Impedance is displayed in real-time as *cell index* (CI), proportional to cell density.

As explained in the introduction, to better set up the invasive experiment from a mathematical point of view, we require more information on gelatin's degradation. Then, we use the QCM™ Gelatin Invadopodia Assay. It allows to plate cells on a culture surface coated with a thin layer of green fluorescent gelatin. Fluorescence is useful to distinguish areas in which gelatin has been consumed by others in which no pores are yet present (see Figure 5.1 - 5.2 B). Such assays have also revealed that invasive cells extend small localised protrusions, called *invadopodia*, from which starts membrane degradation. Pioneered by Wen-Thien Chen in the 1980's ([25, 26, 27]), visualisation of invadopodia ECM degradation by fluorescent gelatin has emerged as the most prevalent technique for evaluating cellular invasive potential, Artym *et al.* [5], Martin *et al.* [88]. Invadopodia are cellular membrane protusions where MMPs enzymes are localized. They mediate matrix degradation by cancer cells. Finally, it is also possible to co-localise the actin cytosckeleton (see Figure 5.1 - 5.2 D), which is a network of filaments made up of polymerized actin that provides mechanical support and determines cell shape, and nuclei (see Figure 5.1 - 5.2 C) with invadopodial degradation sites.

With this technique, biologists can make experiments over 72 hours, taking pictures each day.

Then, shots after 24h, 48h and 72h will be available. Movement of cells and consequent gelatin's consumption are not well known, then a mathematical investigation is required. In any case, the major hypothesis is that cells degrade gelatin below them and, after, they move to degrade around. Gelatin means to mimic basal membrane which has a thickness of 10 to 300 nm, *i.e.* 10^{-7} to $3 \cdot 10^{-6}$ cm, which is smaller that the size of a cell, *i.e.* 10 μm, equal to 10^{-4} cm. In Figure 5.1 and 5.2, an example of experimental data produced by N. Ferrand using the Gelatin Invadopodia Assay.

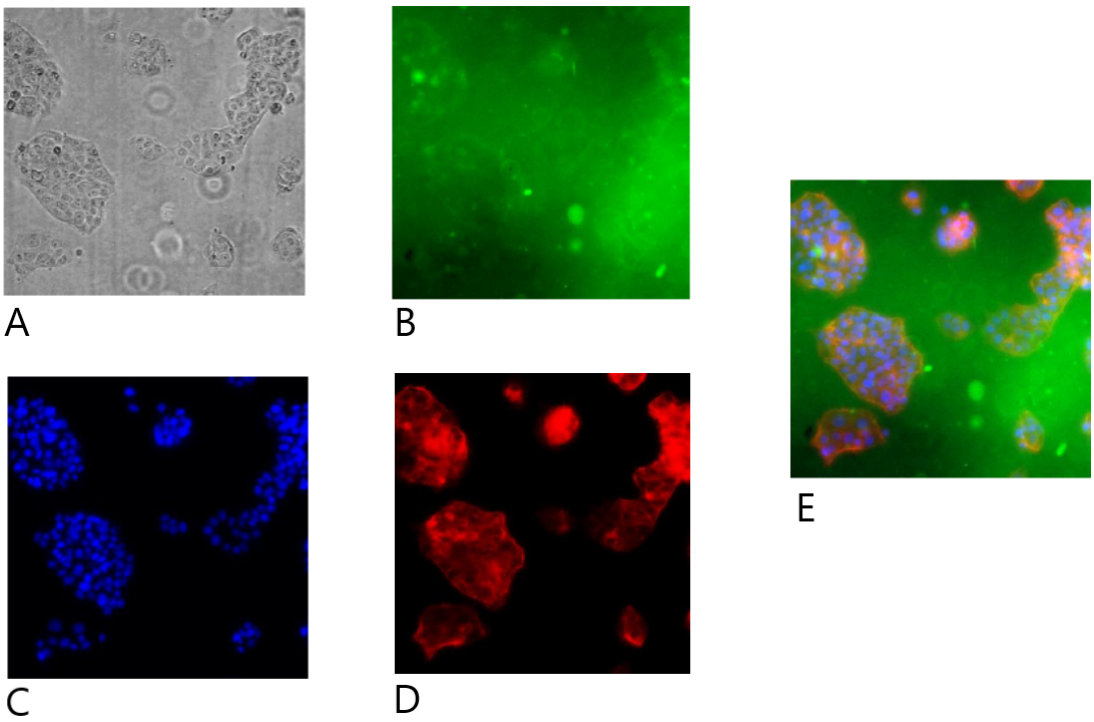

Figure 5.1: *Example of experimental data after 48h for the MCF7, realised by N. Ferrand.* ***A.*** *Contrast phase image representing MCF7 cells.* ***B.*** *Gelatin representation.* ***C.*** *DAPI image representing cells nuclei in blue.* ***D.*** *Representation of actin cytosckeleton in red which delineates cells contouring.* ***E.*** *Overlap of images B,C,D. From these pictures, we can affirm the non-invasive behaviour of normal cells, as expected. Gelatine is entirely green (eventual darker areas are due to instrumentation). Moreover, we remark the formation of clusters.*

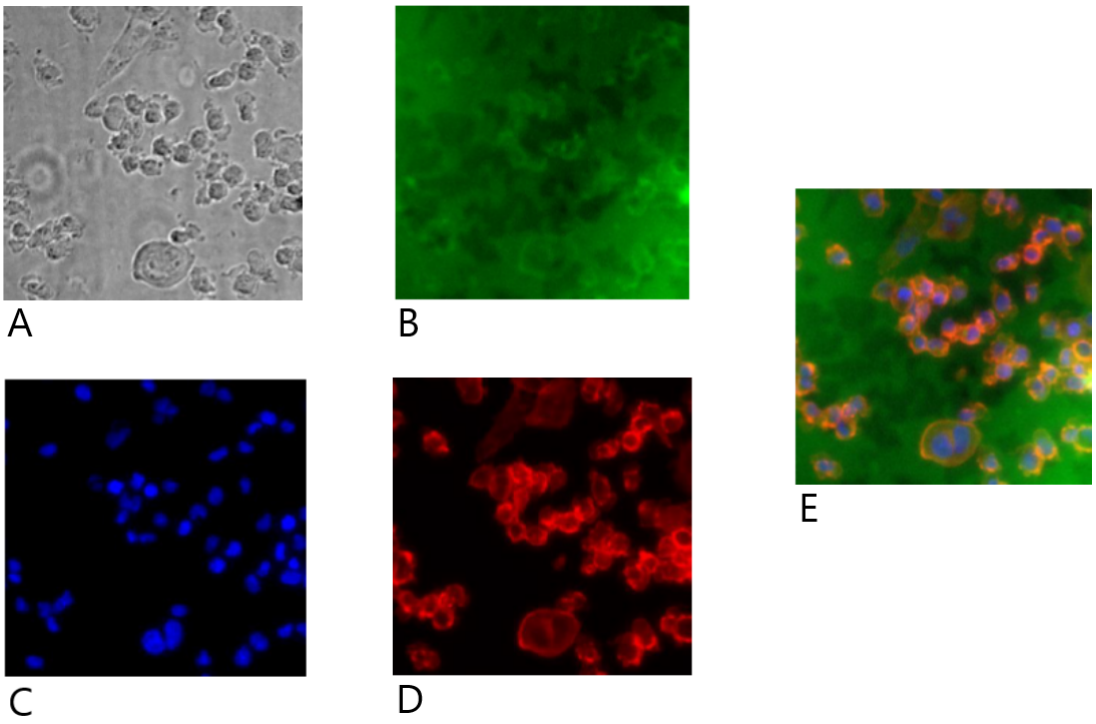

Figure 5.2: *Example of experimental data after 48h for the MCF7 Sh WISP2 (the pictures scale here is bigger than before), realised by N. Ferrand.* ***A.*** *Contrast phase image.* ***B.*** *Image of the left gelatin (in green), whereas black areas are spots without gelatin.* ***C.*** *DAPI image representing cells nuclei in blue.* ***D.*** *Representation of actin cytosckeleton in red which delineates cells contouring.* ***E.*** *Overlap of images B,C,D that relates cells position and gelatin degradation. From these pictures we appreciate gelatin degradation which is quite high, showing the acquired invasive behaviour of MCF7 Sh WISP2. Moreover, emerging black holes correspond to the actual position of cells. Respect to the previous MCF7 pictures, we observe that cells are assembling in circular structures miming the vessels formation.*

5.3 Mathematical model

In accordance to experimental pictures, we consider a domain Ω representing a top view of the gelatin into a single well. For simplicity, we take the rectangular two-dimensional domain $\Omega = [a, b] \times [c, d]$. For $x \in \Omega$, $t > 0$, we consider a three species system for cells density $u(x, t)$, MMPs enzymes concentration $m(t, x)$, and the damage function $d(t, x) \in [0, 1]$, related to the amount of gelatin $q(t, x) = 1 - d(t, x) \in [0, 1]$. Equations write as

$$\begin{cases} \partial_t u = div(D(d)\nabla u) + \alpha_1 u \left(1 - \frac{u}{\alpha_3}\right), & \text{in } \Omega, \\ \partial_t m = D_m \Delta m + \beta(1 - d)u - \alpha m, & \text{in } \Omega, \\ \partial_t d = \gamma m(1 - d), & \text{in } \Omega, \end{cases} \tag{5.1}$$

where

$$D(d) = D_L d + D_G(1 - d) = D_G + (D_L - D_G)d. \tag{5.2}$$

We impose no-flux boundary conditions on $\partial\Omega$ for u and m, *i.e.*

$$\begin{cases} (D(d)\nabla u)\cdot \mathbf{n} = 0, \\ D_m \nabla m \cdot \mathbf{n} = 0, \end{cases} \tag{5.3}$$

where $\mathbf{n}$ is the outward unit normal at the boundary. We complete the system with the following initial conditions

$$\begin{cases} u(0,x) = u_0(x), \\ m(0,x) = m_0(x) = 0, \\ d(0,x) = d_0(x) = 0, \end{cases} \tag{5.4}$$

with u_0 a random function on Ω.

Equation for u. The first equation in (5.1) describes the evolution of the cells density. The diffusion coefficient depends on the diffusion $D_L > 0$ into the liquid and $D_G > 0$ on the gelatin. Interesting scenarios are when $D_L \neq D_G$, otherwise we would have a standard diffusion equation. We observe that when the gelatin is intact ($d = 0$, then $q = 1$), cells move randomly on the gelatin, whereas when it is completely destroyed ($d = 1$, then $q = 0$), cells diffuse into the liquid. We add also a logistic growth term (with $\alpha_1, \alpha_3 > 0$), since experiments are available until 72 hours, then proliferation is present, Pearl and Reed [102].

Equation for m. The second equation is a reaction-diffusion like equation for the MMPs with diffusion coefficient $D_m > 0$, production rate $\beta > 0$ and death rate $\alpha > 0$. In particular, production of MMPs is due to cells and to the fact that they sense the gelatin below them. Moreover, we assume that MMPs diffuse locally and, consequently, we add the condition

$$\sqrt{\frac{D_m}{\alpha}} << 1, \tag{5.5}$$

where $\sqrt{\frac{D_m}{\alpha}}$ is proportional to $\sqrt{x^2}$ and it corresponds to the diffusion length.

Equation for d. Finally, the equation for the damage derives from the damage mechanics, Kachanov [69]. It can be written in terms of the gelatin q as

$$\partial_t q = -\gamma m q,$$

which has an exponential decreasing solution. The damage is produced at rate γ by the MMPs m.

5.4 Dimensionless model

Before analysing the model, we propose a nondimensional form. It has several advantages, as the reduction of the number of parameters and the fact that their units are unimportant, see Murray [94], Segel [119]. Upon changes of time and space variables

$$\tilde{t} = \alpha t, \quad \tilde{x} = \sqrt{\frac{\alpha}{D_m}}x, \tag{5.6}$$

and appropriate scaling for u, m, and d, namely

$$\begin{aligned} u(t,x) &= \tilde{u}\left(\alpha t, \sqrt{\tfrac{\alpha}{D_m}}x\right), \\ m(t,x) &= \tfrac{\alpha}{\gamma}\tilde{m}\left(\alpha t, \sqrt{\tfrac{\alpha}{D_m}}x\right), \\ d(t,x) &= \tfrac{D_m}{D_L - D_G}\tilde{d}\left(\alpha t, \sqrt{\tfrac{\alpha}{D_m}}x\right), \end{aligned} \tag{5.7}$$

we find a parametrised version, again with homogeneous Neumann boundary conditions. For simplicity in notation, eliminating the tilde, we find

$$\begin{cases} \partial_t u = div((\theta + d)\nabla u) + k_2 u\left(1 - \frac{u}{\alpha_3}\right), & \text{in } \Omega, \\ \partial_t m = \Delta m + k_1(1 - pd)u - m, & \text{in } \Omega, \\ \partial_t d = \frac{1}{p} m(1 - pd), & \text{in } \Omega, \end{cases} \tag{5.8}$$

where $\theta = \frac{D_G}{D_m}, p = \frac{D_m}{D_L - D_G}, k_1 = \frac{\gamma\beta}{\alpha^2}, k_2 = \frac{\alpha_1}{\alpha}$. Here, $D(d) = \theta + d$. We assume all parameters positive, except p that satisfies the restriction $p \leqslant 1$, since we require $1 - pd \geqslant 0$.

5.5 Numerical results for the nondimensional model

We investigate the numerical behaviour of our mathematical nondimensional model. Waiting for additional biological data, we test our model with data from the literature.

We perform numerical simulations of System (5.8) in a spatial domain $\Omega = [0, 20] \times [0, 20]$, with discretisation step $\Delta x = 0.21$. All simulations have been performed with the software Matlab, using finite difference schemes (see Appendix 5.B for more details). We take as initial data

$$\begin{aligned} &u(t = 0, x) \text{ a random function mostly zero}, \\ &m(t = 0, x) = 0, \\ &d(t = 0, x) = 0. \end{aligned} \tag{5.9}$$

We show the evolution of cells u, enzymes m, and gelatin $q = 1 - d$ at three different time intervals (using a time step $\Delta t = 9 \cdot 10^{-3}$, corresponding to 1 hour): 24h, 48h, 72h. Based on parameters from Di Costanzo *et al* [38], and Braun [12], we choose

$$\begin{gathered} D_L = 7 \cdot 10^{-7}\ cm^2\, s^{-1}, \quad D_G = 10^{-7}\ cm^2\, s^{-1}, \quad D_m = 5 \cdot 10^{-7}\ cm^2\, s^{-1}, \\ \alpha_1 = 3.75 \cdot 10^{-5}\ s^{-1}, \quad \alpha_3 = 2.26 \cdot 10^5\, cell. \end{gathered} \tag{5.10}$$

From Franssen *et al* [49], we have

$$\alpha = 2.5 \cdot 10^{-6}\ s^{-1}, \quad \beta = 4.875 \cdot 10^{-6}\ M\, s^{-1}. \tag{5.11}$$

We remark that with this choice $\sqrt{\frac{D_m}{\alpha}} < 1$, then MMPs diffuse locally. In accordance with biologists, we choose as degradation rate $\gamma = 10^{-6}\ Ms^{-1}$. We have tested also $\gamma = 10^{-4}\ Ms^{-1}$ (taken from Franssen *et al.* [49]) and $10^{-5}\ Ms^{-1}$ but degradation turns out to be too fast in that cases. Consequently, the nondimensional parameters are

$$\theta = 0.2, \quad p = 0.83, \quad k_2 = 15, \quad \alpha_3 = 2.26 \cdot 10^5, \quad k_1 = 0.78. \tag{5.12}$$

In Figures 5.3 - 5.6, we illustrate from left to right: cells and their density, enzymes concentration, and gelatin concentration. Cells (represented with magenta dots through a density to particle transformation, see Appendix 5.A) are diffusing and proliferating on the gelatin. The scale of values from black to red is relative to cells density, in the background of the picture. Enzymes concentration is increasing in time, and locally around cells. We remark that the scale of values of the concentration is changing with time. Concerning the gelatin, its concentration q has values between 0 and 1: $q = 0$, corresponds to the black color and to the spots where no gelatin is left, in the contrary $q = 1$ in green defines area with gelatin. We can observe a correspondence between dots position and enzymes concentration, as well as gelatin degradation.

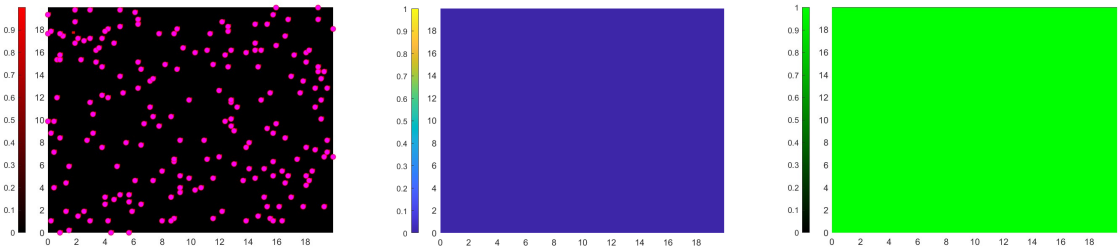

Figure 5.3: ***t*=0*h*.** *Initial data for cells is random, whereas for MMP and gelatin is zero since at the beginning there is no enzyme and the gelatin fully covers the plate.*

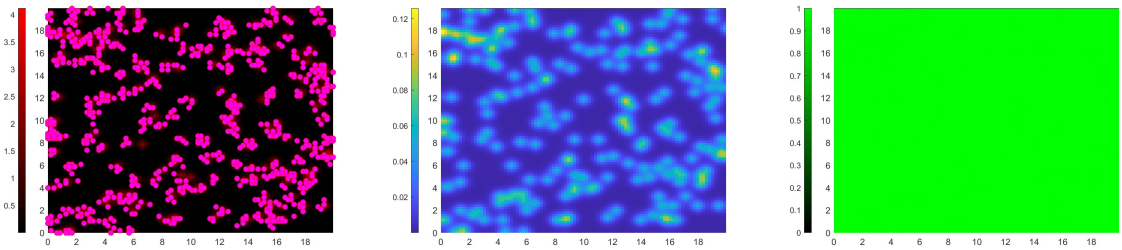

Figure 5.4: ***t*=24*h*.** *After one day, cells diffuse and proliferate. The production of the enzymes is started, even if not enough to observe holes in the gelatin.*

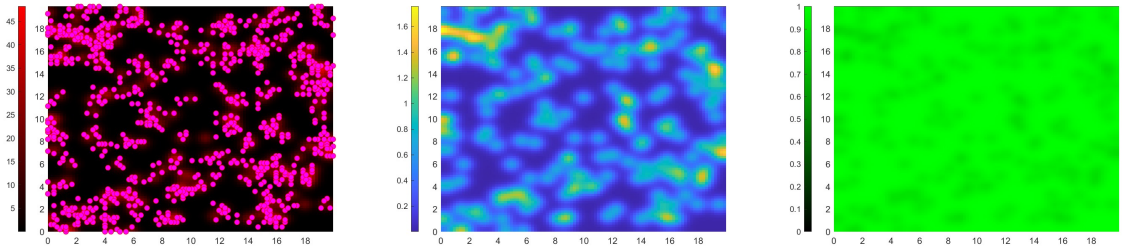

Figure 5.5: ***t*=48*h*.** *After* 2 *days, cells and enzymes increase. At the same time, we can remark that gelatin degradation has started.*

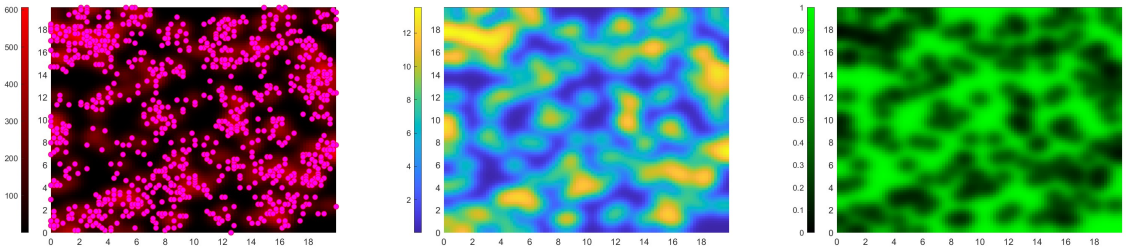

Figure 5.6: ***t*=72*h*.** *Finally, we observe that the gelatin is well degraded in some spots corresponding to the areas in which the enzymes are.*

5.6 Sensitivity analysis and parameter estimation

In order to compare the experimental data (Figures 5.1 - 5.2) to the numerical solutions of the Model (5.8), we need to determine the parameters correctly because they are not accessible by direct measurements. This problem is called *inverse problem*. Since we still do not have enough biological data, we want to test our scheme in order to be ready to receive them and we can then use the so-called *artificial data*. The idea is that we create an artificial solution, through our numerical model, using data from the literature. Then, we find the set of parameters that solves the inverse problem and we can evaluate the error made in the choice of parameters, see Subsection 5.6.2.

Another useful study that can be done in parallel is the *sensitivity analysis*, see Subsection 5.6.1. It provides us with an instrument to examine how the choice of the parameters affects the dynamics of the model. This is also a key indicator in the case in which the error between one of the estimated parameters and its corresponding real one, that have generated the numerical solution, is too big. In fact, the sensitivity analysis could show us that some parameters do not have important effects on solutions. Thus, a huge error on their estimation is not so important.

In the following, we integrate the theory with our model's analysis. In Subsection 5.6.1 and 5.6.2, we consider Model (5.8) without cells proliferation, using parameters in (5.12). Indeed, a different study can be done for cells proliferation, see Subsection 5.6.3. In here, we propose a logistic fitting. We do not show the application to our model since it requires experimental data.

5.6.1 Sensitivity analysis

The lack of data availability from experiments imposes an uncertainty in the output of the model. To obtain as reliable results as possible, we have to study the influence of the parameters on the model dynamics through a *local sensitivity analysis*. Local methods are the simplest and the most common. They are based on a one-factor-at-a-time (OAT) method. It consists in perturbing one parameter at a time to see the effect on the output for each parameter of the model. Sensitivity analysis (SA) is then performed monitoring changes in the output through, for example, a derivative-based approach.

SA determines dependencies of input parameters $\mathcal{Q} = (\mathcal{Q}_1, ..., \mathcal{Q}_n)$ and output of the model $\mathcal{Y}$. We illustrate in the following the procedure. The measure of the influence of the parameter $\mathcal{Q}_i$ on the output $\mathcal{Y}(\mathcal{Q})$ is calculated by the partial derivative with respect to this parameter. Since the model parameters differ by several orders of magnitude, we introduce a normalisation with respect to the mean value. Using the finite difference approach, the sensitivity of the output

respect to the parameter $\mathcal{Q}_i$ is obtained as

$$S = \frac{\mathcal{Y}(\mathcal{Q}_1, ..., \mathcal{Q}_i \pm \delta, ..., \mathcal{Q}_n) - \mathcal{Y}(\mathcal{Q}_1, ..., \mathcal{Q}_n)}{\mathcal{Y}(\mathcal{Q}_1, ..., \mathcal{Q}_n)} \frac{\mathcal{Q}_i}{\delta}, \tag{5.13}$$

where δ is taken as the 5% of the parameter $\mathcal{Q}_i$, namely $\delta = 5\% \cdot \mathcal{Q}_i$.

For our model. We report here the results obtained in our Model (5.8) without cells proliferation, using data in Section 5.5. We have evaluated sensitivity of parameters $\mathcal{Q} = [\theta, p, k_1]$, taking as output $\mathcal{Y}$ the maximum value at the final time for cells density and the total mass of enzymes and gelatin at the final time. It is not interesting to consider the total mass also for cells since, ignoring proliferation, this is a conserved quantity. In Table 5.1 below, we show for each changed parameter $\mathcal{Q}_i \pm \delta$, the sensitivity $S_{\mathcal{Y}}$ related to the output $\mathcal{Y}$. Sensitivity should be less than one or around it but not much bigger, namely $S_{\mathcal{Y}} \lesssim 1$, in order to have low sensitivity of the model respect to parameters. Here it is the case.

$\mathcal{Q}_i \pm \delta$ \ $S_{\mathcal{Y}}$	$S_{\max_u}$	S_{mass_m}	S_{mass_d}
$\theta + \delta$	0.6262	$6.57 \cdot 10^{-4}$	$7.05 \cdot 10^{-5}$
$\theta - \delta$	0.6705	$7.03 \cdot 10^{-4}$	$7.48 \cdot 10^{-4}$
$p + \delta$	0.0141	$2.44 \cdot 10^{-4}$	0.9524
$p - \delta$	0.0155	$2.70 \cdot 10^{-6}$	1.0526
$k_1 + \delta$	0.0146	0.9980	0.9982
$k_1 - \delta$	0.01469	0.9982	0.9972

Table 5.1: *We collect sensitivity values $S_{\mathcal{Y}}$ par each parameter $\mathcal{Q}_i \pm \delta$. S_{max_u} is the sensitivity with output the maximum of cell density at the final time (72h), S_{mass_m} is the sensitivity with output the amount of enzymes again at 72h and the same for S_{mass_d} respect to gelatin degradation. Since the sensitivity is at maximum around 1, we deduce that solutions have not a great influence on big changes in parameters. Of course, the bigger is the sensitivity, the bigger is the influence on solutions. For example, looking at the first column, we observe that cells behaviour is mainly influenced by their diffusion coefficient θ rather than on p and k_1 which affect more gelatin degradation.*

From Table 5.1, we remark that the diffusion parameter does not play a remarkable role in the behaviour of enzymes m and degradation d, whereas it is the most 'critical' parameter for cells evolution. In this case, in fact, p and k_1 are of order 10^{-2}. More critical is the influence of p on degradation and k_1 on both degradation and enzymes concentration, but still sensitivity is good enough. From SA, we infer that changings in our parameters do not greatly affect solutions behaviour. Not knowing real solutions of the model, this is a good estimate to know about.

From biological experiments, the main knowledge is on cancer cells density. We can calculate at each time interval cells position and number. More difficult is the evaluation of the amount of gelatin, as noticed with biologists. One of the reasons is that cells have their own fluorescence, but still there is no matches between numbers and observations. Up to our knowledge, it is very difficult to have data on enzymes. In conclusion, the output of interest regards cells (the first column in Table 5.1). As underlined before, sensitivity is low especially for p and k_1, thus we expect that the solution u will be mainly affected by changes in θ. In the following

Subsection 5.6.2, we are going to examine errors among solutions, obtained with a parameter estimation method.

5.6.2 Inverse problem: parameter estimation with artificial data

With the knowledge that changing our parameters we do not modify too much solutions (Subsection 5.6.1), we can now estimate, through an inverse problem, the good parameters useful, in a second step, to recover the experimental results.

We can distinguish a *forward problem* from an *inverse problem*. The first one consists in fact in calculating a solution of the model, given its parameters (as done in Section 5.5). Instead, the latter verifies that we are using the appropriate parameters such that the model successfully describes the dynamics observed in the experiments. So, if the forward problem aims at finding the solution, knowing the parameters, the inverse problem wants to find the right parameters, given the solution (that will be the experimental solution in our case). In this case, the inverse problem is called *parameter estimation problem*.

A convenient reformulation of the inverse problem is to write it as a minimization problem.

Definition 5.6.1. *Let $F(\mathcal{Q}) = \mathcal{Y}$ be the forward problem with $\mathcal{Q} = (\mathcal{Q}_1, ..., \mathcal{Q}_n)$ the parameters and $\mathcal{Y}$ the numerical solution found with the finite difference scheme. The inverse problem is defined as a minimisation problem of the form*

$$\mathcal{Q}_{opt} := \underset{\mathcal{Q}\in\mathbb{R}^n}{\operatorname{argmin}} \|F(\mathcal{Q}) - \mathcal{Y}_{exp}\|_{L^2}^2, \tag{5.14}$$

where Q_{opt} are the estimated parameters and $\mathcal{Y}_{exp}$ are the experimental data.

Unfortunately, inverse problems are usually ill-posed. Then, initial small perturbations can lead to large ones in the results. In other words, small errors between the solution of the forward problem and the experimental data can lead to arbitrary large errors between the given parameters and the estimated ones. Hence the necessity of a regularisation method to compute a stable approximation of the minimiser, Braun [12].

Definition 5.6.2 (Tikhonov regularisation)**.** *We define the Tikhonov regularisation as*

$$\mathcal{R}(\mathcal{Q}) = \lambda\|T(\mathcal{Q} - \mathcal{Q}_0)\|_{L^2}^2,$$

where $\lambda > 0$ is the regularisation parameter, T is a Tikhonov matrix and a priori estimate $\mathcal{Q}_0 \in \mathbb{R}^n$ representing an a priori knowledge about the parameters. This term extends the inverse problem as

$$\mathcal{Q}_{opt} := \underset{\mathcal{Q}\in\mathbb{R}^n}{\operatorname{argmin}}(\|F(\mathcal{Q}) - \mathcal{Y}_{exp}\|_{L^2}^2 + \lambda\|T(\mathcal{Q} - \mathcal{Q}_0)\|_{L^2}^2).$$

The choice of Tikhonov matrix normally depends on the experiments. In our case, we will choose the identity $T = I$ in order to better analyse parameters with smaller norms. A more precise analysis can be read in Braun [12, Section 6.2.1, Example 2]. Moreover, we remember that consistent data from experiments come only from cells observation, thus we will take $\mathcal{Y} = u$ and $\mathcal{Y}_{exp} = u_{exp}$. Ignoring $\mathcal{Q}_0$, we infer that

$$\mathcal{Q}_{opt} := \underset{\theta,k_1\in\mathbb{R},p\leqslant 1}{\operatorname{argmin}} (\|F(\mathcal{Q}) - u_{exp}\|_{L^2}^2 + \lambda\|\mathcal{Q}\|_{L^2}^2), \quad \text{where } \mathcal{Q} = [\theta, p, k_1]. \tag{5.15}$$

In this way, if an unknown noise is included in the data, there might be different solutions that minimise $\|F(\mathcal{Q}) - u_{exp}\|_2^2$, but among these solutions only the one which minimises $\|\mathcal{Q}\|_2^2$ is selected.

Further problems are the nonlinearity of the optimisation method, which can result in the presence of numerous local minima, and the large computational cost. To overcome these difficulties and to find a stable solution, we can apply a multigrid method, Braun [12], Liu [85]. The idea is that coarser grids are more efficient and reduce the number of local minima, allowing to find the best parameter estimation. This is not our case due to the fact that we are considering simple equations without nonlinear diffusion or convection terms, which normally make the analysis more complex.

Parameter estimation with artificial data for our model. Now, we explain the procedure used to estimate parameters for our Model (5.8) without cells proliferation. We take numerical solutions as in Section 5.5. Then, choosing parameters $\mathcal{Q}_{lit}$ as

$$\theta = 0.2, \qquad p = 0.83, \qquad k_1 = 0.78,$$

we derive numerical solutions u, m and $q = 1 - d$. We choose the artificial experimental data u_{exp}, which in our examples will be either u or a perturbation of it. Now, we want to move away from the parameters $\mathcal{Q}_{lit}$ describing our artificial data. Indeed, starting from perturbed parameters we would like to recover the best ones such that the functional in (5.15) is minimised, or equivalently such that the error among their corresponding solution and the experimental one is small. Thus, we perturb parameters with a $n\% = 10\%$, 20% or 40% Gaussian noise, namely $\mathcal{Q}_{pert}$ is composed by

$$\theta_{pert} = \theta + \omega_\theta \cdot n\% \cdot \theta, \qquad p_{pert} = p + \omega_p \cdot n\% \cdot p, \qquad k_{1_{pert}} = k_1 + \omega_{k_1} \cdot n\% \cdot k_1, \tag{5.16}$$

with ω_θ and ω_{k_1} random numbers in $[-1, 1]$, whereas ω_p is again a random number in $[-1, 1]$ in the case $n = 10\%$, 20% and $[-1, 0]$ if $n = 40\%$. Indeed, we recall that $p \leqslant 1$, so that $1 - pd \geqslant 0$.

Then, we look for the best parameters that solve the inverse Problem (5.15) in an interval given by $[\mathcal{Q}_{lit} - 50\%\mathcal{Q}_{lit}, \mathcal{Q}_{lit} + 50\%\mathcal{Q}_{lit}]$ and starting with the perturbed parameters in (5.16). So, we evaluate the parameters that minimise the error $E(\mathcal{Q})$ between our artificial data and the new solution $\widehat{u}$ obtained with one of the parameters $\mathcal{Q}$ in the research interval $[\mathcal{Q}_{lit} - 50\%\mathcal{Q}_{lit}, \mathcal{Q}_{lit} + 50\%\mathcal{Q}_{lit}]$ plus the Tikhonov regularisation with $\lambda = 10^{-6}$, namely

$$E(\mathcal{Q}) = \|\widehat{u}(t) - u_{exp}(t)\|_2^2 + \lambda \|\mathcal{Q}\|_2^2, \qquad \text{for } t = 48 \text{ hours.} \tag{5.17}$$

We have chosen an intermediate time $t = 48h$, since diffusion problems have a dissipative behaviour and we can loose information at the final time. Instead, we have not to consider $t = 0$, since initial data do not depend on parameters and the error appears fixed. Finally, we calculate the relative error between the estimated parameters $\mathcal{Q}_{opt}$ and the original ones, *i.e.*

$$E_\theta = \frac{\|\theta - \theta_{opt}\|_2}{\|\theta\|_2}, \qquad E_p = \frac{\|p - p_{opt}\|_2}{\|p\|_2}, \qquad E_{k_1} = \frac{\|k_1 - k_{1_{opt}}\|_2}{\|k_1\|_2}. \tag{5.18}$$

We also estimate the relative error between the experimental artificial data u_{exp} and the solution with the estimated parameters, that is defined as

$$E_{\mathcal{Q}_{opt}}(t) = \frac{\|u_{exp}(t) - u_{\mathcal{Q}_{opt}}(t)\|_2}{\|u_{exp}(t)\|_2}, \qquad \text{for } t = 0, 24, 48, 72 \text{ hours.} \tag{5.19}$$

Artificial data: exact numerical solution

At first, we choose as artificial data the exact numerical solution u. The results are in Example 5.6.1 and Remark 5.6.1.

Example 5.6.1. *We consider a* 10% *perturbation on parameters* $\mathcal{Q}_{lit} = [\theta, p, k_1] = [0.2, 0.83, 0.78]$, *randomly extracting* $\omega_\theta = -0.48$, $\omega_p = -0.49$ *and* $\omega_{k_1} = 0.51$. *We deduce*

$$\mathcal{Q}_{pert} = [0.19, \quad 0.871, \quad 0.82].$$

Solving the inverse problem in (5.15), *we infer that*

$$\mathcal{Q}_{opt} = [0.199, \quad 0.415, \quad 0.39].$$

The errors on parameters, see Equations (5.18), *are*

$$E_\theta = 10^{-4}\%, \quad E_p = 50\%, \quad E_{k_1} = 50\%.$$

Unfortunately, errors on p *and* k_1 *are high. However, as expected from the sensitivity analysis in Subsection 5.6.1, this do not impact solutions. In Figure 5.7, we show the error* $E_{\mathcal{Q}_{opt}}$ *between the data* u *and the solution with estimated parameters. The same is provided also for* q, *since they are both quantities experimentally of interest.*

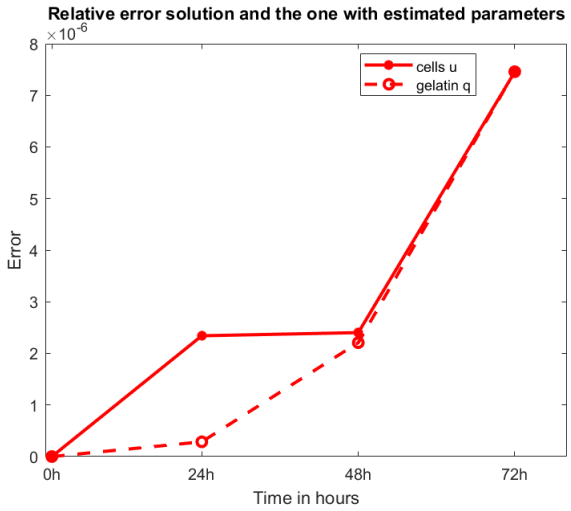

Figure 5.7: *We show the variation in time of error* $E_{\mathcal{Q}_{opt}}$ *in* (5.19), *both for cells* u *and gelatin* q *(dash line) which are the quantities experimentally of interest. The daily time step is highlighted. Considering estimated parameters the error on them is below* $8 \cdot 10^{-4}\%$.

Remark 5.6.1. *The same results are obtained considering* 20% *perturbation on parameters with* $\omega_\theta = 0.66$, $\omega_p = -0.62$ *and* $\omega_{k_1} = 0.15$ *and* 40% *perturbation with* $\omega_\theta = -0.19$, $\omega_p = -0.76$ *and* $\omega_{k_1} = 0.68$.

A property of our model is stability and this is reflected on a good approximation of solutions (around $10^{-3}\%$), or equivalently on a low value for the functional (around $3 \cdot 10^{-7}$). Unfortunately, errors on parameters are high for p and k_1, but without any effect on solutions, see the sensitivity analysis in Subsection 5.6.1.

We conclude the example with a final observation. The relative error between solutions is of the same order of $\lambda = 10^{-6}$, and also lower. This implies that the minimisation do not consider any more the norm of solutions, but only the norm of parameters $\mathcal{Q}$, see Equation (5.17). This is why we end up with a big error on parameters: the algorithm is trying to find very small parameters. Then, considering a lower $\lambda = 10^{-12}$, we could force the minimiser to decrease only solutions norms. The results are just below. We take the same data as before and, solving the inverse problem, we obtain

$$\mathcal{Q}_{opt} = [0.2, \quad 0.809, \quad 0.761].$$

The errors on parameters are significantly smaller, *i.e.*

$$E_\theta = 10^{-6}\%, \quad E_p = 2.4\%, \quad E_{k_1} = 2.4\%.$$

Again, we have a good estimate of solutions as before, see Figure 5.8.

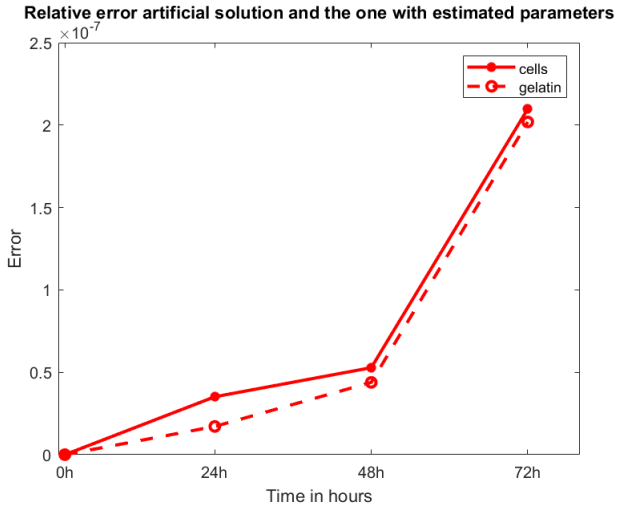

Figure 5.8: *We show the variation in time of error $E_{\mathcal{Q}_{opt}}$ in (5.19), both for cells u and gelatin q (dash line) which are the quantities experimentally of interest. The daily time step is highlighted. Considering estimated parameters the error on them is below $3 \cdot 10^{-5}\%$.*

At the same time, (non artificial) experimental data have always some unknown noise due for instance to instrumentation. This is why in the following we consider a more realistic setting in which the artificial data are a perturbation of the numerical solutions.

Artificial data: perturbed numerical solution

We perturb with 5% Gaussian noise the exact numerical solutions, *i.e.*

$$u_{pert} = u + \omega_u \cdot 5\% \cdot u, \qquad m_{pert} = m + \omega_m \cdot 5\% \cdot m, \qquad q_{pert} = q + \omega_q \cdot 5\% \cdot q,$$

where ω_u and ω_m are random matrices with entries in $[-1, 1]$, whereas ω_q has entries in $[-1, 0]$, so that d_{pert} keeps being in $[0, 1]$. The perturbed solutions should simulate experimental data, introducing the idea that they are characterised by some unknown noise. Moreover, in the case of u and m, this Gaussian noise is with 0 mean, thus perturbed solutions are the original numerical solutions on average. The results are in Example 5.6.2, 5.6.3, 5.6.4.

Example 5.6.2. *We consider a* 10% *perturbation on parameters* $\mathcal{Q}_{lit} = [\theta, p, k_1] = [0.2, 0.83, 0.78]$. *Randomly extracting* $\omega_\theta = -0.11$, $\omega_p = -0.15$ *and* $\omega_{k_1} = -0.83$, *we deduce*

$$\mathcal{Q}_{pert} = [0.198, \quad 0.817, \quad 0.715].$$

Solving the inverse problem in (5.15), *we get*

$$\mathcal{Q}_{opt} = [0.199, \quad 0.415, \quad 0.539].$$

This infers an error on parameters, see Equations (5.18), *such that*

$$E_\theta = 0.07\%, \qquad E_p = 50\%, \qquad E_{k_1} = 31\%.$$

As before, errors on p *and* k_1 *are high. In Figure 5.9, we show the errors* $E_{\mathcal{Q}_{opt}}$, *which are for both* u *and* q *below the initial error of* 5% *(the error between the artificial data and the solution with the original parameters).*

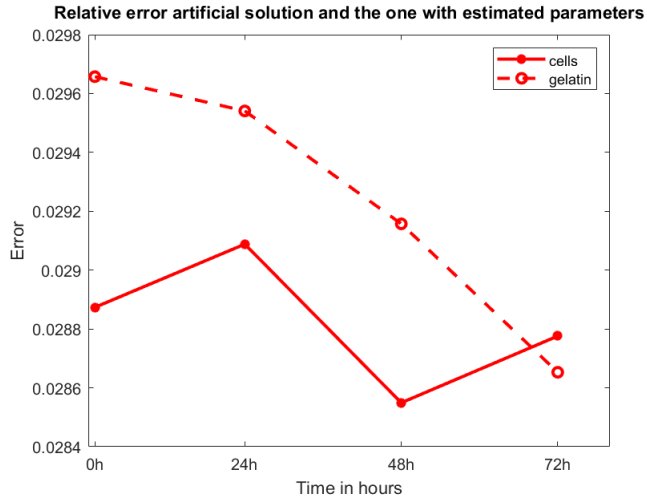

Figure 5.9: *We show the variation in time of errors* $E_{\mathcal{Q}_{opt}}$ *in* (5.19) *both for cells* u *and gelatin* q *(dash line) which are the quantities experimentally of interest.* $E_{\mathcal{Q}_{opt}}$ *is below* 3%.

Remark 5.6.2. *We do not get very satisfactory results in terms of parameter estimation. However, the real aim of parameter estimation is that solutions with* $\mathcal{Q}_{opt}$ *do not greatly differ from the experimental data (the perturbed solutions in this artificial case), as studied in Subsection 5.6.1. In contrast, we remark that having more information also on gelatin and enzymes concentration could bring us also a good estimation on the other parameters. In particular, the parameter* p *is present both in the equation for enzymes concentration* m *and gelatin degradation* d, *then we should need both of them to obtain a good estimate on* p. *The parameter* k_1 *is only in the equation for the enzymes and, indeed, we can approximate it having experimental data on enzymes.*

Example 5.6.3. *A different situation promises to be the case with* 20% *perturbation on parameters* $\mathcal{Q}_{lit} = [\theta, p, k_1] = [0.2, 0.83, 0.78]$. *Randomly extracting* $\omega_\theta = 0.28$, $\omega_p = -0.13$ *and* $\omega_{k_1} = -0.81$, *we deduce*

$$\mathcal{Q}_{pert} = [0.211, \quad 0.809, \quad 0.653].$$

Solving the inverse problem in (5.15)*, we get*

$$\mathcal{Q}_{opt} = [0.199, \quad 0.415, \quad 0.809].$$

This infers an error on parameters, see Equations (5.17)*, such that*

$$E_\theta = 0.2\%, \qquad E_p = 50\%, \qquad E_{k_1} = 3.7\%.$$

So, here we notice a better convergence rate for k_1 respect to Example 5.6.2, probably due to a better formulation of the minimisation problem which well represent the final minima. Again, we have good final errors on solutions. In Figure 5.10, we show the errors $E_{\mathcal{Q}_{opt}}$, which are below the initial 5% noise.

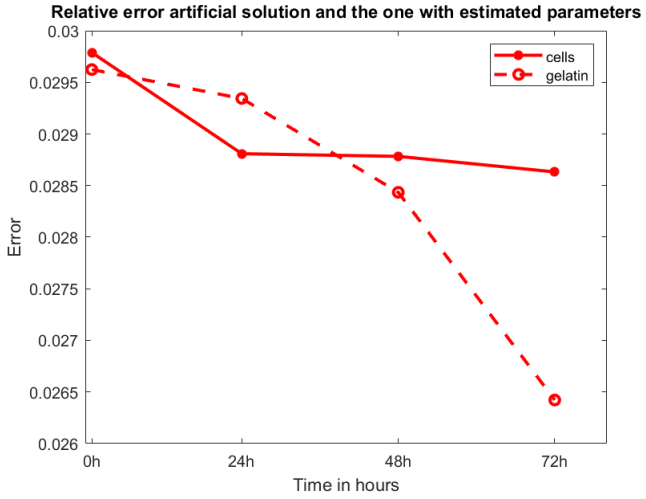

Figure 5.10: *We show the variation in time of errors $E_{\mathcal{Q}_{opt}}$ in* (5.19) *both for cells u and gelatin q (dash line) which are the quantities experimentally of interest. Again, they are below 3%.*

Remark 5.6.3. *Of course the randomness on perturbations influence the final error. As confirmation, we report that repeating the same experiment, but again randomly choosing perturbations, we can end up on a worst estimate on k_1 as the one in Example 5.6.2.*

Example 5.6.4. *We consider a 40% perturbation on parameters $\mathcal{Q}_{lit} = [\theta, p, k_1] = [0.2, 0.83, 0.78]$. Randomly extracting $\omega_\theta = 0.27$, $\omega_p = -0.56$ and $\omega_{k_1} = -0.81$, we get similar values as in Example 5.6.3. We deduce*

$$\mathcal{Q}_{pert} = [0.222, \quad 0.643, \quad 0.526].$$

Solving the inverse problem in (5.15)*, we get*

$$\mathcal{Q}_{opt} = [0.199, \quad 0.415, \quad 0.801].$$

The results are then the same as in Example 5.6.3. Indeed, we have

$$E_\theta = 0.2\%, \qquad E_p = 50\%, \qquad E_{k_1} = 3.7\%.$$

In Figure 5.11, we show the errors $E_{\mathcal{Q}_{opt}}$.

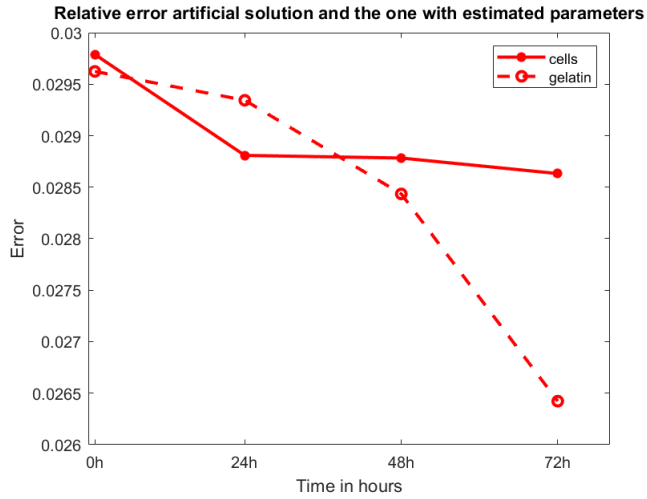

Figure 5.11: *We show the variation in time of errors $E_{\mathcal{Q}_{opt}}$ in (5.19) both for cells u and gelatin q (dash line) which are the quantities experimentally of interest. We have the same results as in the previous Examples 5.6.2, 5.6.3.*

So if we look for the optimal parameters describing the artificial experimental data (chosen as the perturbed numerical solution u_{pert}), we deduce:

- a good approximation of θ with an error around $10^{-1}\%$;
- a maximal error on p (since we are looking for parameters in an interval of $\pm 50\%$ of their values);
- a varying error on k_1, which is around 4% or 30% in the examples presented.

Despite the perturbation on parameters, we end up with the same value of the functional $E(\mathcal{Q})$ in (5.17), which is around $6 \cdot 10^{-3}$, thus we have the same error $E_{\mathcal{Q}_{opt}} \sim 3\%$. A good error is also appreciated on the gelatin q, which is always around 3%.

Finally, we conclude that we can recover experimental data on cells and, possibly, even gelatin satisfactorily. In order to obtain the optimal parameters accurately, we should need either more experimental data or to change the definition of the functional $E(\mathcal{Q})$ in (5.17) or eventually a model reduction. Indeed, concerning $E(\mathcal{Q})$, we could modify the value of λ, maybe a lower one, at least for Example 5.6.1, where the error between solutions is of the same order of λ. Regarding a model reduction, even if relatively simple, System (5.8) could still be too complex to describe experiments. A detailed analysis of it could highlight particular behaviours that we currently ignore. We could also add $\mathcal{Q}_0 = \mathcal{Q}_{lit}$. This last addition would be less realistic but, at least, we force the minimisation to consider parameters not too far away from the original ones. In fact, the inverse Problem (5.15) looks for minimisation of solutions with a preference to small parameters. An example is shown just below.

Example 5.6.5. *Let $\lambda = 10^{-3}, \mathcal{Q}_0 = \mathcal{Q}_{lit}$. We consider a 10% perturbation on parameters $\mathcal{Q}_{lit} = [\theta, p, k_1] = [0.2, 0.83, 0.78]$, randomly extracting $\omega_\theta = 0.27$, $\omega_p = -0.12$ and $\omega_{k_1} = -0.81$. Solving the inverse problem in (5.15), we get*

$$\mathcal{Q}_{opt} = [0.2, \quad 0.806, \quad 0.803].$$

This infers an error on parameters, see Equations (5.18), such that

$$E_\theta = 0.3\%, \qquad E_p = 2.8\%, \qquad E_{k_1} = 3\%.$$

In Figure 5.12, we show the errors $E_{\mathcal{Q}_{opt}}$, which are for both u and q below the initial error of 5% (the error between the artificial data and the solution with the original parameters).

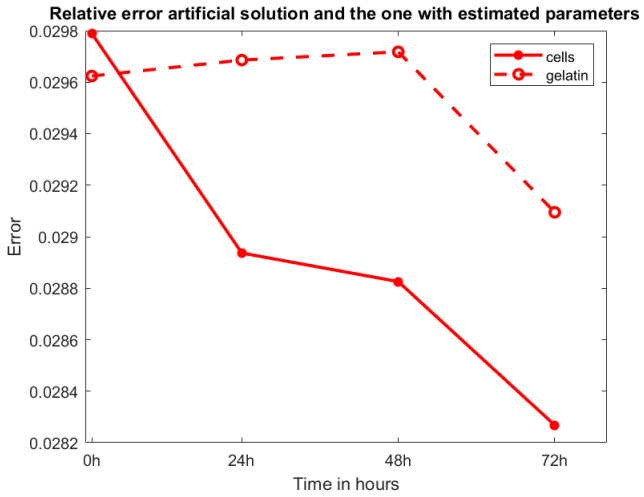

Figure 5.12: *We show the variation in time of errors $E_{\mathcal{Q}_{opt}}$ in (5.19) both for cells u and gelatin q (dash line) which are the quantities experimentally of interest. $E_{\mathcal{Q}_{opt}}$ is below 3%.*

5.6.3 Cell proliferation: a logistic fitting

As biological experiments are over 72 hours, cells have also the time to replicate. This is why we had to add a proliferation term in our model, which is preferentially logistic. Knowing cells duplication time, we can also estimate the growth parameters. This information can be extrapolated from the same experiments described in Section 5.2. Hence, we still do not have experimental data. However, we illustrate here the procedure that we will follow.

The population size or total number of cells $U = \int_\Omega u$ grows in the domain Ω following a logistic equation

$$\frac{dU}{dt} = \alpha U(\overline{U} - U),$$

with $\overline{U}, \alpha$ unknown parameters, Pearl and Reed [102]. Here, α is related to the duplication time of the population. This equation can be rewritten as

$$\frac{dU}{dt} = rU\left(1 - \frac{U}{k}\right),$$

where $r := \alpha\overline{U}$ is the growth rate and $k := \overline{U}$ is called carrying capacity and it stands for the level of saturation, *i.e.* the maximum population size of a biological specie that can be sustained by a specific environment. So, at the beginning, the population size grows exponentially, then slows down converging to the carrying capacity. The logistic solution is then

$$U(t) = \frac{k}{1 - \frac{k-U_0}{U_0}e^{-rt}},$$

where $U_0 = U(t = 0)$. For the estimation of parameters of a logistic curve, we can use the method of three selected points given by Pearl and Reed [102]. Given three equally spaced times t_1, t_2, t_3 at which we evaluate U_1, U_2, U_3, then

$$k = \frac{U_2^2(U_1 + U_3) - 2U_1U_2U_3}{U_2^2 - U_1U_3}, \qquad r = \frac{1}{t_2 - t_1} \ln\left(\frac{(k - U_1)U_2}{(k - U_2)U_1}\right).$$

In our case, we could take $t_1 = 24h$, $t_2 = 48h$, $t_3 = 72h$ and U_1, U_2, U_3 will be the experimental values of the mass of cells at these times.

5.7 Conclusions and future works

We set up the mathematical model and tools to deal with biological experiments on membrane degradation. This biological process is fundamental in invasion of cells and, then, in tumor metastasis as well as in its inflammation and development. Therefore, a closer knowledge of degradation of ECM layers is the key point to a better understanding of invasion, from both a biological and mathematical point of view. Indeed, we can recover both the behaviour of cells and pictures of the degradation of a layer, which are not provided by invasion experiments.

The chapter is an ongoing work, since we will apply the mathematical results presented to biological experiments, as soon as available. The complete work represents also a starting point to study invasion experiments through the XCELLigence technology, that we leave right now as an open problem. The difference with degradation will be the introduction of membrane Kedem-Katchalsky conditions. Actually as soon as cells have degraded the ECM layer, they pass through it. Moreover, the XCELLigence allows us to consider different gelatin thicknesses and we will be able to evaluate the consequent different times of degradation. Indeed, unfortunately QCM™ Gelatin Invadopodia Assay has not this possibility.

In the short term, obtained the experimental data for degradation, we will have pictures of both cells and gelatin at the interesting times of $0, 24, 48, 72$ hours. For cells, biologists are able to obtain DAPI images, representing colored cells nuclei, which will enable us to know the number of cells at each interesting time. This is fundamental to the logistic fitting in cells proliferation, see Subsection 5.6.3. Moreover, we will have to recover the dimension of the domain Ω, corresponding to the well coated of gelatin. Then, we could perform the parameter estimation, see Subsection 5.6.2. In this case, the experimental data will be the biological ones and we will need to perturb them by the transformation process of particles into densities. In fact, since biologists have pictures of cells as a microscopic quantity, we will need to transform particles into densities in order to obtain a macroscopic representation of cells. This procedure consists of centering a Gaussian kernel on each cells, see Braun [12]. Finally, we will substitute the numerical results in Section 5.5, with the one in which cells initial data u_0 is the experimental one, treated with the particles to density transformation.

5.A Density to particle transformation

In the previous numerical results in Figures 5.3 - 5.6, we present cells as particles even if dealing with a macroscopic model. In fact, this kind of pictures is comparable to experimental data, available as microscopic observations representing cells (as seen in Figures 5.1 and 5.2). At the same time, they are more understandable, even outside the mathematical community. This is the reason why we introduce here the useful technique of transforming macroscopic data into microscopic ones, called *acceptance-rejection method* or simply *rejection method*, Braun [12],

Hörmann *et al.* [67]. The inverse is also possible, but it is not of interest at this stage.

We remember that partial differential equations can be derived from probabilistic microscopic models, where each particle moves following a random walk. In the limit of the number of particles, we can obtain a partial differential equation of the probability that a particle is located at a certain point in space. This probability density is associated to a continuous random variable. The acceptance-rejection method is based upon the property that if a random point $(X, Y) \in \mathbb{R}^2$ is uniformly distributed in the area between the graph of the density function f and the x-axis, then X is distributed according to f (see Figure 5.13). The formal result is the following.

Theorem 5.A.1. *Let $f(x)$ be a density function and α a positive constant. If X and Y are uniformly distributed on*

$$G_{\alpha,f} := \{(x, y) : 0 < y \leqslant \alpha f(x)\},$$

then X is a random variable with density $f(x)$.

This method can be easily generalised to higher dimensions.

Algorithm in 1D

$X = [\,]$; counter= 0; $\alpha = \max_{x\in[a,b]} f(x)$;
while counter< M *do*
  generate $x \sim U(a, b)$
  generate $y \sim U(0, \alpha)$
  if $y \leqslant f(x)$
    $X = [X; x]$;
    counter= counter+1;
  end
end

Algorithm in 2D

$X = [\,]$; counter= 0; $\alpha = \max_{x,y} f(x, y),\ \forall x \in [a, b], y \in [c, d]$;
while counter< M *do*
  generate $x \sim U(a, b)$
  generate $y \sim U(c, d)$
  generate $z \sim U(0, \alpha)$
  if $z \leqslant f(x, y)$
    $X = [X; (x, y)]$;
    counter= counter+1;
  end
end

With regards to partial differential equations, where the analytical solution is often unknown, we can use the discrete form of the acceptance-rejection method applied to the numerical solution, calculated via a finite difference scheme. Thus, the choice of the random variables X and Y has to be done on the grid points on which is constructed the numerical scheme. The previous theorem becomes in two-dimension

Theorem 5.A.2. *Let $\Omega = [a,b] \times [c,d]$ be the spatial domain and $u^n_{i,j}$ the discrete values of the density function obtained through a finite difference scheme on the discretised domain with $x_i = a + i\Delta x$, $y_j = b + j\Delta y$, for $i = 1, ..., N_x + 1$ and $j = 1, ..., N_y + 1$. If X, Y are distributed according to a discrete uniform distribution, i.e. $X \sim U(0, N_x + 1), Y \sim U(0, N_y + 1)$ and Z is uniformly distributed $Z \sim U(0,1)$ on*

$$G_{\alpha,u^n} := \{(i,j,z) : 0 < z \leqslant \alpha u^n_{i,j}\},$$

then (X,Y) is a random variable with density u^n.

Discrete algorithm in 2D

$X = [\,]$; counter$= 0$; $\alpha = \max_{i,j} u^n_{i,j}$;

while counter$<$ M *do*

generate $i \sim U(1, ..., N_x + 1)$

generate $j \sim U(1, ..., N_y + 1)$

generate $z \sim U(0, \alpha)$

if $z \leqslant u^n_{i,j}$

$X = [X; (x_i, y_j)]$;

counter$=$ counter$+1$;

end

end

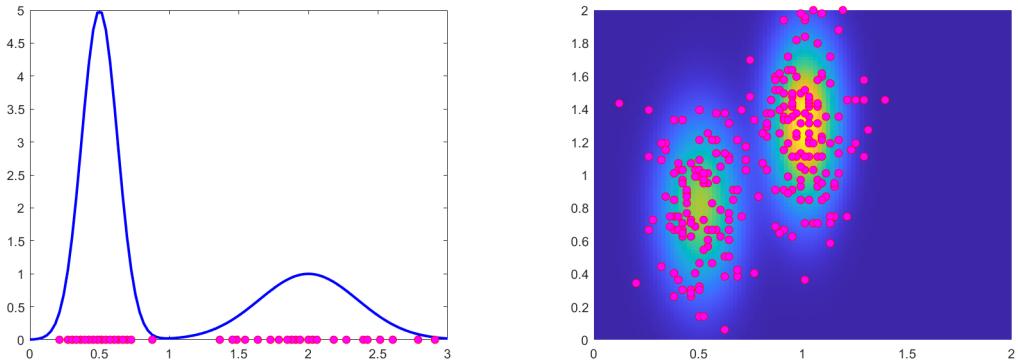

Figure 5.13: *On the left, we represent the one-dimensional acceptance-rejection method applied to $f(x) = 5e^{-30(x-0.5)^2} + e^{-4(x-2)^2}$ with $x \in (0,3)$ and the counter limit $M = 100$. On the right, a two-dimensional example with $f(x,y) = 5e^{-30(x-0.5)^2-4(y-0.8)^2} + 7e^{-40(x-1)^2-4(y-1.3)^2}$ with $x, y \in (0,2)$ and the counter limit $M = 250$.*

A discrete example can be seen in Figures 5.3 - 5.6 in Section 5.5, where we have considered $M = 1000$. In this case, the idea of the acceptance-rejection method is to collect random points (x_i, y_j) corresponding to cells coordinates positions. The higher is the density value, the higher will be the concentration of magenta dots that we can interpreter as tumor cell.

5.B Discretisation

We illustrate the two-dimension numerical method, Morton and Mayers [92], Quarteroni *et al.* [111]. We present the discretisation of the two-dimensional System (5.8) on the domain $\Omega = [a, b] \times [c, d]$. The main ideas are the same as in Section 4.B.

Concerning space discretisation, we consider a mesh over Ω such that $\Delta x = \frac{b-a}{N_x+1} = \Delta y$. Thus, we divide $[a, b]$ into $N_x \in \mathbb{N}$ intervals such that a (respectively, b) corresponds to $j = 1$ ($j = N_x + 1$), and $[c, d]$ into $N_y \in \mathbb{N}$ intervals such that c (respectively, d) corresponds to $i = 1$ ($i = N_y + 1$). The mesh is formed by the intervals

$$J_j = \left(x_{j-\frac{1}{2}}, x_{j+\frac{1}{2}}\right),\ j = 1, ..., N_x + 1, \qquad I_i = \left(y_{i-\frac{1}{2}}, y_{i+\frac{1}{2}}\right),\ i = 1, ..., N_y + 1.$$

The intervals are centred in $x_j = j\Delta x$, $j = 1, ..., N_x+1$ and $y_i = i\Delta y$, $i = 1, ..., N_y+1$. Moreover, we add ghost points to build the extremal intervals centred at the boundaries for $x = a, b$ and $y = c, d$. At a given time, the spatial discretisation of $u(t, x, y)$ (the same for functions m and d), interpreted in the finite volume sense, is of the form

$$u_{i,j}(t) \approx \frac{1}{\Delta x}\frac{1}{\Delta y}\int_{J_j}\int_{I_i} u(t, x, y)\, dx\, dy, \qquad \text{for } j = 1, ..., N_x + 1,\ i = 1, ..., N_y + 1.$$

For the time discretisation, we consider a time step Δt, and set $t^n = n\Delta t$, with $n \in \mathbb{N}$. The discrete approximation of $u(t, x, y)$ (or of functions m or d), for $n \in \mathbb{N}$, $j = 1, ..., N_x + 1$, $i = 1, ..., N_y + 1$ is now

$$u^n_{i,j} \approx \frac{1}{\Delta x}\frac{1}{\Delta y}\int_{J_j}\int_{I_i} u(t^n, x, y)\, dx\, dy.$$

Equation for d. We solve $\partial_t d = \frac{1}{p} m \left(1 - \frac{1}{p} d\right)$. We discretise the solution $d = \frac{1}{p}\left(1 - e^{\int_0^t m ds}\right)$, $\forall x, y \in \Omega$, using the trapezoidal rule for the integral

$$\int_0^t m\, ds \approx \frac{\Delta t}{2}\left[m^n_{i,j} + 2\sum_{k=1}^{n-1} m^k_{i,j}\right],$$

for $j = 1, ..., N_x + 1$, $i = 1, ..., N_y + 1$. We remember that initially $d^0_{i,j} = 0$, $\forall i = 1, ..., N_y + 1, j = 1, ..., N_x + 1$, since the gelatin is not damaged.

Discretisation for D(d). We analyse separately the diffusion coefficient for cell density u. We recall the expression in (5.2), namely $D(d) = \theta + d$ in the parametrised version. Its discretisation is easy, but we have to deal with ghost points that appear in the discretisation for u. We derived boundary conditions which preserve the mass in our system. Namely, we obtain

$$\begin{aligned} D(d)^n_{i,0} &= D(d)^n_{i,2}, \quad D(d)^n_{i,N_x+2} = D(d)^n_{i,N_x}, \\ D(d)^n_{0,j} &= D(d)^n_{2,j}, \quad D(d)^n_{N_y+2,j} = D(d)^n_{N_y,j}. \end{aligned} \tag{5.20}$$

Equation for u. To achieve the time discretisation, we adopt an Euler method, and we write $\frac{du}{dt}(t)$ as $\frac{u^{n+1}-u^n}{\Delta t}$. To obtain space discretisation, we recall the following explicit one-dimensional method

$$\partial_x(a(x)\partial_x u) \approx \frac{(a_{j+1}+a_j)(u_{j+1}-u_j)-(a_{j-1}+a_j)(u_j-u_{j-1})}{2\Delta x^2}.$$

In the vector analysis, we can use this one-dimensional approximation on each axis derivative. Then, full discretisation of System (5.8) reads for $n \in \mathbb{N}, j = 1, ..., N_x + 1, i = 1, ..., N_y + 1$ as

$$\begin{aligned} u_{i,j}^{n+1} - u_{i,j}^n = \mu[&(D_{i-1,j}^n + D_{i,j}^n)u_{i-1,j}^n + (D_{i+1,j}^n + D_{i,j}^n)u_{i+1,j}^n + \\ -&(D_{i-1,j}^n + D_{i+1,j}^n + 4D_{i,j}^n + D_{i,j-1}^n + D_{i,j+1}^n)u_{i,j}^n + (D_{i,j-1}^n + D_{i,j}^n)u_{i,j-1}^n + \\ &+(D_{i,j+1}^n + D_{i,j}^n)u_{i,j+1}^n] + k_2 u_{i,j}^n \left(1 - \tfrac{u_{i,j}^n}{\alpha_3}\right), \end{aligned} \tag{5.21}$$

with $\mu_u = \frac{\Delta t}{2\Delta x^2}$. Finally, we deduce the system

$$\begin{aligned} u_{i,j}^{n+1} &= [1 - \mu(D_{i-1,j}^n + D_{i+1,j}^n + 4D_{i,j}^n + D_{i,j-1}^n + D_{i,j+1}^n)]u_{i,j}^n + \\ &+\mu(D_{i-1,j}^n + D_{i,j}^n)u_{i-1,j}^n + \mu(D_{i+1,j}^n + D_{i,j}^n)u_{i+1,j}^n + \mu(D_{i,j-1}^n + D_{i,j}^n)u_{i,j-1}^n + \\ &+\mu(D_{i,j+1}^n + D_{i,j}^n)u_{i,j+1}^n + k_2 u_{i,j}^n \left(1 - \tfrac{u_{i,j}^n}{\alpha_3}\right), \end{aligned} \tag{5.22}$$

with second order discretisation of the Neumann boundary conditions in $x = a, b$, and $y = c, d$ as

$$u_{i,0}^n = u_{i,2}^n, \quad u_{i,N_x+2}^n = u_{i,N_x}^n, \quad u_{0,j}^n = u_{2,j}^n, \quad u_{N_y+2,j}^n = u_{N_y,j}^n. \tag{5.23}$$

Previous conditions give the relations of the extremal ghost points. Substituting ghost points Relations (5.20), (5.23) into Equation (5.22), we obtain the discretised equation for u of System (5.8) defined on the spatial grid.

Equation for m. Instead of the equation for m, in order to avoid stiffness problems due to the presence of the term $-m$, we discretise the equation for $w = e^t m$ which is of the form $\partial_t w = \Delta w + k_1 u(1 - pd)e^t$. At the end, the discretised density for the enzymes m can be derived from the numerical solution w, as $m_{i,j}^n = e^{-t^n} w_{i,j}^n$. We infer that

$$w_{i,j}^{n+1} = (1 - 4\mu_m)w_{i,j}^n + \mu_m(w_{i-1,j}^n + w_{i+1,j}^n + w_{i,j-1}^n + w_{i,j+1}^n) + k_1 u_{i,j}^n(1 - pd_{i,j}^n)e^{n\Delta t}, \tag{5.24}$$

with $\mu_m = \frac{\Delta t}{\Delta x^2}$. Boundary conditions are the same as in (5.23).

Calling the vector solutions at time t^n as

$$U^n = \left(u_{i,1}^n, \ldots, u_{i,N_x+1}^n\right)^T, \qquad W^n = \left(w_{i,1}^n, \ldots, w_{i,N_x+1}^n\right)^T,$$

and the reaction vectors as

$$R^n = k_2 U^n \left(1 - \frac{U^n}{\alpha_3}\right), \quad S^n = e^{\alpha n \Delta t}\beta U^n,$$

we can write the discretised systems in a matrix form as $U^{n+1} = AU^n + \Delta t R^n$ coupled with $W^{n+1} = BW^n + \Delta t S^n$. Coefficients of the matrices A and B can be found substituting ghost points in the discretised equations. In particular, B is the standard matrix related to the heat

equation.

It is important to guarantee the positiveness of the coefficients in the previous Equations (5.22), (5.24), in order to preserve positiveness and stability. This brings conditions on the time interval Δt which has to be such that

$$\Delta t < \min(dt_1, dt_2), \quad \text{where} \quad dt_1 = \frac{\Delta x^2}{4(\theta+1)}, \quad dt_2 = \frac{\Delta x^2}{4}, \tag{5.25}$$

since $dt_1 = \min\left(\frac{2\Delta x^2}{8\theta+(d^n_{i-1,j}+d^n_{i+1,j}+4d^n_{i,j}+d^n_{i,j-1}+d^n_{i,j+1})}\right) = \left(\frac{2\Delta x^2}{8\theta+\max(d^n_{i-1,j}+d^n_{i+1,j}+4d^n_{i,j}+d^n_{i,j-1}+d^n_{i,j+1})}\right)$, and the maximum value for d is 1.

Bibliography

[1] N. Aceto, A. Bardia, D. T. Miyamoto, M. C. Donaldson, B. S. Wittner, J. A. Spencer, M. Yu, A. Pely, A. Engstrom, H. Zhu, et al. "Circulating tumor cell clusters are oligoclonal precursors of breast cancer metastasis". In: *Cell* 158.5 (2014), pp. 1110–1122. URL: https://doi.org/10.1016/j.cell.2014.07.013.

[2] R. A. Adams and J. J. Fournier. *Sobolev spaces*. Elsevier, 2003. URL: https://www.elsevier.com/books/sobolev-spaces/adams/978-0-12-044143-3.

[3] A. M. Alizadeh, S. Shiri, and S. Farsinejad. "Metastasis review: from bench to bedside". In: *Tumor Biol.* 35.9 (2014), pp. 8483–8523. URL: https://doi.org/10.1007/s13277-014-2421-z.

[4] L. Almeida, F. Bubba, B. Perthame, and C. Pouchol. "Energy and implicit discretization of the Fokker-Planck and Keller-Segel type equations". In: *Netw. Heterog. Media* 14.1 (2019), pp. 23–41. URL: http://dx.doi.org/10.3934/nhm.2019002.

[5] V. V. Artym, Y. Zhang, F. Seillier-Moiseiwitsch, K. M. Yamada, and S. C. Mueller. "Dynamic interactions of cortactin and membrane type 1 matrix metalloproteinase at invadopodia: defining the stages of invadopodia formation and function". In: *Cancer Res.* 66.6 (2006), pp. 3034–3043. URL: https://doi.org/10.1158/0008-5472.CAN-05-2177.

[6] J.-P. Aubin. "Un théorème de compacité". In: *C. R. Acad. Sci. Paris* 256 (1963), pp. 5042–5044. URL: https://gallica.bnf.fr/ark:/12148/bpt6k4006n/f1164.item.

[7] P. Baras and M. Pierre. "Problemes paraboliques semi-lineaires avec donnees mesures". In: *Appl. Anal.* 18.1-2 (1984), pp. 111–149. URL: https://doi.org/10.1080/00036818408839514.

[8] M. Bathory, M. Bulıček, and O. Souček. "Existence and qualitative theory for nonlinear elliptic systems with a nonlinear interface condition used in electrochemistry". In: *Z. Angew. Math. Phys.* 71.3 (2020), pp. 1–24. URL: https://doi.org/10.1007/s00033-020-01293-w.

[9] M. Bissell and W. Hines. "Why don't we get more cancer? A proposed role of the microenvironment in restraining cancer progression". In: *Nat. Med.* (2011), pp. 320–329. URL: https://doi.org/10.1038/nm.2328.

[10] D. Bothe and M. Pierre. "Quasi-steady-state approximation for a reaction–diffusion system with fast intermediate". In: *J. Math. Anal. Appl.* 368.1 (2010), pp. 120–132. URL: https://doi.org/10.1016/j.jmaa.2010.02.044.

[11] E. C. Braun, G. Bretti, and R. Natalini. "Parameter estimation techniques for a chemotaxis model inspired by Cancer-on-Chip (COC) experiments". In: *Int. J. Non-Linear Mech.* 140 (2022), p. 103895. URL: https://doi.org/10.1016/j.ijnonlinmec.2021.103895.

[12] E. C. Braun. "Organs-On-Chips: mathematical modelling and parameter estimation". PhD thesis. Università degli Studi di Roma Tre, 2021. URL: http://www.matfis.uniroma3.it/Allegati/Dottorato/TESI/ecbraun/Thesis%20Braun%20Revision.pdf.

[13] E. C. Braun, G. Bretti, and R. Natalini. "Mass-preserving approximation of a chemotaxis multi-domain transmission model for microfluidic chips". In: *Mathematics* 9.6 (2021), p. 688. URL: https://doi.org/10.3390/math9060688.

[14] D. Bresch, T. Colin, E. Grenier, B. Ribba, and O. Saut. "Computational modeling of solid tumor growth: the avascular stage". In: *SIAM J. Sci. Comput.* 32.4 (2010), pp. 2321–2344. URL: https://doi.org/10.1137/070708895.

[15] H. Brezis. *Functional analysis, Sobolev spaces and partial differential equations*. Vol. 2. 3. Springer, 2011. URL: https://doi.org/10.1007/978-0-387-70914-7.

[16] H. Brezis, L. A. Caffarelli, and A. Friedman. "Reinforcement problems for elliptic equations and variational inequalities". In: *Ann. Mat. Pura Appl.* 123.1 (1980), pp. 219–246. URL: https://doi.org/10.1007/BF01796546.

[17] F. Bubba, C. Pouchol, N. Ferrand, G. Vidal, L. Almeida, B. Perthame, and M. Sabbah. "A chemotaxis-based explanation of spheroid formation in 3D cultures of breast cancer cells". In: *J. Theor. Biol.* 479 (2019), pp. 73–80. URL: https://doi.org/10.1016/j.jtbi.2019.07.002.

[18] H. M. Byrne and M. A. J. Chaplain. "Modelling the role of cell-cell adhesion in the growth and development of carcinomas". In: *Math. Comput. Modelling* 24 (1996), pp. 1–17. URL: https://doi.org/10.1016/S0895-7177(96)00174-4.

[19] H. M. Byrne and D. Drasdo. "Individual-based and continuum models of growing cell populations: a comparison". In: *J. Math. Biol.* 58.4-5 (2009), pp. 657–687. URL: https://doi.org/10.1007/s00285-008-0212-0.

[20] F. Calabrò and P. Zunino. "Analysis of parabolic problems on partitioned domains with nonlinear conditions at the interface. Application to mass transfer through semi-permeable membranes". In: *Math. Models Methods Appl. Sci.* 16.4 (2006), pp. 479–501. URL: https://doi.org/10.1142/S0218202506001236.

[21] A. Cangiani and R. Natalini. "A spatial model of cellular molecular trafficking including active transport along microtubules". In: *J. Theoret. Biol.* 267.4 (2010), pp. 614–625. URL: https://doi.org/10.1016/j.jtbi.2010.08.017.

[22] J. A. Cañizo, L. Desvillettes, and K. Fellner. "Improved duality estimates and applications to reaction-diffusion equations". In: *Comm. Partial. Differ. Equ.* 39.6 (2014), pp. 1185–1204. URL: https://doi.org/10.1080/03605302.2013.829500.

[23] P. Carmeliet and R. K. Jain. "Angiogenesis in cancer and other diseases". In: *Nature* 407.6801 (2000), pp. 249–257. URL: https://doi.org/10.1038/35025220.

[24] M. A. J. Chaplain, C. Giverso, T. Lorenzi, and L. Preziosi. "Derivation and application of effective interface conditions for continuum mechanical models of cell invasion through thin membranes". In: *SIAM J. Appl. Math.* 79.5 (2019), pp. 2011–2031. URL: https://doi.org/10.1137/19M124263X.

[25] W.-T. Chen, J.-M. Chen, S. J. Parsons, and J. T. Parsons. "Local degradation of fibronectin at sites of expression of the transforming gene product pp60src". In: *Nature* 316.6024 (1985), pp. 156–158. URL: https://doi.org/10.1038/316156a0.

[26] W.-T. Chen, K. Olden, B. A. Bernard, and F. F. Chu. "Expression of transformation-associated protease (s) that degrade fibronectin at cell contact sites." In: *J. Cell. Biol.* 98.4 (1984), pp. 1546–1555. URL: https://doi.org/10.1083/jcb.98.4.1546.

[27] W.-T. Chen and S. Singer. "Fibronectin is not present in the focal adhesions formed between normal cultured fibroblasts and their substrata". In: *Proc. Natl. Acad. Sci.* 77.12 (1980), pp. 7318–7322. URL: https://doi.org/10.1073/pnas.77.12.7318.

[28] S.-W. Cho, S. Kwak, T. E. Woolley, M.-J. Lee, E.-J. Kim, R. E. Baker, H.-J. Kim, J.-S. Shin, C. Tickle, P. K. Maini, et al. "Interactions between Shh, Sostdc1 and Wnt signaling and a new feedback loop for spatial patterning of the teeth". In: *Development* 138.9 (2011), pp. 1807–1816. URL: https://doi.org/10.1242/dev.056051.

[29] G. Ciavolella. "Effect of a membrane on diffusion-driven Turing instability". In: *Acta Appl. Math.* 178.1 (2022), pp. 1–21. URL: https://doi.org/10.1007/s10440-022-00475-0.

[30] G. Ciavolella, N. David, and A. Poulain. "Effective interface conditions for a model of tumour invasion through a membrane". In: *preprint* (2021). URL: https://arxiv.org/abs/2105.02063.

[31] G. Ciavolella and B. Perthame. "Existence of a global weak solution for a reaction–diffusion problem with membrane conditions." In: *J. Evol. Equ.* 21.2 (2020), pp. 1513–1540. URL: https://doi.org/10.1007/s00028-020-00633-7.

[32] M. A. Cichon, A. C. Degnim, D. W. Visscher, and D. C. Radisky. "Microenvironmental influences that drive progression from benign breast disease to invasive breast cancer". In: *J. Mammary Gland Biol. Neoplasia* 15.4 (2010), pp. 389–397. URL: https://doi.org/10.1007/s10911-010-9195-8.

[33] A. G. Clark and D. M. Vignjevic. "Modes of cancer cell invasion and the role of the microenvironment". In: *Curr. Opin. Cell Biol.* 36 (2015), pp. 13–22. URL: https://doi.org/10.1016/j.ceb.2015.06.004.

[34] L. Connolly and P. Maxwell. "Image analysis of Transwell assays in the assessment of invasion by malignant cell lines". In: *Br. J. Biomed. Sci.* 59.1 (2002), pp. 11–14. URL: https://doi.org/10.1080/09674845.2002.11783627.

[35] E. N. Dancer, D. Hilhorst, M. Mimura, and L. A. Peletier. "Spatial segregation limit of a competition–diffusion system". In: *Eur. J. Appl. Math.* 10.2 (1999), pp. 97–115. URL: https://doi.org/10.1017/S0956792598003660.

[36] F. Demengel, G. Demengel, and R. Erné. *Functional spaces for the theory of elliptic partial differential equations*. Springer, 2012. URL: http://dx.doi.org/10.1007/978-1-4471-2807-6.

[37] E. Denicolai, S. Honoré, F. Hubert, and R. Tesson. "Microtubules (MT) a key target in oncology: mathematical modeling of anti-MT agents on cell migration". In: *Math. Model. Nat. Phenom.* 15 (2020), p. 63. URL: https://doi.org/10.1051/mmnp/2020004.

[38] E. Di Costanzo, V. Ingangi, C. Angelini, M. F. Carfora, M. V. Carriero, and R. Natalini. "A macroscopic mathematical model for cell migration assays using a real-time cell analysis". In: *PLoS One* 11.9 (2016), e0162553. URL: https://doi.org/10.1371/journal.pone.0162553.

[39] H. Dillekås, M. S. Rogers, and O. Straume. "Are 90% of deaths from cancer caused by metastases?" In: *Cancer med.* 8.12 (2019), pp. 5574–5576. URL: https://doi.org/10.1002/cam4.2474.

[40] L. Dimitrio. "Modelling nucleocytoplasmic transport with application to the intracellular dynamics of the tumor suppressor protein p53". PhD thesis. Université Pierre et Marie Curie-Paris VI and Universitá degli Studi di Roma La Sapienza, 2012. URL: https://tel.archives-ouvertes.fr/tel-00769901/document.

[41] C. Eck, H. Garcke, and P. Knabner. *Mathematical modeling*. Springer, 2017. URL: https://doi.org/10.1007/978-3-319-55161-6.

[42] A. D. Economou, A. Ohazama, T. Porntaveetus, P. T. Sharpe, S. Kondo, M. A. Basson, A. Gritli-Linde, M. T. Cobourne, and J. B. Green. "Periodic stripe formation by a Turing mechanism operating at growth zones in the mammalian palate". In: *Nat. Genet.* 44.3 (2012), pp. 348–351. URL: https://doi.org/10.1038/ng.1090.

[43] M. Egeblad, E. S. Nakasone, and Z. Werb. "Tumors as organs: complex tissues that interface with the entire organism". In: *Dev. Cell* 18.6 (2010), pp. 884–901. URL: https://doi.org/10.1016/j.devcel.2010.05.012.

[44] S. Eikenberry, C. Thalhauser, and Y. Kuang. "Tumor-immune interaction, surgical treatment, and cancer recurrence in a mathematical model of melanoma". In: *PLoS Comput. Biol.* 5.4 (2009), e1000362. URL: https://doi.org/10.1371/journal.pcbi.1000362.

[45] L. C. Evans. *Partial differential equations*. American Mathematical Soc., 2010.

[46] L. C. Evans. "A convergence theorem for a chemical diffusion-reaction system". In: *Houst. J. Math.* (1980), pp. 259–267.

[47] N. Ferrand, A. Gnanapragasam, G. Dorothee, G. Redeuilh, A. K. Larsen, and M. Sabbah. "Loss of WISP2/CCN5 in estrogen-dependent MCF7 human breast cancer cells promotes a stem-like cell phenotype". In: *PloS One* 9.2 (2014), e87878. URL: https://doi.org/10.1371/journal.pone.0087878.

[48] G. Fiandaca, M. Delitala, and T. Lorenzi. "A mathematical study of the influence of hypoxia and acidity on the evolutionary dynamics of cancer". In: *Bull. Math. Biol.* 83.7 (2021), pp. 1–29. URL: https://doi.org/10.1007/s11538-021-00914-3.

[49] L. C. Franssen, T. Lorenzi, A. E. Burgess, and M. A. Chaplain. "A mathematical framework for modelling the metastatic spread of cancer". In: *Bull. Math. Biol.* 81.6 (2019), pp. 1965–2010. URL: https://doi.org/10.1007/s11538-019-00597-x.

[50] L. C. Franssen. "Mathematical modelling of cancer invasion and metastatic spread". PhD thesis. University of St Andrews, 2019. URL: https://doi.org/10.17630/10023-19080.

[51] M. Gahn. "Singular limit for reactive transport through a thin heterogeneous layer including a nonlinear diffusion coefficient". In: *Commun. Pure Appl. Anal.* 21.1 (2022), pp. 61–82. URL: http://dx.doi.org/10.3934/cpaa.2021167.

[52] M. Gahn, W. Jäger, and M. Neuss-Radu. "Correctors and error estimates for reaction–diffusion processes through thin heterogeneous layers in case of homogenized equations with interface diffusion". In: *J. Comput. Appl. Math.* 383 (2021), p. 113126. URL: https://doi.org/10.1016/j.cam.2020.113126.

[53] O. Gallinato, T. Colin, O. Saut, and C. Poignard. "Tumor growth model of ductal carcinoma: from in situ phase to stroma invasion". In: *J. Theoret. Biol.* 429 (2017), pp. 253–266. URL: https://doi.org//%2010.1016/j.jtbi.2017.06.022.

[54] R. A. Gatenby and E. T. Gawlinski. "A reaction-diffusion model of cancer invasion". In: *Cancer Res.* 56.24 (1996), pp. 5745–5753.

[55] G. Ghersi, Q. Zhao, M. Salamone, Y. Yeh, S. Zucker, and W.-T. Chen. "The protease complex consisting of dipeptidyl peptidase IV and seprase plays a role in the migration and invasion of human endothelial cells in collagenous matrices". In: *Cancer Res.* 66.9 (2006), pp. 4652–4661. URL: https://doi.org/10.1158/0008-5472.CAN-05-1245.

[56] A. Gierer and H. Meinhardt. "A theory of biological pattern formation". In: *Kybernetik* 12.1 (1972), pp. 30–39. URL: https://doi.org/10.1007/BF00289234.

[57] C. Giverso, T. Lorenzi, and L. Preziosi. "Effective interface conditions for continuum mechanical models describing the invasion of multiple cell populations through thin membranes". In: *Appl. Math. Lett.* 125 (2022), p. 107708. URL: https://doi.org/10.1016/j.aml.2021.107708.

[58] H. P. Greenspan. "On the growth and stability of cell cultures and solid tumors". In: *J. Theoret. Biol.* 56.1 (1976), pp. 229–242. URL: https://doi.org/10.1016/S0022-5193(76)80054-9.

[59] P. Gwiazda, B. Perthame, and A. Świerczewska-Gwiazda. "A two-species hyperbolic–parabolic model of tissue growth". In: *Commun. Partial Differ. Equ.* 44.12 (2019), pp. 1605–1618. URL: https://doi.org/10.1080/03605302.2019.1650064.

[60] D. Hanahan and L. M. Coussens. "Accessories to the crime: functions of cells recruited to the tumor microenvironment". In: *Cancer cell* 21.3 (2012), pp. 309–322. URL: %7Bhttps://doi.org/10.1016/j.ccr.2012.02.022%7D.

[61] D. Hanahan and R. A. Weinberg. "Hallmarks of cancer: the next generation". In: *Cell* 144.5 (2011), pp. 646–674. URL: https://doi.org/10.1016/j.cell.2011.02.013.

[62] D. Hanahan and R. A. Weinberg. "The hallmarks of cancer". In: *Cell* 100.1 (2000), pp. 57–70. URL: https://doi.org/10.1016/S0092-8674(00)81683-9.

[63] D. Hanahan and R. A. Weinberg. "Biological hallmarks of cancer". In: *Holland-Frei Cancer Medicine*. John Wiley & Sons, Ltd, 2017, pp. 1–10.

[64] N. Harbeck, F. Penault-Llorca, J. Cortes, M. Gnant, N. Houssami, P. Poortmans, K. Ruddy, J. Tsang, and F. Cardoso. "Breast cancer". In: *Nat. Rev. Dis. Primers* 5.1 (2019), pp. 1–31. URL: https://doi.org/10.1038/s41572-019-0111-2.

[65] F. Hillen and A. W. Griffioen. "Tumour vascularization: sprouting angiogenesis and beyond". In: *Cancer Metastasis Rev.* 26.3 (2007), pp. 489–502. URL: https://doi.org/10.1007/s10555-007-9094-7.

[66] Y. Hong, F. Fang, and Q. Zhang. "Circulating tumor cell clusters: What we know and what we expect". In: *Int. J. Oncol.* 49.6 (2016), pp. 2206–2216. URL: https://doi.org/10.3892/ijo.2016.3747.

[67] W. Hörmann, J. Leydold, and G. Derflinger. *Automatic nonuniform random variate generation*. Springer, 2004. URL: https://doi.org/10.1007/978-3-662-05946-3.

[68] A. Jüngel. *Entropy methods for diffusive partial differential equations*. Vol. 804. Springer, 2016. URL: https://doi.org/10.1007/978-3-319-34219-1.

[69] L. Kachanov. *Introduction to continuum damage mechanics*. Vol. 10. Springer Science & Business Media, 1986. URL: https://doi.org/10.1007/978-94-017-1957-5.

[70] T. Kato. "Schrödinger operators with singular potentials". In: *Israel J. Math.* 13.1 (1972), pp. 135–148. URL: https://doi.org/10.1007/BF02760233.

[71] N. Ke, X. Wang, X. Xu, and Y. A. Abassi. "The xCELLigence system for real-time and label-free monitoring of cell viability". In: *Mammalian cell viability*. Springer, 2011, pp. 33–43. URL: https://doi.org/10.1007/978-1-61779-108-6_6.

[72] O. Kedem and A. Katchalsky. "A physical interpretation of the phenomenological coefficients of membrane permeability". In: *J. Gen. Physiol.* 45.1 (1961), pp. 143–179. URL: https://doi.org/10.1085/jgp.45.1.143.

[73] I. Kim and N. Požár. "Porous medium equation to Hele-Shaw flow with general initial density". In: *Trans. Amer. Math. Soc.* 370.2 (2018), pp. 873–909. URL: https://doi.org/10.1090/tran/6969.

[74] Y. Kim and A. Friedman. "Interaction of tumor with its micro-environment: A mathematical model". In: *Bull. Math. Biol.* 72.5 (2010), pp. 1029–1068. URL: https://doi.org/10.1007/s11538-009-9481-z.

[75] V. Klika, R. E. Baker, D. Headon, and E. A. Gaffney. "The influence of receptor-mediated interactions on reaction-diffusion mechanisms of cellular self-organisation". In: *Bull. Math. Biol.* 74.4 (2012), pp. 935–957. URL: https://doi.org/10.1007/s11538-011-9699-4.

[76] A. Köhrmann, U. Kammerer, M. Kapp, J. Dietl, and J. Anacker. "Expression of matrix metalloproteinases (MMPs) in primary human breast cancer and breast cancer cell lines: New findings and review of the literature". In: *BMC Cancer* 9.1 (2009), pp. 1–20. URL: https://doi.org/10.1186/1471-2407-9-188.

[77] S. Kondo, M. Iwashita, and M. Yamaguchi. "How animals get their skin patterns: fish pigment pattern as a live Turing wave". In: *Int. J. Dev. Biol.* 53 (2009), pp. 851–856. URL: https://doi.org/10.1387/ijdb.072502sk.

[78] E.-H. Laamri and B. Perthame. "Reaction-diffusion systems with initial data of low regularity". In: *J Differ. Equ.* 269.11 (2020), pp. 9310–9335. URL: https://doi.org/10.1016/j.jde.2020.06.042.

[79] E.-H. Laamri and M. Pierre. "Global existence for reaction–diffusion systems with nonlinear diffusion and control of mass". In: *ANN. I. H. POINCARE-AN.* 34.3 (2017), pp. 571–591. URL: https://doi.org/10.1016/j.anihpc.2016.03.002.

[80] H. Li and X. Wang. "Effective boundary conditions for the heat equation with interior inclusion". In: *Commun. Math. Res.* 36.3 (2020), pp. 272–295. URL: https://doi.org/10.4208/cmr.2020-0012.

[81] J. Li, S. Rosencrans, X. Wang, and K. Zhang. "Asymptotic analysis of a Dirichlet problem for the heat equation on a coated body". In: *Proc. Amer. Math. Soc.* 137.5 (2009), pp. 1711–1721. URL: https://doi.org/10.1090/S0002-9939-08-09766-9.

[82] J. Li, L. Su, X. Wang, and Y. Wang. "Bulk-Surface Coupling: Derivation of Two Models". In: *J. Diff. Eq.* 289 (2021), pp. 1–34. URL: https://doi.org/10.1016/j.jde.2021.04.011.

[83] J.-L. Lions. *Quelques méthodes de résolution des problèmes aux limites non linéaires.* Dunod, 1969.

[84] M. Liu, J. Yang, B. Xu, and X. Zhang. "Tumor metastasis: Mechanistic insights and therapeutic interventions". In: *MedComm* 2.4 (2021), pp. 587–617. URL: https://doi.org/10.1002/mco2.100.

[85] T. Liu. "A nonlinear multigrid method for inverse problem in the multiphase porous media flow". In: *Appl. Math. Comput.* 320 (2018), pp. 271–281. URL: https://doi.org/10.1016/j.amc.2017.09.039.

[86] J. S. Lowengrub, H. B. Frieboes, F. Jin, Y.-L. Chuang, X. Li, P. Macklin, S. M. Wise, and V. Cristini. "Nonlinear modelling of cancer: bridging the gap between cells and tumours".

In: *Nonlinearity* 23.1 (2010), pp. 1–21. URL: https://doi.org/10.1088/0951-7715/23/1/001.

[87] A. Marciniak-Czochra, G. Karch, and K. Suzuki. "Instability of Turing patterns in reaction-diffusion-ODE systems". In: *J. Math. Biol.* 74.3 (2017), pp. 583–618. URL: https://doi.org/10.1007/s00285-016-1035-z.

[88] K. H. Martin, K. E. Hayes, E. L. Walk, A. G. Ammer, S. M. Markwell, and S. A. Weed. "Quantitative measurement of invadopodia-mediated extracellular matrix proteolysis in single and multicellular contexts". In: *J. Vis. Exp.* 66 (2012), e4119. URL: https://dx.doi.org/10.3791/4119.

[89] J. Martinez-Serra, A. Gutierrez, S. Muñoz-Capó, M. Navarro-Palou, T. Ros, J. C. Amat, B. Lopez, T. F. Marcus, L. Fueyo, A. G. Suquia, et al. "xCELLigence system for real-time label-free monitoring of growth and viability of cell lines from hematological malignancies". In: *OncoTargets Ther.* 7 (2014), pp. 985–994. URL: https://doi.org/10.2147/OTT.S62887.

[90] S. Marušić and E. Marušić-Paloka. "Two-scale convergence for thin domains and its applications to some lower-dimensional models in fluid mechanics". In: *Asymptot. Anal.* 23.1 (2000), pp. 23–57. URL: https://content.iospress.com/articles/asymptotic-analysis/asy389.

[91] C. B. Morrey Jr. *Multiple integrals in the calculus of variations*. Springer Science & Business Media, 2009. URL: https://doi.org/10.1007/978-3-540-69952-1.

[92] K. W. Morton and D. F. Mayers. *Numerical solution of partial differential equations: an introduction*. Cambridge university press, 2005. URL: https://doi.org/10.1017/CBO9780511812248.

[93] A. Moussa, B. Perthame, and D. Salort. "Backward Parabolicity, Cross-Diffusion and Turing Instability". In: *J. Nonlinear Sci.* 29 (2019), pp. 139–162. URL: https://doi.org/%2010.1007/s00332-018-9480-z.

[94] J. D. Murray. *Mathematical Biology I. An Introduction*. Springer, 2002. URL: https://doi.org/10.1007/b98868.

[95] J. Murray. *Mathematical biology II: spatial models and biomedical applications*. Springer New York, 2001. URL: https://doi.org/10.1007/b98869.

[96] M. Neuss-Radu and W. Jäger. "Effective transmission conditions for reaction-diffusion processes in domains separated by an interface". In: *SIAM J. Math. Anal.* 39.3 (2007), pp. 687–720. URL: https://doi.org/10.1137/060665452.

[97] N. M. Novikov, S. Y. Zolotaryova, A. M. Gautreau, and E. V. Denisov. "Mutational drivers of cancer cell migration and invasion". In: *Br. J. Cancer* 124.1 (2021), pp. 102–114. URL: https://doi.org/10.1038/s41416-020-01149-0.

[98] A. Obr, P. Röselová, D. Grebeňová, and K. Kuželová. "Real-time monitoring of hematopoietic cell interaction with fibronectin fragment: The effect of histone deacetylase inhibitors". In: *Cell Adh. Migr.* 7.3 (2013), pp. 275–282. URL: https://doi.org/10.4161/cam.24531.

[99] M. Otsuji, S. Ishihara, C. Co, K. Kaibuchi, A. Mochizuki, and S. Kuroda. "A mass conserved reaction–diffusion system captures properties of cell polarity". In: *PLoS Comput. Biol.* 3.6 (2007), e108. URL: https://doi.org/10.1371/journal.pcbi.0030108.

[100] C. M. Overall and C. López-Otín. "Strategies for MMP inhibition in cancer: innovations for the post-trial era". In: *Nat. Rev. Cancer* 2.9 (2002), pp. 657–672. URL: https://doi.org/10.1038/nrc884.

[101] K. Painter, G. Hunt, K. Wells, J. Johansson, and D. Headon. "Towards an integrated experimental–theoretical approach for assessing the mechanistic basis of hair and feather morphogenesis". In: *Interface Focus* 2.4 (2012), pp. 433–450. URL: https://doi.org/10.1098/rsfs.2011.0122.

[102] R. Pearl and L. J. Reed. "On the rate of growth of the population of the United States since 1790 and its mathematical representation". In: *Proc. Natl. Acad. Sci.* 6.6 (1920), pp. 275–288. URL: https://doi.org/10.1073/pnas.6.6.27.

[103] B. Perthame. *Some mathematical models of tumor growth*. 2016. URL: https://www.ljll.math.upmc.fr/perthame/cours_M2.pdf.

[104] B. Perthame, F. Quirós, and J. L. Vázquez. "The Hele-Shaw asymptotics for mechanical models of tumor growth". In: *Arch. Ration. Mech. Anal.* 212.1 (2014), pp. 93–127. URL: https://doi.org/10.1007/s00205-013-0704-y.

[105] B. Perthame and J. Skrzeczkowski. "Fast reaction limit with nonmonotone reaction function". In: *Comm. Pure Appl. Math.* (2022). URL: https://doi.org/10.1002/cpa.22042.

[106] B. Perthame. *Parabolic equations in biology*. Springer, 2015. URL: https://doi.org/10.1007/978-3-319-19500-1.

[107] M. Pierre. "Global Existence in Reaction-Diffusion Systems with Control of Mass: a Survey". In: *Milan J. Math.* 78.2 (2010), pp. 417–455. URL: https://doi.org/10.1007%2Fs00032-010-0133-4.

[108] M. Pierre and G. Rolland. "Global existence for a class of quadratic reaction-diffusion system with nonlinear diffusion and L^1 initial data". In: *Nonlinear Anal.* 138 (2016), pp. 369–387. URL: https://doi.org/10.1016/j.na.2015.11.025.

[109] L. Preziosi and A. Tosin. "Multiphase modelling of tumour growth and extracellular matrix interaction: mathematical tools and applications". In: *J. Math. Biol.* 58.4-5 (2009), pp. 625–656. URL: https://doi.org/10.1007/s00285-008-0218-7.

[110] B. C. Price and X. Xu. "Global existence theorem for a model governing the motion of two cell populations". In: *Kinet. Relat. Models* 13.6 (2020), pp. 1175–1191. URL: https://doi.org/10.3934/krm.2020042.

[111] A. Quarteroni, R. Sacco, and F. Saleri. *Numerical mathematics*. Springer Science & Business Media, 2010. URL: https://doi.org/10.1007/b98885.

[112] A. Quarteroni, A. Veneziani, and P. Zunino. "Mathematical and Numerical Modeling of Solute Dynamics in Blood Flow and Arterial Walls". In: *SIAM J. Numer. Anal.* 39.5 (2002), pp. 1488–1511. URL: https://doi.org/10.1137%2Fs0036142900369714.

[113] P. Quittner and P. Souplet. *Superlinear parabolic problems*. Springer, 2019. URL: https://doi.org/10.1007/978-3-030-18222-9.

[114] J. Raspopovic, L. Marcon, L. Russo, and J. Sharpe. "Digit patterning is controlled by a Bmp-Sox9-Wnt Turing network modulated by morphogen gradients". In: *Science* 345.6196 (2014), pp. 566–570. URL: https://doi.org/10.1126/science.1252960.

[115] B. Ribba, O. Saut, T. Colin, D. Bresch, E. Grenier, and J. P. Boissel. "A multiscale mathematical model of avascular tumor growth to investigate the therapeutic benefit of anti-invasive agents". In: *J. Theoret. Biol.* 243.4 (2006), pp. 532–541. URL: https://doi.org/10.1016/j.jtbi.2006.07.013.

[116] T. Roose, S. J. Chapman, and P. K. Maini. "Mathematical models of avascular tumor growth". In: *SIAM Rev.* 49.2 (2007), pp. 179–208. URL: https://doi.org/10.1137/S0036144504446291.

[117] F. G. Sala, P.-M. Del Moral, C. Tiozzo, D. Al Alam, D. Warburton, T. Grikscheit, J. M. Veltmaat, and S. Bellusci. "FGF10 controls the patterning of the tracheal cartilage rings via Shh". In: *Development* 138.2 (2011), pp. 273–282. URL: https://doi.org/10.1242/dev.051680.

[118] E. Sanchez-Palencia. "Problèmes de perturbations liés aux phénomènes de conduction à travers des couches minces de grande résistivité". In: *J. Math. Pures Appl. (9)* 53 (1974), pp. 251–269.

[119] L. A. Segel. "Simplification and scaling". In: *SIAM review* 14.4 (1972), pp. 547–571. URL: https://doi.org/10.1137/1014099.

[120] A. Serafini. "Mathematical models for intracellular transport phenomena". PhD thesis. Universitá degli Studi di Roma La Sapienza, 2007.

[121] H. Sung, J. Ferlay, R. L. Siegel, M. Laversanne, I. Soerjomataram, A. Jemal, and F. Bray. "Global cancer statistics 2020: GLOBOCAN estimates of incidence and mortality worldwide for 36 cancers in 185 countries". In: *CA Cancer J. Clin.* 71.3 (2021), pp. 209–249. URL: https://doi.org/10.3322/caac.21660.

[122] M. Taylor. *Partial Differential Equations III: Nonlinear Equations*. Springer New York, 2011. URL: https://doi.org/10.1007/978-1-4419-7049-7.

[123] A. M. Turing. "The chemical basis of morphogenesis". In: *Phil. Trans. R. Soc. Lond. B* 237 (1952), pp. 37–72. URL: https://doi.org/10.1098/rstb.1952.0012.

[124] L. Türker Şener, G. Albeniz, B. Dinç, and I. Albeniz. "iCELLigence real-time cell analysis system for examining the cytotoxicity of drugs to cancer cell lines". In: *Exp. Ther. Med.* 14.3 (2017), pp. 1866–1870. URL: https://doi.org/10.3892/etm.2017.4781.

[125] J. L. Vázquez. "An introduction to the mathematical theory of the porous medium equation". In: *Shape optimization and free boundaries*. Springer, 1992, pp. 347–389. URL: https://doi.org/10.1007/978-94-011-2710-3_10.

[126] J. L. Vázquez. "Failure of the strong maximum principle in nonlinear diffusion. Existence of needles". In: *Commun. Partial Differ. Equ.* 30.9 (2005), pp. 1263–1303. URL: https://doi.org/10.1080/10623320500258759.

[127] J. L. Vázquez. *The porous medium equation*. Oxford Mathematical Monographs. The Clarendon Press, Oxford University Press, Oxford, 2007. URL: https://doi.org/10.1093/acprof:oso/9780198569039.001.0001.

[128] A. G. Waks and E. P. Winer. "Breast cancer treatment: a review". In: *Jama* 321.3 (2019), pp. 288–300. URL: https://doi.org/10.1001/jama.2018.19323.

[129] M. Watanabe and S. Kondo. "Is pigment patterning in fish skin determined by the Turing mechanism?" In: *Trends Genet.* 31.2 (2015), pp. 88–96. URL: https://doi.org/10.1016/j.tig.2014.11.005.

[130] D. Wirtz, K. Konstantopoulos, and P. C. Searson. "The physics of cancer: the role of physical interactions and mechanical forces in metastasis". In: *Nat. Rev. Cancer* 11.7 (2011), pp. 512–522. URL: https://doi.org/10.1038/nrc3080.

[131] M. Yamaguchi, E. Yoshimoto, and S. Kondo. "Pattern regulation in the stripe of zebrafish suggests an underlying dynamic and autonomous mechanism". In: *Proc. Natl. Acad. Sci. U.S.A.* 104.12 (2007), pp. 4790–4793. URL: https://doi.org/10.1073/pnas.0607790104.

[132] M. Zaoui, M. Morel, N. Ferrand, S. Fellahi, J.-P. Bastard, A. Lamazière, A. K. Larsen, V. Béréziat, M. Atlan, and M. Sabbah. "Breast-associated adipocytes secretome induce fatty acid uptake and invasiveness in breast cancer cells via CD36 independently of body mass index, menopausal status and mammary density". In: *Cancers* 11.12 (2019), p. 2012. URL: https://doi.org/10.3390/cancers11122012.

Reaction-diffusion equations with membrane conditions describing tumor invasion

Abstract

Reaction-diffusion membrane problems find several applications in physics, biology and medical sciences, both in the case of linear and nonlinear diffusion. We mainly focus on the biological setting of two domains separated by a permeable membrane. At first, extending the work by Sanchez-Palencia to the porous medium case, we rigorously derive the effective interface conditions, called Kedem-Katchalsky conditions, as the limit of transmission conditions when the thickness of the membrane converges to zero. This is biologically relevant and convenient for numerical simulations. Then, the following works regard this limit problem on a zero-thickness membrane, but in the linear case. Extending the theory developed by Pierre and his collaborators, we establish the existence of global weak solutions when initial data have an L^1 regularity and nonlinearities have a sub-quadratic growth. In another work, we look at the situation in which two populations react and diffuse in a single domain creating spatial patterns. We adapt this Turing theory to the case of a permeable membrane. The result is quite similar to the standard case, but pattern formation is influenced both by diffusion and permeability coefficients. Finally, we present a more applied study in collaboration with biologists from the Laboratoire de Biologie et Thérapeutique des Cancers of INSERM at Saint-Antoine Hospital in Paris. In fact, Kedem-Katchalsky conditions can well characterise the flow of tumor cells through the basal membrane, in the so-called invasion process. This is a key step in the metastatic cascade and it is allowed by several stages, among which we distinguish membrane degradation. With the aim of deepening the invasion phenomenon, we propose a mathematical model concerning degradation of a biological layer. We present numerical simulations and an *a priori* analysis on the sensitivity of our system and on the parameter estimation. This is a preparatory work waiting for experimental results.

Keywords: Kedem-Katchalsky conditions, Reaction-diffusion equation, Numerical analysis, Tumor invasion

---

Résumé

Les problèmes de membrane dans les systèmes de réaction-diffusion trouvent de nombreuses applications en physique, en biologie et en médecine, aussi bien dans le cas linéaire que non linéaire. Nous nous intéressons à ces systèmes pour le cas de membranes biologiques. L'exemple représentatif étant donné par deux domaines séparés par une membrane perméable. Dans un premier temps, nous commençons par adapter le travail de Sanchez-Palencia à l'égard de systèmes de type fluide dans un milieu poreux afin de déterminer les conditions de membrane effectives, usuellement appelées conditions de Kedem-Katchalsky, en faisant tendre l'épaisseur de la membrane vers 0. Le modèle limite est à la fois biologiquement pertinent et très bien adapté pour des simulations numériques. Les travaux suivants s'intéressent au cas de diffusion linéaire avec des conditions de membrane effectives. En étendant la théorie développée par Pierre et ses collaborateurs, nous établissons l'existence de solutions faibles globales lorsque les données initiales ont une régularité L^1 et que les non-linéarités ont une croissance sous-quadratique. Dans un autre travail, nous regardons la situation dans laquelle deux populations réagissent et diffusent dans un même domaine en créant des structures spatiales. Nous étendons cette théorie de Turing au cas d'une membrane perméable. Le résultat obtenu est assez similaire au cas sans membrane mais ici vont jouer un rôle aussi bien les coefficients de diffusion que ceux de perméabilité à l'interface. Enfin, nous présentons une étude plus appliquée en collaboration avec le Laboratoire de Biologie et Thérapeutique des Cancers de l'INSERM à l'Hôpital Saint Antoine à Paris. En effet, les conditions de Kedem-Katchalsky permettent de bien caractériser le flux de cellules tumorales à travers la membrane basale, dans le processus dit d'invasion. C'est une étape clé dans la cascade métastatique qui est composée de plusieurs phases, parmi lesquelles on distingue la dégradation de la membrane. Dans le but d'approfondir notre compréhension du phénomène d'invasion, nous proposons un modèle mathématique représentant la dégradation d'une couche biologique. Nous présentons des simulations numériques et une analyse *a priori* sur la sensibilité de notre système et sur l'estimation des paramètres. Il s'agit d'un travail préparatoire en attente des résultats expérimentaux.

Mots clés : Conditions de Kedem-Katchalsky, Équation de réaction-diffusion, Analyse numérique, Invasion tumorale

---

Laboratoire Jacques-Louis Lions – Sorbonne Université – Campus Pierre et Marie Curie – 4 place Jussieu – 75005 Paris – France

Istituto per le Applicazioni del Calcolo 'Mauro Picone' – CNR – Via dei Taurini 19 – 00185 Roma – Italy

Riassunto

I problemi di reazione-diffusione con membrana trovano numerose applicazioni in fisica, biologia e medicina, sia nel caso di diffusione lineare che non lineare. Ci interessiamo a questi sistemi nel caso di membrane biologiche. L'esempio rappresentativo é quello di due domini separati da una membrana permeabile. In un primo tempo, estendendo il lavoro di Sanchez-Palencia per le equazioni dei mezzi porosi, ricaviamo in modo rigoroso le condizioni di interfaccia, chiamate condizioni di Kedem-Katchalsky, come limite di condizioni di trasmissione quando lo spessore della membrana converge a zero. Ciò è rilevante dal punto di vista biologico e conveniente per le simulazioni numeriche. I lavori che seguono riguardano questo problema limite su una membrana di spessore zero, ma guardando al caso di diffusione lineare. In un secondo studio, estendendo la teoria sviluppata da Pierre e dai suoi collaboratori, stabiliamo l'esistenza di soluzioni deboli globali quando i dati iniziali hanno una regolarità L^1 e le nonlinearità hanno una crescita al più quadratica. In un altro lavoro, guardiamo alla situazione in cui due popolazioni reagiscono e si diffondono in un unico dominio creando strutture spaziali. Adattiamo questa teoria di Turing in presenza di una membrana permeabile. Il risultato è abbastanza simile alla classica teoria di Turing, ma la formazione di pattern é influenzata sia dai coefficienti di diffusione che di permeabilità della membrana. Infine, presentiamo un lavoro più applicato in collaborazione con dei biologi del Laboratoire de Biologie et Thérapeutique des Cancers dell'INSERM all'Ospedale Saint Antoine a Parigi. Infatti, le condizioni di Kedem-Katchalsky possono caratterizzare il flusso di cellule tumorali attraverso la membrana basale, nel cosiddetto processo di invasione. Questo è un passaggio chiave nella cascata metastatica ed è consentito da diverse fasi, tra le quali distinguiamo la degradazione della membrana. Con l'obiettivo di approfondire la nostra conoscenza del fenomeno invasivo, proponiamo un modello matematico che rappresenta la degradazione di una membrana biologica. Presentiamo anche simulazioni numeriche e un'analisi *a priori* della sensibilità del nostro sistema e della stima dei parametri. Si tratta di un lavoro preparatorio in attesa dei risultati sperimentali.

Parole chiave: Condizioni di Kedem-Katchalsky, Equazione di reazione-diffusione, Analisi numerica, Invasione tumorale